EVALUATION OF SEISMIC RESPONSE MODIFICATION FACTORS FOR STEEL FRAMES BY NON-LINEAR ANALYSIS

A THESIS SUBMITTED TO
THE GRADUATE SCHOOL OF NATURAL AND APPLIED SCIENCES
OF
MIDDLE EAST TECHNICAL UNIVERSITY

BY

SERHAN BAKIR

IN PARTIAL FULFILLMENT OF THE REQUIREMENTS
FOR
THE DEGREE OF MASTER OF SCIENCE
IN
CIVIL ENGINEERING

NOVEMBER 2006

Approval of the Graduate School of Natural and Applied Sciences

Prof. Dr. Canan Özgen
Director

I certify that this thesis satisfies all the requirements as a thesis for the degree of Master of Science.

Prof. Dr. Erdal Çokça
Head of Department

This is to certify that we have read this thesis and that in our opinion it is fully adequate, in scope and quality, as a thesis for the degree of Master of Science.

Prof. Dr. Çetin Yılmaz
Supervisor

Examining Committee Members

Prof. Dr. Ergin Atımtay	(METU, CE)	
Prof. Dr. Çetin Yılmaz	(METU, CE)	
Assoc. Prof. Dr. Uğur Polat	(METU, CE)	
Assoc. Prof. Dr. Can Balkaya	(METU, CE)	
Dr. Halis Günel	(METU, ARCH)	

I hereby declare that all information in this document has been obtained and presented in accordance with academic rules and ethical conduct. I also declare that, as required by these rules and conduct, I have fully cited and referenced all material and results that are not original to this work.

Name, Last Name: Serhan BAKIR

Signature :

ABSTRACT

EVALUATION OF SEISMIC RESPONSE MODIFICATION FACTORS FOR STEEL FRAMES BY NON-LINEAR ANALYSIS

Bakır, Serhan

M.S., Department of Civil Engineering

Supervisor: Prof. Dr. Çetin Yılmaz

November 2006, 156 pages

In this study steel framing systems are investigated with regards to their lateral load carrying capacity and in this context seismic response modification factors of individual systems are analyzed. Numerous load resisting layouts, such as different bracing systems and un-braced moment resisting frames with various bay and story configurations are designed and evaluated in a parametric fashion. Three types of beam to column connection conditions are incorporated in evaluation process.

Frames, designed according to Turkish seismic code, are investigated by non-linear static analysis with the guidance of previous studies and recent provisions of FEMA. Method of analysis, design and evaluation data are presented in detail. Previous studies in literature, history and the theory of response modification phenomenon is presented.

Results are summarized, main weaknesses and ambiguities introduced to design by the use of “R” factors are stated depending on the observed behavior.

Keywords: response modification factors, steel frames, non-linear static analysis, seismic performance.

ÖZ

TAŞIYICI SİSTEM DAVRANIŞ KATSAYISININ ÇELİK ÇERÇEVELER İÇİN NON-LİNEER ANALİZ İLE ELDE EDİLMESİ

Bakır, Serhan

Yüksek Lisans, İnşaat Mühendisliği Bölümü

Tez Yöneticisi: Prof. Dr. Çetin Yılmaz

Kasım 2006, 156 sayfa

Bu çalışmada çelik çerçeve sistemlerinin yatay yük taşıma kapasiteleri incelenmiş ve bu bağlamda taşıyıcı sistem davranış katsayıları değerlendirilmiştir. Çeşitli tiplerdeki sistemler, örnek olarak değişik çelik çapraz şekilleri ve moment aktaran çerçeveler, farklı kat ve açıklık düzenlerinde boyutlandırılmış ve etüt edilmiştir. Üç farklı kolon kiriş birleşim durumu da değerlendirme sırasında göz önüne alınmıştır.

Türk deprem yönetmeliğine göre tasarlanan çerçeveler, bugüne kadar yapılmış çalışmalar ve güncel FEMA yönergeleri ışığında, doğrusal olmayan statik analiz yöntemi ile irdelenmiştir. Araştırma yöntemi, tasarım ve değerlendirme verileri ayrıntılı bir şekilde aktarılmıştır. Taşıyıcı sistem davranış katsayıları üzerine yapılmış çalışmalar, tarihi ve temel aldığı kuramı da bu tez içersinde sunulmuştur.

Sonuçlar özetlenmiş, “R” katsayısı kullanımının tasarıma getirdiği temel zayıflıklar ve belirsizlikler gözlenen davranışlara bağlı olarak belirtilmeye çalışılmıştır.

Anahtar Sözcükler: taşıyıcı sistem davranış katsayısı, çelik çerçeveler, doğrusal olmayan statik analiz, deprem davranışı.

ACKNOWLEDGEMENTS

I would like to thank to my dear father, Erhan BAKIR and my dear uncle Ali Rıza BAKIR for their invaluable supports and understandings.

I would like to thank to my dear mother, Ayfer BAKIR for taking care of me in every manner and wish good luck to my brother Sinan BAKIR in his academic life.

I would like to thank to my friends who did “not” leave me alone during this period of time.

I would like to thank to my supervisor Prof. Dr. Çetin YILMAZ for the support that he has provided during my study.

TABLE OF CONTENTS

PLAGIARISM iii

ABSTRACT iv

ÖZ v

ACKNOWLEDGMENTS vi

TABLE OF CONTENTS vii

CHAPTER

1 INTRODUCTION 1

1.1 GENERAL INFORMATION 1

1.2 OBJECTIVE AND SCOPE 4

2 RESPONSE MODIFICATION FACTORS 5

2.1 FORMULATION 7

2.2 OVERSTRENGTH FACTOR 9

2.2.1 Local Overstrength 9

2.2.2 Global Overstrength 10

2.2.3 Previous Studies 12

2.2.3.1 Freeman 12

2.2.3.2 Osteraas and Krawinkler 12

2.2.3.3 Rahgozar and Humar 12

2.2.3.4 Kappos 13

2.2.3.5 Balendra and Huang 13

2.2.3.6 Lee, Cho and Ko 13

2.2.3.7 Kim and Choi 13

2.2.4 NEHRP Provisions 14
2.3 DUCTILITY REDUCTION FACTOR 15
2.3.1 Previous Studies 16
2.3.1.1 Newmark and Hall 16
2.3.1.2 Lai and Biggs 17
2.3.1.3 Riddell and Newmark 18
2.3.1.4 Riddell, Hidalgo and Cruz 19
2.3.1.5 Miranda 19
2.3.1.6 Nassar and Krawinkler 20
2.3.1.7 Borzi and Elnashai 20
2.4 DAMPING FACTOR 23
2.4.1 Previous Studies 24
2.4.1.1 Newmark and Hall 24
2.4.1.2 Ashour 24
2.4.1.3 Wu and Hanson 25
2.4.1.4 Ramirez 25
2.4.1.5 Lin and Chang 26
2.5 REDUNDANCY FACTOR 26
2.5.1 Previous Studies 26
2.5.2 NEHRP Provisions 27
3 METHOD OF ANALYSIS 31
3.1 FRAME TYPES 31
3.2 FRAME DESIGN 33
3.2.1 Equivalent Lateral Load Analysis 33

3.2.2 Gravity Load Analysis 37
3.2.3 Sample Design..... 37
3.2.4 Earthquake Zone 38
3.3 NON-LINEAR STATIC ANALYSIS 39
3.3.1 Process of Non-linear Static Analysis..... 40
3.3.2 Force Displacement Relationships..... 40
3.3.2.1 Beam & Column Members 44
3.3.2.2 Bracing Members..... 50
3.3.2.3 Partially Restrained Connections 56
3.3.3 Panel Zone Deformations..... 61
3.3.4 Capacity Curve of Structures 65
3.3.4.1 Idealization of Capacity Curve..... 66
3.3.5 Sample Analysis Evaluation..... 67
4 RESULTS OF ANALYSIS AND FURTHER REMARKS 71
5 SUMMARY OF RESULTS AND CONCLUSIONS 103
5.1 SUMMARY OF RESULTS..... 103
5.2 CONCLUSIONS..... 106
REFERENCES..... 108
APPENDIX
A.1 PROPOSED RESPONSE MODIFICATION FACTORS 118
A.2 FRAME MEMBER LABELS..... 121
A.3 FRAME MEMBER SECTIONS..... 145
A.4 NON-LINEAR FORCE DISPLACEMENT PARAMETERS
For STRUCTURAL COMPONENTS..... 151

CHAPTER 1

INTRODUCTION

1.1 GENERAL INFORMATION

Due to economic and architectural constraints, engineers are compelled to design structural systems which are cost effective and good-looking while adequately safe and strong to satisfy inhabitants who will live and work in them. Scare resources of materials, man & machine power and time, especially in active seismicity areas, mandate the basic objective of structural design as to provide buildings with an ability to withstand strong ground shaking without collapse, but potentially with some significant structural damage. At the present time structural design philosophy residing in codes, emphasizes that absolute safety and no-damage, even in an earthquake with a reasonable probability of occurrence, cannot be achieved. However, letting some structural and non-structural damage, a high level of life safety can be economically achieved in structures by allowing inelastic energy dissipation. As a result of this design philosophy, the design lateral strength prescribed in seismic codes is lower, and in some cases much lower, than the lateral strength required to maintain the structure in the elastic range.

Maintaining the structure in elastic range means that all structural and non-structural members, subjected to lateral motion, are assured to return to the initial state with no permanent deformations and damages. In many cases preserving this state is far from being feasible and rational. On the other hand going beyond the elastic frontier in an earthquake event may lead to yielding and cracking in members which can bring catastrophic results unless these inelastic actions are limited to a certain degree. At this point utilizing inelastic behavior definitely lowers the overall construction costs by reducing member sizes thus reducing material amounts and construction time also providing ease of operability and

erection. Finding the balance in between is the major concern of a designer who is searching for the optimum design by means of sizing the members and making use of different structural systems.

To utilize inelastic behavior in design, first of all, effects of earthquake induced motion on the structure must be examined. Current engineering practice is capable of making close approximations of the structural properties and properly put them into operation of computer aided finite element analysis (formulation of the problem into a set of mathematical equations). Such as the mass, stiffness and damping properties moreover gravity loading conditions may be modeled. On the contrary the earthquake characteristics are unique. The ground motion is unpredictable and irregular in direction, magnitude and duration. Therefore past ground motion records serve as a starting point to form a basic understanding of characteristics of the excitation such as the displacements, velocities, and accelerations.

Structural engineering took advantage of these records by various schemes. Subjecting a model directly to a given motion record as known as Time History Analysis, may provide an insight to what will actually happen during an excitation. In the process of structural design an iterative progression takes place; this kind of simulation may be carried on for linear and non-linear models with different records but such an approach needs huge computational effort and time. Consequently the Response Spectrum Method “which involves the calculation of only the maximum values of the displacements and member forces in each mode using smooth design spectra that are the average of several earthquake motions” [19] is preferred in routine application. The most simplified and striped method for seismic design is the Equivalent Lateral (Static) Load analysis which is easy to employ and the variables (relatively less in number) are defined in the codes.

Plastic design for steel and ultimate strength design for reinforced concrete members are based on inelastic performance of materials. For both design methodologies statistical studies played an important role in defining load factors since members shall not be designed for the working loads anymore. However the overall inelastic behavior is another matter which is also studied by many researchers up to present date. Equivalent Lateral Load and Response Spectrum Analysis methods are by far the most used methods for evaluating earthquake resistance and design of structures since they are actually based on elastic static analysis. However, these are not comprehensive analytical tools that allow for the accurate consideration of very complicated building behavior subjected to earthquake ground motions. A new procedure called Performance Based Design is up and rising now; implementing the inelastic static analysis (pushover) natively in design process, stepping ahead of abovementioned elastic procedures which are most of the time leading to poor approximations of overall behavior.

The main approximation lies in the concept of Response Modification Factors. This vague approach to assign discrete modification factors for structural systems may be very practical when it comes down to routine practice in engineering but simplicity brings higher uncertainty. The structural engineering profession has lacked a codified, traceable, rational and robust method for determining system R factors since their inception. In this particular study past observations and studies are reviewed, factors are tried to be identified with embedded components inside and they tried to be evaluated for steel framing systems.

1.2 OBJECTIVE AND SCOPE

The main aim of this study is to investigate the performance of steel frames designed according to Turkish Seismic Code with non-linear static analysis regarding to their lateral load carrying capacity and to assess pertinent response modification factors based on the literal definition given by past studies. In this context overstrength and ductility reduction factors are evaluated by analyzing the raw pushover data of systems with the help of a custom developed computer program.

Some of the design conditions for framing systems are predetermined such as: seismic zone, soil group, building importance and gravity loading. These values kept constant for all design cases. The main variations are the geometry and the connection modeling through the systems. 3, 4, 5 bay 3, 6, 9 story configurations for 6 different framing systems accompanied by center-line, partially restrained and panel zone deforming models are created. With two limiting top drift states a total of 324 different structural models analyzed in order to evaluate the “R” factors regarding to structures actual lateral capacity.

Response spectrum analysis is performed and resultant base shear is normalized by equivalent lateral load proposed by the code. Steel member design is carried on according to allowable stress design. Design sections are chosen from European sections list such as IPE and HE sections for beams and columns, tube sections are chosen for bracing members. Member sections are assigned with respect to engineering practice, not making any distinct selections but trying to achieve a uniform overall design. Pushover analysis is performed according to FEMA-356 [57] prescriptions. In order to reach structures’ ultimate capacity pushover analysis is run until the system became a mechanism which is unstable. Also an intermediate top drift target is selected as 1% of overall height with the intention of comparison. Brief information and every modeling property data are presented in every section with the intention of providing all details to be benefited, in future investigations or possible extensions of this study.

CHAPTER 2

RESPONSE MODIFICATION FACTORS

The response modification factor, R, simply represents the ratio of the maximum lateral force, *Ve*, which would develop in a structure, responding entirely linear elastic under the specified ground motion, to the lateral force, *Vd*, which it has been designed to withstand. The ratio R, expressed by the equation:

$$R = \frac{V_e}{V_d}$$

The factor R is an empirical response reduction factor intended to account for damping, overstrength, and the ductility inherent in the structural system at displacements great enough to surpass initial yield and approach the ultimate load displacement of the structural system [51]. The concept of a response modification factor was proposed based on the premise that well-detailed seismic framing systems could sustain large inelastic deformations without collapse (ductile behavior) and develop lateral strengths in excess of their design strength (often termed reserve strength) [60].

Engineering practice benefited from these facts of structural behavior. Along with some major assumptions and experiences “R” factor is first introduced in ATC-3-06 [62] in 1978, served to reduce the base shear force (V_e) calculated by elastic analysis using a 5% damped acceleration response spectrum for the purpose of calculating a design base shear (V_d).

R factors are widely used; integrated into the static elastic analysis of structures to account for inelastic response. Major static analysis routines are Equivalent Lateral Force Method and Response Spectrum Method; in both procedures R factors are utilized to calculate the design base shear. One of the

most important assumptions of both methods is that the “inelastic” response quantities are tried to be approximated by the use of “elastic” analysis tools just by introducing a factor. The use of R factors includes another significant ambiguity to the design which is that while assuming considerable damage by reducing the lateral forces, it is not possible to estimate the level of damage by these methods.

As described above, the use of response modification factors will likely ensure that a code compliant building will yield in a design earthquake. The scale and distribution of inelastic response will depend on many factors, including the excitation characteristics, three-dimensional assembly of stiffness and mass in the structure and the soil characteristics. The reasoning behind the use of the response modification factors is to bring economy to the resultant design. The use of static elastic analysis procedures together with the response modification factors are still the cornerstone of seismic design practice. Although being inadequate in predicting some response quantities, static elastic procedures are valuable for the design professional for a number of reasons, including:

1. It is easy to use and does not require the designer to have an in depth understanding of structural dynamics (it may be argued that this is a drawback).

2. It can be used to develop preliminary design a structure for later assessment by more precise methods.

3. It may provide estimates of internal forces of sufficient accuracy for the design of low-rise, regular buildings.

2.1 FORMULATION:

In the mid-1980s, data from an experimental research program at the University of California at Berkeley were used to develop an improved understanding of the seismic response of code-compliant steel braced frame buildings and to propose a draft formulation for the response modification factor. Base shear-roof displacement relationships were established using data acquired from the earthquake simulator testing of two code-compliant steel framing systems, one concentrically braced [1] and one eccentrically braced [2]. The force-displacement curves were developed by plotting the roof displacement at the time corresponding to the maximum base shear force for each earthquake simulation and each model.

For each test, the elastic acceleration response spectrum (Sa,5) was generated using the acceleration-response history of the earthquake simulator platforms. Using the experimental data, the Berkeley researchers described R as the product of three factors that accounted for reserve strength, ductility, and added viscous damping:

$$R = R_S \cdot R_\mu \cdot R_\xi$$

In this equation, R_S is overstrength factor, R_μ is ductility reduction factor and R_ξ is damping factor. The overstrength factor was calculated to be equal to the maximum base shear force at the yield level (V_y) divided by the design base shear force (V_d). The ductility reduction factor was calculated as the base shear (V_e) for elastic response (Sa,5) divided by the yield base shear force (V_y). The damping factor was set equal to 1.0.

Further research ([3] ~ [11], [60]) has been completed since the first proposal for splitting R into component factors. Studies conducted by Applied Technology Council [60] support a new formulation for R in which R is expressed as the product of three factors:

$$R = R_S \cdot R_\mu \cdot R_R$$

where R_S is a strength factor; R_μ is a period dependent ductility factor; and R_R is a redundancy factor. This formulation, with the exception of the redundancy factor, is similar to those proposed by the Berkeley researchers. Here the strength factor (R_S) is the ratio of significant yield strength of the lateral force resisting system to its design strength, while ductility factor (R_μ) is defined as the ratio of the ultimate elastic force demand to the significant yield strength, which are expressed as follows:

$$R_S = \frac{V_y}{V_d} \quad R_\mu = \frac{V_e}{V_y}$$

The redundancy factor is proposed to consider the reliability of seismic framing systems that use multiple lines of vertical seismic framing in each principal direction of a building. The damping factor (R_ξ) is intended to account for the influence of supplemental viscous damping devices. Such a viscous damping factor may be used to reduce displacements in a yielding frame but may not proportionally reduce force demands. Since response modification factors are used with force-based design procedures, the damping factor was excluded from the new formulation.

Differences in the values of the behavior factors specified in various codes for the same type of structure can be significant; for example, the behavior factor for high-ductility reinforced concrete (R/C) frames is equal to 8.5 in UBC [66], but only 5 in EC8 [67]. Tables A.1.1 and A.1.2 in the appendix section are representing response modification factors proposed in NEHRP 2003 [51] and ABYYHY [63].

2.2 OVERSTRENGTH FACTOR

The real strength of a structure will more likely be higher than its design strength. This is due to overall design simplifications; modern computer aided tools however let the engineer model and design the structure as close as to what is built, there are still major simplifications and assumptions that are incorporated through the process. These assumptions and design practices are usually in favor of conservative design as to stay on the safe side. The presence of overstrength in structures may be examined in local and global manner.

2.2.1 Local overstrength

What is meant with the term local is the overstrength as a result of the design process with use of stronger and larger components than required. Main reasons are summarized below.

a) Code Based Strength and Methodology: The design code can mandate a strength level for the material while the actual strength is higher. (e.g., allowable stress design for a steel member may lead to member overstrength due to the significant difference between the allowable stress and the member strength.) Furthermore code design methodology may lead to overstrength by not fully utilizing the member capacity. (e.g., state of the art design codes such as LRFD may produce more economic results and less overdesign when compared to ASD)

b) Code Minimum Requirements and Provisions: There are some circumstances in which the preliminary design of a member may be governed by specific code requirements such as the bracing selection concerning its kl/r or strong column weak beam provision; both not directly linked to strength or serviceability but provide basic solid preventative measures of a design.

c) Governing Design Condition: In the design process member selection is controlled by conditions like strength or serviceability. Besides seismic loads governing conditions may be gravity loading alone or combinations of gravity and

other lateral loads (i.e, wind loads) and especially deflection or drift limits may cause member overstrength.

d) Actual vs. Nominal Material Strength: The actual mean strength of the material used in construction is generally higher than the strength assumed in design.

e) Actual vs. Design Loads: Real life floor live loads are typically less than the code proposed minimum design live load. Point or linear loads of a floor may be modeled as distributed area loads for simplicity and loads greater than the code proposed values may be used if there is any uncertainty of the actual loading values and layout.

f) Discrete Member Selection: Depending on analysis results the design process will point out member sizes different from each other throughout the structure while the designer has the only chance of selecting from one list of available sections. This causes two overdesign issues. First the section selected will likely be larger than the required for that member and the second designer will want to produce a uniform design by making a uniform selection of cross-sections in order to achieve easy fabrication and erection.

2.2.2 Global Overstrength

This type of overstrength comes from overall behavior of the structure to the lateral loading. Plastic hinge occurrence (by yielding) and redistribution of internal forces in the inelastic range allows the structure to resist forces that are significantly higher than the design forces. Two other issues needed to be addressed which have major effect on global overstrength are:

a) Members Neglected in Design: In some cases, certain parts of the structure are neglected such as compression braces and slab systems under lateral action. Furthermore design may be carried out in such a way that the lateral forces are only taken by braced frames, neglecting the rest of the structure. Omitting those

components in design will surely lead to overstrength since their existence in real life will contribute to the general behavior.

b) Non-structural Members: Non-structural members like partition walls, stairways cladding, etc. will contribute to the lateral strength of the structure. It is likely that low-rise buildings shall possess greater overstrength than high-rise buildings since they shall have a greater ratio of non-structural members to structural members moreover their design is mainly controlled by the gravity actions rather than lateral forces.

Here it is necessary to define that “overstrength” is the difference between the significant yield strength and the design strength of the structure (Vy – Vd) however the “overstrength factor” is the ratio between two (Vy / Vd). The term “significant yield” is not the point where first yielding occurs in any member but, rather, it is defined as the stage of complete plastification of at least the most critical region of the structure which can be traced on the capacity curve as a significant change in the slope. An example illustration for significant yield point can be seen in Figure 3.26 at point (Δy, Vy).

Overstrength of a structure due to its inelastic behavior under lateral loading can be assessed by numerical analysis. Non-linear static analysis procedure (pushover) is a functional tool for estimating the lateral yield strength of the structure. Significant yield point is determined by idealizing the resultant capacity curve of the structure. Base shear vs. displacement graph is reformed as a bilinear curve where the deflection point of the curve (start of the non-linearity) indicates the yielding point and the yield base shear is obtained.

2.2.3 Previous Studies

In this section, some of the previous studies about overstrength factors are reviewed

2.2.3.1 Freeman [4]

In this study, conducted in 1990, the author reported overstrength factors for 3 three-story steel moment frames, two constructed in seismic zone 4 and one in seismic zone 3 were 1.9, 3.6, and 3.3, respectively.

2.2.3.2 Osteraas and Krawinkler [5]

In this study overstrength and ductility of steel frames designed in compliance with the Uniform Building Code working stress design provisions were observed. Moment frames, perimeter frames and braced frames having various bay sizes and heights were subjected to non-linear static analysis using an invariant triangular load distribution. For moment frames the overstrength factor ranged from 8.0 in the short period range to 2.1 at a period of 4.0 seconds. For concentric braced frames reported overstrength factors ranged from 2.8 to 2.2 at periods of 0.1s to 0.9s respectively.

2.2.3.3 Rahgozar and Humar [6]

Authors obtained overstrength factors ranging from 1.5 to 3.5 for two types of concentrically braced ten-story frames. Stating as a result of their study the main parameter that controls the reserve strength in those frames was the slenderness ratio of the bracing members. PΔ effect has a negligible effect on the overstrength factor and overstrength increases with an increase in the brace slenderness ratio or a decrease in the design earthquake load.

2.2.3.4 Kappos [7]

In this study five R/C buildings, with one to five stories, consisting of beams, columns, and structural walls are examined and as a result overstrength factors 1.5 to 2.7 are obtained.

2.2.3.5 Balendra and Huang [8]

Authors studied moment, X and V braced 3, 6 and 10 stories steel frames having rigid and semi-rigid connections; reporting overstrength factors ranging 1.9 to 8.0 for moment resisting frames, 2 to 3.4 for X braced and 2.3 to 5.6 for V braced frames. Another conclusion of the study is when the rigid connections are replaced with semi-rigid connections, the overstrength factors of moment resisting frames decrease around 50%, while the ductility factors increase more than 25%.

2.2.3.6 Lee, Cho and Ko [9]

In their study the authors investigated overstrength factors and plastic rotation demands for 5, 10, 15 story R/C buildings designed in low and high seismicity regions utilizing three dimensional pushover analysis. One of their conclusions is that the overstrength factors in low seismicity regions are larger than those of high seismicity regions for structures designed with the same response modification factor. They have reported factors ranging from 2.3 to 8.3

2.2.3.7 Kim and Choi [10]

In this study the overstrength, ductility, and the response modification factors of the 21 special concentric braced steel frames and 9 ordinary concentric braced frames with various stories and span lengths were evaluated by performing pushover analyses. The overstrength factors increased as the structure’s height decreased and the span length increased. In SCBFs, the factors turned out to be 1.9 to 3.2 for a 6m span, 2.4 to 4.1 for an 8m span, and 2.5 to 4.7 for a 10 m span. In OCBFs, factors were found close to 1.5 for all configurations.

2.2.4 NEHRP Provisions

NEHRP Recommended Provisions for Seismic Regulations for New Buildings and Other Structures (Fema 450) - 2003 [51] incorporated the overstrength in design as a component in seismic load effect calculation. The provision is stated as follows:

"Where specifically required by these Provisions, the design seismic force on components sensitive to the effects of structural overstrength shall be as defined by following equations for load combinations in which the effects of gravity are respectively additive with or counteractive to the effect of seismic loads:"

$$E = \Omega_0 \cdot Q_E + 0.2 S_{DS} \cdot D \tag{2.1}$$

$$E = \Omega_0 \cdot Q_E - 0.2 S_{DS} \cdot D \tag{2.2}$$

Where;

E : Effect of horizontal and vertical earthquake induced forces,

Q_E : Effect of horizontal seismic forces

S_{DS}: Design spectral response acceleration parameter at short periods

D : Effect of dead load

Ω_0 : System overstrength factor as given in Table A.1.1 in the appendix section

The term $\Omega_0 . Q_E$ calculated in accordance with Eq. 2.2.1 and 2.2.2 need not exceed the maximum force that can develop in the element as determined by a rational, plastic mechanism analysis or non-linear response analysis utilizing realistic expected values of material strengths.

2.3 DUCTILITY REDUCTION FACTOR

The extent of inelastic deformation experienced by the structural system subjected to a given ground motion or a lateral loading is given by the displacement ductility ratio "μ" (ductility demand) and it is defined as the ratio of maximum absolute relative displacement to its yield displacement.

$$\mu = \frac{u_{\max}}{u_y} \tag{2.3}$$

Displacement ductility ratio is often confused with displacement ductility where displacement ductility is defined as

$$u_{\max} - u_y \tag{2.4}$$

The "ductility reduction factor", in some studies called as "strength reduction factor", (the reduction in strength demand due to post-elastic behavior), $R\mu$, is defined as the ratio of the $Fy(\mu=1)$ (V_E) lateral yield strength required to maintain the system elastic to the $Fy(\mu=\mu_i)$ (V_Y) lateral yield strength required to maintain the displacement ductility ratio μ less or equal to a predetermined target ductility ratio μ_i

$$R\mu = \frac{Fy(\mu = 1)}{Fy(\mu = \mu_i)} \tag{2.5}$$

For a given ground excitation, ductility reduction factor $R\mu$ is defined as a function of the period of the structure, the damping, the type of behavior and the displacement ductility ratio; "Primarily influenced by the period of vibration and the level of inelastic deformation, and to a much lesser degree by the damping and the hysteretic behavior of the system" [11]. Expressed as:

$$R\mu = R\mu(T, \mu_i) \tag{2.6}$$

From the definition of $R\mu$ (Eq. 2.5), it is clear that regardless of the period of the structure or the type of loading applied, for systems behaving elastically (μ_i= 1) the ductility reduction factor must satisfy the condition of:

$$R\mu = R\mu(T, \mu = 1) = 1 \tag{2.7}$$

For very rigid structures where its natural period converges to zero $(T \to 0)$, the structure will not experience any lateral drift relative to the ground but moving synchronously. Thus, for any ground motion, the inelastic strength demand in these systems is the same as the elastic strength demand, so the ductility reduction factor must satisfy the following equation:

$$R\mu = R\mu(T = 0, \mu_i) = 1 \tag{2.8}$$

For very flexible systems $(T \to \infty)$, regardless of the strength of the system, the maximum relative displacement converges to the maximum ground displacement. Therefore, for any ground acceleration the inelastic strength demand $Fy(\mu = \mu_i)$ is equal to the elastic strength demand $Fy(\mu = 1)$ divided by the displacement ductility ratio $\mu = u_{\max} / u_y$ and the strength reduction factor for these systems must satisfy the following equation:

$$R\mu = R\mu(T \to \infty, \mu_i) = \mu \tag{2.9}$$

2.3.1 Previous Studies

In this section, some of the previous studies about ductility reduction factors are reviewed and proposed formulations and plots of Rμ are presented.

2.3.1.1 Newmark and Hall [12]

Based on elastic and inelastic response spectra of the El Centro, California earthquake the authors observed that:

(i) in the high and medium period spectral regions, elastic and inelastic systems have about the same maximum displacement;

(ii) in the extreme low period region, elastic and inelastic systems have the same force;

As a result of their observations authors recommended a procedure to construct inelastic spectra from the elastic spectra as follows:

$$0 \le T < \frac{T_1}{10} \qquad R\mu = 1 \tag{2.10.a}$$

$$\frac{T_1}{10} \le T < \frac{T_1}{4} \qquad R\mu = \sqrt{2\mu - 1}\left[\frac{T_1}{4T}\right]^{2.513\left[\frac{1}{\sqrt{2\mu-1}}\right]} \tag{2.10.b}$$

$$\frac{T_1}{4} \le T < T_1' \qquad R\mu = \sqrt{2\mu - 1} \tag{2.10.c}$$

$$T_1' \le T < T_1 \qquad R\mu = \frac{T \cdot \mu}{T_1} \tag{2.10.d}$$

$$T_1 \le T < T_2 \qquad R\mu = \mu \tag{2.10.e}$$

$$T_1 \le T < 10.0s \qquad R\mu = \mu \tag{2.10.f}$$

Where limiting periods are given by:

$$T_1 = 2\pi \frac{\phi_{ev} V}{\phi_{ea} A} \qquad T_1' = T_1 \frac{\mu}{\sqrt{2\mu - 1}} \qquad T_2 = 2\pi \frac{\phi_{ed} D}{\phi_{ev} V} \tag{2.11}$$

A, V and D are the maximum ground acceleration, velocity and displacement

ϕ_{ea} ϕ_{ev} and ϕ_{ed} are factors applied to give the ordinates of the elastic design spectrum in the acceleration, velocity and displacement spectral regions. Pertinent results are shown on Figure 2.1.a

2.3.1.2 Lai and Biggs [13]

In this study design inelastic response spectra were based on mean inelastic spectra computed for 20 artificial ground motions. Analyses carried on for periods equally spaced between 0.1s and 10s with 50 natural periods. The ductility reduction factors corresponding to the proposed coefficients are given by the Equation 2.12 and plotted on Figure 2.1.b

$$R\mu = \alpha + \beta(\log T) \tag{2.12}$$

Table 2.1: α & β coefficients proposed by authors Lai & Biggs [13]

Period Range	Coefficient	μ=2	μ=3	μ=4	μ=5
0.1 < T < 0.5	α β	1.6791 0.3291	2.2296 0.7296	2.6587 1.0587	3.1107 1.4307
0.5 < T < 0.7	α β	2.0332 1.5055	2.7722 2.5320	3.3700 3.4217	3.8336 3.8323
0.7 < T < 4.0	α β	1.8409 0.2642	2.4823 0.6605	2.9853 0.9380	3.4180 1.1493

2.3.1.3 Riddell and Newmark [14]

This study is based on statistical analysis of inelastic spectra of recorded ground motions, considering ten earthquake ground motions recorded on rock and alluvium sites. In contrast to the Newmark-Hall deamplification factors, in this study the damping ratio μ is also taken into account in forming deamplification factors. The strength reduction factors, Rμ proposed by the Riddell and Newmark procedure are shown on Figure 2.1.c and are defined as:

$$0 \le T < 0.0303s \qquad R\mu = 1 \tag{2.13.a}$$

$$0.0303 \le T < 0.125s \qquad R\mu = (p_a\mu - q_a)^{ra}\left[\frac{1}{8T}\right]^{1.625\log\left[(p_a\mu - q_a)^{-ra}\right]} \tag{2.13.b}$$

$$0.125 \le T < T_1' \qquad R\mu = (p_a\mu - q_a)^{ra} \tag{2.13.c}$$

$$T_1' \le T < T_1 \qquad R\mu = \frac{T}{T_1}(p_v\mu - q_v)^{rv} \tag{2.13.d}$$

$$T_1 \le T < T_2' \qquad R\mu = (p_v\mu - q_v)^{rv} \tag{2.13.e}$$

$$T_2' \le T < T_2 \qquad R\mu = \frac{T}{T_2 p_d \mu^{-rd}} \qquad 1.5 \le \mu < 10 \tag{2.13.f}$$

$$T_2 \le T < 10.0s \qquad R\mu = \frac{1}{p_d \mu^{-rd}} \qquad 1.5 \le \mu < 10 \tag{2.13.g}$$

Where parameters are defined as:

$$p_a = q_a + 1 \qquad q_a = 3\cdot\beta^{-0.3} \qquad r_a = 0.48\cdot\beta^{-0.08} \qquad 2 \le \beta \le 10 \tag{2.14.a}$$

$$p_v = q_v + 1 \qquad q_v = 2.7\cdot\beta^{-0.4} \qquad r_v = 0.66\cdot\beta^{-0.04} \qquad 2 \le \beta \le 10 \tag{2.14.b}$$

$$p_a = 0.87\cdot\beta^{0.055} \qquad r_d = 1.07 \qquad 2 \le \beta \le 10 \tag{2.14.c}$$

Where limiting periods are given by:

$$T_1 = 2\pi\frac{\phi_{ev}V}{\phi_{ea}A} \qquad T_1' = T_1\frac{(p_a\mu - q_a)^{ra}}{(p_v\mu - q_v)^{rv}} \tag{2.15.a}$$

$$T_2 = 2\pi\frac{\phi_{ed}D}{\phi_{ev}V} \qquad T_2' = T_2 p_d \mu^{-rd}\left(p_v\mu - q_v\right)^{rv} \tag{2.15.b}$$

2.3.1.4 Riddell, Hidalgo and Cruz [15]

This study was based on inelastic spectra computed for four different earthquake records using SDOF systems with an elasto-plastic behavior and with 5 percent damping. The ductility reduction factors proposed in this study is set in two period intervals defined as follows also plotted on Figure 2.1.d

$$0 \le T < T^* \qquad R\mu = 1 + \frac{R^* - 1}{T^*} \cdot T \tag{2.16.a}$$

$$T \ge T^* \qquad R\mu = R^* \tag{2.16.b}$$

Table 2.2: R* & T* values proposed by authors Riddell, Hidalgo and Cruz [15]

Parameter	μ=2	μ=3	μ=4	μ=5	μ=6	μ=7	μ=8
R*	2.0	3.0	4.0	5.0	5.6	6.2	6.8
T*	0.1	0.2	0.3	0.4	0.4	0.4	0.4

2.3.1.5 Miranda [16]

In this study, 124 ground motions recorded on rock, alluvium and soft soil conditions belonging to various earthquakes were utilized. Ductility reduction factors were computed for 5% damped bilinear SDOF systems with displacement ductility ratios between 2 and 6. The study also showed that magnitude and distance has insignificant results while soil condition has a major effect on the ductility reduction factor. Here ϕ is a function of soil condition, μ and T. T_g is defined as the predominant period of the motion. Proposed formulation plotted for rock and alluvium sites on Figures 2.2 a,b respectively is as follows:

$$R\mu = \frac{\mu - 1}{\phi} + 1 \ge 1 \tag{2.17}$$

Rock Sites $$\phi = 1 + \frac{1}{10T - \mu T} - \frac{1}{2T}\exp\left[-\frac{3}{2}\left(\ln T - \frac{3}{5}\right)^2\right] \tag{2.18.a}$$

Alluvium Sites $$\phi = 1 + \frac{1}{12T - \mu T} - \frac{2}{5T}\exp\left[-2\left(\ln T - \frac{1}{5}\right)^2\right] \tag{2.18.b}$$

Soft Soil Sites $$\phi = 1 + \frac{T_g}{3T} - \frac{3T_g}{4T}\exp\left[-3\left(\ln\frac{T}{T_g} - \frac{1}{4}\right)^2\right] \tag{2.18.c}$$

2.3.1.6 Nassar and Krawinkler [17]

This study is based on the response of SDOF non-linear systems subjected to 15 ground motions belonging to alluvium and rock sites. The effect of the structural natural period, strain-hardening ratio, yield level and the type of inelastic material behavior to the ductility reduction factor were considered and examined. The resulting formulation defined as follows is also plotted on Fig. 2.1.e

$$R\mu = \left[c\left(\mu - 1\right) + 1 \right]^{1/c} \tag{2.19.a}$$

$$c(T, \alpha) = \frac{T^a}{1 + T^a} + \frac{b}{T} \tag{2.19.b}$$

Table 2.3.3: a & b coefficients per strain-hardening ratio

α	a	b
0.00	1.00	0.42
0.02	1.00	0.37
0.10	0.80	0.29

2.3.1.7 Borzi and Elnashai [18]

Following the definition of ductility reduction factor, regression analyses for the evaluation of the ratio between the elastic and inelastic acceleration spectra (q-factor) were observed in this study. The period dependent behavior factor functions calculated were approximated with a trilinear spectral shape. The formulation is presented in Eq. 2.20 & 2.21 along with coefficient in Table 2.3

$$T < T_1 \qquad q = 1 + (q_1 - 1)\frac{T}{T_1} \tag{2.20.a}$$

$$T_1 < T < T_2 \qquad q = 1 + q_1 + (q_2 - q_1)\frac{T - T_1}{T_2 - T_1} \tag{2.20.b}$$

$$T > T_2 \qquad q = q_2 \tag{2.20.c}$$

Where limiting periods and coefficients are defined as:

$b_{T1} = 0.25 \quad a_{T2} = 0.163 \quad b_{T2} = 0.60$

$$T_1 = b_{T1} \qquad T_2 = a_{T2}\mu + b_{T2} \tag{2.21.a}$$

$$q_1 = a_{q1}\mu + b_{q1} \qquad q_2 = a_{q2}\mu + b_{q2} \tag{2.21.b}$$

Table 2.3: various coefficients according to structures post-yield behavior

		a_{g1}	b_{g1}	a_{g2}	b_{g2}
K_3=0	Elastic Perfectly Plastic	0.55	1.37	1.33	0
K_3=0.1K_y	Hardening Behavior	0.32	1.69	0.96	0.51
K_3=-0.2K_y	Softening Behavior	0.38	1.67	1.24	0
K_3=-0.3K_y	Softening Behavior	0.29	1.83	1.21	0

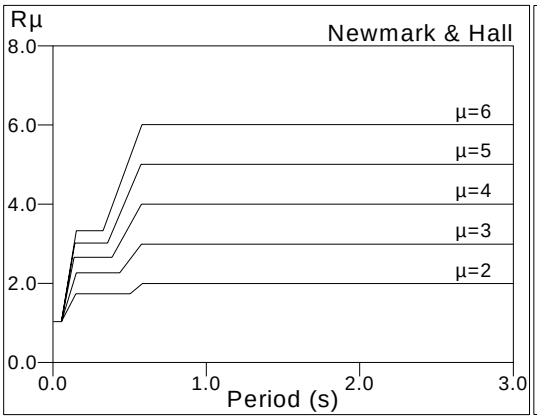

2.1.a

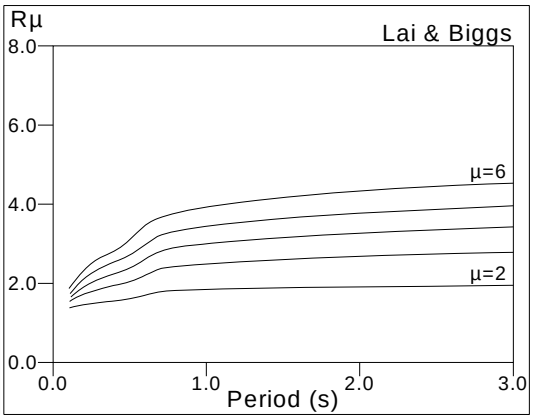

2.1.b

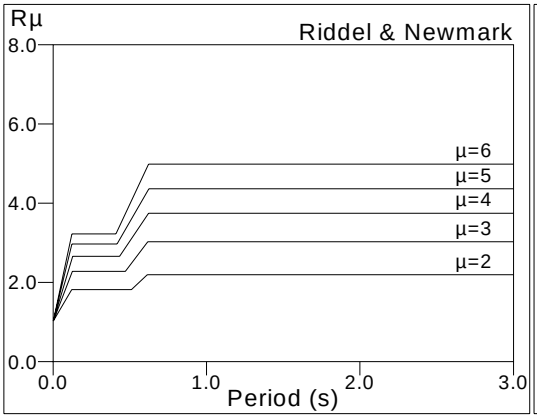

2.1.c

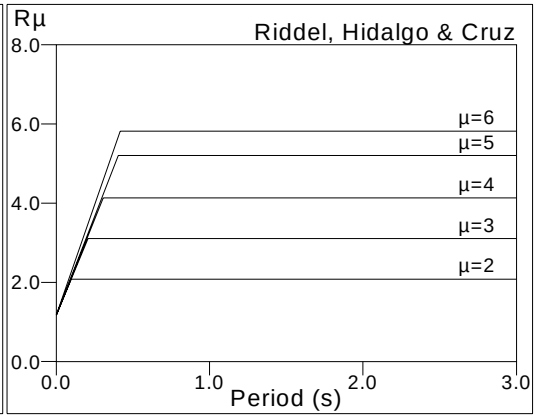

2.1.d

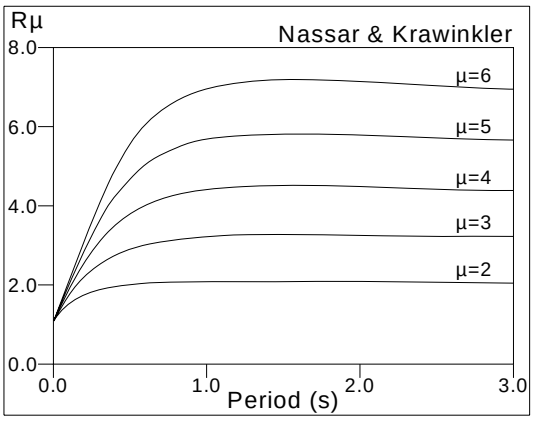

2.1.e

Figure 2.1: Plots of Proposed Ductility Reduction Factors

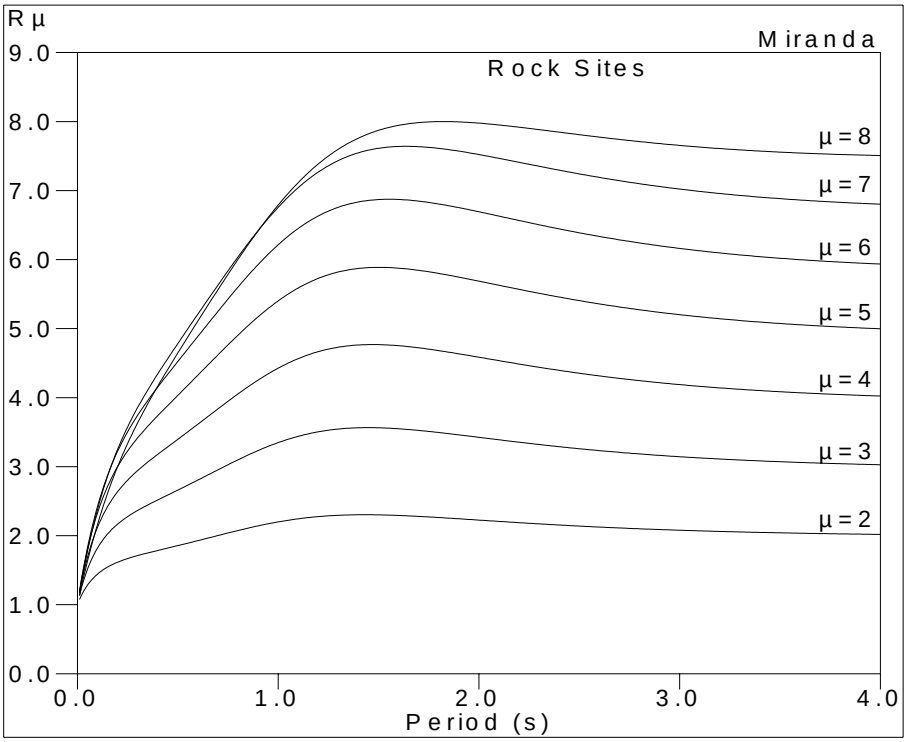

2.2.a

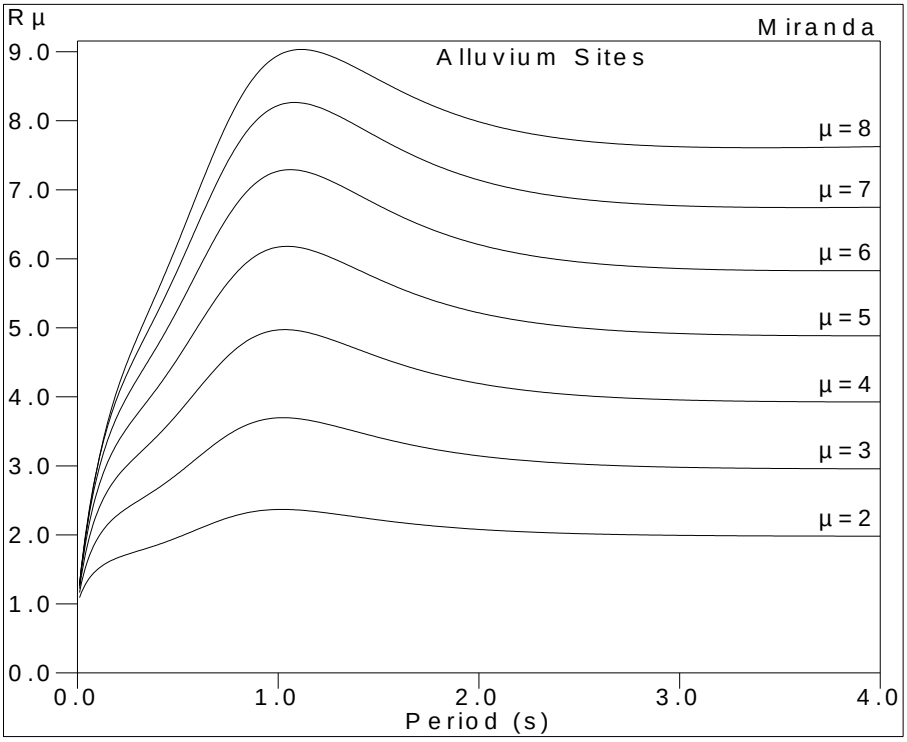

2.2.b

Figure 2.2: Plots of Ductility Reduction Factors Proposed by Miranda [16]

2.4 DAMPING FACTOR

Damping is the general the term used to characterize energy dissipation in a building frame, irrespective of whether the energy is dissipated by hysteretic behavior or by viscous damping [60]. It is an effect, either intentionally created or inherent to a system that tends to reduce the amplitude of oscillations of an oscillatory system, with magnitude proportional to that of the velocity of the system but opposite in direction to the displacement. The decay in the oscillation indicates that energy dissipation is taking place. In structural engineering the cause of this energy dissipation is related to the material internal friction, friction at joints, radiation damping at the supports (vibration waves fading away in the infinite foundation material) or the hysteretic behavior of the system.

Viscous velocity-dependent damping is very difficult to visualize in most real structural systems. In most cases, modal damping ratios are used in the computer model to approximate unknown non-linear energy dissipation within the structure. Another form of damping, referred to as Rayleigh damping, is often used in the mathematical model for the simulation of the dynamic response of a structure; “Rayleigh damping is proportional to the stiffness and mass of the structure. Both modal and Rayleigh damping are used to avoid the need to form a damping matrix based on the physical properties of the real structure” [19].

The damping reduction factors are used in a variety of building codes in order to estimate the elastic response spectrum with higher or lower damping ratios (ξ) from 5% critical damping.

Table 2.4: Comparison of proposed factors in some US codes

	UBC 94 NEHRP 94	UBC 97 IBC2000 NEHRP 97	ATC40		FEMA-273 1997		NEHRP 2000 NEHRP 2003
Damping Ratio	**B**	**B**	**B_S**	**B_1**	**B_S**	**B_1**	**B**
0.02	-	1.25	1.28	1.23	1.25	1.25	1.25
0.05	1.00	1.00	1.00	1.00	1.00	1.00	1.00
0.10	0.84	0.83	0.77	0.83	0.77	0.83	0.83
0.20	0.64	0.67	0.55	0.65	0.56	0.67	0.67
0.30	0.53	0.59	0.42	0.56	0.43	0.59	0.56
0.40	-	0.53	0.33	0.48	0.37	0.53	0.48
0.50	-	0.50	0.26	0.43	0.33	0.50	0.42

In FEMA 273-2003 and ATC40 codes, “B” is given in form of B_S and B_1, where B_S is valid when $T<Ts.B_1/B_S$ and B_1 is valid when $T>Ts.B_1/B_S$ and T_S is the value where constant acceleration and constant velocity regions of the spectrum intersects.

2.4.1 Previous Studies

So far a number of expressions for the damping reduction factor have been proposed; studies based on single degree of freedom systems subjected to various earthquake excitations. Results reported by authors Newmark and Hall [20] have been implemented in the ATC-40 [61], FEMA-273 [52] and IBC 2000 [65] for the displacement-based evaluation design of existing buildings. Results obtained from Ashour [21] were adopted in the UBC-94 [66] and NEHRP 94 [48] for the design of buildings with passive energy dissipation systems. Moreover, results from Ramirez et al. [22], [23] have been implemented in the NEHRP 2000 [50] for the design of buildings with damping systems.

2.4.1.1 Newmark and Hall [20]

The method proposed by authors is the earliest and the best known. The data are limited to the viscous damping ratio of 20%. Their results have been adopted by most design codes and guidelines. In this method, the damping reduction factors (B) for are expressed as:

$$B = \begin{bmatrix} 1514 - 0.321\ln(\xi) \text{ for constant acceleration region} \\ 1514 - 0.321\ln(\xi) \text{ for constant velocity region} \\ 1514 - 0.321\ln(\xi) \text{ for constant displacement region} \end{bmatrix} \quad (2.22)$$

2.4.1.2 Ashour [21]

In his study author developed a relationship that described the decrease in displacement response spectrum for elastic systems with changes in viscous damping. Viscous damping ratios of 0, 2, 5, 10, 20, 30, 50, 75, 100, 125 and 150% were considered. The damping reduction factor is formulated as:

$$B = \sqrt{\frac{0.05(1-e^{-\alpha\xi})}{\xi(1-e^{-0.05\alpha})}} \tag{2.23}$$

where α is a coefficient that was set to be 18 and 65 for the upper and low bound of B. α=18 was adopted by NEHRP 94 [48] for the design of buildings with passive energy dissipation systems.

2.4.1.3 Wu and Hanson [22]

Authors obtained a formulation for damping reduction factor from a statistical study of non-linear response spectra with high damping ratios. Ten earthquake records were used as input ground motions for elasto-plastic SDOF systems with damping ratios between 10% and 50%.

$$B = \frac{\psi(\xi, T)}{\psi(\xi = 5\%, T)} \tag{2.24}$$

$T = 0.1s \qquad \psi = -0.349\ln(0.0959\xi)$

$T = 0.5s \qquad \psi = -0.547\ln(0.417\xi)$

$0.5 < T < 3s \qquad \psi = -0.471\ln(0.524\xi)$

$T = 3.0s \qquad \psi = -0.478\ln(0.475\xi)$

$T = 10.0s \qquad \psi = -0.291\ln(0.0473\xi)$

2.4.1.4 Ramirez et al. [23], [24]

Author derived damping factor data, utilizing ten earthquake histories for linear elastic single degree of freedom systems having damping ratios ranging from 2% to 100%. Resultant damping factors are given in Table 2.5

Table 2.5: Bs & B1 values derived by Ramirez [22],[23]

β	B_S	B_1
2	0.8	0.8
5	1.00	1.00
10	1.20	1.20
20	1.50	1.50
30	1.70	1.70
40	1.90	1.90

β	B_S	B_1
50	2.20	2.20
60	2.30	2.60
70	2.35	2.90
80	2.40	3.30
90	2.45	3.70
100	2.50	4.00

where B_S and B_1 are the damping reduction factors for periods (T) equal to 0.2Ts and Ts, respectively. Ts is defined as the period at the intersection of the constant velocity and constant acceleration regions. Based on this study, a two-parameter model was adopted by the NEHRP 2000 [50] for design of structures with damping systems.

2.4.1.5 Lin and Chang [25]

In their study authors subjected 102 earthquake records to linear elastic SDOF systems with damping ratios between 2%~50% and with periods ranging from 0.01 to 10 s to develop the following expression of period dependent damping factor:

$$B = 1 - \frac{a \cdot T^{0.30}}{(T+1)^{0.65}} \qquad a = 1.303 + 0.436\ln(\xi) \tag{2.25}$$

2.5. REDUNDANCY FACTOR

Redundancy and overstrength are two concepts needed to be distinguished clearly. Redundant is usually defined as: exceeding what is necessary or naturally excessive. The same definition could probably be applied to overstrength, but it will be misleading, because, in the perspective of structural engineering, redundancy does not point to what is unnecessary or excess. A more accurate but indirect definition of redundancy may be given as: In a nonredundant system the failure of a member is equivalent to the failure of the entire system however in a redundant system failure will occur if more than one member fails. Thus the reliability of a system will be a function of the system's redundancy meaning that the reliability depends on whether the system is redundant or nonredundant.

Redundancy in a system may be of the active or standby type. In the case of actively redundant systems, all the members of a system do participate in load carrying; on the other hand for systems with standby redundancies, some of the members are inactive and become active only when some of the active

components fail. Generally in earthquake design redundancy in a structural system is of the active type.

A redundant seismic framing system should be composed of multiple vertical lines of framing, each designed and detailed to transfer seismic-induced inertial forces to the foundation. The multiple lines of framing must be strength and deformation compatible to be capable of good response in a design earthquake. Seismic frames not meeting these conditions should probably not be considered redundant systems [60].

Because of the many unknowns and uncertainties in the magnitude and characteristics of earthquake loading, in the materials and systems of construction for resisting earthquake loadings, and in the methods of analysis, good earthquake engineering practice has been to provide as much redundancy as possible in the seismic-force-resisting system of buildings. In a structural system without redundant components, every component must remain operative to preserve the integrity of the building structure. “On the other hand, in a highly redundant system, one or more redundant components may fail and still leave a structural system that retains its integrity and can continue to resist lateral forces” [59].

2.5.1 Previous Studies

Furuta et al. [26] pointed out the difficulty of defining and quantifying the amount and effect of redundancy on their study who used probabilistic and fuzzy interpretations to review several definitions of structural redundancy. A paper by Frangopol and Curley [27] illustrated how damage studies can be carried out to identify members that are critical to the integrity of a structure. In another paper, Tang and Yao [28] derived a relationship among structural damage, member damage, and redundancy on the basis of expected ultimate strength of structure and a reserve resistance factor. However, most of the definitions of redundancy used in the abovementioned papers in fact refer to what is called overstrength or to an index of the strength reduction due to the failure of individual structural elements.

There is very little research that speaks directly to the merits of redundancy in buildings for seismic resistance. Bonowitz et al. [29] studied the relationships between damage to welded steel moment frame connections and redundancy. While this study found no specific correlation between damage and the number of bays of moment resisting framing per moment frame, it did find increased rates of damage in connections that resisted loads for larger floor areas. Another study by Wood [30] addressed the potential effects of redundancy; evaluating the performance of 165 Chilean concrete buildings ranging in height from 6 to 23 stories. These concrete shear wall buildings with non-ductile details experienced moderately strong shaking with duration of over 60 seconds, yet performed well. One reasonable explanation for this generally good performance stated by the author was the substantial amount of wall area (2 to 4 percent of the floor area) commonly used in Chile. However, this study found no correlation between damage rates and higher redundancy in buildings with wall areas greater than 2 percent.

In his study, Moses [31] stated that safety margins for wind framing system collapse modes depend on the sum of several strength and load variables. Therefore, the reliability of the framing system will be higher than the reliability of individual members. A mean strength reduction factor inversely proportional to the square root of the number of independent strength terms (e.g., plastic hinges in a lateral mechanism) in the redundant wind framing system was proposed. Applying the same logic to seismic framing systems can be illustrated with an example.

Two systems with identical geometry shown in Figure 2.3; first one is composed of one bay of lateral load resisting framing with each beam member capable of developing a plastic moment of 200 units, the second one is composed of two bays of lateral load resisting framing with each beam member capable of developing a plastic moment of 100 units. Non-linear static analysis would produce the same amount of ultimate lateral strength for both systems, however utilizing the methodology proposed by Moses [31] for wind framing systems the

ratio of the nominal moment strength of the beams of first system which have the capability to form 8 plastic hinges to the second system with the capacity of 16 plastic hinges should be:

$$\frac{M_P^1}{M_P^2} = \frac{1/\sqrt{8}}{1/\sqrt{16}} = 1.41$$

To this end it can be stated that the first framing needed to be 41% stronger than the second one in order to achieve a similar level of reliability.

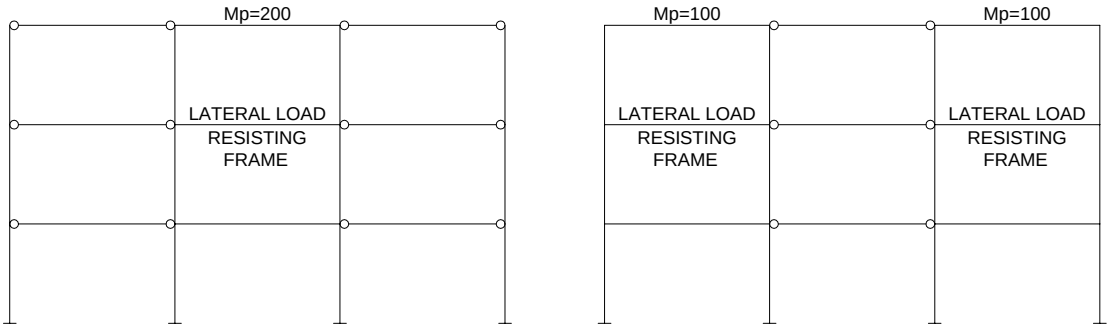

Figure 2.3: Redundancy in Moment Resisting Frames

2.5.2 NEHRP Provisions

NEHRP Recommended Provisions for Seismic Regulations for New Buildings and Other Structures (Fema 450) - 2003 [51] incorporated the redundancy in design as an amplification factor for design forces.

$$E = \rho \cdot Q_E + 0,2S_{DS} \cdot D \tag{2.26}$$

ρ is the redundancy factor given as 1.3 if the following criteria are not satisfied:

1. Systems with braced frames: Removal of an individual brace, or connection thereto, would not result in more than a 33 percent reduction in story strength, nor create an extreme torsional irregularity (plan structural irregularity Type 1b).

2. Systems with moment frames: Loss of moment resistance at the beam to column connections at both ends of a single beam would not result in more than a 33 percent reduction in story strength, nor create an extreme torsional irregularity (plan structural irregularity Type 1b).

3. Systems with shear walls or wall piers: Removal of a shear wall or wall pier with a height to length ratio greater than 1.0 within any story, or collector connections thereto, would not result in more that a 33 percent reduction in story strength, nor create an extreme torsional irregularity.

CHAPTER 3

METHOD OF ANALYSIS

In this chapter the intention is to represent the overall design and evaluation process of the thesis study. Design methodology and non-linear analysis procedure can be followed throughout this chapter along with the properties of the studied framing systems. For the design of the structures and their performance evaluation, analysis of the structure's mathematical model is required. Today's computer processing speed and the available software packages together presents a very powerful toolset for the analyst. In this particular study SAP2000 v9.03 [68] "Integrated software for structural analysis & design" is used for both linear elastic analysis & design and for non-linear static analysis (pushover) for capacity evaluation of the individual systems.

3.1 FRAME TYPES

Different types of steel framing systems are taken into consideration and subjected to the analysis (the un-braced moment resisting frame is both investigated as high ductility and normal ductility). Six frame systems and their variations of 3, 6, 9 stories and 3, 4, 5 bays and in addition to these geometrical variations, 3 different connection types are modeled which were center-line models, partially restrained connections and connections with panel zone deformation are modeled. Thus analysis, design and evaluation process is carried on for a grand sum of 162 structural systems and repeated for two limit states. Frame types are illustrated in Figure 3.1, story & bay variations along with the bracing locations are illustrated in Figure 3.2 (X type bracing is placed for convenience of the illustration.). "B-3-3-PR" is an example for the naming convention which will be used throughout the thesis. First letter denotes the type of framing A,B,C… following numbers denote the bay and story numbers

respectively. The suffix denotes the connection type; center-line models with no special connection have “CL” suffix and partially restrained connections and panel zone deforming connections have “PR” and “PZ” suffixes respectively.

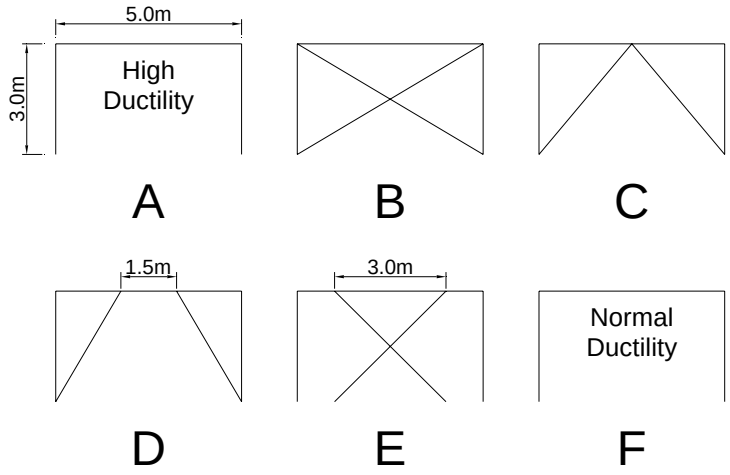

Figure 3.1: Frame Types

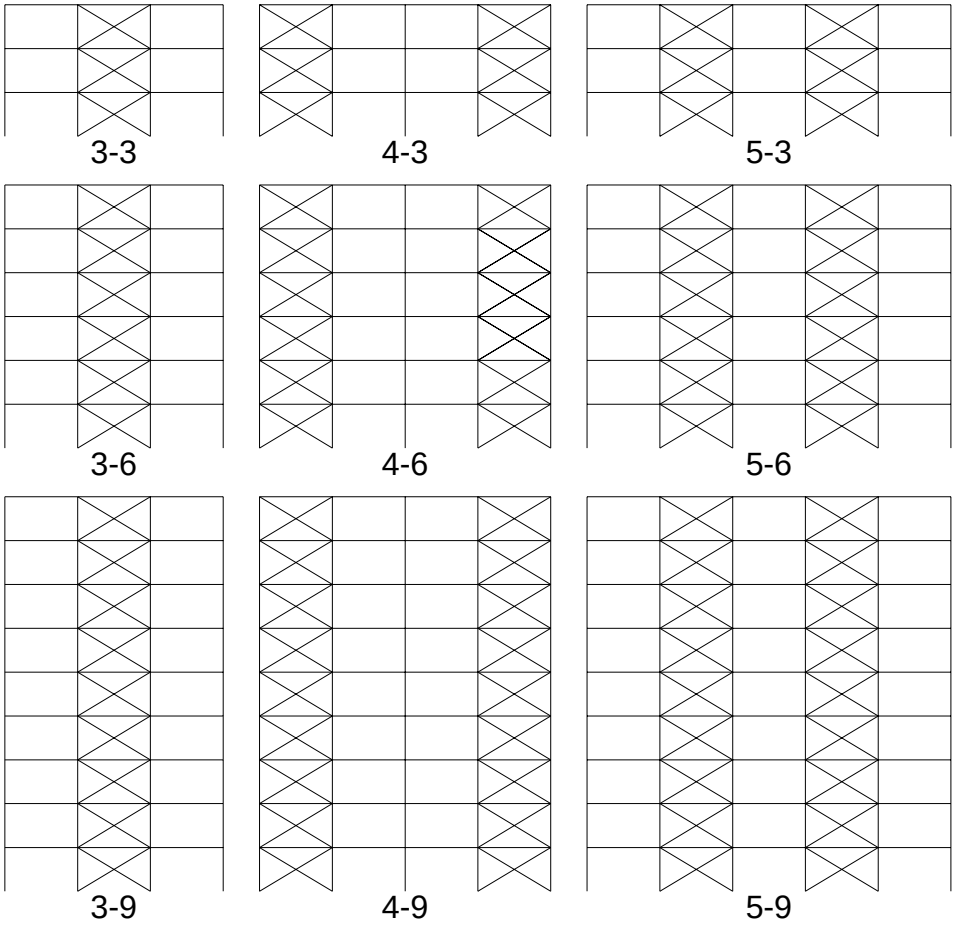

Figure 3.2: Story & Bay variations and Bracing Locations of frames

3.2 FRAME DESIGN

Aforementioned frames are designed according to the Turkish Seismic Code “Afet Bölgelerinde Yapılacak Yapılar Hakkında Yönetmelik” [63] and the steel member design is carried on according to the AISC - Allowable Stress Design [70] in an automated fashion by the software package. The calculation of the equivalent lateral load is based on Turkish seismic code; response spectrum method is utilized to propagate the lateral load which is a more robust procedure than the code based manual operation. Frame member labels are presented in Figures A.2.1 ~ A.2.24 and resultant design sections are presented in Tables A.3.1 ~ A.3.6 in the appendix section.

3.2.1 Equivalent Lateral Load Analysis

According to the Turkish Seismic Code, Total Equivalent Lateral Load (base shear), Vt, acting on the entire building in the earthquake direction considered shall be determined by Eq. 3.1

$$V_t = \frac{W \cdot A(T)}{R_a(T)} \geq 0.10 A_0 \cdot I \cdot W \tag{3.1}$$

The base shear equation consists of three main items which are:

W: Total Seismic Weight of the structure

A(T) : Spectral Acceleration Coefficient

$R_a(T)$: Seismic Load Reduction Factor

Total Seismic Weight of the structure, *W*, shall be calculated by Eq. 3.2 where n is the Live Load Participation Factor given in table 3.1. In this study n is taken as 0.3

$$W = g + n \cdot q \tag{3.2}$$

The Spectral Acceleration Coefficient, *A(T)*, is given by the equation:

$$A(T) = A_0 \cdot I \cdot S(T) \tag{3.3}$$

A_0 is the "Effective Ground Acceleration Coefficient" defined in Table 3.2, in this study Seismic Zone is considered as "1" thus A_0 is taken as 0.40.

I is the "Building Importance Factor", specified in Table 3.3, in this study the structures are considered to be occupied intensively thus the factor is taken as 1.2.

The Spectrum Coefficient, *S(T)*, shall be determined by following equations:

$$\begin{aligned} S(T) &= 1 + 1.5T / T_A \qquad (0 \le T \le T_A) \\ S(T) &= 2.5 \qquad (T_A < T \le T_B) \\ S(T) &= 2.5(T_B / T)^{0.8} \qquad (T > T_B) \end{aligned} \tag{3.4}$$

Spectrum Characteristic Periods, T_A and T_B, are specified in Table 3.4, depending on Local Site Classes defined in Table 3.5 which is dependent on soil groups defined in Table 3.6. In this study Soil group is selected as "Group C" thus Local Site Class is selected as "Z4" and as a result the Characteristic Periods, T_A and T_B, are taken as 0.2 and 0.9 respectively.

Table 3.1: "*n*" Live Load Participation Factor

Purpose of Occupancy of Building	***n***
Depot, warehouse, etc.	**0.80**
School, dormitory, sport facility, cinema, theatre, concert hall, car park, restaurant, shop, etc.	**0.60**
Residence, office, hotel, hospital, etc.	**0.30**

Table 3.2: "A_0" Effective Ground Acceleration Coefficient

Seismic Zone	A_0
1	0.40
2	0.30
3	0.20
4	0.10

Table 3.3: "*I*" Building Importance Factor

Purpose of Occupancy or Type of Building	Importance Factor (I)
1. Buildings to be utilized after the earthquake and buildings containing hazardous materials **a)**Buildings required to be utilized immediately after the earthquake (Hospitals, dispensaries, health wards, fire department buildings and facilities, PTT and other telecommunication facilities, transportation stations and terminals, power generation and distribution facilities; governorate, county and municipality administration buildings, first aid and emergency planning stations) **b)**Buildings containing or storing toxic, explosive and flammable materials, etc.	1.5
2. Intensively and long-term occupied buildings and buildings preserving valuable goods **a)** Schools, other educational buildings and facilities, dormitories and hostels, military barracks, prisons, etc. **b)** Museums	1.4
3. Intensively but short-term occupied buildings Sport facilities, cinema, theatre and concert halls, etc.	1.2
4. Other buildings Buildings other than above defined buildings. (Residential and office buildings, hotels, building-like industrial structures, etc.)	1.0

Table 3.4: Spectrum Characteristic Periods

Local Site Classes	TA (s)	TB (s)
Z1	0.10	0.30
Z2	0.15	0.40
Z3	0.15	0.60
Z4	0.20	0.90

Table 3.5: Local Site Classes

Local Site Class	Soil Group
Z1	**Group (A)** soils **Group (B)** soils with h1 < 15 m
Z2	**Group (B)** soils with h1 > 15 m **Group (C)** soils with h1 < 15 m
Z3	**Group (C)** soils with 15 m < h1 < 50 m **Group (D)** soils with h1 < 10 m
Z4	**Group (C)** soils with h1 > 50 m **Group (D)** soils with h1 > 10 m

Elastic acceleration spectrum may be determined through special investigations by considering local seismic and site conditions. The proposed spectrum by the code is illustrated in Figure 3.3.

Table 3.6: Soil Groups

Soil Group	Description of Soil Group
(A)	**1.** Massive volcanic rocks, un-weathered sound metamorphic rocks, stiff cemented sedimentary rocks **2.** Very dense sand, gravel **3.** Hard clay, silty lay
(B)	**1.** Soft volcanic rocks such as tuff and agglomerate, weathered cemented sedimentary rocks with planes of discontinuity…… **2.** Dense sand, gravel **3.** Very stiff clay, silty clay
(C)	**1.** Highly weathered soft metamorphic rocks and cemented sedimentary rocks with planes of discontinuity **2.** Medium dense sand and gravel **3.** Stiff clay, silty clay
(D)	**1.** Soft, deep alluvial layers with high water table **2.** Loose sand **3.** Soft clay, silty clay

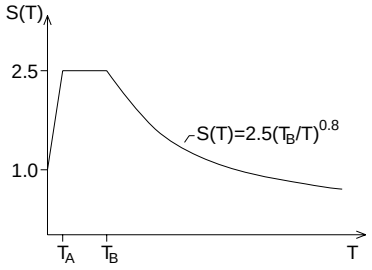

Figure 3.3: Design Acceleration Spectra

Elastic seismic load determined in terms of spectral acceleration coefficient is then divided by the "Seismic Load Reduction Factor" to account for the non-linear behavior of the structural system during earthquake. Seismic Load Reduction Factor, $R_a(T)$, shall be determined by Eq. 3.5 in terms of Structural Behavior Factor, R, given in Table A.1.2 in the appendix section and the natural vibration period T.

$$\begin{aligned} R_a(T) &= 1.5 + (R-1.5)\cdot T/T_A && (0 \le T \le T_A) \\ R_a(T) &= R && (T > T_A) \end{aligned} \qquad (3.5)$$

Code states that (for structures without irregularities) the results obtained from a response spectrum analysis shall be normalized so that the base shear is at least equal to the 90% of the value obtained from an equivalent lateral load analysis.

3.2.2 Gravity Load Analysis

The floor area load values are obtained from the Turkish Code of "Design Loads for Buildings" (TS-498) [71] and converted to uniform span loads with respect to standard 5m span, presented in Table 3.7.

Table 3.7: Gravity Loads

Roof	Floor
$dead = 3\,kN/m^2$	$dead = 4\,kN/m^2$
$snow = 0,75\,kN/m^2$	$wall = 0,8\,kN/m^2$
$wall = 0,2\,kN/m^2$	$live = 5\,kN/m^2$
$live = 2\,kN/m^2$	$g\ (dead + wall) = 4,8\,kN/m^2 \times 5m =$ ***24 kN/m***
$g\ (dead + wall) = 3,2\,kN/m^2 \times 5m =$ ***16 kN/m***	$q\ (live) = 5\,kN/m^2 \times 5m =$ ***25 kN/m***
$q\ (snow + live) = 2,75\,kN/m^2 \times 5m =$ ***13,75 kN/m***	

3.2.3 Sample Design:

Two sample frames are designed to illustrate the process, both are 1 story, 1 bay frames in typical 3m height, 5m span configuration, one is designed as high ductility and the other as normal ductility. Analysis quantities are given in Table 3.8. Geometry and the resultant design sections can be seen in Figure 3.4.

Table 3.8: Sample Frame Analysis Quantities

	Frame Y-1-1	**Frame Z-1-1**	**Description**
Total Weight	W = **167.65 kN**	W = **173.48 kN**	Dead+0.3Live+Self
Acceleration Coefficient	A_0 = **0,4**	A_0 = **0,4**	Seismic Zone 1
Importance Factor	I = **1,2**	I = **1,2**	
Characteristic Periods	T_A = **0,2** T_B = **0,9**	T_A = **0,2** T_B = **0,9**	Foundation Type Z4
Fundamental Period	T = **0,5035**	T = **0,225**	1st Mode
Behavior Factor	R = **5**	R = **8**	Normal, High Ductility Mom. Res. Steel Frame
Seismic Mod. Factor	$R_a(T)$= **5**	$R_a(T)$= **8**	$T_A < T$
Spectrum Coefficient	$S(T)$ = **2,5**	$S(T)$ = **2,5**	$T_A < T < T_B$
Spectral Accel. Coefficient	$A(T)= A_0.I.S(T)$ = **1,2**	$A(T)= A_0.I.S(T)$ = **1,2**	
Base Shear	V_t = **36,21** kN	V_t = **23,42** kN	

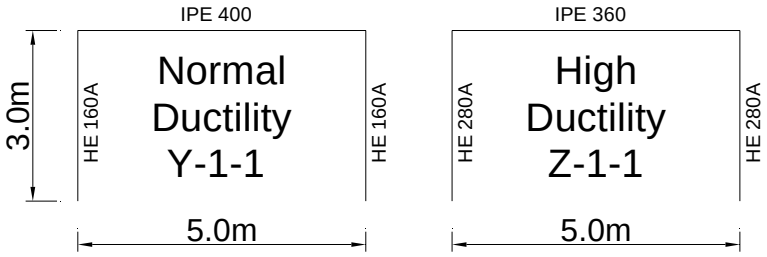

Figure 3.4: Geometry and Sections of the Sample Frames

According to the strong column weak beam design provision, for the high ductility frame Z-1-1 column sections needed to be bigger while normal ductility frame Y-1-1 has a bigger beam section due to weaker columns causing higher moment values at the mid-span. Ductile design permitted the behavior factor to be 8 which is considerably higher when compared to the value of 5 selected for the normal ductility frame. To this end the resultant base shear values differ in favor of the ductile frame as 23.2 kN is 56% lower than the calculated value for normal frame which is 36.2 kN. Non-linear analysis evaluation of these frames can found in section 3.3.6.

3.2.4 Earthquake Zone:

In order to examine the effect of change in seismic zoning, six studied frames have been redesigned for seismic zone 4. Equivalent framing systems are subjected to the same evaluation process with the former “zone 1” systems. 4 bay 9 story systems are chosen for the comparison and are named in a different fashion where equivalent names are given as:

A-4-9 → G-4-1	D-4-9 → G-4-4
B-4-9 → G-4-2	E-4-9 → G-4-5
C-4-9 → G-4-3	F-4-9 → G-4-6

In this part of the study “Effective Ground Acceleration Coefficient” for the G type frames is taken as 0.1. Redesigning the framing sections according to the lowered base shear led to new designs which are mainly governed by gravity actions and lighter by %2.5 than the original ones. Results are given in Table 4.4 - 4.5 and discussed in section 5.1

3.3 NON-LINEAR STATIC ANALYSIS

Non-linear static analysis (pushover analysis), has been developed over the past years and has become a useful analysis procedure for design and performance evaluation purposes. Since the procedure is relatively simple, it does involve certain approximations and simplifications so that some amount of variation is always expected to exist in seismic demand evaluation.

Although, pushover analysis has been shown to capture essential structural response characteristics, the accuracy and the reliability in predicting global and local seismic demands for all structures have been a subject of discussion and improved pushover procedures have been proposed to overcome the certain limitations. However, the improved procedures are mostly computationally demanding and conceptually complex that uses of such procedures are impractical in engineering profession and codes.

The function of the pushover analysis is to evaluate the expected performance of a structural system by estimating its strength and deformation demands in design earthquakes by means of a static inelastic analysis, and comparing these demands to available capacities. Pushover analysis can be viewed as a tool for predicting seismic force and deformation demands, which accounts in an approximate manner for the redistribution of internal forces occurring when the structure is subjected to inertia forces that no longer can be resisted within the elastic range of structural behavior.

In the recent NEHRP guidelines [52], the seismic demands are computed by non-linear static analysis of the structure subjected to monotonically increasing lateral forces with an invariant height-wise distribution until a target displacement is reached. Both the force distribution and target displacement are based on the assumption that the response is controlled by the fundamental mode and that the mode shape remains unchanged which both assumptions are approximate after the structure yields.

With the recent publication of the FEMA-273 [52], FEMA-356 [57] and FEMA-440 [58] documents which include extensive recommendations for the load-deformation modeling of individual elements and for acceptable values of force and deformation parameters for performance evaluation, the non-linear structural analysis procedure has been taken one step further.

3.3.1 Process of Non-linear Static Analysis

A two or three dimensional mathematical model of the structure which includes load-deformation relationship of all members is first created and gravity loads are applied first. A lateral load pattern which is distributed along the building's height is then applied. In this particular study the lateral load pattern is selected as the first mode shape of the structure. The lateral forces are increased in a step by step fashion until a member yields (plastic hinge occurrence). The model is then modified to account for the change in stiffness of yielded member and lateral forces are increased until additional members yield. The process is continued until the control displacement reaches a certain level or structure becomes a mechanism which is unstable. In this particular study the typical end state of the analysis was the mechanism condition as to investigate the full capacity of the system. However in some cases to prevent occurrence of further excrescent results the target displacement is, at most, kept 3% of the total height as the ultimate performance point. The plot of the displacement versus the base shear gives global capacity curve of the structure. In this study displacement is monitored as the mean value of the displacement of the roof nodes.

3.3.2 Force Deformation Relationships

One of the key steps in non-linear analysis is to properly model the force-deformation relationships for individual members. This basic relationship is often represented by concentric plastic hinges assigned to desired locations along the frame members. As it's most probable that the yielding will occur at the ends of the members which are subjected to lateral loads, the plastic hinges are assigned to those locations. Yielding and post-yielding behavior can be modeled as a moment-

rotation curve for flexural yielding (typical for beam members), as a three dimensional axial force – bending moment interaction for column members or as an axial force – axial deformation curve for brace members.

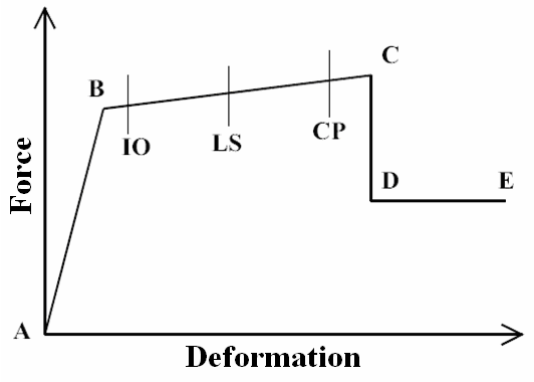

Figure 3.5: Component Force-Deformation Curve

A generic component behavior curve is represented in Figure 3.5. The points marked on the curve are expressed by the software vendor [69] as follows:

- Point A is the origin.
- Point B represents yielding. No deformation occurs in the hinge up to point B, regardless of the deformation value specified for point B. The deformation (rotation) at point B will be subtracted from the deformations at points C, D, and E. Only the plastic deformation beyond point B will be exhibited by the hinge.
- Point C represents the ultimate capacity for pushover analysis. However, a positive slope from C to D may be specified for other purposes.
- Point D represents a residual strength for pushover analysis. How ever, a positive slope from C to D or D to E may be specified for other purposes.
- Point E represents total failure. Beyond point E the hinge will drop load down to point F (not shown) directly below point E on the horizontal axis. If it is not desired that the hinge to fail this way, a large value for the deformation at point E may be specified.

One can specify additional deformation measures at points IO (immediate occupancy), LS (life safety), and CP (collapse prevention). These are informational measures that are reported in the analysis results and used for performance-based design. They do not have any effect on the behavior of the structure.

Prior to reaching point B, all deformation is linear and occurs in the Frame element itself, not the hinge. Plastic deformation beyond point B occurs in the hinge in addition to any elastic deformation that may occur in the element. When the hinge unloads elastically, it does so with out any plastic deformation, i.e., parallel to slope A-B.

The force - deformation curve of a member, for structural modeling purposes, in FEMA-356 [57] is shown in the Figure 3.6 and proposal for the parameters a, b, c are given in the Table A.4.1 in the appendix section. The highlighted rows in tables indicate the selected parameters to model the behavior curve in this particular study.

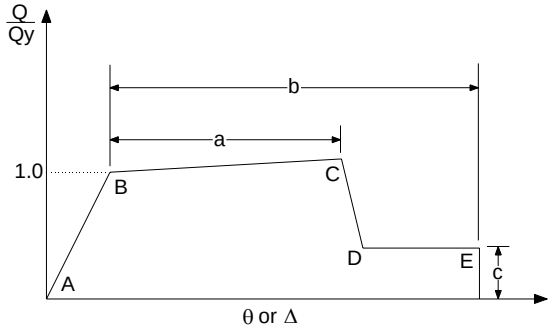

Figure 3.6: Component Force-Deformation Curve as given in FEMA-356 [57]

Following equations are given in FEMA-356 [57], to calculate the yield moment and yield rotation of steel beams and columns.

Beams: $\theta_y = \dfrac{Z \cdot F_{ye} \cdot l_b}{6EI_b}$ $\qquad M_y = Z \cdot F_{ye}$ (3.6)

Columns: $\theta_y = \dfrac{Z \cdot F_{ye} \cdot l_c}{6EI_c}\left(1 - \dfrac{P}{P_{ye}}\right)$ $\qquad M_y = 1.18 \cdot Z \cdot F_{ye}\left(1 - \dfrac{P}{P_{ye}}\right) \le Z \cdot F_{ye}$ (3.7)

where, θ_y : Yield Rotation

M_y : Yield Moment

F_{ye} : Yield strength of steel

Z : Plastic section modulus

l_b : Beam length

l_c : Column length

E : Modulus of elasticity

I_b : Moment of inertia of beam with respect to the bending axis

I_c : Moment of inertia of Column with respect to the bending axis

P : Axial force in the member

P_{ye}: Expected axial yield force of the member ($A_g F_{ye}$)

The idealized force deformation curves are derived from the "backbone curves" which are also fundamentally derived from experimental data of a hysteretic behavior of a member. A schematic representation of how a plastic hinge model data can be acquired is shown in Figures 3.7 and 3.8. In Figure 3.8 the behavior is also classified as ductile, semi-ductile and brittle where it is apparent that the post-yield performance determines the characteristics.

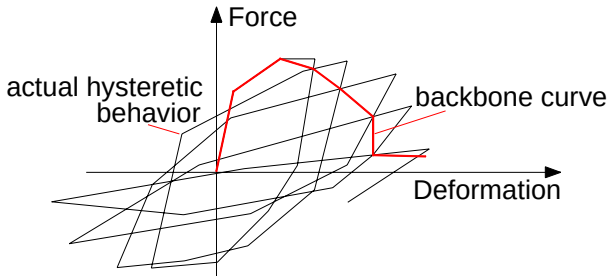

Figure 3.7: Actual Hysteretic Behavior and its Backbone

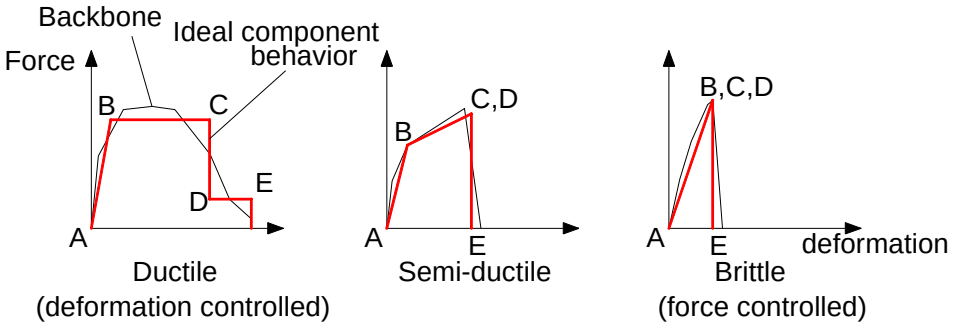

Figure 3.8: Backbone Curves Further Idealized as Component Behavior Curves

First curve in Figure 3.8 is of a typical ductile behavior. It is characterized by an elastic range (point A to point B on the curve), followed by a plastic range (points B to E) that may include strain hardening or softening (points B to C), and a strength-degraded range (points C to D) in which the residual force that can be resisted is significantly less than the ultimate strength, but still substantial. Component actions exhibiting this behavior are considered deformation-controlled.

The second curve is representative of another type of ductile behavior. It is characterized by an elastic range and a plastic range, followed by a quick and complete loss of strength. If the plastic range is sufficiently large (2 times the elastic deformation range), this behavior is categorized as deformation-controlled otherwise it is categorized as force-controlled.

The third curve presented in figure 3.8 is showing a brittle (or non-ductile) behavior. It is characterized just by an elastic range, followed by a complete loss of strength. Components displaying this behavior are always categorized as force-controlled.

3.3.2.1 Beam & Column Members

Steel moment frames develop their seismic resistance through bending of steel beams and columns, and moment-resisting beam-column connections. Such frame connections are designed to develop moment resistance at the joint between the beam and the column. To this end, the behavior of steel moment-resisting frames is generally dependent on connection configuration and detailing. In FEMA-356 [57] various connection types are identified as fully-restrained or partially restrained, presented in Table A.4.2 in the appendix section.

Along with the limits of web and flange slenderness, FEMA-356 [57] classified the beam & column members' behavior (Table A.4.1); in this particular study, selected IPE sections for beams and HE sections for columns are within the limits of web & flange slenderness as shown in the Table 3.9. Thus alteration is not needed for the provided parameters; highlighted values presented in Tables A.4.1 are used to construct the force deformation curves of beams & columns.

For beam and column sections pertinent ratios are smaller than the limits. $\left(F_{ye} = 36kips\right)$

$$Beam: \quad bf/2tf \le \frac{52}{\sqrt{F_{ye}}} = 8,67 \qquad h/tw \le \frac{418}{\sqrt{F_{ye}}} = 69,67$$

$$Column: \quad bf/2tf \le \frac{65}{\sqrt{F_{ye}}} = 10,83 \quad h/tw \le \frac{640}{\sqrt{F_{ye}}} = 106,67$$

Table 3.9: Beam & Column Member Local Slenderness Ratios

Units in (m)	Outside Height	Web Height (*h*)	Flange Width (*bf*)	Flange Thick. (*tf*)	Web Thick. (*tw*)	$bf/2tf$	h/tw
IPE400	0,40	0,3730	0,18	0,0135	0,0086	6,67	43,37
IPE450	0,45	0,4208	0,19	0,0146	0,0094	6,51	44,77
IPE500	0,50	0,4680	0,20	0,0160	0,0102	6,25	45,88
IPE550	0,55	0,5156	0,21	0,0172	0,0111	6,10	46,45
HE200-A	0,19	0,170	0,20	0,010	0,0065	10,00	26,15
HE220-A	0,21	0,188	0,22	0,011	0,0070	10,00	26,86
HE280-A	0,27	0,244	0,28	0,013	0,0080	10,77	30,50
HE300-A	0,29	0,262	0,30	0,014	0,0085	10,71	30,82
HE340-A	0,33	0,297	0,30	0,0165	0,0095	9,09	31,26
HE360-A	0,35	0,315	0,30	0,0175	0,0100	8,57	31,50
HE400-A	0,39	0,352	0,30	0,0190	0,0110	7,89	32,00
HE450-A	0,44	0,398	0,30	0,0210	0,0115	7,14	34,61
HE500-A	0,49	0,444	0,30	0,0230	0,0120	6,52	37,00

Beam and column sectional properties and corresponding yield rotation, yield moment and yield axial force values calculated according to equations 3.6 & 3.7 are presented in Table 3.10. These cross-sectional properties form a basis to the construction of behavior curves. With a 3% strain-hardening ratio the basic force – deformation curve constructed with selected parameters from Table A.4.1 is plotted in figure 3.9. Derived data for beam and column sections are presented in Tables 3.11-3.12 and plotted in Figures 3.10, 3.11 & 3.12 respectively.

Table 3.10: Beam, Column Sectional Properties & Yield Quantities

L = Length of Member A = Cross-section Area Z = Plastic Modulus I = Moment of Inertia Θy = Yield Rotation My = Yield Moment Py = Yield Axial Force				HE200-A
E = $2e^8$ kNm^2				L = 3,0 m A = 0,005380 m^2 Z = 0,000429 m^3 I = 0,000037 m^4 Θy = 0,0068 rad My = 100,97 kNm Py = 1266,24 kN
Fy = 235360 kN/m^2				
HE220-A	HE280-A	HE300-A	HE340-A	
L = 3,0 m A = 0,006430 m^2 Z = 0,000568 m^3 I = 0,000054 m^4 Θy = 0,0062 rad My = 133,68 kNm Py = 1513,36 kN	L = 3,0 m A = 0,009730 m^2 Z = 0,001112 m^3 I = 0,000137 m^4 Θy = 0,0048 rad My = 261,72 kNm Py = 2290,05 kN	L = 3,0 m A = 0,011300 m^2 Z = 0,001383 m^3 I = 0,000183 m^4 Θy = 0,0045 rad My = 325,50 kNm Py = 2659,57 kN	L = 3,0 m A = 0,013300 m^2 Z = 0,001850 m^3 I = 0,000277 m^4 Θy = 0,0039 rad My = 435,42 kNm Py = 3130,29 kN	
HE360-A	HE400-A	HE450-A	HE500-A	
L = 3,0 m A = 0,014300 m^2 Z = 0,002088 m^3 I = 0,000331 m^4 Θy = 0,0037 rad My = 491,43 kNm Py = 3365,65 kN	L = 3,0 m A = 0,015900 m^2 Z = 0,002562 m^3 I = 0,000451 m^4 Θy = 0,0033 rad My = 602,99 kNm Py = 3742,22 kN	L = 3,0 m A = 0,017800 m^2 Z = 0,003216 m^3 I = 0,000637 m^4 Θy = 0,0030 rad My = 756,92 kNm Py = 4189,41 kN	L = 3,0 m A = 0,019800 m^2 Z = 0,003949 m^3 I = 0,000870 m^4 Θy = 0,0027 rad My = 929,44 kNm Py = 4660,13 kN	
IPE 400	IPE 450	IPE 500	IPE 50	
L = 5,0 m Z = 0,001307 m^3 I = 0,000231 m^4 Θy = 0,0055 rad My = 307,62 kNm	L = 5,0 m Z = 0,001702 m^3 I = 0,000337 m^4 Θy = 0,0050 rad My = 400,58 kNm	L = 5,0 m Z = 0,002194 m^3 I = 0,000482 m^4 Θy = 0,0045 rad My = 516,38 kNm	L = 5,0 m Z = 0,002787 m^3 I = 0,000671 m^4 Θy = 0,0041 rad My = 655,95 kNm	

Table 3.11: Moment – Plastic Rotation Data for Beam Members

Plastic Mom. Rot.		**IPE 400**		**IPE 450**		**IPE 500**		**IPE 550**	
		Mp	Θp	Mp	Θp	Mp	Θp	Mp	Θp
M/Mp	Θ/Θp	307,616	0,0055	400,583	0,0049	516,380	0,0045	655,948	0,0041
-0,6	-11	-184,569	-0,0610	-240,350	-0,0544	-309,828	-0,0491	-393,569	-0,0448
-0,6	-9	-184,569	-0,0499	-240,350	-0,0445	-309,828	-0,0402	-393,569	-0,0366
-1,27	-9	-390,672	-0,0499	-508,740	-0,0445	-655,802	-0,0402	-833,054	-0,0366
-1	0	-307,616	0	-400,583	0	-516,380	0	-655,948	0
0	0	0	0	0	0	0	0	0	0
1	0	307,616	0	400,583	0	516,380	0	655,948	0
1,27	9	390,672	0,0499	508,740	0,0445	655,802	0,0402	833,054	0,0366
0,6	9	184,569	0,0499	240,350	0,0445	309,828	0,0402	393,569	0,0366
0,6	11	184,569	0,0610	240,350	0,0544	309,828	0,0491	393,569	0,0448

Table 3.12: Force – Deformation Data for Column Members

HE 200			HE 220			HE 280		
My	Py	Θy	My	Py	Θy	My	Py	Θy
100,97	1266,24	0,01	133,68	1513,36	0,0062	261,72	2290,05	0,0048
-60,58	-759,74	-0,0752	-80,21	-908,02	-0,0680	-157,03	-1374,03	-0,0527
-60,58	-759,74	-0,0615	-80,21	-908,02	-0,0556	-157,03	-1374,03	-0,0431
-128,23	-1608,12	-0,0615	-169,78	-1921,97	-0,0556	-332,38	-2908,37	-0,0431
-100,97	-1266,24	0,0000	-133,68	-1513,36	0	-261,72	-2290,05	0
0,00	0,00	0,0000	0,00	0,00	0	0,00	0,00	0
100,97	1266,24	0,0000	133,68	1513,36	0	261,72	2290,05	0
128,23	1608,12	0,0615	169,78	1921,97	0,0556	332,38	2908,37	0,0431
60,58	759,74	0,0615	80,21	908,02	0,0556	157,03	1374,03	0,0431
60,58	759,74	0,0752	80,21	908,02	0,0680	157,03	1374,03	0,0527
HE 300			**HE 340**			**HE 360**		
My	Py	Θy	My	Py	Θy	My	Py	Θy
325,50	2659,57	0,00	435,42	3130,29	0,0039	491,43	3365,65	0,0037
-195,30	-1595,74	-0,0490	-261,25	-1878,17	-0,0432	-294,86	-2019,39	-0,0409
-195,30	-1595,74	-0,0401	-261,25	-1878,17	-0,0354	-294,86	-2019,39	-0,0334
-413,39	-3377,65	-0,0401	-552,98	-3975,47	-0,0354	-624,12	-4274,37	-0,0334
-325,50	-2659,57	0,0000	-435,42	-3130,29	0	-491,43	-3365,65	0
0,00	0,00	0,0000	0,00	0,00	0	0,00	0,00	0
325,50	2659,57	0,0000	435,42	3130,29	0	491,43	3365,65	0
413,39	3377,65	0,0401	552,98	3975,47	0,0354	624,12	4274,37	0,0334
195,30	1595,74	0,0401	261,25	1878,17	0,0354	294,86	2019,39	0,0334
195,30	1595,74	0,0490	261,25	1878,17	0,0432	294,86	2019,39	0,0409
HE 400			**HE 450**			**HE 500**		
My	Py	Θy	My	Py	Θy	My	Py	Θy
602,99	3742,22	0,0033	756,92	4189,41	0,0030	929,44	4660,13	0,0027
-361,80	-2245,33	-0,0368	-454,15	-2513,64	-0,0327	-557,66	-2796,08	-0,0294
-361,80	-2245,33	-0,0301	-454,15	-2513,64	-0,0267	-557,66	-2796,08	-0,0241
-765,80	-4752,62	-0,0301	-961,29	-5320,55	-0,0267	-1180,38	-5918,36	-0,0241
-602,99	-3742,22	0	-756,92	-4189,41	0	-929,44	-4660,13	0,0000
0,00	0,00	0	0,00	0,00	0	0,00	0,00	0,0000
602,99	3742,22	0	756,92	4189,41	0	929,44	4660,13	0,0000
765,80	4752,62	0,0301	961,29	5320,55	0,0267	1180,38	5918,36	0,0241
361,80	2245,33	0,0301	454,15	2513,64	0,0267	557,66	2796,08	0,0241
361,80	2245,33	0,0368	454,15	2513,64	0,0327	557,66	2796,08	0,0294

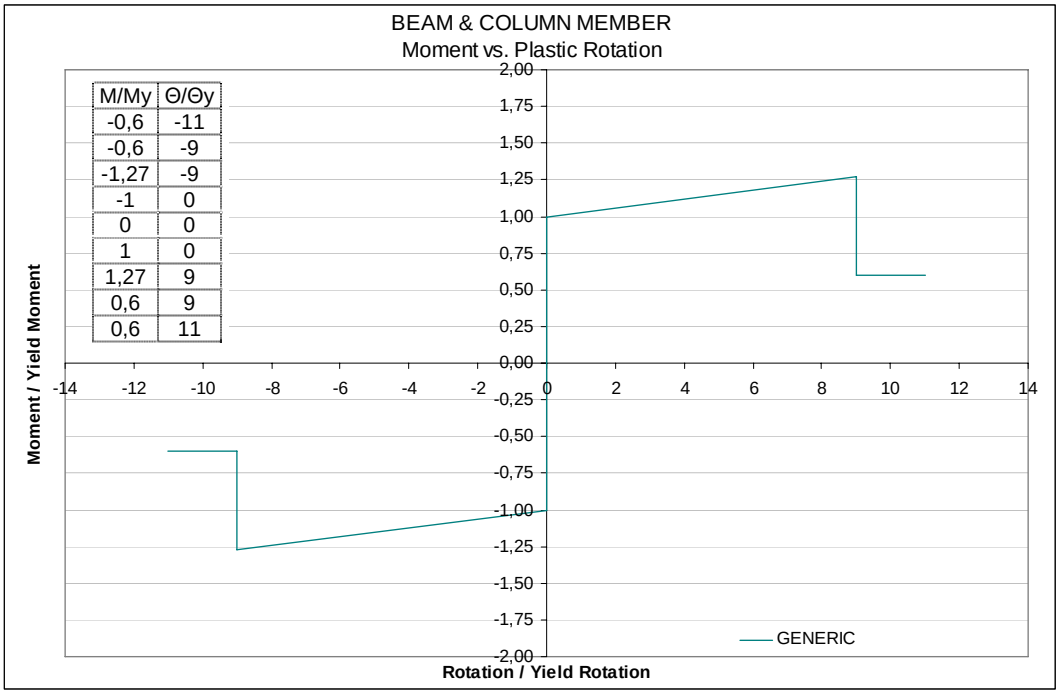

Figure 3.9: Basic Force – Deformation Curve for Beam & Column Members

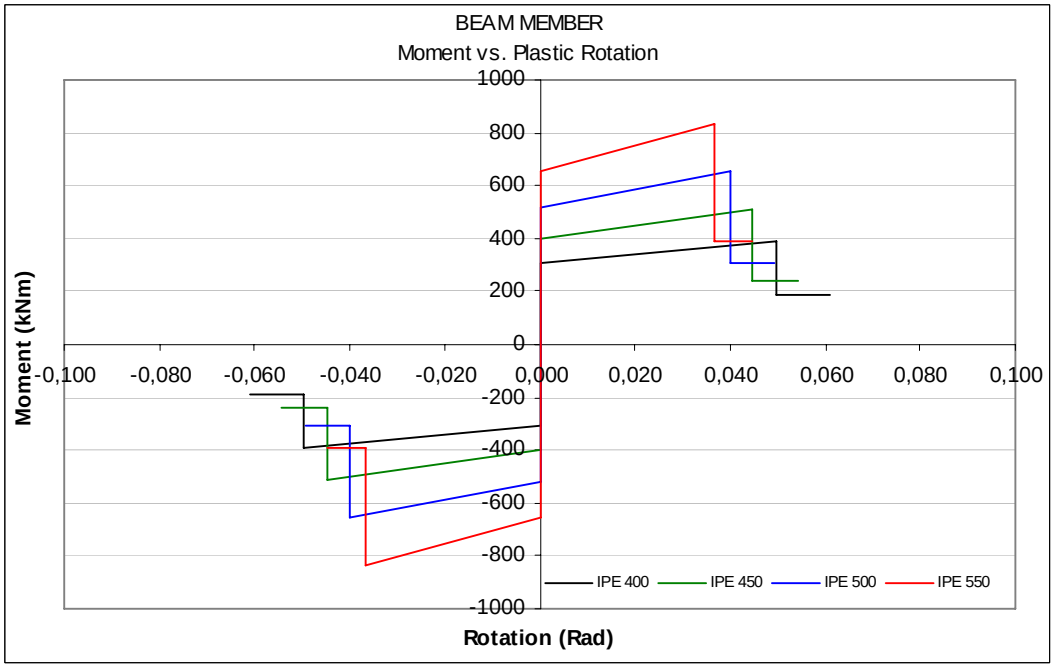

Figure 3.10: Moment – Plastic Rotation Curve for Beam Members

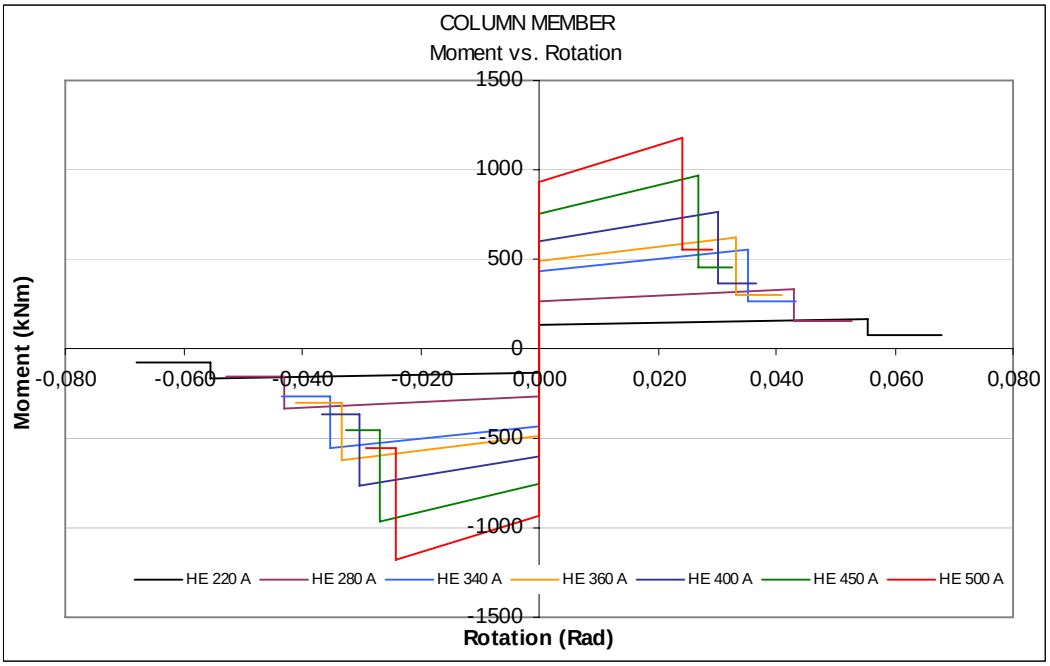

Figure 3.11: Moment – Plastic Rotation Curve for Column Members

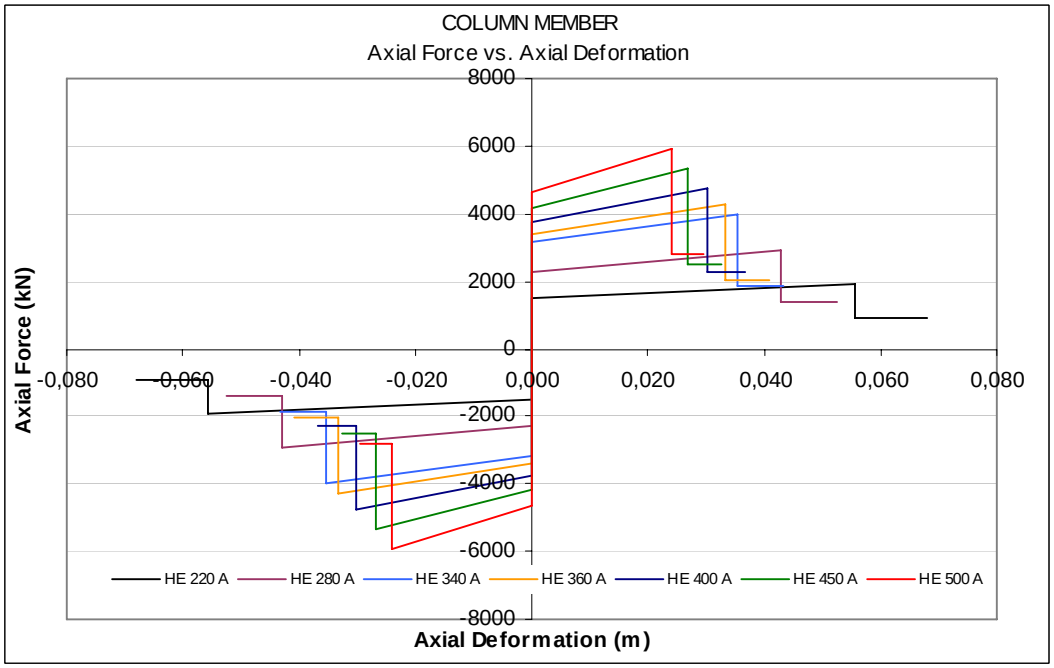

Figure 3.12: Axial Force – Axial Deformation Curve for Column Members

3.3.2.2 Bracing Members

Steel braces are defined as those frame members that develop seismic resistance primarily through axial forces. Braced frames act as vertical trusses where the columns are the chords and the beams and braces are the web members.

Concentric braced frames are very efficient structural systems in steel for resisting lateral forces due to wind or earthquakes because they provide complete truss action. However this framing system is not considered as ductile in design practice for earthquake resistance. The non-ductile behavior of these structures mainly results from early cracking and fracture of bracing members or connections during large cyclic deformations in the post-buckling range. The reason lies in the code philosophy. Instead of requiring the bracing members and their connections to withstand cyclic post-buckling deformations without premature failures (i.e., supply adequate ductility), the codes generally specify increased lateral design forces [53].

Numerous experimental studies have been performed on the inelastic cyclic response of bracing members for concentrically braced steel frames, valuable information and results can be found in references [32] through [39]. These studies showed that bracing members typically show nonsymmetrical hysteretic behavior, with a degradation of their strength in compression and increase in permanent deformation in tension. Also, their energy dissipation capacity generally increases when the brace slenderness is reduced.

Brace slenderness can be reduced by adopting an X-bracing configuration. Theoretical and experimental studies by Picard and Beaulieu [40], [41] showed that the tension acting brace can provide an efficient support at the brace intersecting point for the compression brace. For symmetrical bracing configuration, an effective length factor, K, of 0.5 was recommended for pin-ended braces, both for in-plane and out-of-plane buckling.

A typical force versus axial deformation response of a steel brace is shown in Figure 3.13. For this brace the residual force was about 20% of the buckling load, a percentage that is about the same for many brace configurations.

In this study for both concentric and eccentric structural systems, axial plastic hinges are placed at the mid-length of the brace elements which are modeled to represent the buckling action under compression.

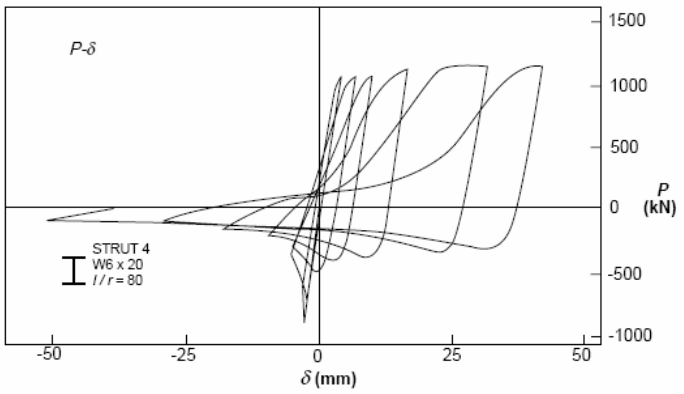

Figure 3.13: Hysteretic Behavior of a Bracing Member

Eccentric braced frames shall be defined as braced frames where component axes do not intersect at a single point and the eccentricity exceeds the width of the smallest member at the joint. The section between these points is defined as the link component with a span equal to the eccentricity. For a short link, energy is dissipated primarily through inelastic shearing of the link web on the other hand for a long link, the energy is dissipated primarily through flexural yielding at the ends of the link. The shear yielding energy dissipation mechanism is more efficient than the flexural plastic hinging mechanism. [53] In this particular study it's assumed that the link component is detailed as to prevent occurrence of any shear hinges; eccentric braced frames are modeled to develop flexural hinges in the neighborhood of the link element as well as beam-column connections.

Brace member sectional properties and corresponding axial yield force and deformation, values calculated according to Equation 3.8, buckling strength of

steel braces under axial compression are calculated in accordance with AISC - LRFD Specifications. Calculated data are presented in Table 3.13 and plotted in Figures 3.15 ~ 3.18. A basic force – deformation curve constructed with selected parameters from Table A.4.1 is plotted in figure 3.14. Derived data for brace sections are presented in Tables 3.14 and plotted in Figures 3.15 ~ 3.18.

Braces: $P_y = F_{ye} \cdot A \qquad \Delta_y = \frac{P_y \cdot l_{br}}{E \cdot A}$ (3.8)

where, Δ_y : Yield Deformation P_y : Yield Axial Force

F_{ye} : Yield strength of steel l_{br} : Brace length

E : Modulus of elasticity A : Cross-sectional Area

Table 3.13: Bracing Member Sectional Properties & Yield-Buckling Quantities

	TUBE 120 B	**TUBE 140 B**	**TUBE 160 B**	**TUBE 180 B**	
L=	5,831	5,831	5,831	5,831	m
I=	8,947E-06	1,473E-05	2,260E-05	3,287E-05	kNm2
A=	0,0044	0,0052	0,006	0,0068	m2
Pty=	1035,584	1223,872	1412,16	1600,448	kN
Dty=	6,862E-03	6,862E-03	6,862E-03	6,862E-03	m
Pcy=	450	685	925	1165	kN
Dcy=	2,982E-03	3,841E-03	4,495E-03	4,995E-03	m
	TUBE 120 C	**TUBE 140 C**	**TUBE 160 C**	**TUBE 180 C**	
L=	3,9051	3,9051	3,9051	3,9051	m
I=	8,947E-06	1,473E-05	2,260E-05	3,287E-05	kNm2
A=	0,0044	0,0052	0,006	0,0068	m2
Pty=	1035,584	1223,872	1412,16	1600,448	kN
Dty=	4,596E-03	4,596E-03	4,596E-03	4,596E-03	m
Pcy=	736	972	1204	1428	kN
Dcy=	3,266E-03	3,650E-03	3,918E-03	4,100E-03	m
	TUBE 120 D	**TUBE 140 D**	**TUBE 160 D**	**TUBE 180 D**	
L=	3,4731	3,4731	3,4731	3,4731	m
I=	8,947E-06	1,473E-05	2,260E-05	3,287E-05	kNm2
A=	0,0044	0,0052	0,006	0,0068	m2
Pty=	1035,584	1223,872	1412,16	1600,448	kN
Dty=	4,087E-03	4,087E-03	4,087E-03	4,087E-03	m
Pcy=	798	1030	1259	1479	kN
Dcy=	3,149E-03	3,440E-03	3,644E-03	3,777E-03	m
	TUBE 120 E	**TUBE 140 E**	**TUBE 160 E**	**TUBE 180 E**	
L=	4,2426	4,2426	4,2426	4,2426	m
I=	8,947E-06	1,473E-05	2,260E-05	3,287E-05	kNm2
A=	0,0044	0,0052	0,006	0,0068	m2
Pty=	1035,584	1223,872	1412,16	1600,448	kN
Dty=	4,993E-03	4,993E-03	4,993E-03	4,993E-03	m
Pcy=	685	924	1157	1388	kN
Dcy=	3,302E-03	3,769E-03	4,091E-03	4,330E-03	m

L=Length of Member I =Moment of Inertia A=Cross-section Area

Pty=Tension Yield Force Dty = Tension Yield Deformation Pcy= Buckling Force

Dcy = Buckling Deformation Fy = 235360 kN/m^2 E = $2e^8$ kNm^2

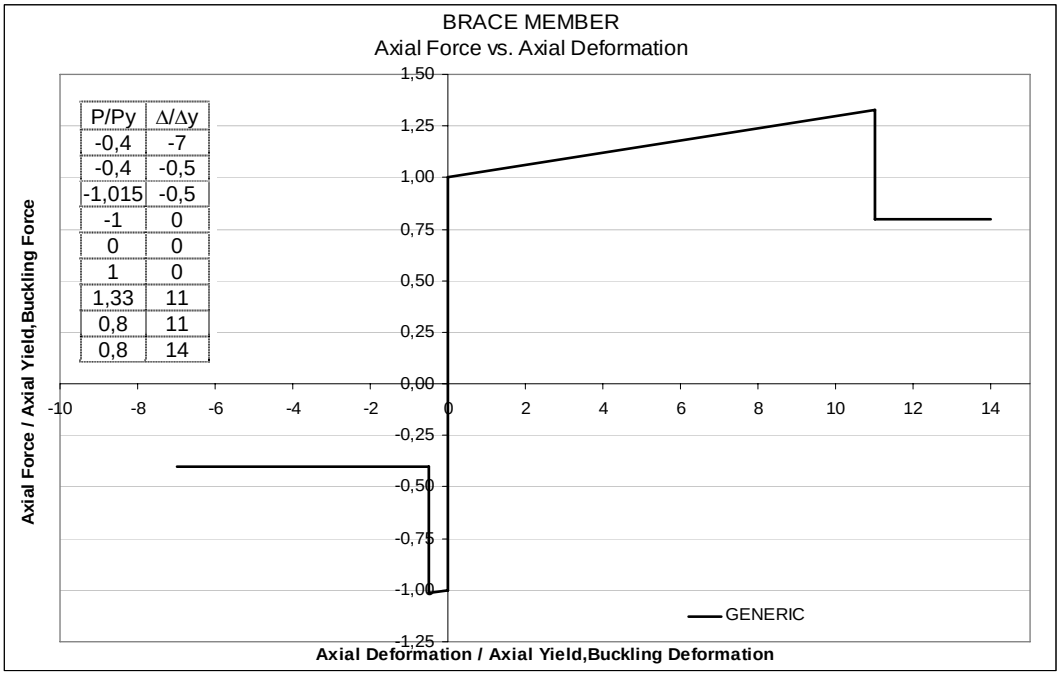

Figure 3.14: Basic Force – Deformation Curve for Bracing Members

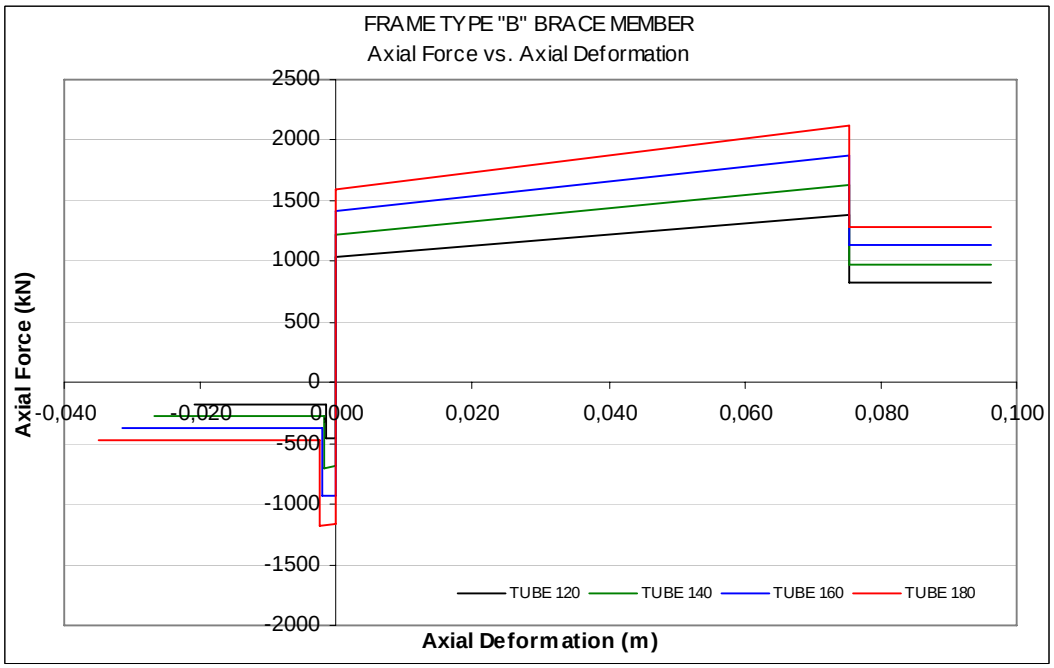

Figure 3.15: Axial Force – Axial Deformation Curve for Type “B” Bracing

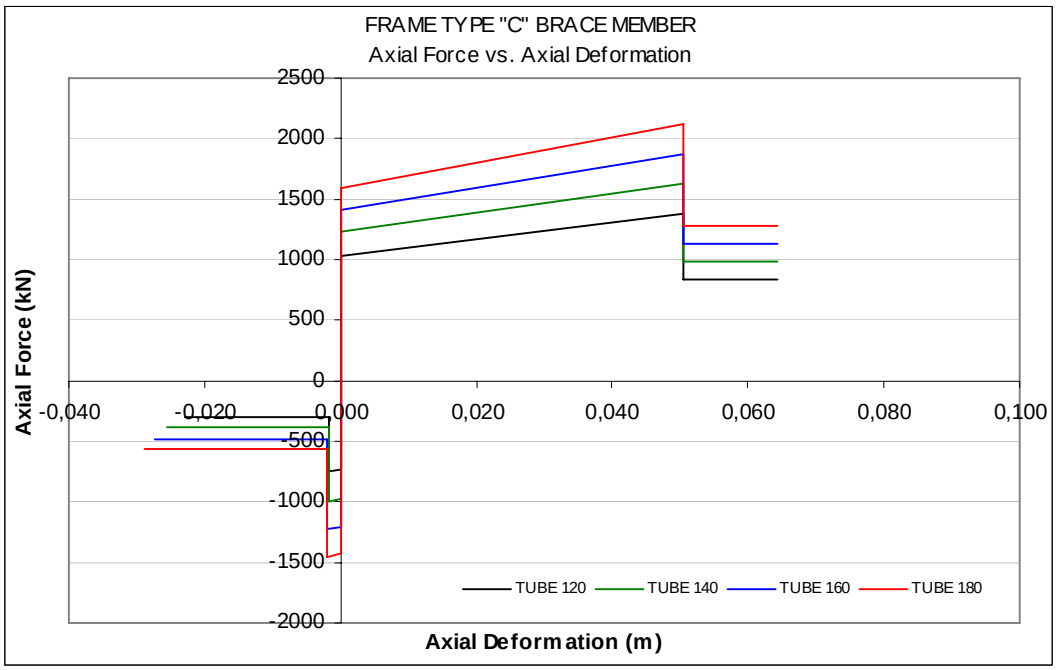

Figure 3.16: Axial Force – Axial Deformation Curve for Type “C” Bracing

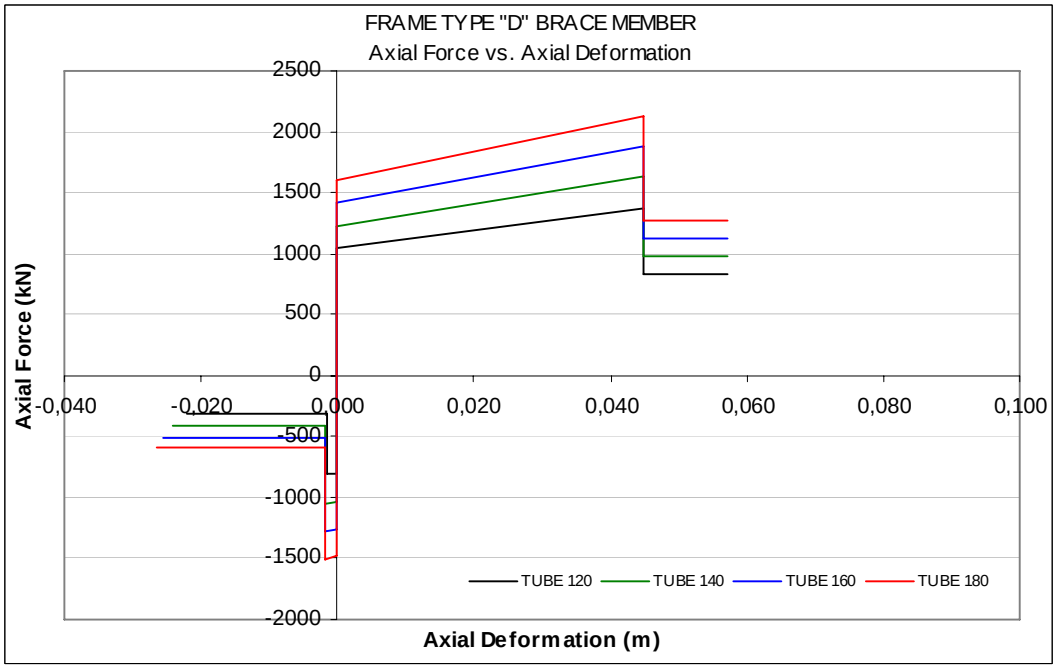

Figure 3.17: Axial Force – Axial Deformation Curve for Type “D” Bracing

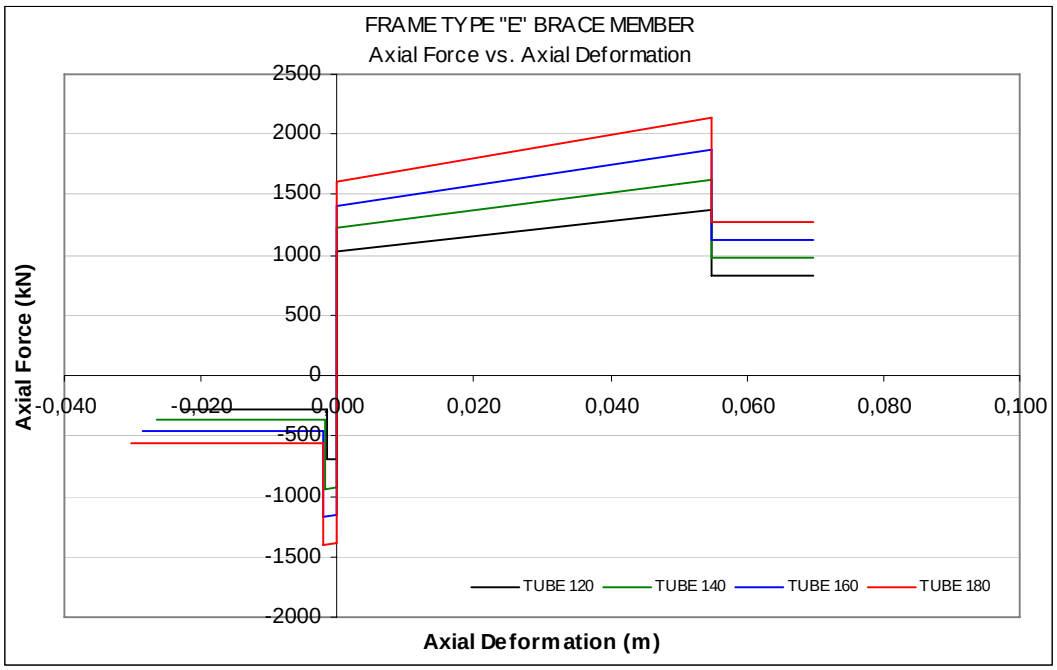

Figure 3.18: Axial Force – Axial Deformation Curve for Type “E” Bracing

Table 3.14: Force – Deformation Data for Brace Members

FRAME TYPE B		TUBE 120 B		TUBE 140 B		TUBE 160 B		TUBE 180 B	
		Pp	Δp	Pp	Δp	Pp	Δp	Pp	Δp
P/Pp	Δ/Δp	1035,584	0,006862	1223,872	0,006862	1412,16	0,006862	1600,45	0,006862
		450	0,0030	685	0,003841	925	0,004495	1165	0,004995
-0,4	-7	-180,000	-0,0209	-274,000	-0,0269	-370,000	-0,0315	-466,000	-0,0350
-0,4	-0,5	-180,000	-0,0015	-274,000	-0,0019	-370,000	-0,0022	-466,000	-0,0025
-1,015	-0,5	-456,750	-0,0015	-695,275	-0,0019	-938,875	-0,0022	-1182,475	-0,0025
-1	0	-450,000	0	-685,000	0	-925,000	0	-1165,000	0
0	0	0	0	0	0	0	0	0	0
1	0	1035,584	0	1223,872	0	1412,160	0	1600,448	0
1,33	11	1377,327	0,0755	1627,750	0,0755	1878,173	0,0755	2128,596	0,0755
0,8	11	828,467	0,0755	979,098	0,0755	1129,728	0,0755	1280,358	0,0755
0,8	14	828,467	0,0961	979,098	0,0961	1129,728	0,0961	1280,358	0,0961

FRAME TYPE C		TUBE 120 C		TUBE 140 C		TUBE 160 C		TUBE 180 C	
		Pp	Δp	Pp	Δp	Pp	Δp	Pp	Δp
P/Pp	Δ/Δp	1035,584	0,004596	1223,872	0,004596	1412,16	0,004596	1600,45	0,004596
		736	0,0033	972	0,00365	1204	0,003918	1428	0,004100
-0,4	-7	-294,400	-0,0229	-388,800	-0,0255	-481,600	-0,0274	-571,200	-0,0287
-0,4	-0,5	-294,400	-0,0016	-388,800	-0,0018	-481,600	-0,0020	-571,200	-0,0021
-1,015	-0,5	-747,040	-0,0016	-986,580	-0,0018	-1222,060	-0,0020	-1449,420	-0,0021
-1	0	-736,000	0	-972,000	0	-1204,000	0	-1428,000	0
0	0	0	0	0	0	0	0	0	0
1	0	1035,584	0	1223,872	0	1412,160	0	1600,448	0
1,33	11	1377,327	0,0506	1627,750	0,0506	1878,173	0,0506	2128,596	0,0506
0,8	11	828,467	0,0506	979,098	0,0506	1129,728	0,0506	1280,358	0,0506
0,8	14	828,467	0,0643	979,098	0,0643	1129,728	0,0643	1280,358	0,0643

Table 3.14: Force – Deformation Data for Brace Members (cont.)

FRAME TYPE D		TUBE 120 D		TUBE 140 D		TUBE 160 D		TUBE 180D	
		Pp	Δp	Pp	Δp	Pp	Δp	Pp	Δp
P/Pp	Δ/Δp	1035,584	0,0041	1223,872	0,0041	1412,16	0,0041	1600,45	0,0041
		798	0,0031	1030	0,0034	1259	0,0036	1479	0,0038
-0,4	-7	-319,200	-0,0220	-412,000	-0,0241	-503,600	-0,0255	-591,600	-0,0264
-0,4	-0,5	-319,200	-0,0016	-412,000	-0,0017	-503,600	-0,0018	-591,600	-0,0019
-1,015	-0,5	-809,970	-0,0016	-1045,450	-0,0017	-1277,885	-0,0018	-1501,185	-0,0019
-1	0	-798,000	0	-1030,000	0	-1259,000	0	-1479,000	0
0	0	0	0	0	0	0	0	0	0
1	0	1035,584	0	1223,872	0	1412,160	0	1600,448	0
1,33	11	1377,327	0,0450	1627,750	0,0450	1878,173	0,0450	2128,596	0,0450
0,8	11	828,467	0,0450	979,098	0,0450	1129,728	0,0450	1280,358	0,0450
0,8	14	828,467	0,0572	979,098	0,0572	1129,728	0,0572	1280,358	0,0572

FRAME TYPE E		TUBE 120 E		TUBE 140 E		TUBE 160 E		TUBE 180 E	
		Pp	Δp	Pp	Δp	Pp	Δp	Pp	Δp
P/Pp	Δ/Δp	1035,584	0,004993	1223,872	0,004993	1412,16	0,004993	1600,45	0,004993
		685	0,003302	924	0,003769	1157	0,004091	1388	0,004330
-0,4	-7	-274,000	-0,0231	-369,600	-0,0264	-462,800	-0,0286	-555,200	-0,0303
-0,4	-0,5	-274,000	-0,0017	-369,600	-0,0019	-462,800	-0,0020	-555,200	-0,0022
-1,015	-0,5	-695,275	-0,0017	-937,860	-0,0019	-1174,355	-0,0020	-1408,820	-0,0022
-1	0	-685,000	0	-924,000	0	-1157,000	0	-1388,000	0
0	0	0	0	0	0	0	0	0	0
1	0	1035,584	0	1223,872	0	1412,160	0	1600,448	0
1,33	11	1377,327	0,0549	1627,750	0,0549	1878,173	0,0549	2128,596	0,0549
0,8	11	828,467	0,0549	979,098	0,0549	1129,728	0,0549	1280,358	0,0549
0,8	14	828,467	0,0699	979,098	0,0699	1129,728	0,0699	1280,358	0,0699

3.3.2.3 Partially Restrained Connections

The Load and Resistance Factor Design 1999 (LRFD-99) specification of the American Institute of Steel Construction (AISC) [64] categorizes two basic types of steel frame construction as follows:

1. Fully Restrained (FR), commonly designated as “rigid-frame” (continuous frame), assumes that connections have sufficient stiffness to maintain the angles between intersecting members.
2. Partially Restrained (PR), assumes that connections have insufficient stiffness to maintain the angles between intersecting members.

In analysis and design of a steel-framed structure, the actual behavior of beam-to-column connection is generally simplified to the two ideal models of either rigid-joint or pinned-joint behavior. Rigid joints, where no relative rotations occur between the connected members, transfer all internal actions to one another. On the other hand, pinned joints are characterized by free rotation movement between the connected elements that prevents the transmission of bending moments. Yet it

is known that the great majority of real connections do not show these idealized behaviors. Such connections which possess moment capacity in between complete fixity and the pin connection are partially restrained connections.

In September 2000 FEMA published a series of documents related to detailed derivations and explanations of the basis for the steel structure design and evaluation recommendations including the document no 355D [56]; a report on connection performance. This document classified the PR connections in three types with in depth investigations on real life connection practices. This categorization, based upon the connection stiffness, is determined from experimental results combined with the analytical studies.

First type is named as Stiff PR Connections where they develop larger connection bending moments at smaller connection rotations. These connections are often stiff enough that their behavior is very close to rigid connections. Furthermore, they are often strong enough to reach the full plastic capacity of the member. “Extended End Plate” and “Bolted Flange Plate” connections can be examples of stiff PR connections.

Another type is the PR Connections with Intermediate Stiffness. These connections usually require consideration of the connection stiffness in the structural analysis, and depending on their design they sometimes have a resistance which is less than the plastic capacity of the member. “Bolted T-Stub” connection is classified as PR with Intermediate Stiffness.

Third and the last type is the Flexible PR Connections which always require consideration of the connection spring stiffness in mathematical models. Besides, the more flexible PR connections will only be able to develop a small portion of the plastic moment capacity of the member. “Top-Bottom Clip Angle”, “Bolted Web-Angle” and Shear Tab connections are flexible PR connections. Abovementioned examples of PR connections are presented in Figure 3.19.

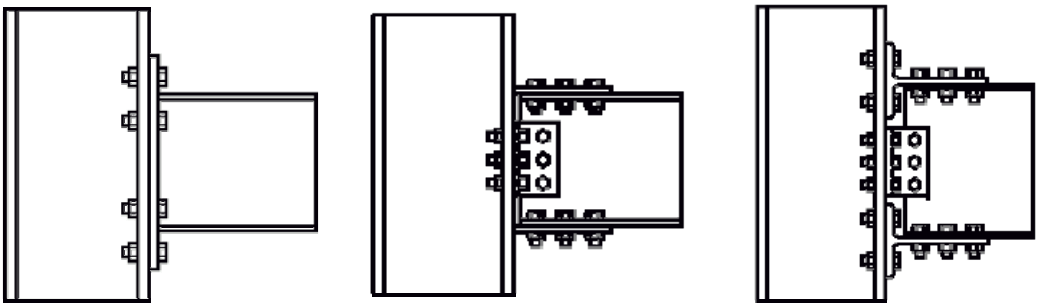

a) Extended End Plate b) Bolted Flange Plate c) Bolted T-Stub

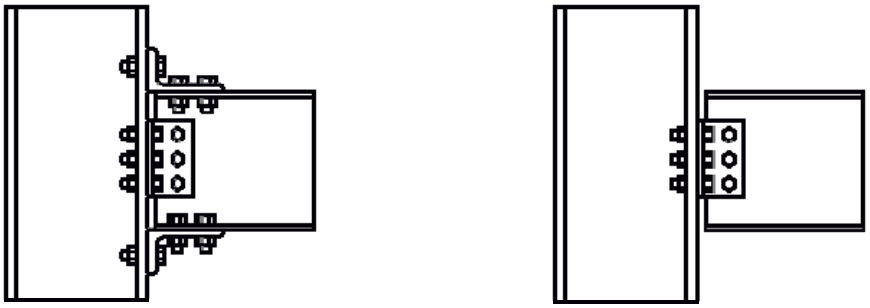

d) Top and Bottom Clip Angle e) Bolted Web-Angle

Figure 3.19 Partially Restrained Connection Examples

In this study one particular type of PR connection is modeled and introduced to all framing systems in order to examine the effects of connection modeling on seismic response. It is not intended to change the elastic response of the structure with the introduction of the PR connection; the primary purpose is to examine the general behavior in the post-elastic region. To this end the connection shown in Figure 3.19.d “Top and Bottom Clip Angle” is modeled as to transfer all elastic demands as a rigid connection however exhibit a poor plastic performance preventing the beam section reaching its full plastic moment capacity. By this way it’s wanted to simulate a scenario where the engineer designs such a connection as fully restrained under elastic design forces but the connection is inadequate under inelastic actions.

In FEMA 356 [57] this type of connection is characterized by four limiting states according to their unique yield mechanisms and failure modes and the moment strength of the connection is determined by the smallest value of these limits.

Limit State 1: If the shear connectors between the beam flange and the flange angle control the capacity of the connection, M_{CE} shall be computed in accordance with Equation 3.9

$$M_{CE} = d_b \left(F_{ve} \cdot A_b \cdot N_b \right) \tag{3.9}$$

Limit State 2: If the tensile capacity of the horizontal leg of the connection controls the capacity, P_{CE} shall be taken as the smaller of that computed by Equations 3.10.a or 3.10.b. and M_{CE} shall be calculated by Equation 3.10.c

$$P_{CE} \leq F_{ye} \cdot A_g \tag{3.10.a}$$

$$P_{CE} \leq F_{te} \cdot A_g \tag{3.10.b}$$

$$M_{CE} \leq P_{CE} \left(d_b + t_a \right) \tag{3.10.c}$$

Limit State 3: If the tensile capacity of the rivets or bolts attaching the vertical outstanding leg to the column flange controls the capacity of the connection, M_{CE} shall be computed in accordance with Equation 3.11

$$M_{CE} = \left(d_b + b_a \right) \cdot \left(F_{te} \cdot A_b \cdot N_b \right) \tag{3.11}$$

Limit State 4: If the flexural yielding of the flange angles controls the capacity of the connection, M_{CE} shall be computed by Equation 3.12

$$M_{CE} = \frac{w \cdot t_a \cdot F_{ye}}{4\left[b_a - \frac{t_a}{2} \right]} \left(d_b + b_a \right) \tag{3.12}$$

where:

Ab = Gross area of rivet or bolt

Ae = Effective net area of the horizontal leg

Ag = Gross area of the horizontal leg

ba = Distance between the bolt connecting the flange angle and the bottom of the flange

db = Overall beam depth

Fve = nominal shear strength of the bolts or rivets given in AISC LRFD Specifications

Fte = Expected tensile strength of the angle

Fye = Expected yield strength of the angle

ta = Thickness of angle

Nb = Least number of bolts or rivets connecting top or bottom angle to column flange

w = Length of the flange angle

In Table 3.15 calculated connection limit states along with section elastic and plastic capacities are summarized. It can be seen that for all beam sections the governing limit state of the connection appeared to be the last one which is the flexural yielding of flange angles.

Table 3.15: Partially Restrained Connection Strength Data

	Flexural Strength of Section		Connection Strength at Limit States				Yield Rotation
	Elastic	Plastic	1	2	3	4	θ_y
IPE 400	163.9	307.7	250	364.2	375.0	**180**	0.003243
IPE 450	211.9	407.7	281.3	408.3	416.7	**230**	0.002840
IPE 500	272.6	516.6	312.5	452.5	458.3	**300**	0.002593
IPE 550	344.8	656.2	398.7	496.6	579.9	**380**	0.002359

In order to obtain the moment-rotation curve the underlined parameters presented in Table A.4.1 in appendix section are used. These values are originally proposed by FEMA 356 [57] particularly for Top and Bottom Clip Angle connections limit state 4. Force-deformation data calculated according to the given parameters are presented in Table 3.16 and plotted in Figure 3.20

Table 3.16: Force – Deformation Data for PR Connections

IPE 400				**IPE 450**			
		Mp	Θp			Mp	Θp
M/Mp	Θ/Θp	**180**	**0,003243**	M/Mp	Θ/Θp	**230**	**0,00284**
-0,2	-25,9	-36,000	-0,0840	-0,2	-29,6	-46,000	-0,0841
-0,2	-13	-36,000	-0,0422	-0,2	-14,8	-46,000	-0,0420
-1,39	-13	-250,200	-0,0422	-1,444	-14,8	-332,120	-0,0420
-1	0	-180,000	0,0000	-1	0	-230,000	0,0000
0	0	0	0,0000	0	0	0	0,0000
1	0	180,000	0,0000	1	0	230,000	0,0000
1,39	13	250,200	0,0422	1,444	14,8	332,120	0,0420
0,2	13	36,000	0,0422	0,2	14,8	46,000	0,0420
0,2	25,9	36,000	0,0840	0,2	29,6	46,000	0,0841
IPE 500				**IPE 550**			
		Mp	Θp			Mp	Θp
M/Mp	Θ/Θp	**300**	**0,002593**	M/Mp	Θ/Θp	**380**	**0,002359**
-0,2	-32,4	-60,000	-0,0840	-0,2	-35,6	-76,000	-0,0840
-0,2	-16,2	-60,000	-0,0420	-0,2	-17,8	-76,000	-0,0420
-1,486	-16,2	-445,800	-0,0420	-1,534	-17,8	-582,920	-0,0420
-1	0	-300,000	0,0000	-1	0	-380,000	0,0000
0	0	0	0,0000	0	0	0	0,0000
1	0	300,000	0,0000	1	0	380,000	0,0000
1,486	16,2	445,800	0,0420	1,534	17,8	582,920	0,0420
0,2	16,2	60,000	0,0420	0,2	17,8	76,000	0,0420
0,2	32,4	60,000	0,0840	0,2	35,6	76,000	0,0840

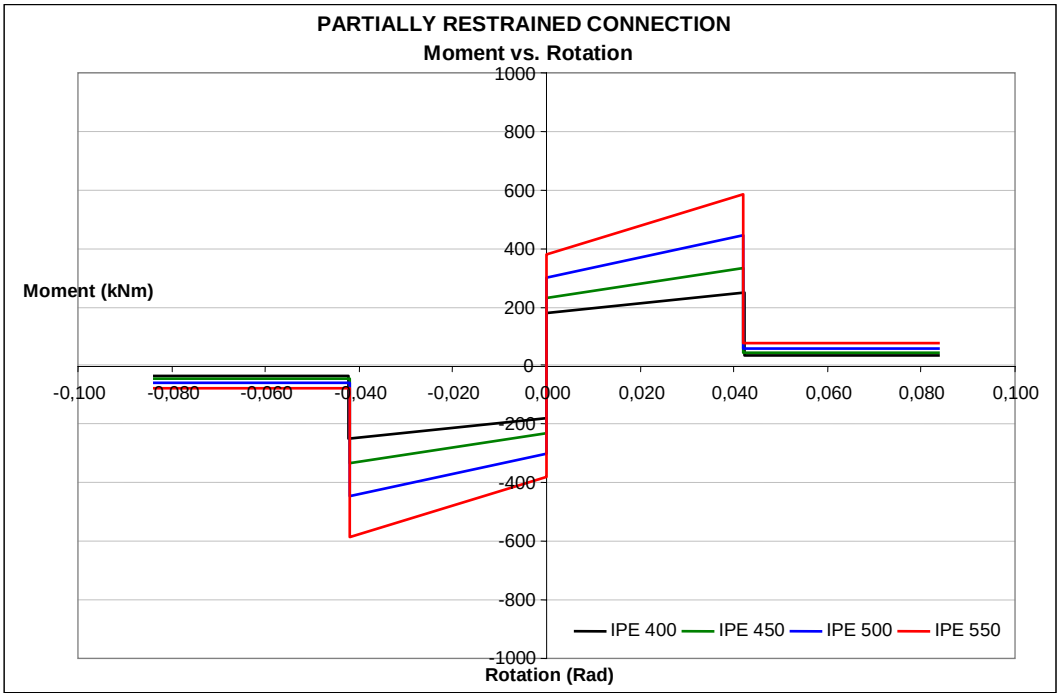

Figure 3.20: Moment – Plastic Rotation Curve for PR Connections

3.3.3 Panel Zone Deformations

The panel zone is defined as the region in the column web limited by the extension of the beam flange lines into the column as shown in Figure 3.21. A simple way to employ the panel zone deformations for linear analysis is the scissors model as shown in Figure 3.22. Beams and columns are modeled with a rigid link through the panel zone region and a hinge is placed at the intersection of the beam and column centerlines. A rotational spring is then introduced to tie the beam and column together permitting a relative rotation between them. Given equation 3.13 is for determining the stiffness of the panel zone spring, based on the yield properties of the panel zone.

$$\theta_y = \frac{F_y}{\sqrt{3}G} \qquad M_y = V_y \cdot d_b = 0.55F_y \cdot d_c \cdot t \cdot d_b \quad \rightarrow \quad K_\theta = \frac{M_y}{\theta_y} \qquad (3.13)$$

where, F_y : Yield strength of steel G : Shear Modulus

d_c : Depth of column d_b : Depth of Beam

t : Thickness of Panel Zone K_θ : Stiffness of the Panel Zone

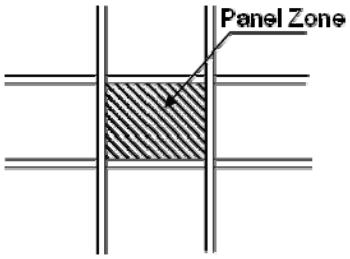

Figure 3.21: Panel Zone Region

While the rigid links stiffen the structure, the panel zone spring adds flexibility. The overall behavior is needed to be investigated per system basis not letting a strict comment like panel zone modeling stiffens or softens the structure.

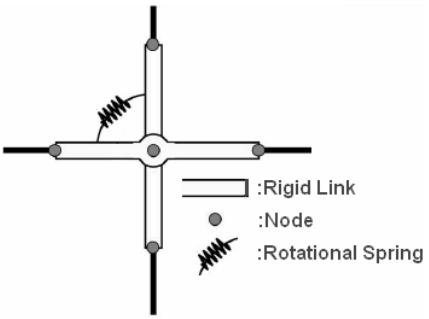

Figure 3.22: Scissors Model for Panel Zone

The actual panel zone behavior is more complex than the basic scissors model. Bending moment transfers between beams and columns causes a complicated state of stress and strain in the connection area. Within the column part of the connection, high normal stresses occur in the flanges and high shear stresses occur in the panel zone. Forces around a general beam column connection which will be transferred through the panel zone are shown in Figure 3.23.

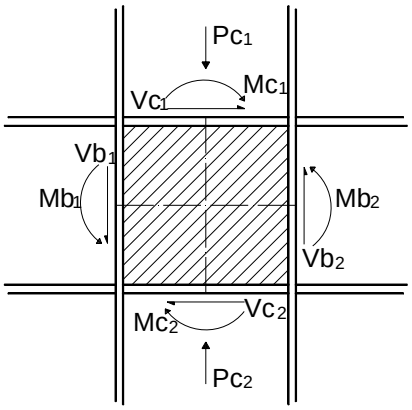

Figure 3.23: Forces acting on the Panel Zone

An improved model for the panel zone, proposed by Krawinkler [42] which also presented in the state of the art report FEMA 355C [55] is illustrated in Figure 3.24. This model overcomes the inabilities of the scissors model by eliminating two approximations. Firstly, in scissors model the relationship between the moment at the spring location and the panel zone shear force needs to be estimated from the beam moments at the column face. Secondly, the right angles between the panel zone boundaries and the adjacent beams and columns are not maintained, which results in approximations in deflections. The model given in Figure 3.24 holds the full dimension of the panel zone with rigid boundary element and controls the deformation of the panel zone by means of two bilinear springs that simulate a tri-linear behavior. Pertinent formulation is given in Equation 3.14 and trilinear spring load deformation curve is given in Figure 3.25.

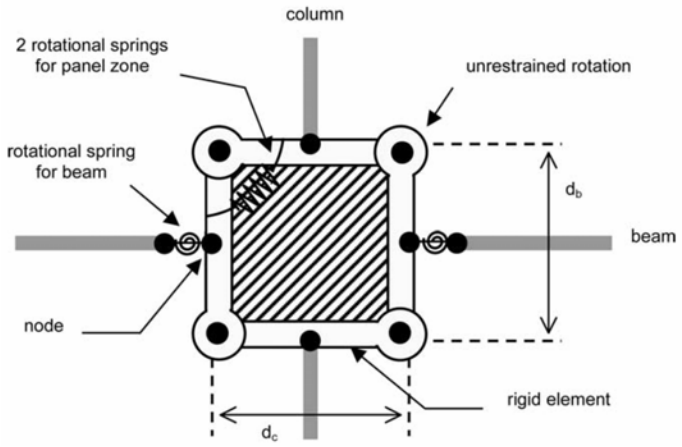

Figure 3.24: Improved Model for Panel Zone

$$\theta_y = \frac{F_y}{\sqrt{3}G} \quad \theta_p = 4 \cdot \theta_y \quad V_y = 0.55 F_y \cdot d_c \cdot t \quad V_p = V_y \cdot \left(1 + \frac{3 \cdot b_c \cdot t_{cf}^2}{d_b \cdot d_c \cdot t_p}\right) \quad (3.14)$$

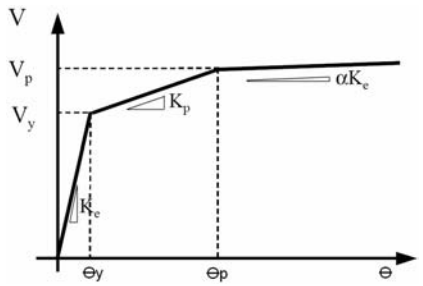

Figure 3.25: Tri-linear Behavior Curve of Improved Model for Panel Zone Spring

Connection performance can be affected either positively or negatively by panel zone strength. Even if plastic hinging in the column is prevented, there is no guarantee that energy in a severe earthquake will be dissipated just by plastic hinging in beams. Excessive internal forces may lead to a shear yield in the panel zone. On the positive side panel zones have shown [42] ~ [46] to present stable strength and stiffness characteristics in the inelastic range. “Panel zones also have a greater slope of strain-hardening compared to the plastic hinge characteristics of a wide flange shape and are less prone to local buckling. Therefore, due to their stable hysteretic behavior, panel zones are considered to be a very good source of energy dissipation” [47]. “Some shear yielding of the panel zone can relieve the amount of plastic deformation that must be accommodated in other regions of the frame and many connections have been found to provide the largest inelastic deformation capacity when yielding is balanced between the panel zone and other connection elements. However, excessive panel zone deformation can induce large secondary stresses into the connection that can degrade connection performance.” [54] It is a good practice to design the connection area well proportioned so that flexural yielding of the beam starts at the same point where shear yielding of the panel zone starts. FEMA 350, a part of the document series published in 2000, proposed a formulation to calculate the thickness of the panel zone. If the calculated thickness is greater than the column web, commentary of the document recommends to increase the column size or to use “Doubler Plate” to increase the web thickness properly.

In this particular study panel zones of the frames are modeled with the abovementioned scissors model with respect to the columns web thickness. No additional doubler plate thickness is introduced and the spring stiffness is calculated according to the Equation 3.13. It’s been considered that non-linear modeling of the panel zone element is beyond the scope of this thesis work therefore panel zone springs in the mathematical models are linear link elements. Modeling properties (stiffness) of the springs per beam to column connection are presented in Table 3.17.

Table 3.17: Panel Zone Spring Stiffness per Member Connection (kNm/rad)

	HE200-A	HE220-A	HE280-A
IPE400	36199,9	43088,1	63313,1
IPE450	40724,8	48474,1	71227,3
IPE500	45249,8	53860,1	79141,4
IPE550	49774,8	59246,1	87055,5
	HE300-A	HE340-A	HE360-A
IPE400	72253,2	91892,0	102590,7
IPE450	81284,8	103378,5	115414,5
IPE500	90316,5	114864,9	128238,4
IPE550	99348,1	126351,4	141062,2
	HE400-A	HE450-A	HE500-A
IPE400	125746,9	148316,8	172352,4
IPE450	141465,2	166856,4	193896,4
IPE500	157183,6	185396,1	215440,5
IPE550	172902,0	203935,7	236984,5

3.3.4 Capacity Curve of Structures

Capacity (pushover) curve is defined as the plot of the total applied lateral force, V_i, versus the lateral displacement of the control point, Δ_i, as determined in a non-linear static analysis. As previously discussed the chosen method for the pushover analysis is to apply the lateral load until the control node reaches a target displacement. The lateral load pattern is the first mode shape of the structure in which the applied forces are in proportion to the amplitude of the elastic first mode for each node. The control point is selected as the center of mass at the roof level to index the lateral displacement of the structure in the analysis. Capacity curve is then constructed with the pushover analysis data by plotting the lateral load value with respect to the control point displacement for each successive load increment. The curve continues until the target displacement is reached or the structure became unstable forming a global mechanism. The effects of inelasticity on lateral load pattern and higher modes on target displacement are neglected. Thus, the accuracy of the predictions depends on the approximations involved. Resultant plots for each type of structural systems can be found on the chapter 4 “Results of Analysis”. This traced relationship, referred to as a capacity curve, (because it characterizes the overall performance of the system) is the fundamental product of a pushover analysis and the sole resource of this particular thesis study.

3.3.4.1 Idealization of Capacity Curve

The capacity curve presents the primary data for the evaluation of the response modification factor for structures, but first of all it must be idealized in order to extract the relevant information from the plot. The intention is to obtain the overstrength factor and the ductility reduction factor by studying the pushover curve.

To this end a bi-linear curve is fitted to the capacity curve, such that the first segment starts from the origin, intersects with the second segment at the significant yield point and the second segment starting from the intersection ends at the ultimate displacement point. The slope of the first segment is found by tracing the individual changes in slopes of the plot increments; the mean slope of the all increments are calculated for each step and compared with the latter, searching for a dramatic change. First segment, referred to as elastic portion, is then obtained with a mean slope of the successive parts of the curve until a remarkable change occurs. The second segment, referred to as post-elastic portion, is plotted by acquiring the significant yield point by means of equal energy concept in which the area under the capacity curve and the area under the bi-linear curve is kept equal. An AutoLISP program is developed to read and plot the pushover data then fit the bi-linear curve by utilizing the abovementioned methodology.

This method is an improved version of the one, proposed by FEMA 273 [52] which offers a visual trial & error process and suggests that the first segment intersects the original curve at 60% of the significant yield strength. However in the studied plots, intersecting the curve at the 60% of the significant yield strength is by no means form a boundary condition since all curves already satisfy that condition with their almost straight elastic portions. The method is improved in such a way that there is no need for the visual trial & error anymore; nevertheless resultant bi-linear curves are checked against a faulty interpretation. A generic illustration of the bi-linear approximation is given in Figure 3.26.

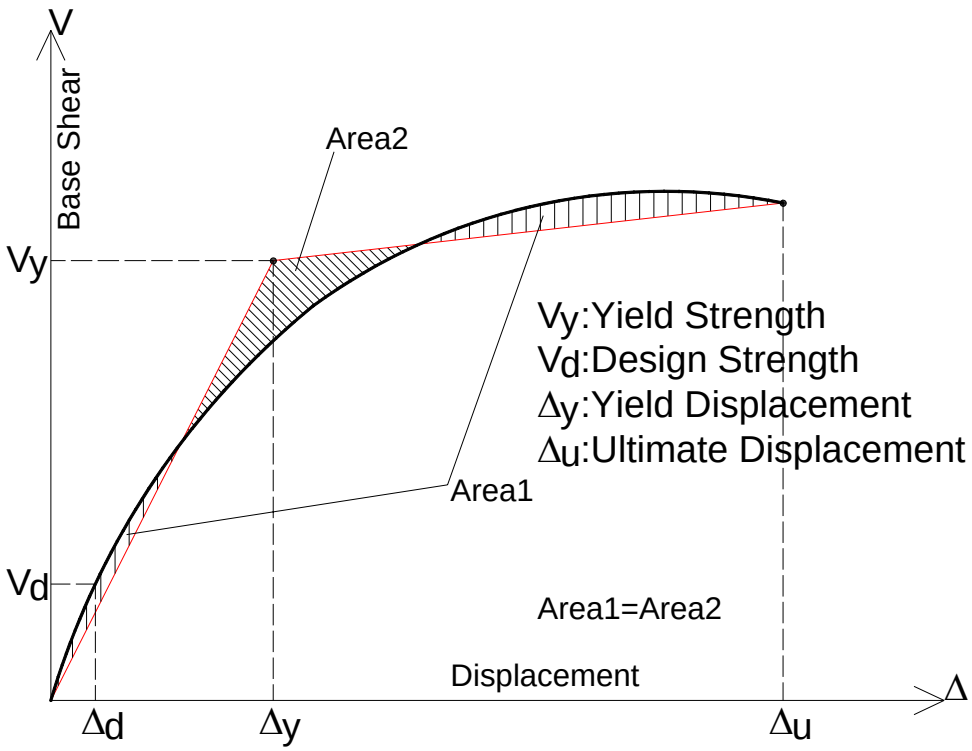

Figure 3.26: Bi-linear Idealization of a Generic Capacity Curve

Bi-linear idealization provides the essential components, which are significant yield strength and the significant yield displacement as well as the predetermined design strength and the ultimate displacement. With these resultant data in hand, the overstrength factor which is overviewed in section 2.2 can be calculated easily as the ratio of the yield strength to the design strength. Furthermore the ductility ratio can be calculated as the ratio of ultimate displacement to yield displacement which is the key element in calculation of the ductility reduction factor according to the Eq. 2.3.32 as proposed by Miranda [16].

3.3.5 Sample Analysis Evaluation

Previously in section 3.2.3 two single bay, single story steel frames were designed; one in normal ductility class, the other in high ductility class according to the Turkish seismic code and the design base shears were 36.21kN and 23.42kN respectively. Figures 3.27 a & b show the capacity curves of the systems along with the pertinent analysis data.

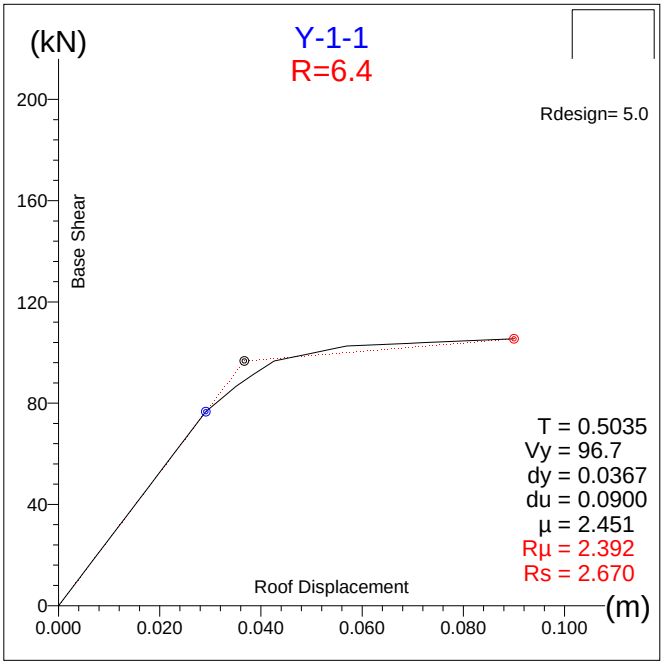

3.27.a

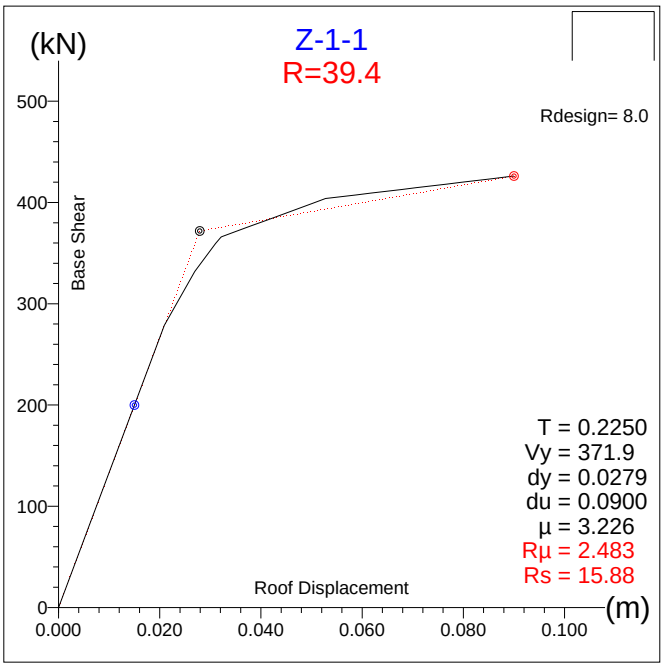

3.27.b

Figure 3.27: a) Normal Ductility Frame b) High Ductility Frame

In Figures 3.27 a & b the plot of the pushover data is presented for two systems. At the uppermost side of the figures, name of the model is printed (following the naming convention which is mentioned in section 3.1).

Under the model's name, the calculated Response Modification Factor, *R*, is printed as the product of calculated Ductility Reduction Factor, $R\mu$, and the Overstrength Factor, *Rs*. The initial design value of the R factor is printed below the sketch of the framing system which is placed at the top right corner. Base Shear and Roof Displacement axes are plotted in units of kN and meters respectively. At the lower right corner resultant data of the analysis are presented. Where;

- "T" is the elastic first mode period of the system, obtained as a result of the modal analysis.
- "Vy" is the significant yield strength of the system, obtained by bi-linear idealization of the capacity curve.
- "dy "is the significant yield displacement of the system, corresponding to the significant yield strength
- "du" is the ultimate displacement value of the system where the analysis ended according to a limit state (which may be a target value or a global collapse).
- μ is the ductility ratio which is defined as the ratio of the ultimate displacement to the yield displacement.
- Rμ is the ductility reduction factor, calculated according to the Equation 2.3.32 proposed by Miranda [16].
- Rs is the overstrength factor defined as the ratio of the yield strength to the design strength.

Blue, black and red points on the plot indicate first yield of a member, significant yield of the system and the ultimate displacement respectively. The calculated equivalent lateral load for the systems Y-1-1 and Z-1-1 were 36.21kN and 23.42kN respectively, the idealization of the capacity curve showed that the significant yield strength of the systems are at 96.7kN and 371.9kN respectively. Overstrength factors are found to be:

$$\text{Y-1-1: } Rs = \frac{V_y}{V_d} = \frac{96.7}{36.21} = 2,67$$

$$\text{Z-1-1: } Rs = \frac{V_y}{V_d} = \frac{371.9}{23.42} = 15,88$$

In this study the Ductility Reduction Factor is calculated by utilizing the formulation proposed by Miranda [16] with respect to the ϕ coefficient for alluvium sites. Factors are found to be:

For Y-1-1:

$$\mu = \frac{du}{dy} = \frac{0.09}{0.0367} = 2.451$$

$$\phi = 1 + \frac{1}{12T - \mu T} - \frac{2}{5T}\exp\left[-2\left(\ln T - \frac{1}{5}\right)^2\right] = 1.042$$

$$R\mu = \frac{\mu - 1}{\phi} + 1 = \frac{2.451 - 1}{1.042} + 1 = 2.392$$

Applying the same procedure for Z-1-1:

$$\mu = 3,226 \quad \phi = 1.501$$

$$R\mu = \frac{\mu - 1}{\phi} + 1 = \frac{3,226 - 1}{1.501} + 1 = 2.483$$

Damping and redundancy factors are kept constant at 1.0, thus the *R* factor is calculated as the product of $R\mu$ and *Rs* factors. Which are found to be;

$$Y-1-1: \quad R = Rs \cdot R\mu = 2.67 \times 2.392 = 6.39 \sim \mathbf{6.4}$$

$$Z-1-1: \quad R = Rs \cdot R\mu = 15.88 \times 2.483 = 39.43 \sim \mathbf{39.4}$$

Notice the significant difference in overstrength factors while ductility reduction factor remains close for both systems. Results of all analysis cases can be found on Chapter 4 and further discussion on the results can be found on Chapter 5.

CHAPTER 4

RESULTS OF ANALYSIS AND FURTHER REMARKS

In this chapter analysis results are compiled and presented as graphics, including capacity curves accompanied with various evaluation results. Graphics representing “Base Shear vs. Roof Displacement” for center-line, partially restrained and panel zone deforming models are given in figures 4.2~4.7, 4.8~4.13 and 4.14~4.19 respectively. Modification factors relationship with period of vibration is also represented in figures 4.20~4.28, which can be followed in an order of ductility reduction, overstrength and response modification factors for center-line, partially restrained and panel zone deforming models (In figure definitions CL, PR and PZ abbreviations are used instead of “center-line”, “partially restrained” and “panel zone”). Tables 4.1, 4.2 and 4.3 are presenting the results in a tabulated format for convenience, in which analysis results for %1 top displacement (height wise) is also included.

At this point it is necessary to recall the fundamental assumption for the definition of the response modification factors which is called the “equal displacement rule” [72]; a well known empirical proposal for the evaluation of the non-linear behavior of structures subjected to ground motion. As illustrated in Figure 4.1, the theory states that inelastic peak displacements (Δu) will be the same as elastic peak displacement (Δe). The rule was intensively investigated numerically for recorded earthquakes as well as for synthetic earthquakes; significant investigations are reviewed in section 2.3.1

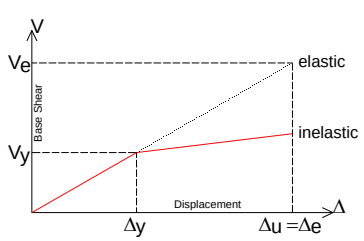

Figure 4.1: Illustration of the “Equal Displacement Rule”

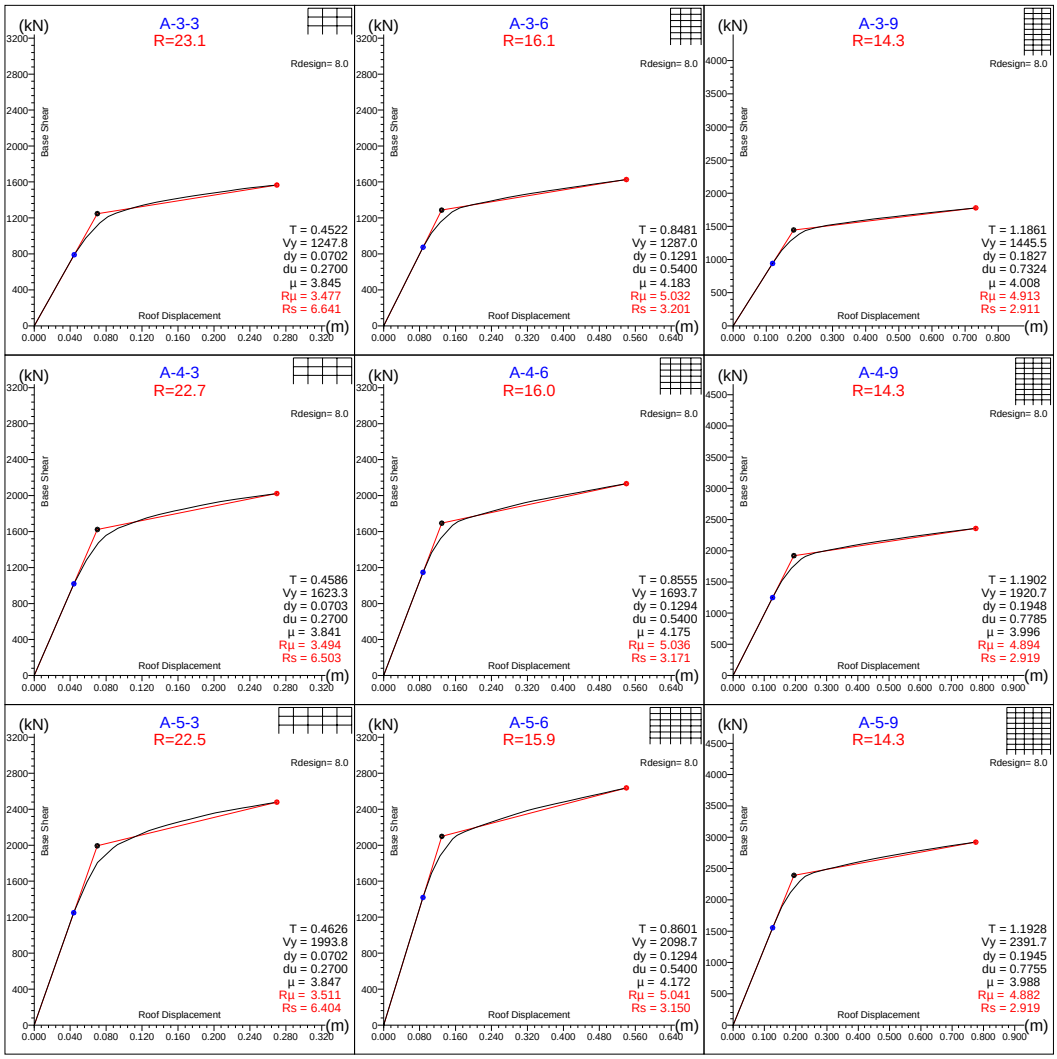

Figure 4.2: Frame Type **A** – "**CL**"
Base Shear vs. Roof Displacement Diagram

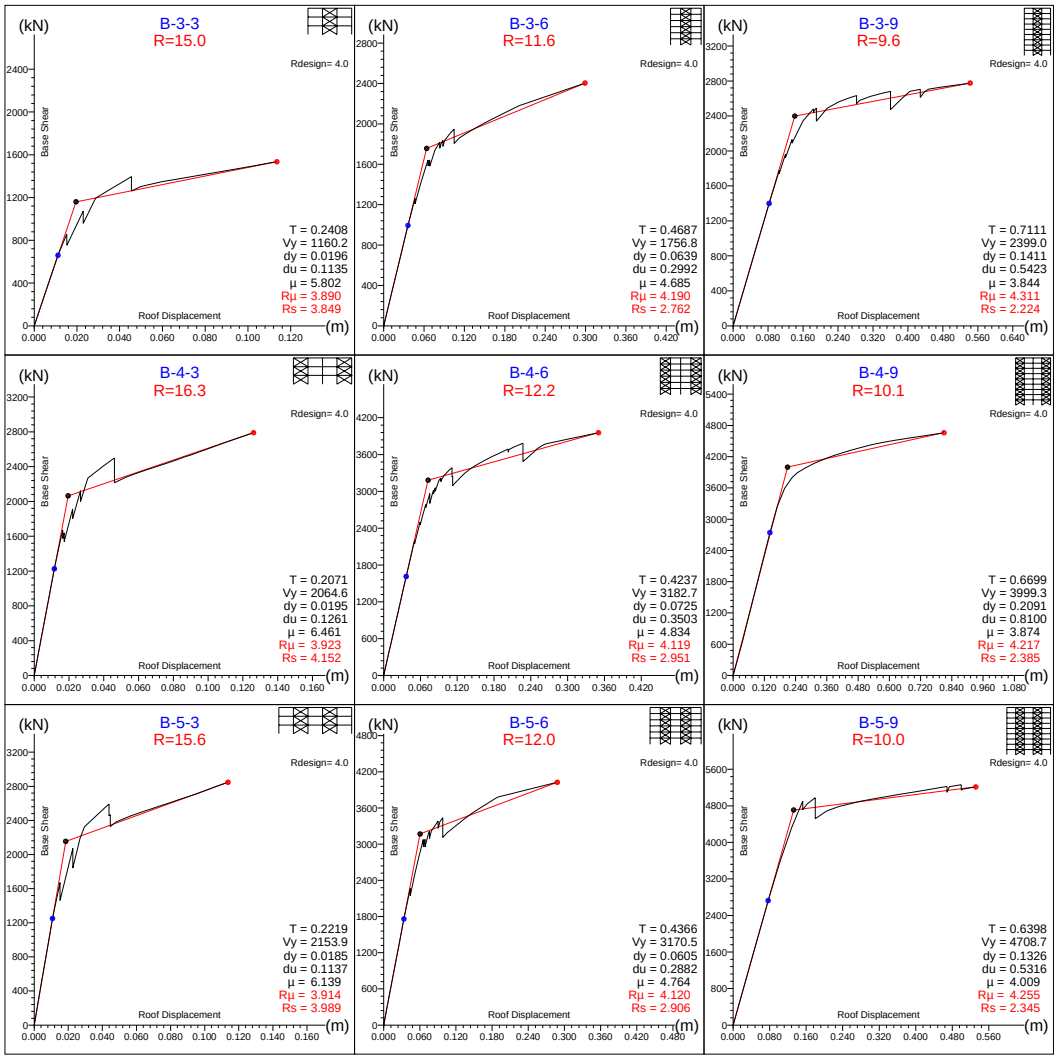

Figure 4.3: Frame Type **B** – **"CL"**
Base Shear vs. Roof Displacement Diagram

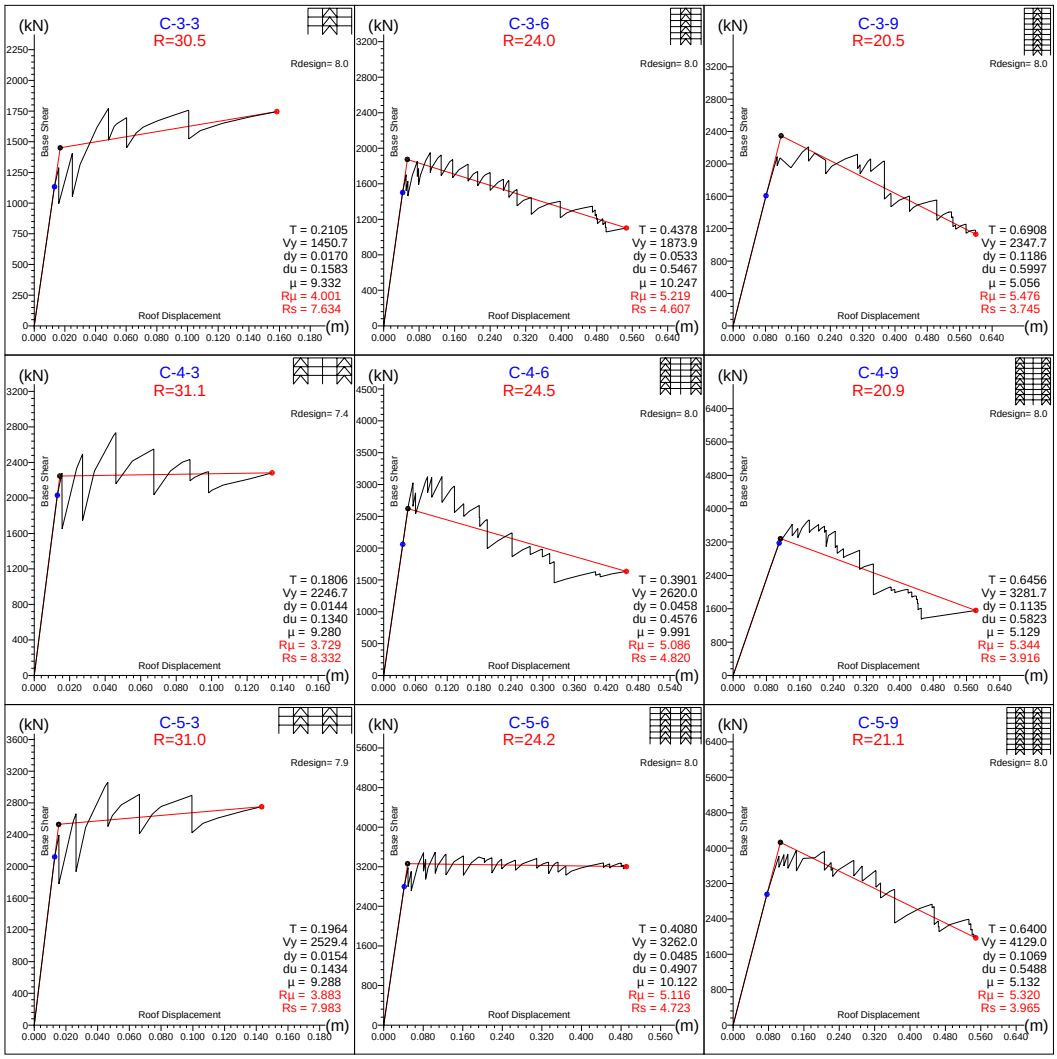

Figure 4.4: Frame Type **C** – **"CL"**
Base Shear vs. Roof Displacement Diagram

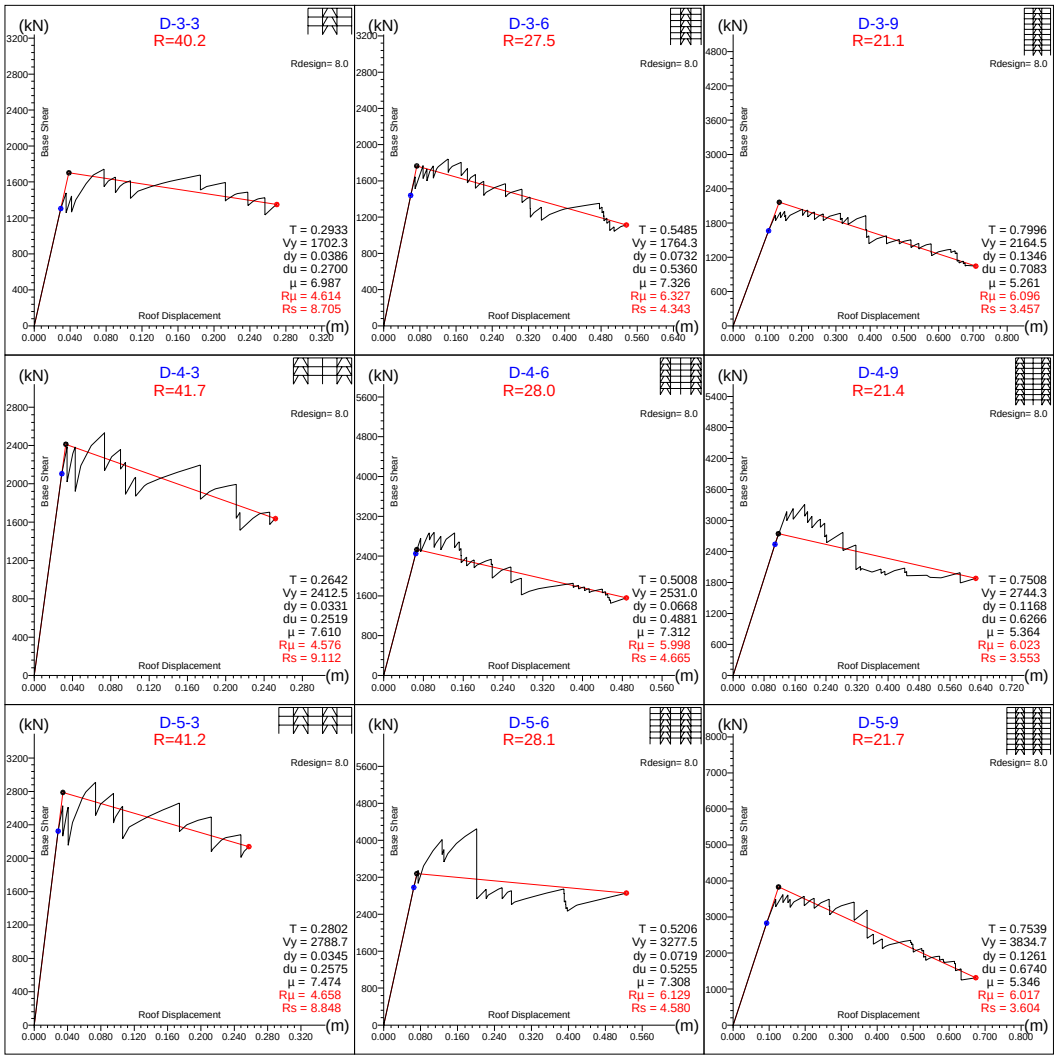

Figure 4.5: Frame Type **D** – **"CL"**
Base Shear vs. Roof Displacement Diagram

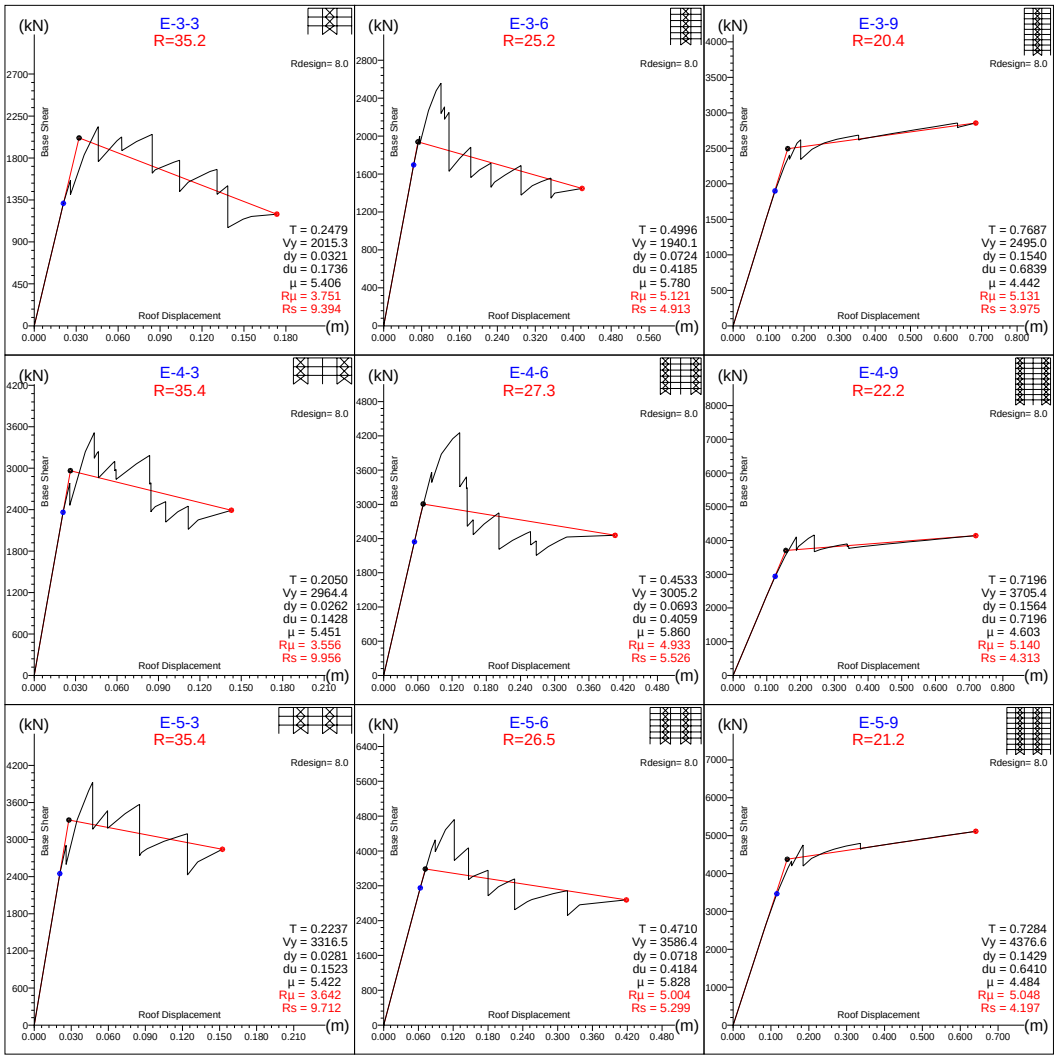

Figure 4.6: Frame Type **E** – **"CL"**
Base Shear vs. Roof Displacement Diagram

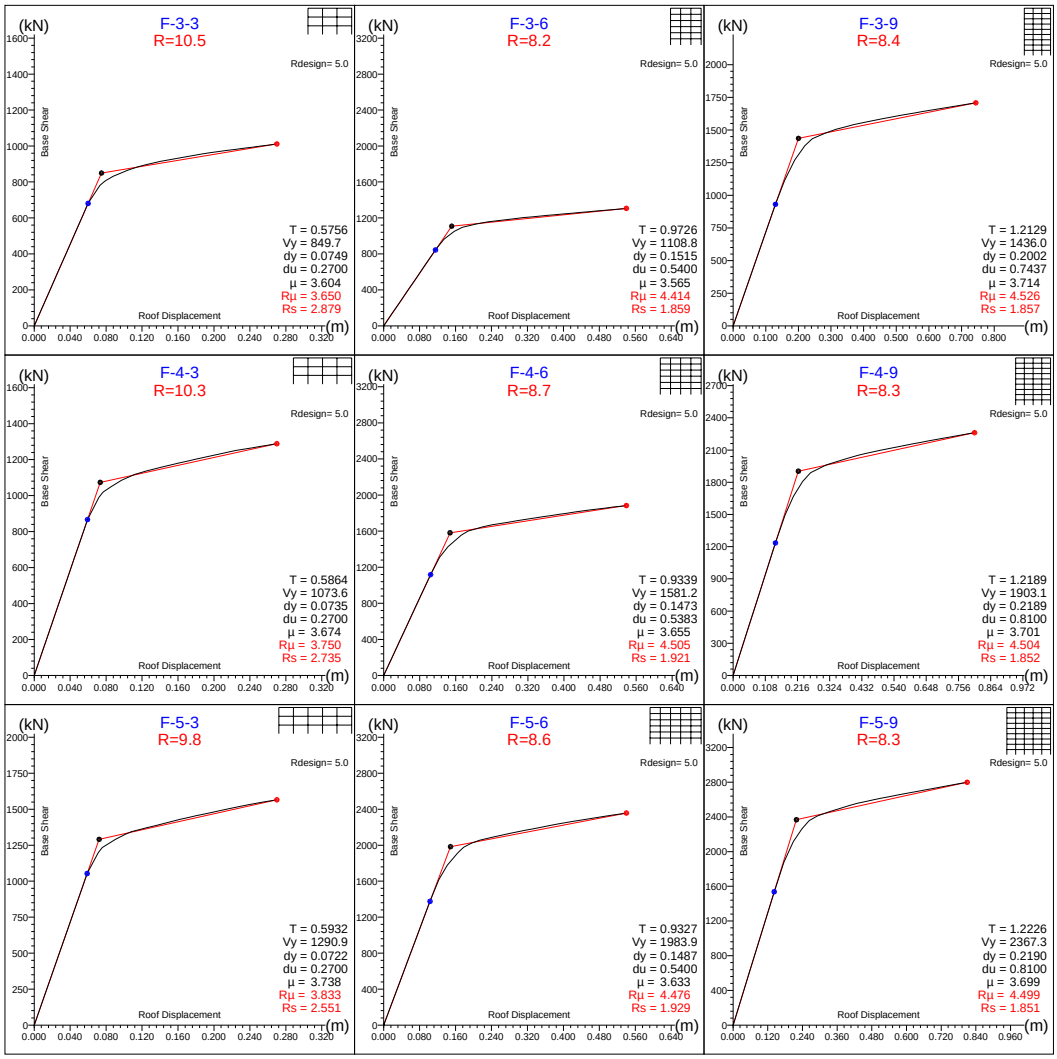

Figure 4.7: Frame Type **F – "CL"**
Base Shear vs. Roof Displacement Diagram

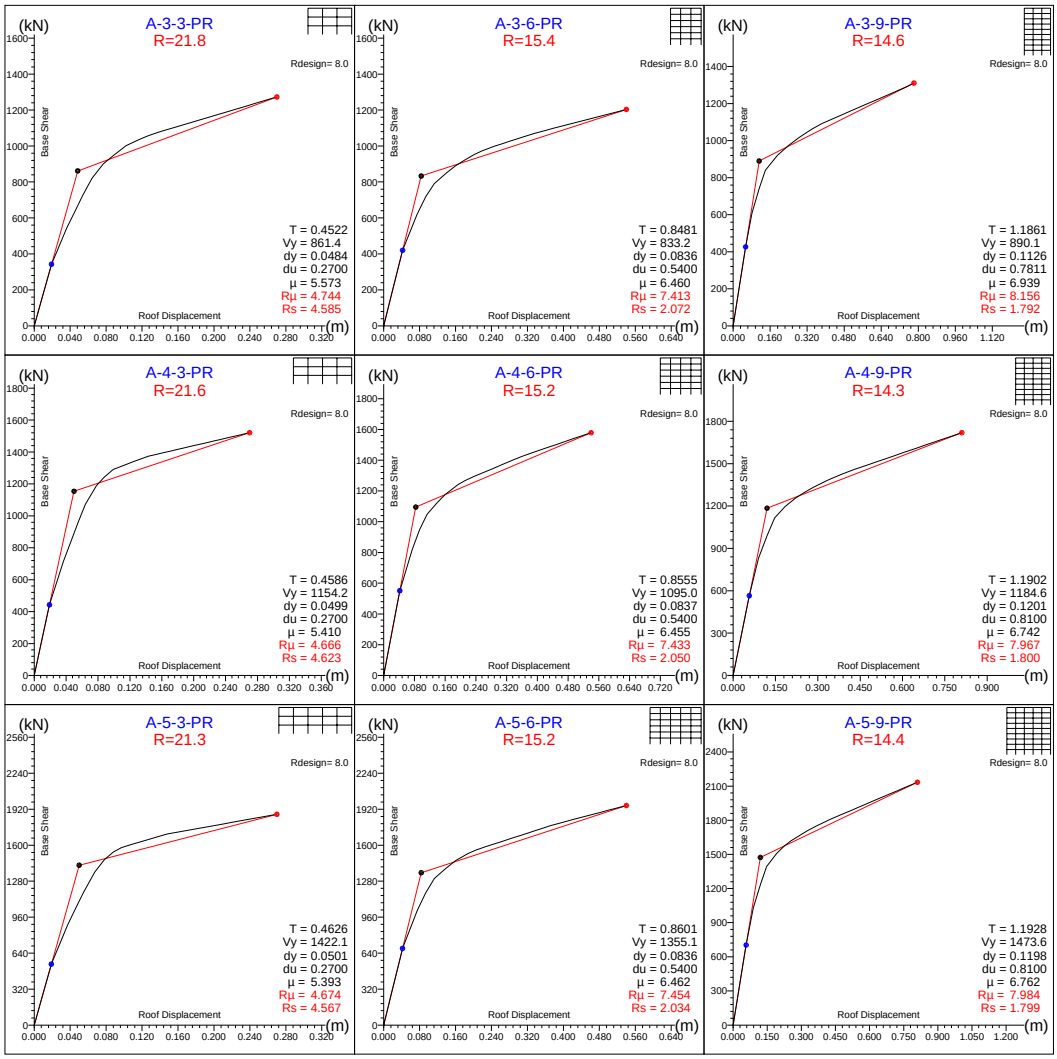

Figure 4.8: Frame Type **A** – "**PR"**
Base Shear vs. Roof Displacement Diagram

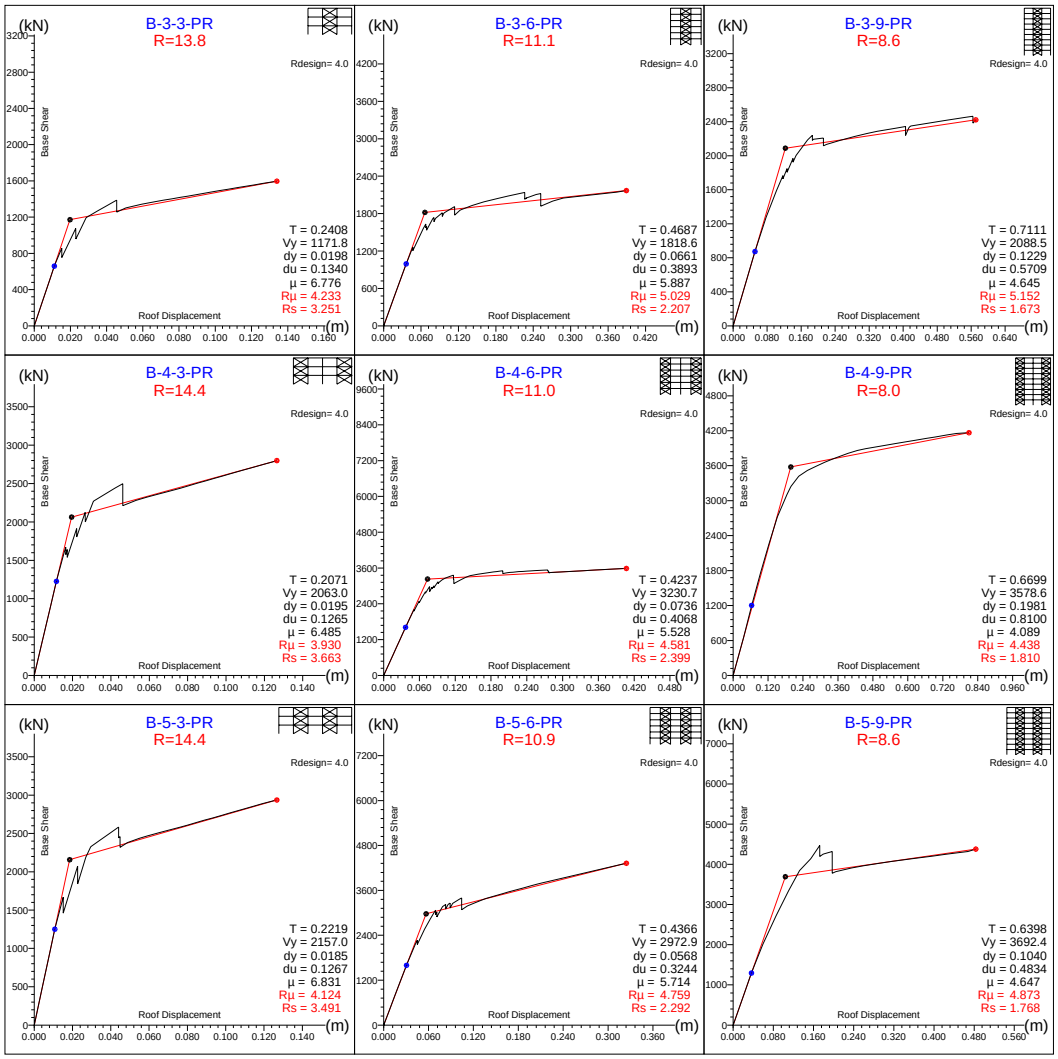

Figure 4.9: Frame Type **B** – "**PR**"
Base Shear vs. Roof Displacement Diagram

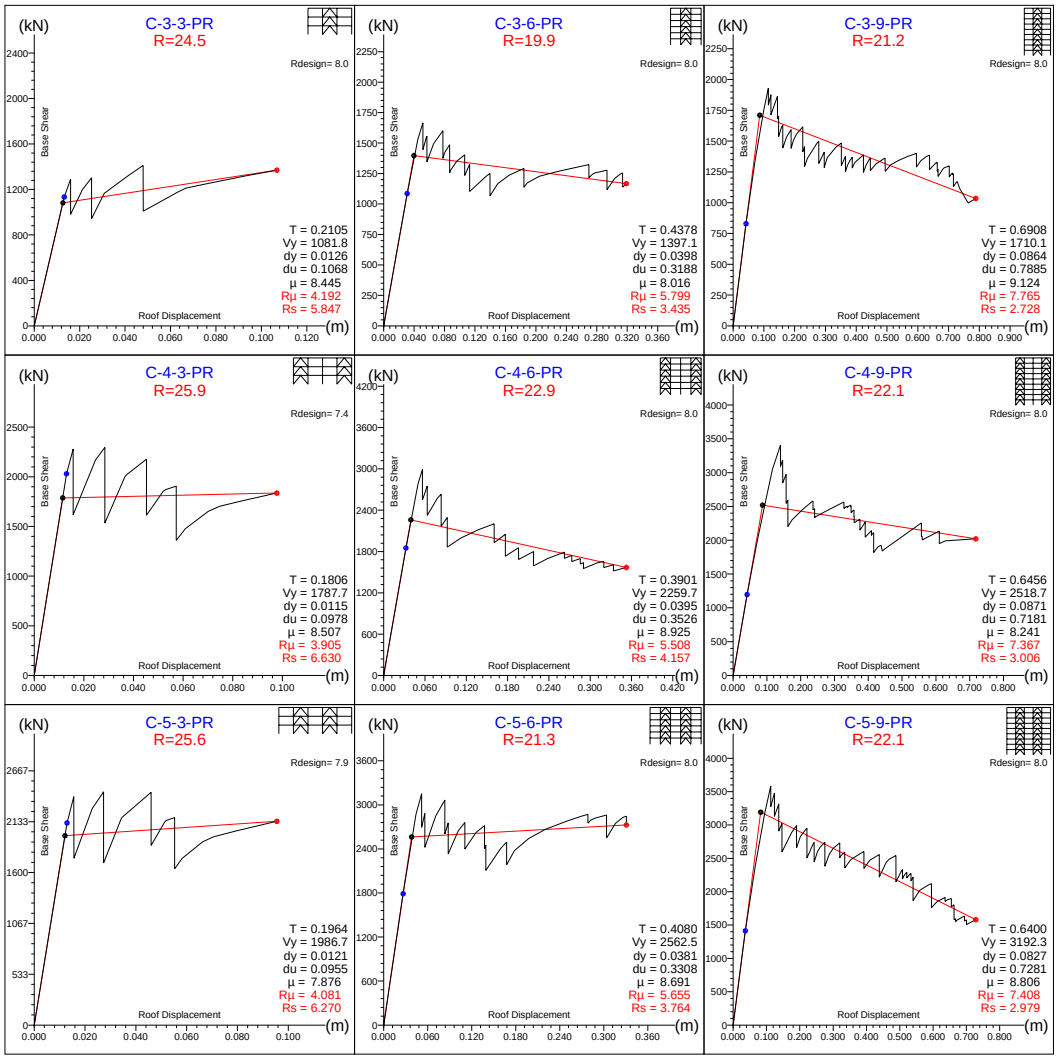

Figure 4.10: Frame Type **C** – "**PR**"
Base Shear vs. Roof Displacement Diagram

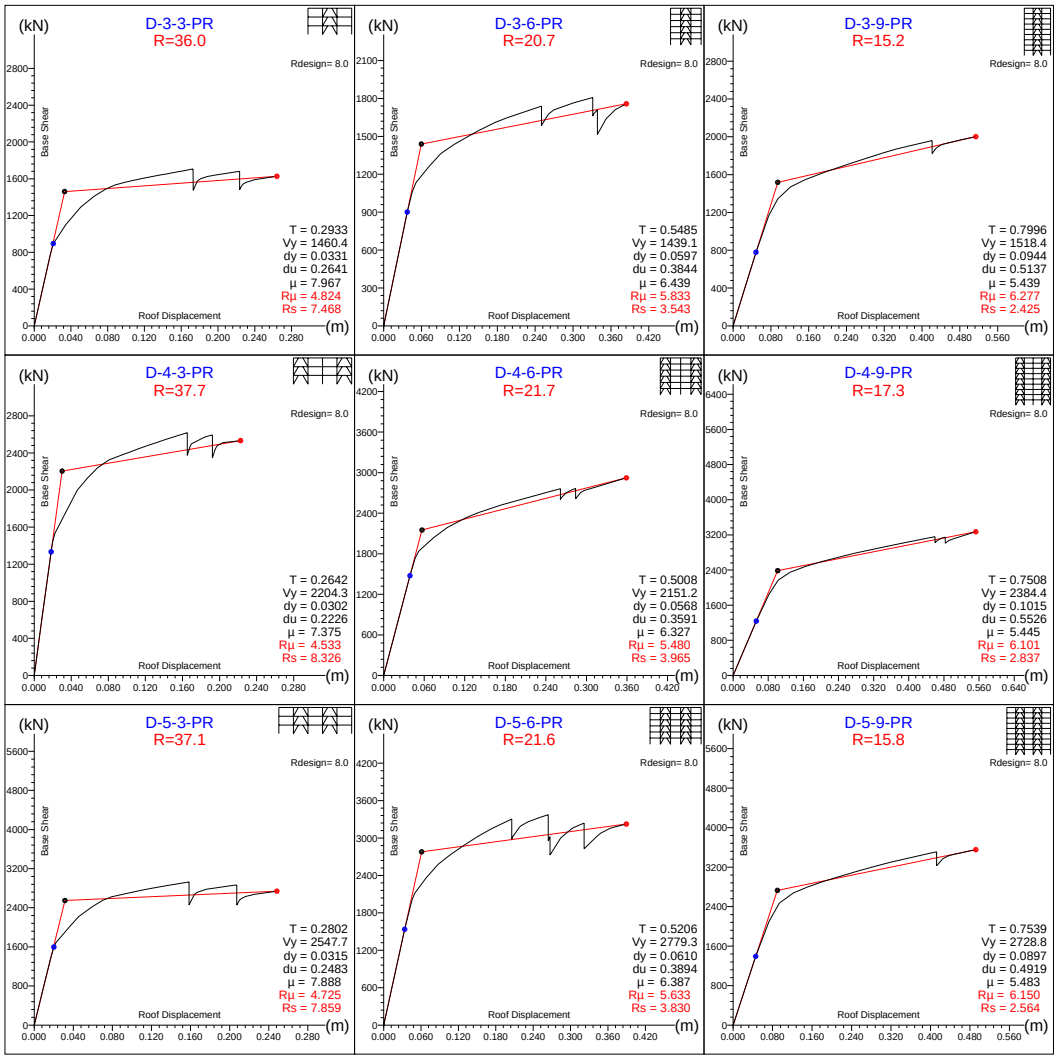

Figure 4.11: Frame Type **D** – "**PR**"
Base Shear vs. Roof Displacement Diagram

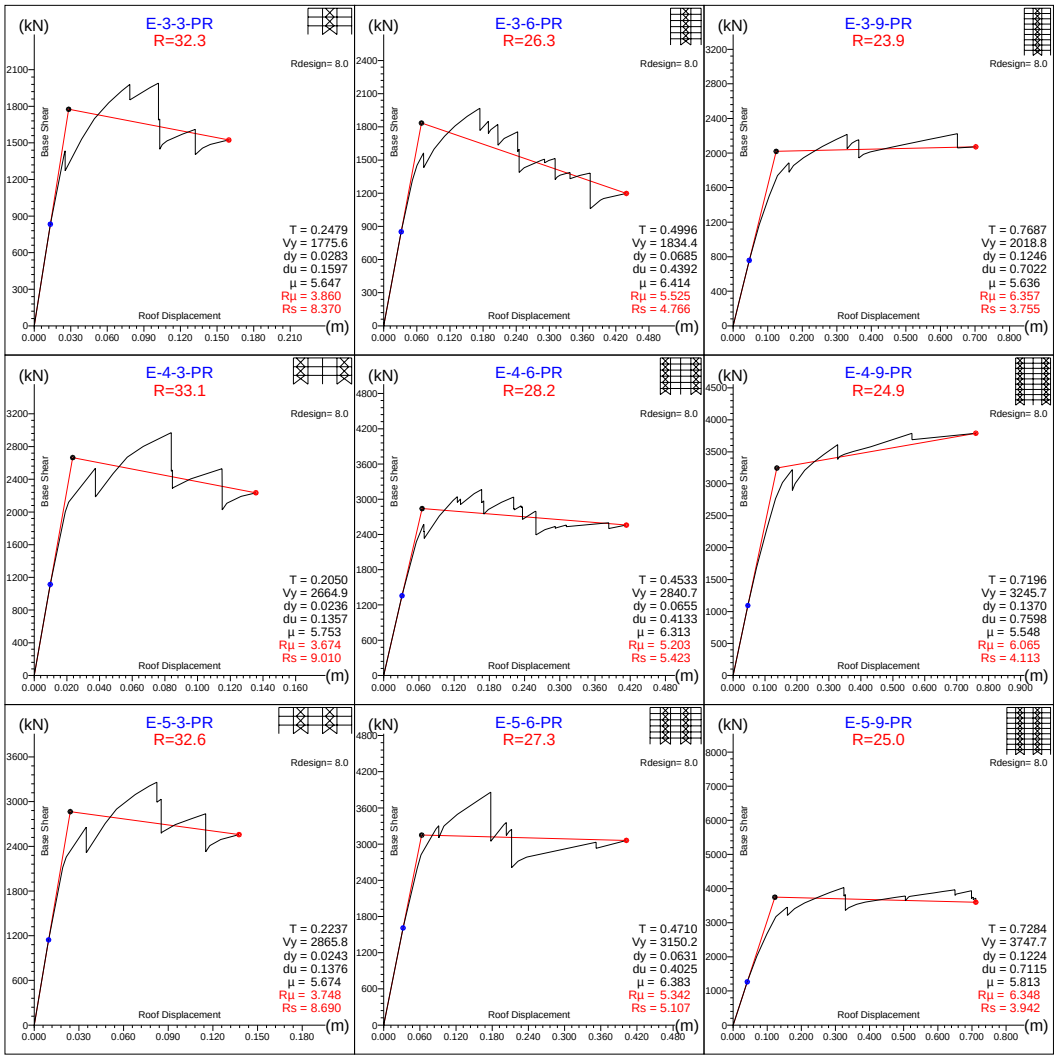

Figure 4.12: Frame Type **E** – "**PR**"
Base Shear vs. Roof Displacement Diagram

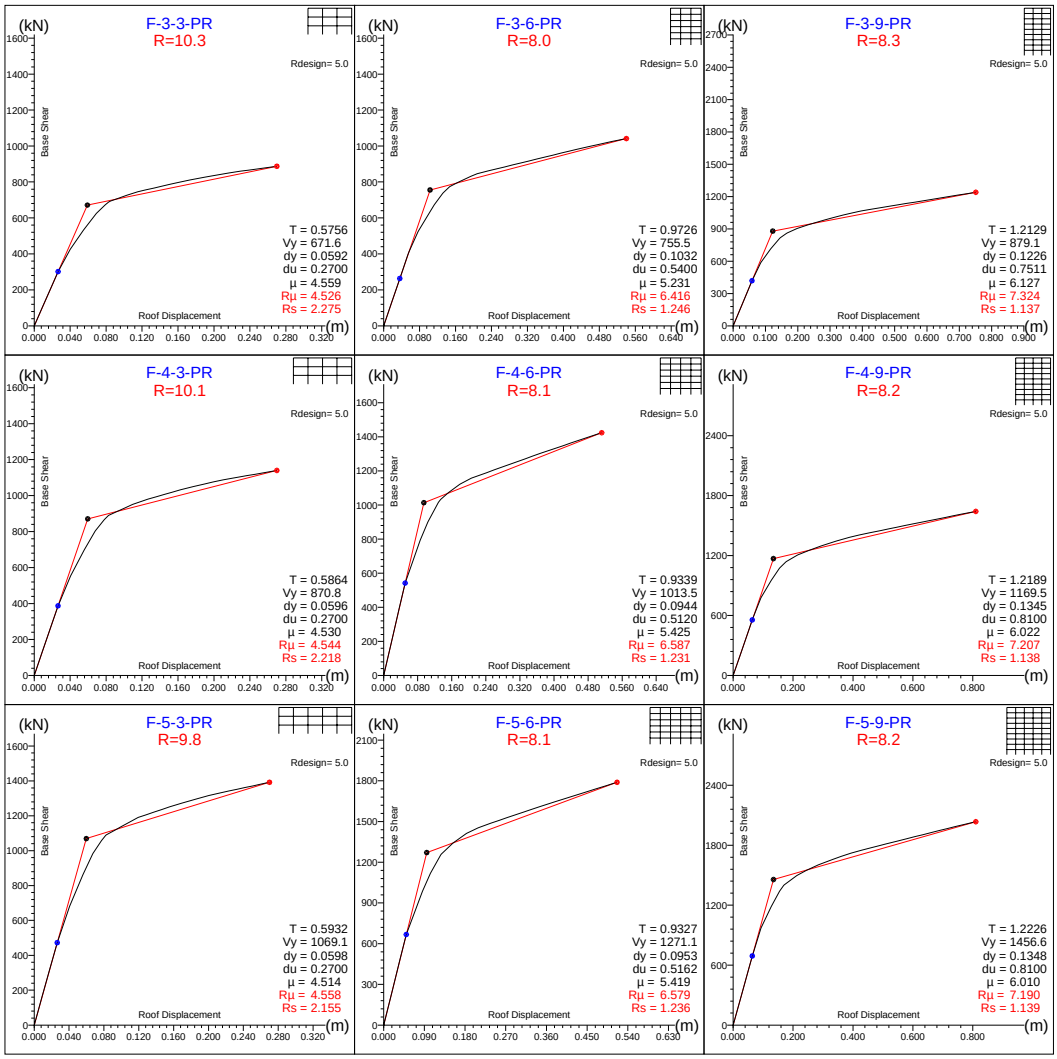

Figure 4.13: Frame Type **F** – "**PR"**
Base Shear vs. Roof Displacement Diagram

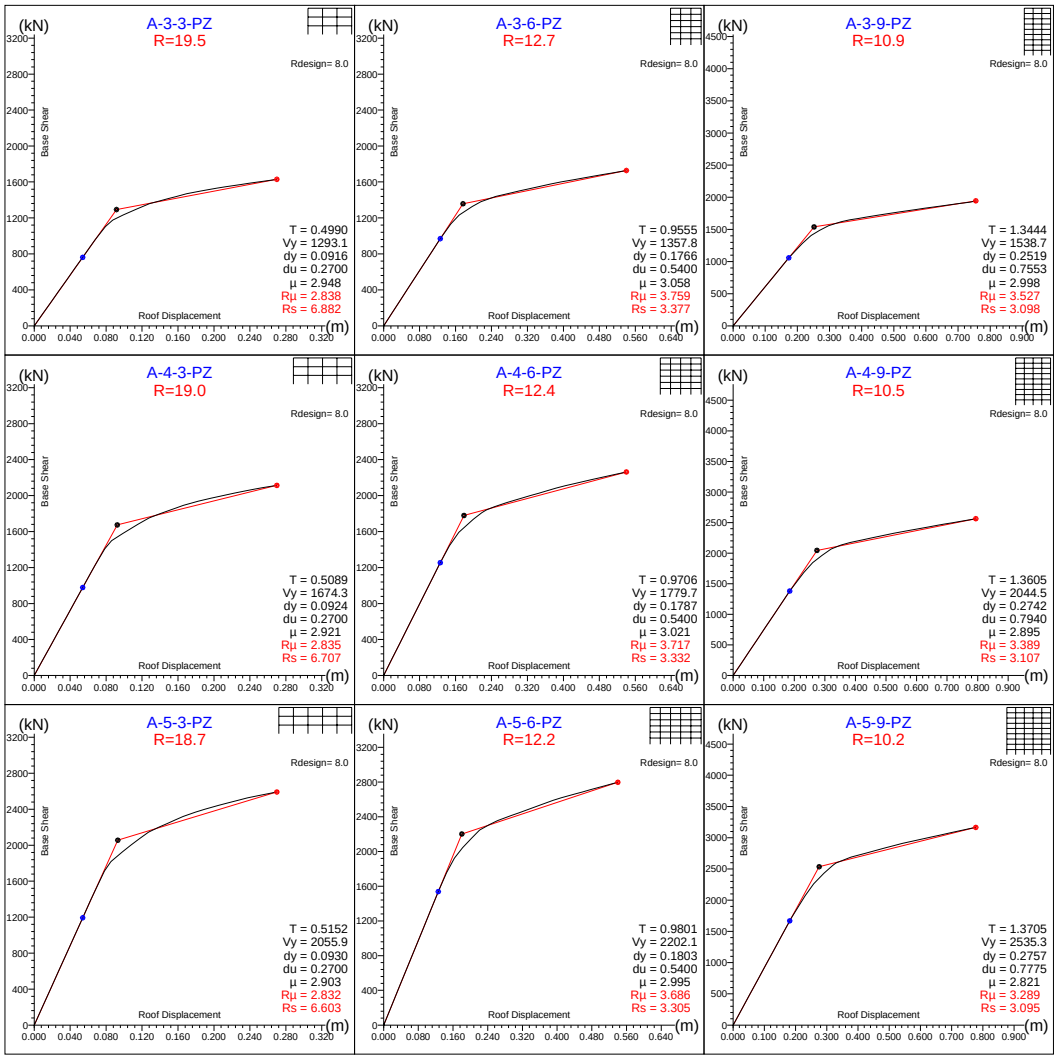

Figure 4.14: Frame Type **A** – "**PZ**"
Base Shear vs. Roof Displacement Diagram

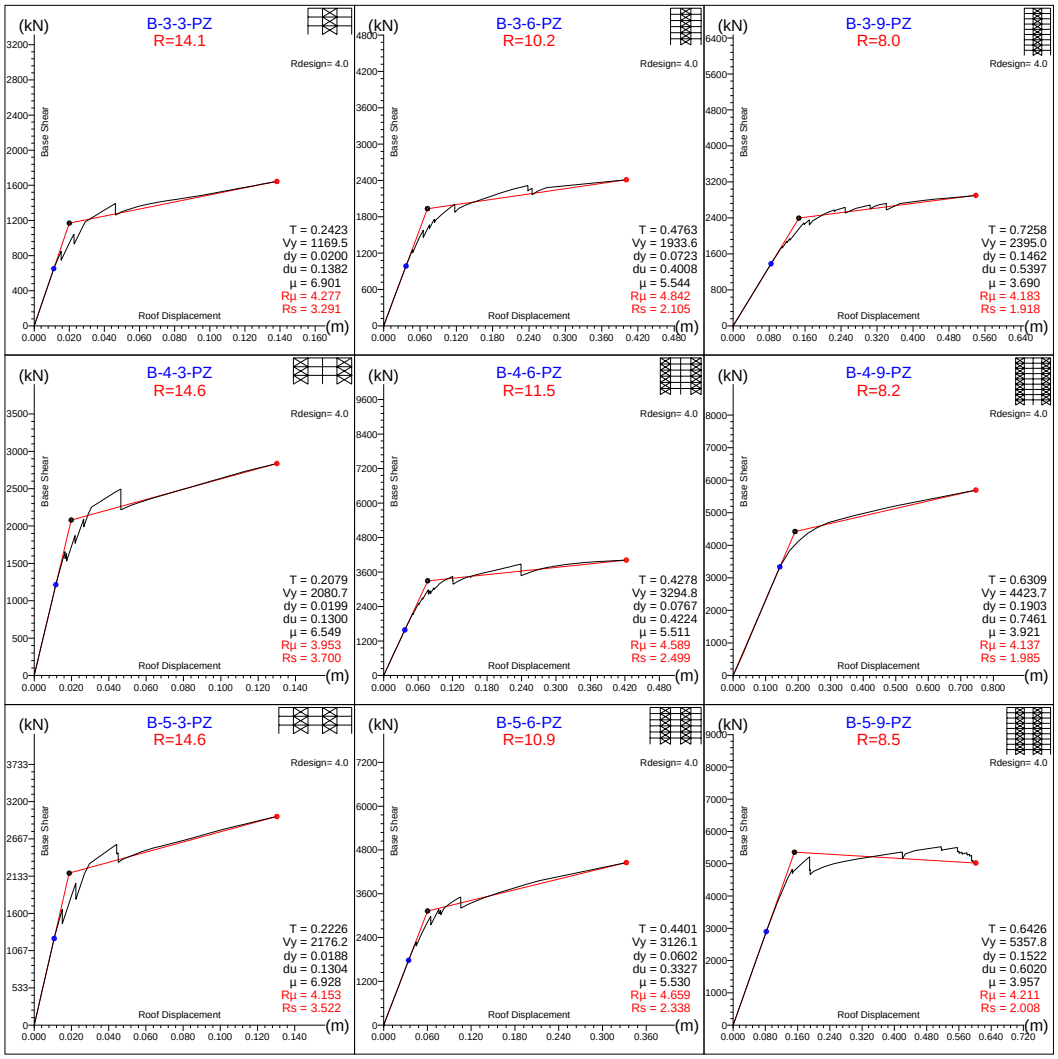

Figure 4.15: Frame Type **B** – "**PZ**"
Base Shear vs. Roof Displacement Diagram

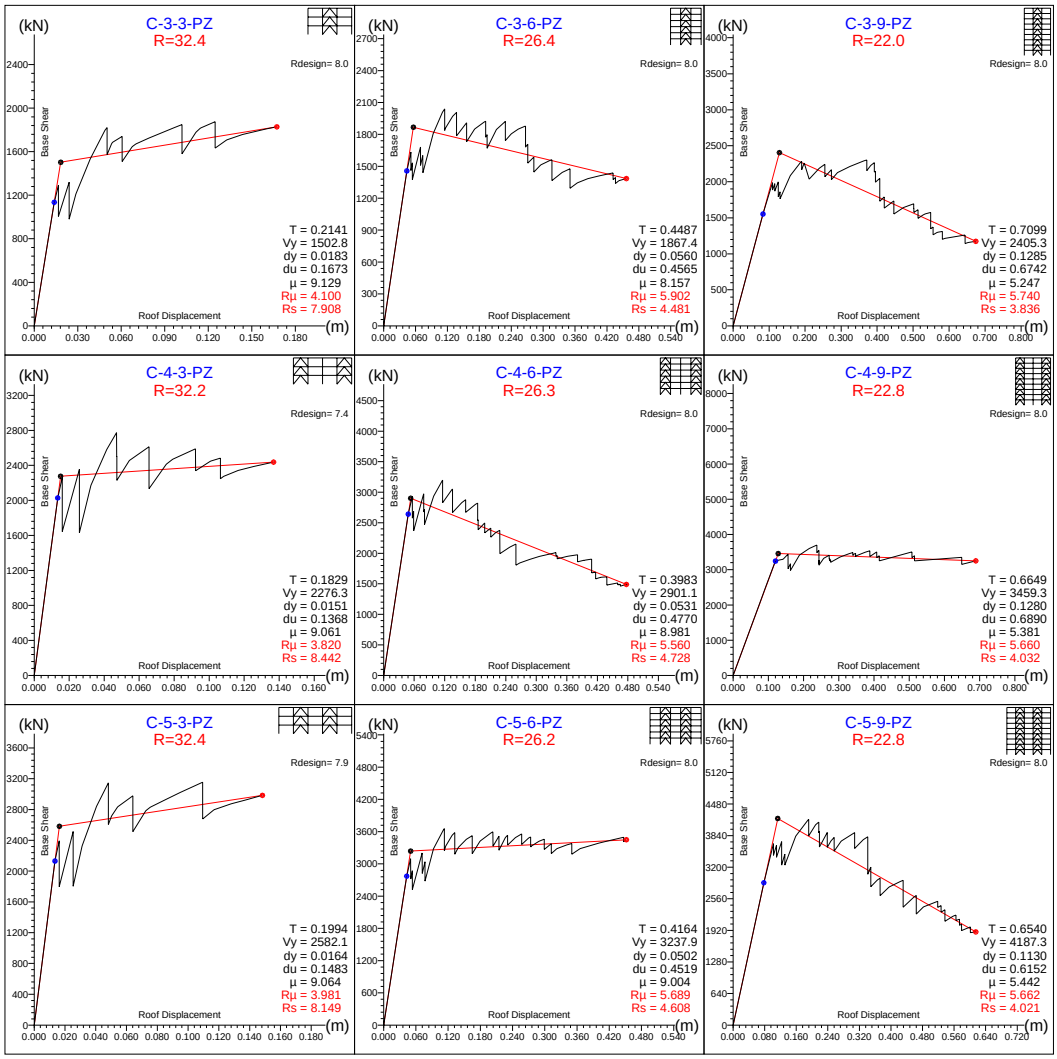

Figure 4.16: Frame Type **C** – "**PZ**"
Base Shear vs. Roof Displacement Diagram

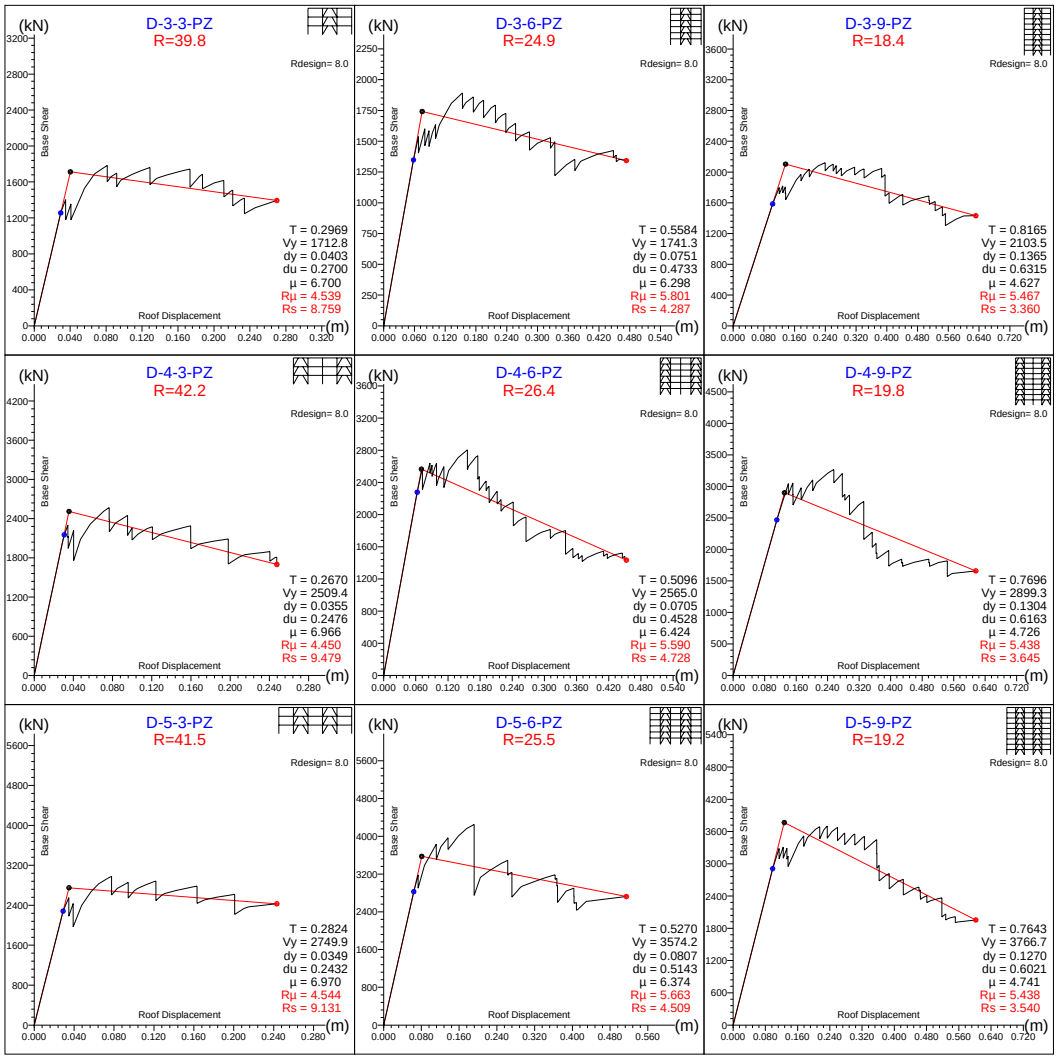

Figure 4.17: Frame Type **D** – **"PZ"**
Base Shear vs. Roof Displacement Diagram

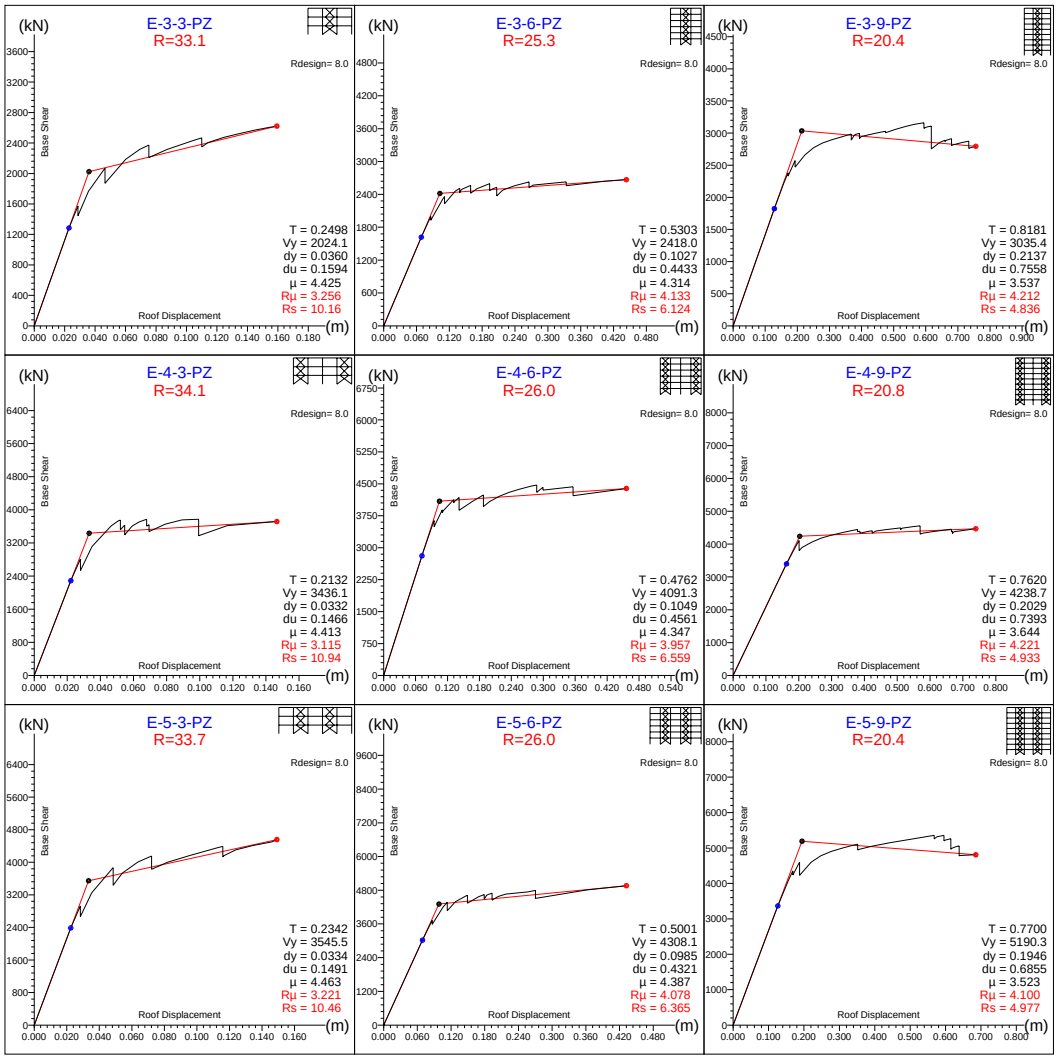

Figure 4.18: Frame Type **E** – "**PZ**"
Base Shear vs. Roof Displacement Diagram

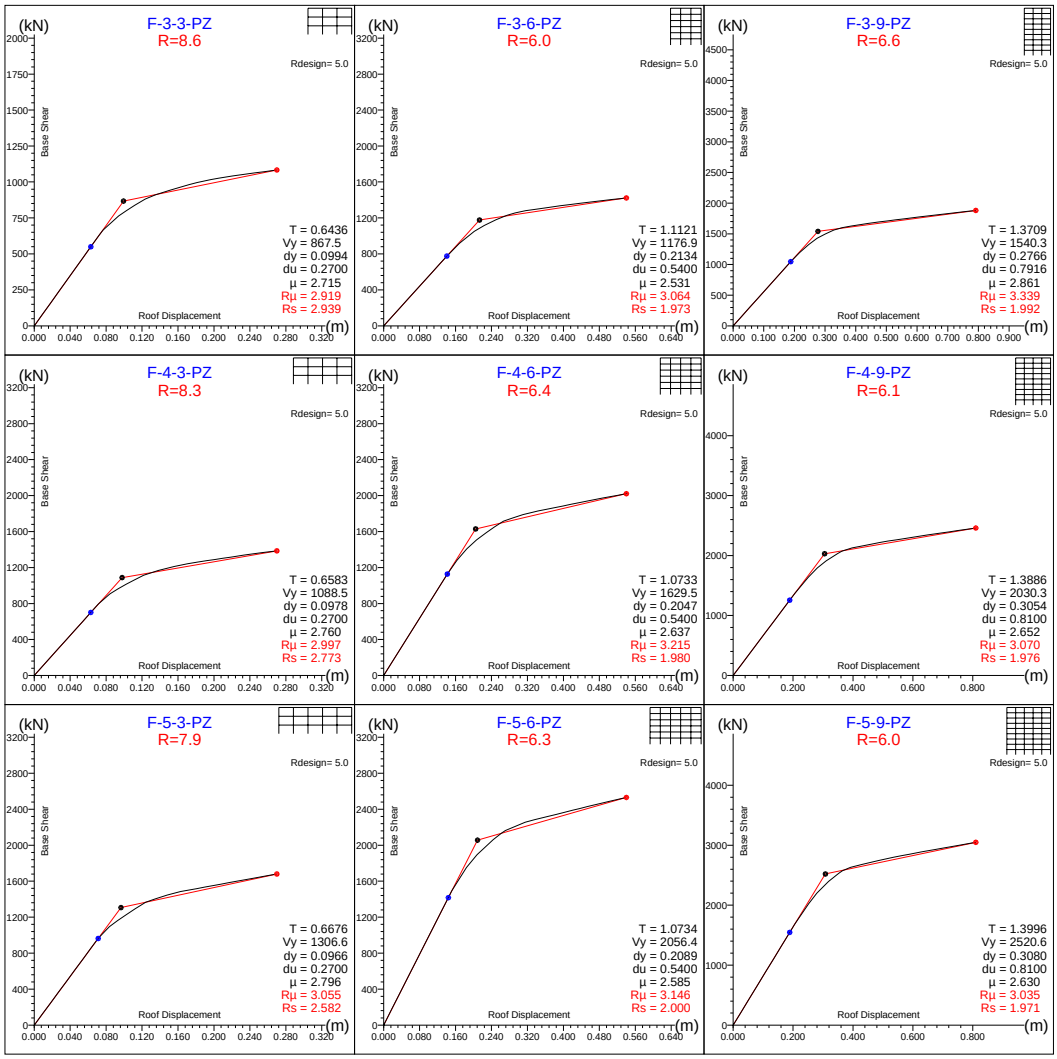

Figure 4.19: Frame Type **F** – "**PZ**"
Base Shear vs. Roof Displacement Diagram

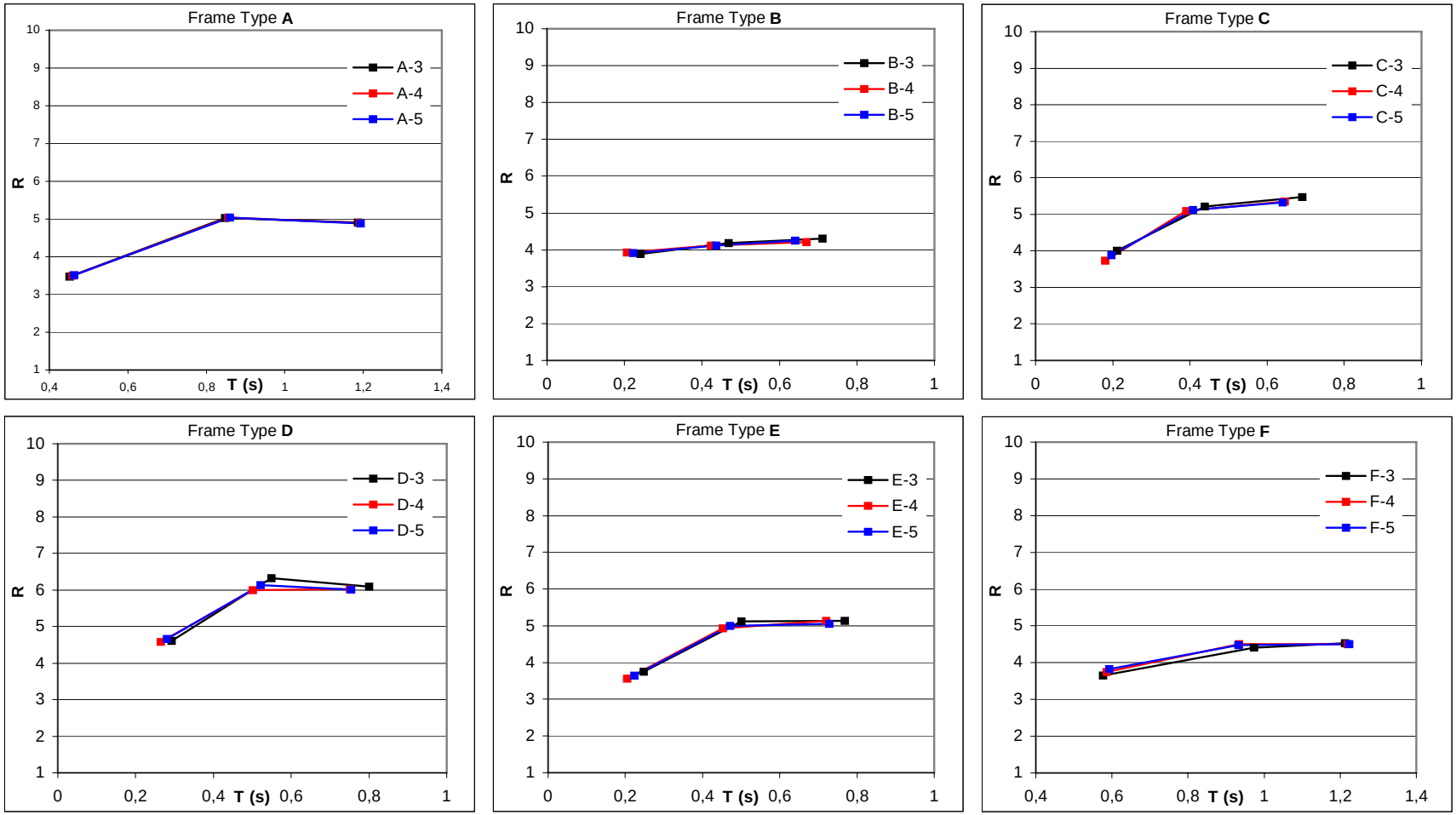

Figure 4.20: Ductility Reduction Factor (Rμ) vs. Period (T) – "**CL"**

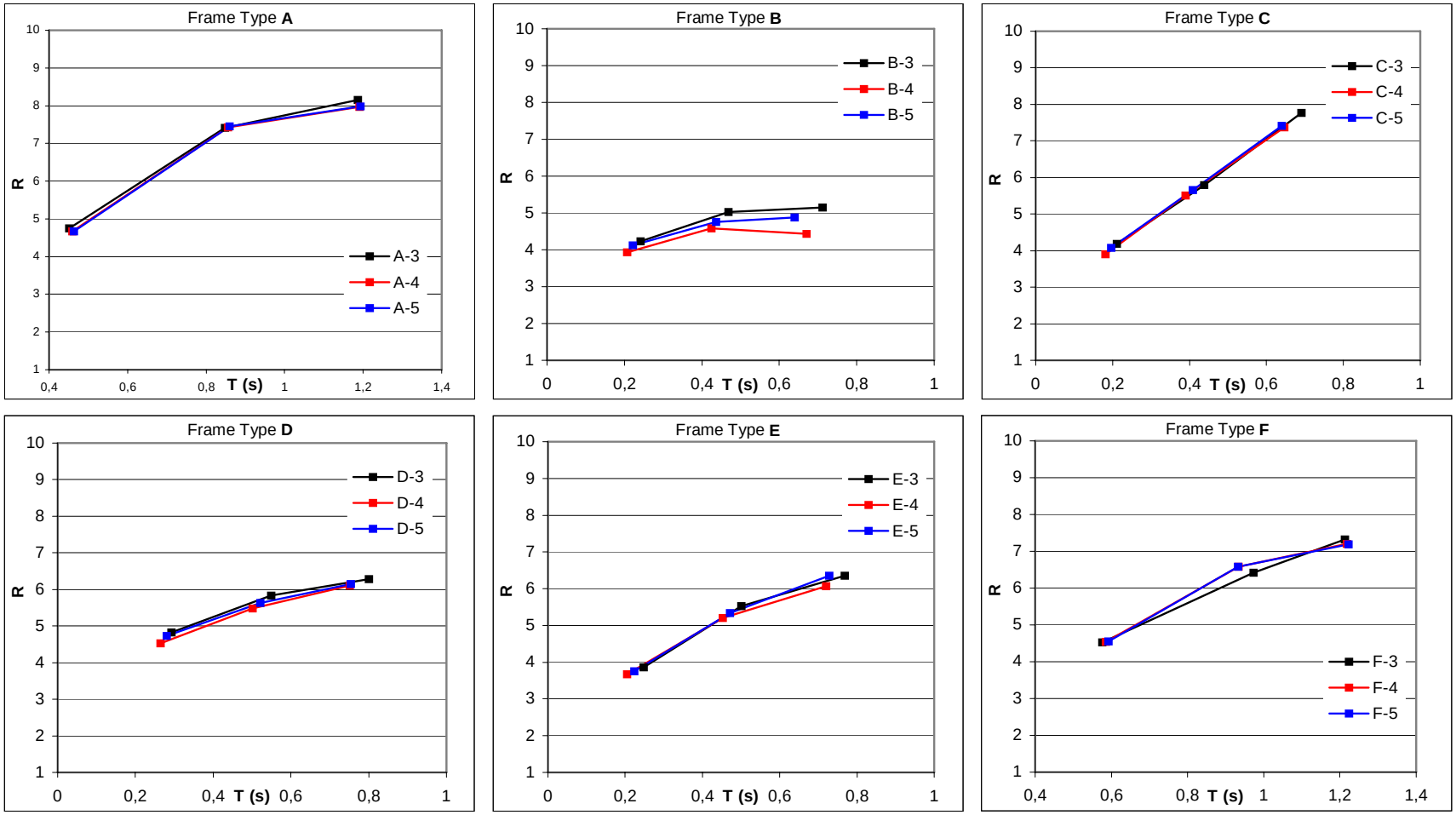

Figure 4.21: Ductility Reduction Factor (Rμ) vs. Period (T) – "**PR"**

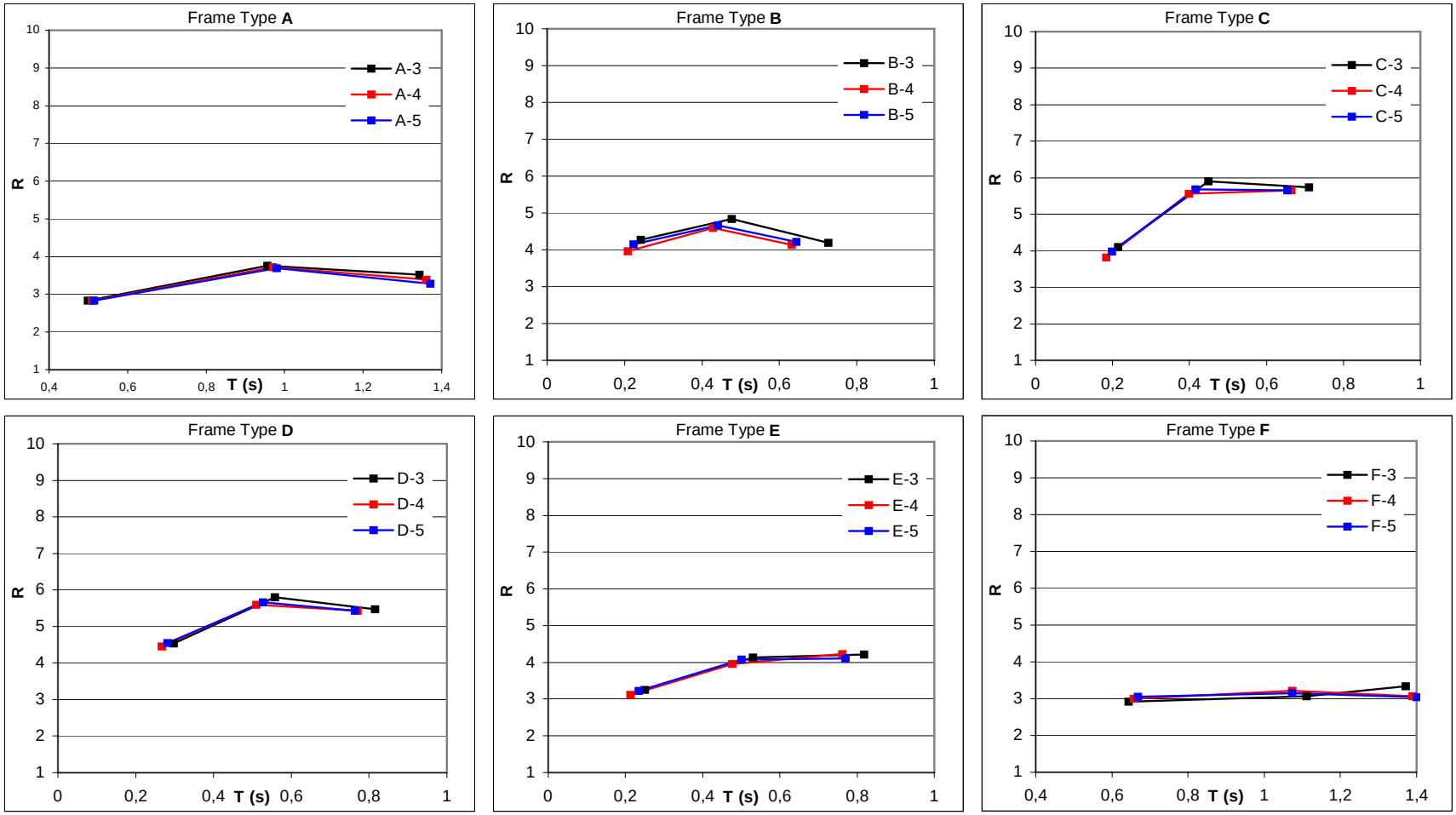

Figure 4.22: Ductility Reduction Factor (Rμ) vs. Period (T) – "**PZ**"

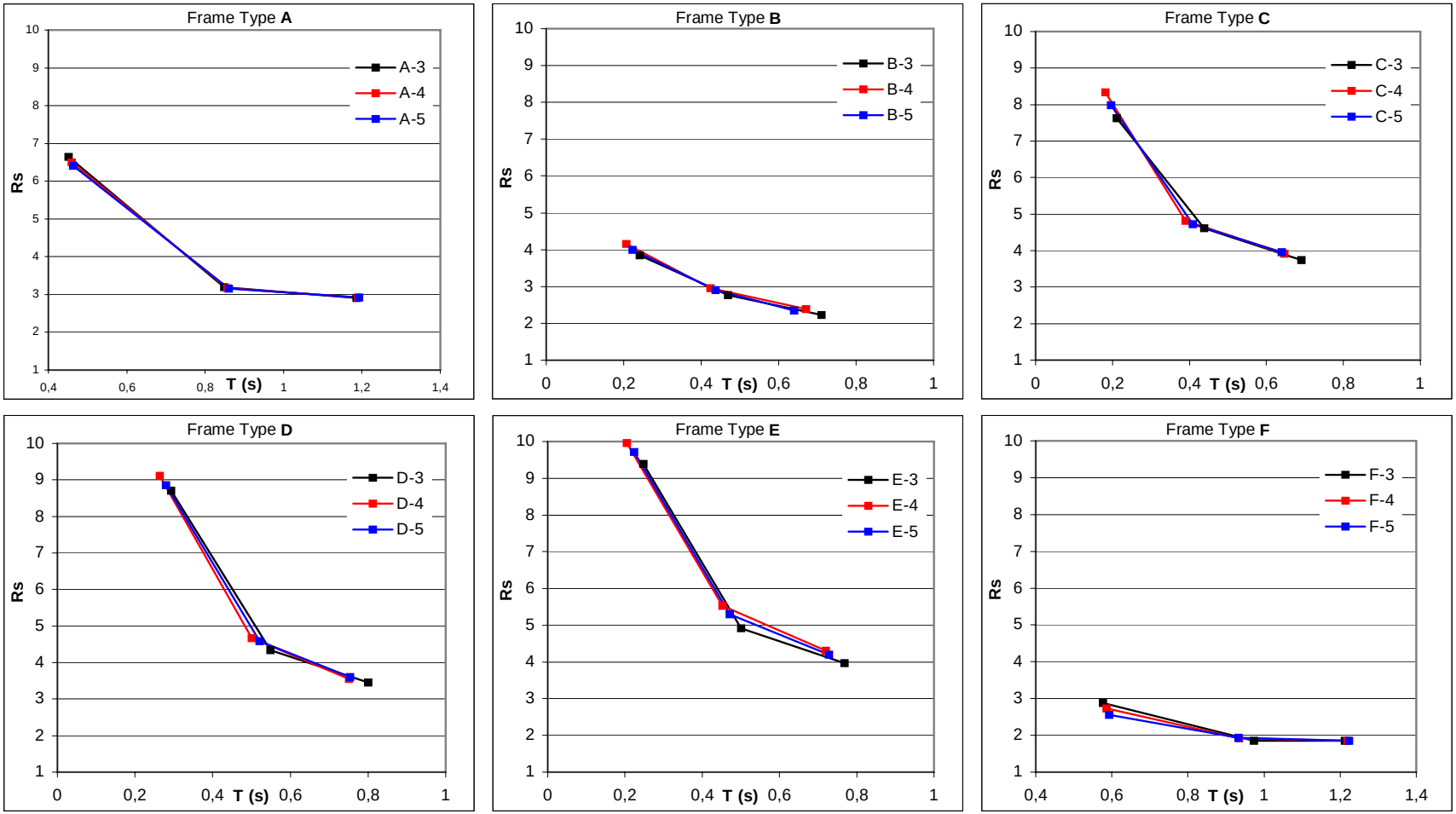

Figure 4.23: Overstrength Factor (Rs) vs. Period (T) – "**CL"**

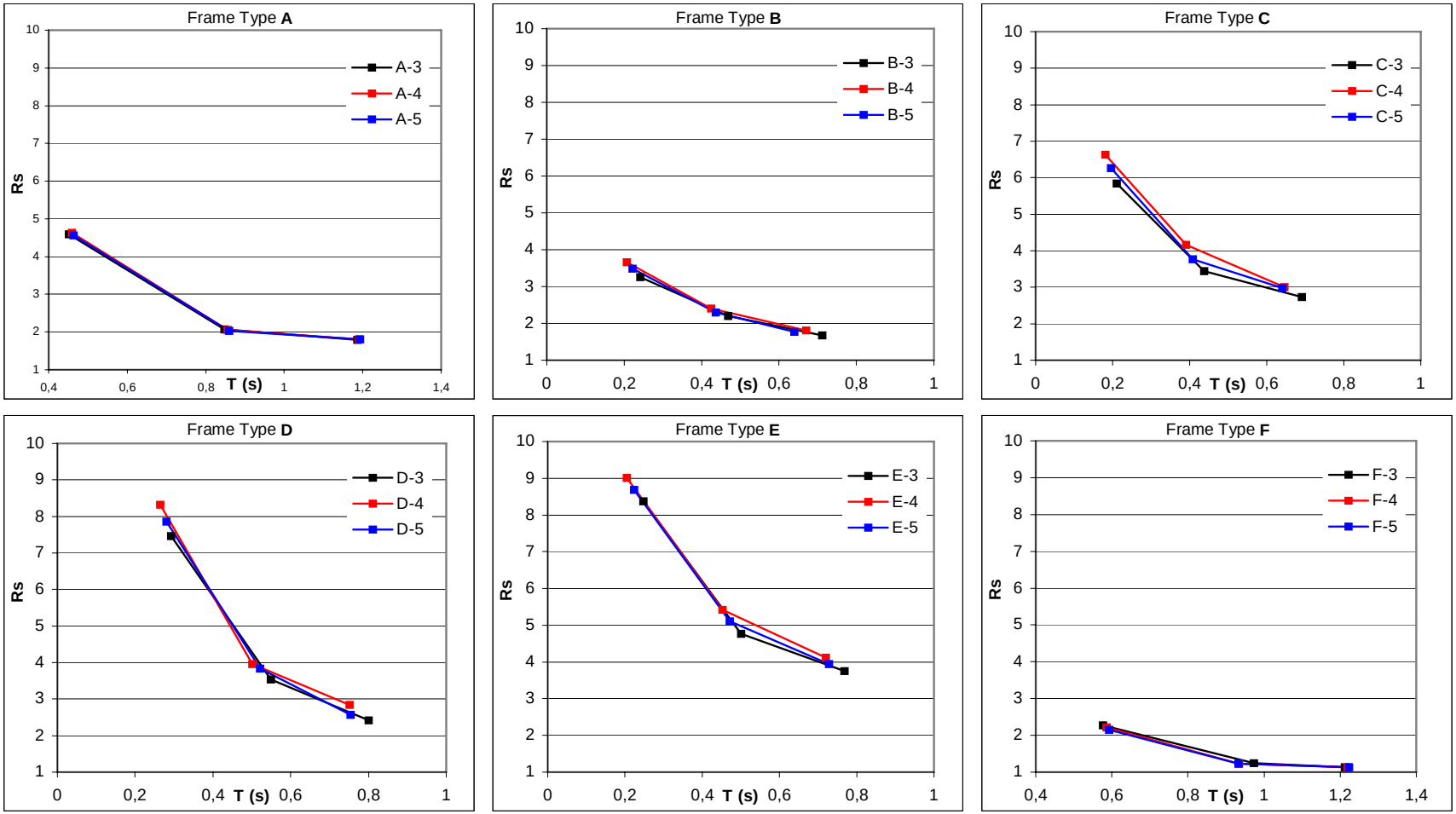

Figure 4.24: Overstrength Factor (Rs) vs. Period (T) – "**PR"**

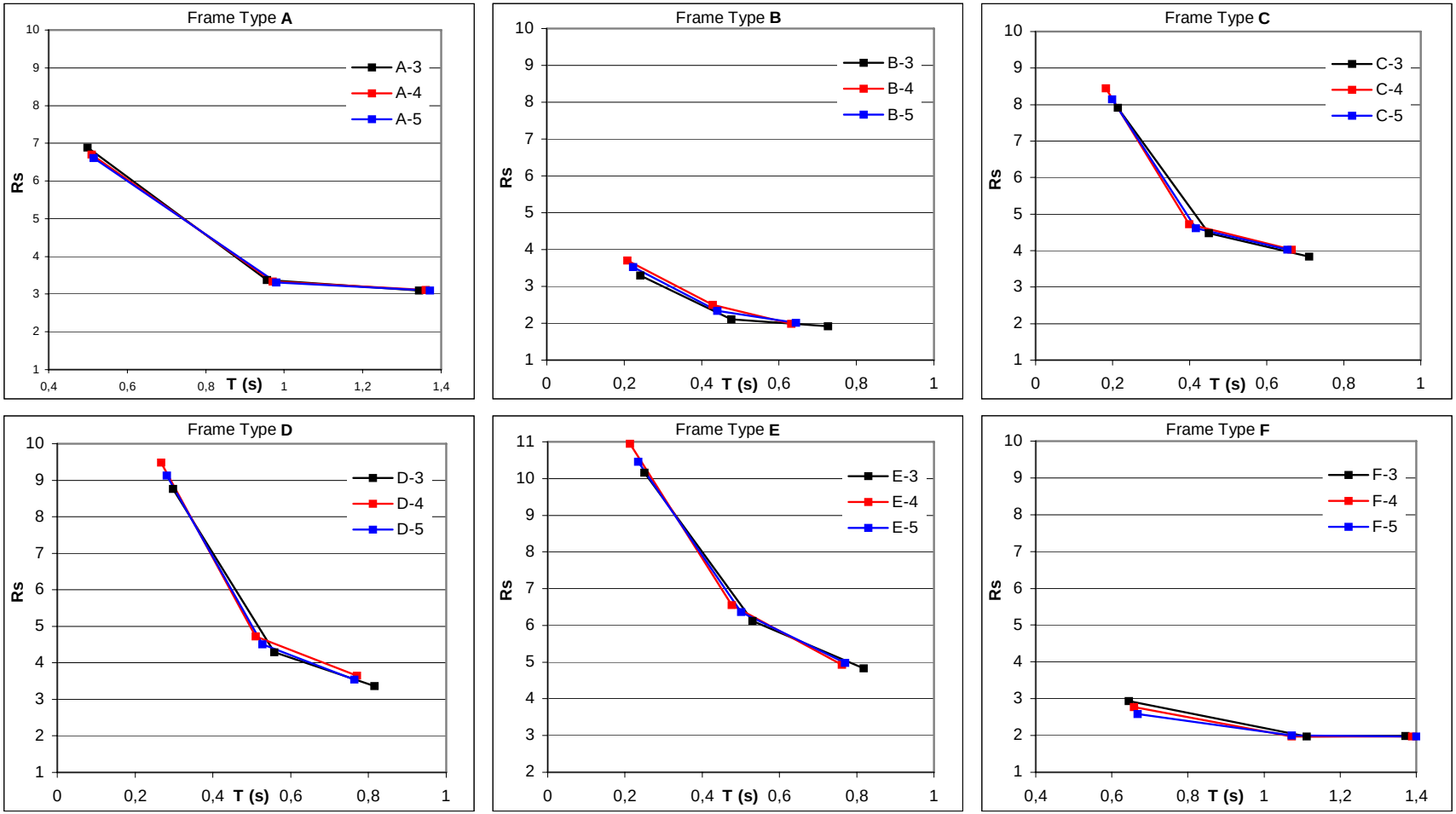

Figure 4.25: Overstrength Factor (Rs) vs. Period (T) – "**PZ**"

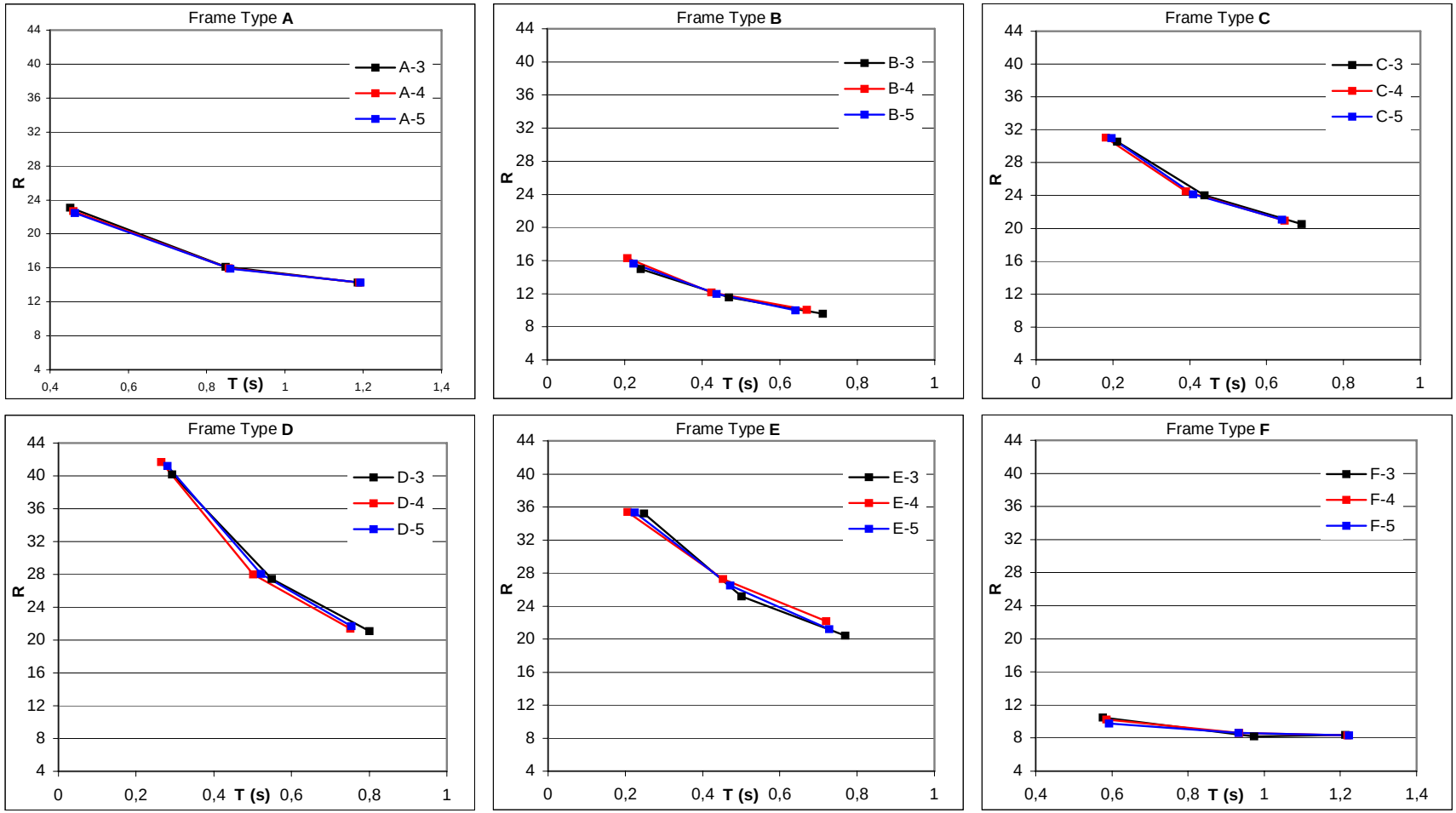

Figure 4.26: Response Modification Factor (R) vs. Period (T) – "**CL**"

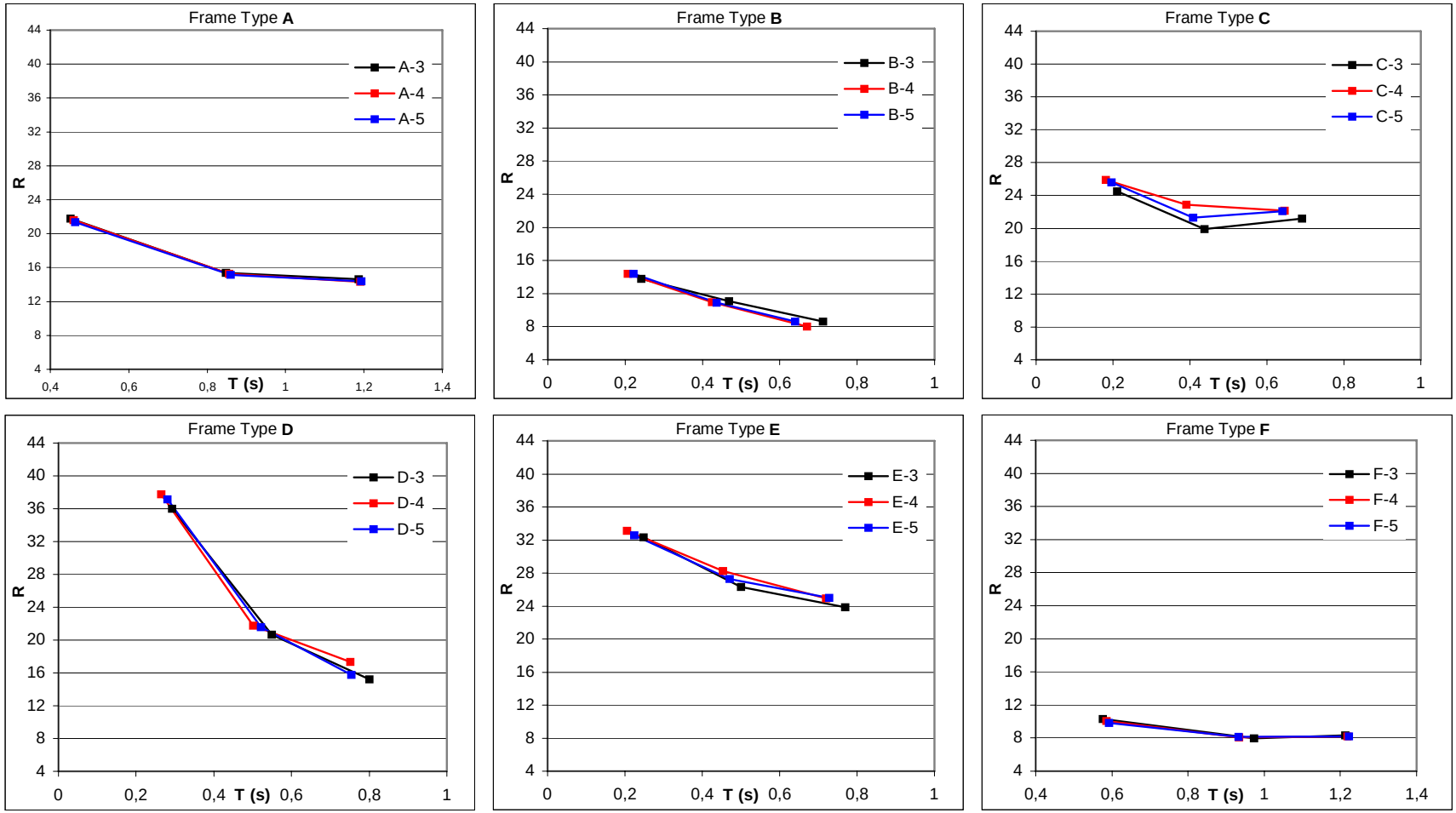

Figure 4.27: Response Modification Factor (R) vs. Period (T) – "**PR**"

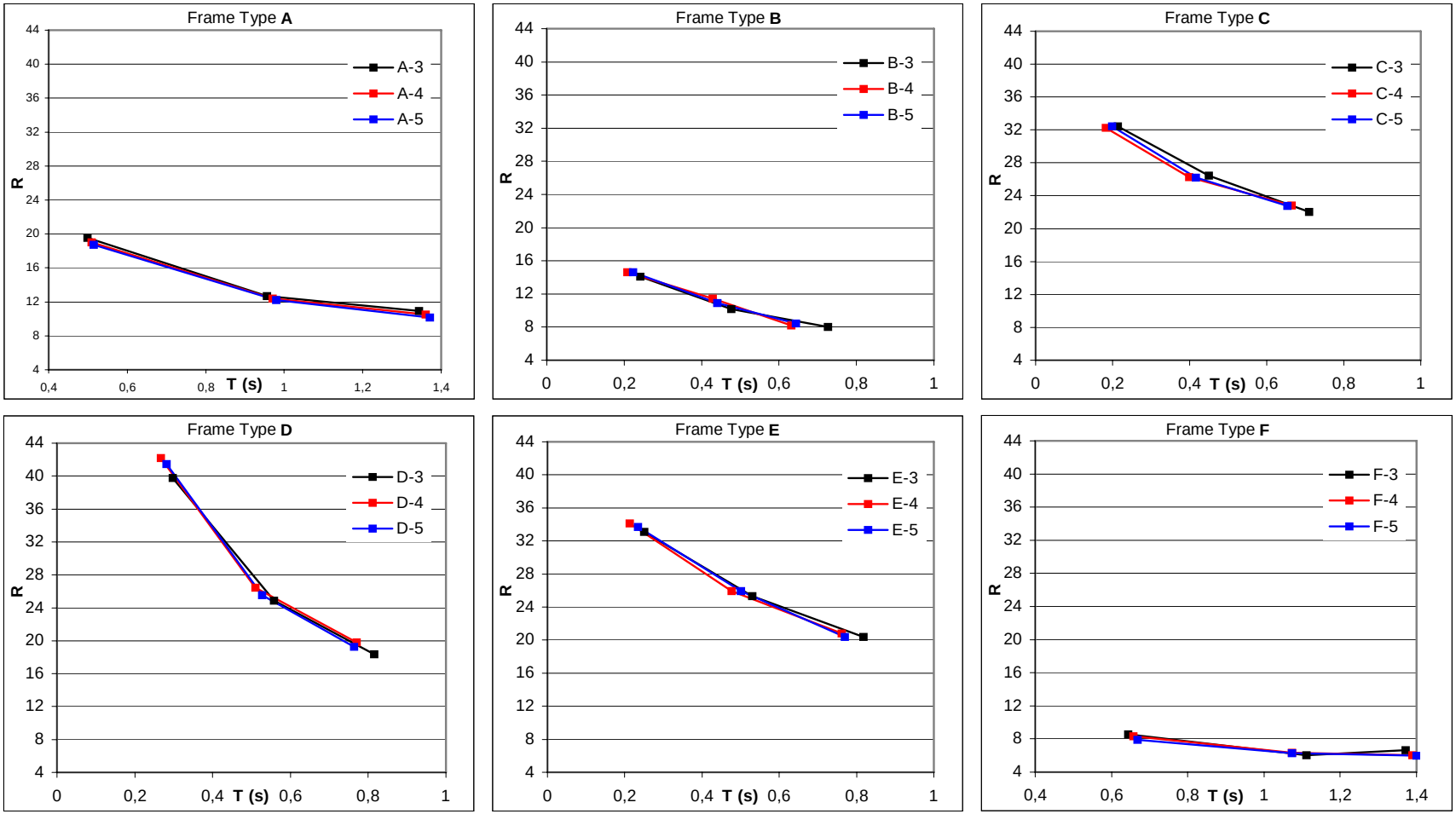

Figure 4.28: Response Modification Factor (R) vs. Period (T) – "**PR**"

Table 4.1: Calculated R Factors – "**CL"**

	1% Top Drift			Collapse State		
	Rμ	Rs	R	Rμ	Rs	R
A-3-3	1,55	5,33	8,25	3,48	6,64	23,09
A-3-6	1,81	2,78	5,02	5,03	3,20	16,11
A-3-9	1,86	2,62	4,88	4,91	2,91	14,30
A-4-3	1,53	5,29	8,10	3,49	6,50	22,72
A-4-6	1,79	2,78	4,96	5,04	3,17	15,97
A-4-9	1,76	2,59	4,55	4,89	2,92	14,29
A-5-3	1,53	5,24	8,00	3,51	6,40	22,48
A-5-6	1,78	2,77	4,92	5,04	3,15	15,88
A-5-9	1,74	2,61	4,54	4,88	2,92	14,25
B-3-3	3,35	3,10	10,36	3,89	3,85	14,97
B-3-6	2,80	2,07	5,78	4,19	2,76	11,57
B-3-9	2,30	1,77	4,07	4,31	2,22	9,59
B-4-3	3,18	4,17	13,26	3,92	4,15	16,29
B-4-6	2,49	2,70	6,71	4,12	2,95	12,16
B-4-9	1,55	2,11	3,26	4,22	2,39	10,06
B-5-3	3,38	3,48	11,75	3,91	3,99	15,61
B-5-6	2,93	2,19	6,41	4,12	2,91	11,97
B-5-9	2,25	2,27	5,09	4,26	2,35	9,98
C-3-3	3,69	7,09	26,16	4,00	7,63	30,54
C-3-6	3,26	4,29	13,97	5,22	4,61	24,04
C-3-9	2,73	3,45	9,42	5,48	3,75	20,51
C-4-3	3,67	8,43	30,97	3,73	8,33	31,07
C-4-6	3,06	5,37	16,43	5,09	4,82	24,51
C-4-9	2,16	4,61	9,95	5,34	3,92	20,93
C-5-3	3,74	7,65	28,57	3,88	7,98	31,00
C-5-6	3,36	4,65	15,61	5,12	4,72	24,16
C-5-9	3,04	3,54	10,74	5,32	3,97	21,09
D-3-3	2,29	7,65	17,50	4,61	8,71	40,16
D-3-6	2,51	4,29	10,75	6,33	4,34	27,48
D-3-9	2,49	3,21	8,00	6,10	3,46	21,07
D-4-3	2,38	8,83	20,98	4,58	9,11	41,70
D-4-6	2,29	5,35	12,28	6,00	4,67	27,98
D-4-9	2,22	3,83	8,52	6,02	3,55	21,40
D-5-3	2,39	7,96	18,99	4,66	8,85	41,21
D-5-6	2,38	5,05	12,01	6,13	4,58	28,07
D-5-9	2,73	3,26	8,90	6,02	3,60	21,69
E-3-3	2,40	9,20	22,04	3,75	9,39	35,24
E-3-6	2,07	5,61	11,60	5,12	4,91	25,16
E-3-9	2,09	3,75	7,81	5,13	3,98	20,40
E-4-3	2,48	11,29	27,93	3,56	9,96	35,40
E-4-6	1,88	7,35	13,84	4,93	5,53	27,26
E-4-9	1,76	4,70	8,28	5,14	4,31	22,17
E-5-3	2,46	10,00	24,59	3,64	9,71	35,37
E-5-6	1,98	6,40	12,68	5,00	5,30	26,52
E-5-9	2,20	4,00	8,80	5,05	4,20	21,19
F-3-3	1,39	2,54	3,52	3,65	2,88	10,51
F-3-6	1,48	1,64	2,42	4,41	1,86	8,21
F-3-9	1,72	1,63	2,80	4,53	1,86	8,40
F-4-3	1,40	2,44	3,42	3,75	2,74	10,26
F-4-6	1,60	1,64	2,61	4,51	1,92	8,65
F-4-9	1,58	1,59	2,51	4,50	1,85	8,34
F-5-3	1,41	2,30	3,25	3,83	2,55	9,78
F-5-6	1,58	1,64	2,59	4,48	1,93	8,63
F-5-9	1,58	1,59	2,51	4,50	1,85	8,33

Table 4.2: Calculated R Factors – "**PR"**

	1% Top Drift			Collapse State		
	Rμ	Rs	R	Rμ	Rs	R
A-3-3	2,65	2,99	7,93	2,65	2,99	21,75
A-3-6	3,32	1,61	5,33	3,32	1,61	15,36
A-3-9	3,39	1,54	5,20	3,39	1,54	14,62
A-4-3	2,65	2,94	7,80	2,65	2,94	21,57
A-4-6	3,28	1,61	5,28	3,28	1,61	15,24
A-4-9	3,18	1,53	4,86	3,18	1,53	14,34
A-5-3	2,64	2,93	7,72	2,64	2,93	21,35
A-5-6	3,26	1,61	5,25	3,26	1,61	15,16
A-5-9	3,17	1,54	4,87	3,17	1,54	14,36
B-3-3	3,36	3,08	10,35	3,36	3,08	13,76
B-3-6	2,85	2,03	5,77	2,85	2,03	11,10
B-3-9	2,67	1,54	4,11	2,67	1,54	8,62
B-4-3	3,18	4,17	13,25	3,18	4,17	14,40
B-4-6	2,51	2,68	6,70	2,51	2,68	10,99
B-4-9	1,65	1,89	3,10	1,65	1,89	8,03
B-5-3	3,39	3,47	11,74	3,39	3,47	14,40
B-5-6	2,98	2,15	6,40	2,98	2,15	10,91
B-5-9	2,75	1,86	5,11	2,75	1,86	8,62
C-3-3	4,09	5,77	23,59	4,09	5,77	24,51
C-3-6	4,04	3,35	13,52	4,04	3,35	19,92
C-3-9	3,53	2,68	9,46	3,53	2,68	21,18
C-4-3	3,93	7,08	27,80	3,93	7,08	25,89
C-4-6	3,31	4,89	16,18	3,31	4,89	22,90
C-4-9	2,99	3,35	10,02	2,99	3,35	22,15
C-5-3	4,03	6,36	25,62	4,03	6,36	25,59
C-5-6	3,75	4,08	15,31	3,75	4,08	21,29
C-5-9	3,65	2,92	10,67	3,65	2,92	22,07
D-3-3	2,92	5,71	16,67	2,92	5,71	36,03
D-3-6	3,52	3,01	10,58	3,52	3,01	20,67
D-3-9	3,69	2,22	8,18	3,69	2,22	15,22
D-4-3	2,88	6,97	20,09	2,88	6,97	37,74
D-4-6	3,27	3,67	12,00	3,27	3,67	21,73
D-4-9	3,27	2,66	8,71	3,27	2,66	17,31
D-5-3	2,91	6,26	18,20	2,91	6,26	37,13
D-5-6	3,44	3,41	11,76	3,44	3,41	21,57
D-5-9	3,78	2,41	9,12	3,78	2,41	15,77
E-3-3	2,87	7,87	22,62	2,87	7,87	32,31
E-3-6	2,85	4,01	11,40	2,85	4,01	26,33
E-3-9	3,14	2,57	8,06	3,14	2,57	23,87
E-4-3	3,09	8,40	25,99	3,09	8,40	33,10
E-4-6	2,60	5,15	13,40	2,60	5,15	28,22
E-4-9	2,72	3,14	8,55	2,72	3,14	24,95
E-5-3	2,90	8,07	23,44	2,90	8,07	32,57
E-5-6	2,83	4,78	13,54	2,83	4,78	27,28
E-5-9	3,21	3,07	9,87	3,21	3,07	25,02
F-3-3	2,20	1,62	3,55	2,20	1,62	10,30
F-3-6	2,61	0,99	2,60	2,61	0,99	7,99
F-3-9	3,09	0,97	2,99	3,09	0,97	8,33
F-4-3	2,15	1,61	3,46	2,15	1,61	10,08
F-4-6	2,82	1,00	2,82	2,82	1,00	8,11
F-4-9	2,82	0,96	2,70	2,82	0,96	8,20
F-5-3	2,12	1,55	3,30	2,12	1,55	9,82
F-5-6	2,83	0,99	2,81	2,83	0,99	8,13
F-5-9	2,81	0,96	2,70	2,81	0,96	8,19

Table 4.3: Calculated “R” Factors – “**PZ”**

	1% Top Drift			Collapse State		
	Rμ	Rs	R	Rμ	Rs	R
A-3-3	1,17	5,74	6,74	1,17	5,74	19,53
A-3-6	1,32	2,80	3,69	1,32	2,80	12,69
A-3-9	1,40	2,53	3,55	1,40	2,53	10,93
A-4-3	1,17	5,60	6,52	1,17	5,60	19,01
A-4-6	1,32	2,73	3,59	1,32	2,73	12,39
A-4-9	1,32	2,44	3,23	1,32	2,44	10,53
A-5-3	1,16	5,50	6,38	1,16	5,50	18,70
A-5-6	1,32	2,68	3,53	1,32	2,68	12,18
A-5-9	1,33	2,41	3,20	1,33	2,41	10,18
B-3-3	3,35	3,06	10,23	3,35	3,06	14,08
B-3-6	2,77	2,04	5,66	2,77	2,04	10,19
B-3-9	2,22	1,77	3,94	2,22	1,77	8,02
B-4-3	3,17	4,16	13,17	3,17	4,16	14,63
B-4-6	2,44	2,71	6,60	2,44	2,71	11,47
B-4-9	1,74	2,26	3,93	1,74	2,26	8,21
B-5-3	3,39	3,45	11,69	3,39	3,45	14,63
B-5-6	2,92	2,19	6,39	2,92	2,19	10,89
B-5-9	2,21	2,29	5,05	2,21	2,29	8,46
C-3-3	3,67	6,94	25,43	3,67	6,94	32,42
C-3-6	3,24	4,14	13,42	3,24	4,14	26,45
C-3-9	2,75	3,28	9,01	2,75	3,28	22,02
C-4-3	3,74	8,15	30,46	3,74	8,15	32,25
C-4-6	3,04	5,21	15,82	3,04	5,21	26,29
C-4-9	2,39	4,00	9,53	2,39	4,00	22,82
C-5-3	3,74	7,44	27,79	3,74	7,44	32,44
C-5-6	3,33	4,54	15,10	3,33	4,54	26,21
C-5-9	2,88	3,62	10,40	2,88	3,62	22,77
D-3-3	2,31	7,34	16,91	2,31	7,34	39,76
D-3-6	2,58	4,03	10,40	2,58	4,03	24,87
D-3-9	2,53	3,06	7,72	2,53	3,06	18,37
D-4-3	2,41	8,42	20,31	2,41	8,42	42,18
D-4-6	2,35	4,99	11,74	2,35	4,99	26,43
D-4-9	2,36	3,46	8,15	2,36	3,46	19,82
D-5-3	2,42	7,65	18,48	2,42	7,65	41,49
D-5-6	2,39	4,90	11,73	2,39	4,90	25,53
D-5-9	2,75	3,21	8,83	2,75	3,21	19,25
E-3-3	2,17	9,99	21,69	2,17	9,99	33,07
E-3-6	1,88	5,55	10,41	1,88	5,55	25,31
E-3-9	1,80	3,79	6,82	1,80	3,79	20,37
E-4-3	2,22	12,83	28,50	2,22	12,83	34,09
E-4-6	1,81	6,94	12,55	1,81	6,94	25,95
E-4-9	1,58	4,57	7,24	1,58	4,57	20,82
E-5-3	2,22	10,88	24,17	2,22	10,88	33,69
E-5-6	1,84	6,21	11,45	1,84	6,21	25,96
E-5-9	1,89	4,06	7,67	1,89	4,06	20,41
F-3-3	1,20	2,28	2,72	1,20	2,28	8,58
F-3-6	1,25	1,41	1,76	1,25	1,41	6,05
F-3-9	1,35	1,53	2,06	1,35	1,53	6,65
F-4-3	1,21	2,16	2,61	1,21	2,16	8,31
F-4-6	1,20	1,52	1,82	1,20	1,52	6,37
F-4-9	1,23	1,48	1,82	1,23	1,48	6,07
F-5-3	1,22	2,02	2,47	1,22	2,02	7,89
F-5-6	1,21	1,50	1,81	1,21	1,50	6,29
F-5-9	1,23	1,46	1,80	1,23	1,46	5,98

Table 4.4: “R” Factors Comparison for Frame Type **G**

(Zone 1)	Rμ		(Zone 4)
A-4-9 →	**4.894**	**3.733**	**← G-4-1**
B-4-9 →	**4.217**	**4.241**	**← G-4-2**
C-4-9 →	**5.344**	**4.518**	**← G-4-3**
D-4-9 →	**6.023**	**3.991**	**← G-4-4**
E-4-9 →	**5.14**	**3.249**	**← G-4-5**
F-4-9 →	**4.504**	**3.955**	**← G-4-6**
Rs			
A-4-9 →	**2.919**	**7.580**	**← G-4-1**
B-4-9 →	**2.385**	**7.667**	**← G-4-2**
C-4-9 →	**3.926**	**13.29**	**← G-4-3**
D-4-9 →	**3.553**	**10.67**	**← G-4-4**
E-4-9 →	**4.313**	**14.17**	**← G-4-5**
F-4-9 →	**1.852**	**5.015**	**← G-4-6**
R			
A-4-9 →	**14.3**	**28.3**	**← G-4-1**
B-4-9 →	**10.1**	**32.5**	**← G-4-2**
C-4-9 →	**20.9**	**60.1**	**← G-4-3**
D-4-9 →	**21.4**	**42.6**	**← G-4-4**
E-4-9 →	**22.2**	**46.0**	**← G-4-5**
F-4-9 →	**8.3**	**19.8**	**← G-4-6**

Table 4.5: Design Base Shear Comparison for Frame Type **G**

(Zone 1)	Vd (kN)		(Zone 4)
A-4-9 →	**657.96**	**122.49**	**← G-4-1**
B-4-9 →	**1677.04**	**410.65**	**← G-4-2**
C-4-9 →	**838.01**	**203.45**	**← G-4-3**
D-4-9 →	**836.33**	**209.08**	**← G-4-4**
E-4-9 →	**839.70**	**209.93**	**← G-4-5**
F-4-9 →	**1027.50**	**188.45**	**← G-4-6**

CHAPTER 5

SUMMARY OF RESULTS AND CONCLUSIONS

5.1 SUMMARY OF RESULTS

In this section, results of the analysis and evaluations of this study are tried to be summarized.

Ductility reduction factor (Rμ) shows an increasing trend when raised to 6 stories from 3 stories. Except from PR frames this rise is followed by a constant plateau or a slight increase/decrease while reaching nine stories. PR frames possess greater Rμ of all; followed by CL and PZ frames afterwards for both collapse and 1% top drift states.

On the contrary significant decreasing trend of overstrength factor (Rs) with increasing period can be traced for all framing systems except for type “F”. However the fall from 6 stories to 9 stories is not as substantial as the fall from 3 stories to 6 stories. For all connection types Frame type “F” (normally ductility moment resisting frame) shows an almost constant trend of Rs.

Obviously it is not expected to obtain different overstrength levels between collapse and 1% drift states however an insignificant increase in Rs is observed for all systems due to the bilinear approximation. Panel zone inclusion seems to elevate the yield level of frames resulting higher Rs. PZ frames are followed by CL and PR frames with respect to overstrength factors.

The overall response modification factor which is the product of abovementioned sub-factors, have a tendency to decrease with the increasing period. This is valid for each system without exceptions. Again the frame type “F” shows a little change in behavior.

If connection performance is to be compared, it can be said that panel zone modeling, while increasing the structural period, decreases the lateral load carrying capacity of frames thus resulting in slightly lower values of R factors. Partially restrained connections add significant ductility to the frames but the particular connection type chosen, has considerable reduction on plastic moment capacity which directly results in lower values of R factors. Center-line modeled frames possess greater R of all; followed by PR and PZ frames afterwards for both collapse and 1% top drift states.

A generalized behavior trend for frame types can not be justified from results of this parametric study. However it can be said that (for all connection types) frame type C, D and E compete in lateral strength levels, they are followed by A, B and F (in exact order) for both collapse and 1% top drift states. The same outcome can be projected to pertinent R values.

Based on this study, overall results of "R" factors obtained for most of the systems are considerably higher when compared to code values. This result may be issued to some facts such as:

- Frames designed as high ductility, had to fulfill the requirement of columns being stronger than beams. This practice brings high ratios of overdesign since beam design is mostly governed by gravity loads. Therefore columns having larger plastic modules than beams leave a considerable unused capacity for lateral loads. Even in design phase this is noticed as column sections hardly being utilized to 50% of their allowable stress level. "F" type frames have reasonable values since they possess lower overdesign.

- Especially in 3 story frames, gravity loads govern the design instead of lateral loads, which results an excess lateral strength, raising the overstrength factor.

- Discrete selection of member sections is another reason for systems being over-designed. Moreover braces designed to be code compliant, show significant overstrength due to the slenderness (kl/r) recommendation.

- The target displacement value (used for the pushover analysis) is corresponding to the collapse state of the structure. Thus any given frame is evaluated with its full capacity. However if target values according to a design state were to be chosen, significantly lower ductility ratios may be obtained. Results based on 1% top drift (defined as life safety level) produces a mean value of 50% lower values of "Rμ" thus 50% lower "R" values.

- Using allowable stress design instead of a more up to date method may be also mentioned as a cause of high values of "R".

Lowering "Effective Ground Acceleration Coefficient" by 4 times significantly reduced the design base shear and thus the governing lateral actions in design phase seemed to be disappeared. This dramatic change in seismic zoning resulted in lighter systems with reduced sections which are mainly stressed by gravity actions. Changing the earthquake zone effected the non-linear evaluation as expected; lower design base shears resulted in very high overstrength factors while ductility reduction factor decreased very little.

5.2 CONCLUSIONS

Conclusions derived based on this thesis study, are presented in this section as follows:

Methodology, in determination of “R”, is based on equal displacement rule. This idea simplifies the application but completely neglects the post-elastic behavior of the structure. Positive or negative slopes of inelastic behavior, strength and stiffness degradation affects are completely omitted. Alternatively, another idea called equal area rule, equals the total energy absorbed thus inelastic behavior is included to some degree. However it is far from even roughly estimating the displacement demands. Both approaches are unrealistic and lead to vague results of “R”.

Seismic design using the response modification factors listed in seismic codes and guidelines will most probably not result in a uniform level of risk for all seismic framing systems since there is no sound mathematical basis of the application.

Current seismic code is capable of adjusting the “R” factor according to the “stiffness” of the structure. “R” is streamlined to lower values if structure has very short periods of vibration. “Strength” on the other hand has never been issued in R determination. Structural strength level also needed to be controlled since over-design or under-design may both result in unexpected and unfavorable behaviors. Some of the structures, designed in this study, seem to never even yield in a moderate earthquake.

The use of response modification factors will likely not produce the desired performance in the design earthquake. A single value of “R” for a given framing type, without the correlation of basic structural properties such as height, plan geometry, framing layout, connection type, can not be obtained. Since every structure and its boundary conditions are unique, conducting parametric studies to form a detailed tabulation will not be enough to provide a well controlled seismic

behavior. However many design variables are tied to a single value of R; it is believed that incorporating various parameters into to R factor selection, would result in better and more reliable seismic performance.

The major intention of “R” factor is to utilize the inelastic capacity of the structure. Designing the building for a significantly lower base shear than expected will lead to inelasticity but in an uncontrolled manner; key components of inelastic behavior such as story drift ratios, overall displacement and plastic rotations will be unknown.

In current Turkish seismic design code damping in structures are fixed in 5% modal damping. There is an intensive research in literature on highly damped response of structures; more insightful provisions may be provided especially for structures with damping systems.

Current Turkish seismic design code never mentions about redundancy in structures. While irregularities in structural layout are punished, providing redundancy must be encouraged by the code.

REFERENCES

[1] Uang, C.-M. and Bertero, V.V., "*Earthquake Simulation Tests And Associated Studies of A 0.3-Scale Model of A Six-Story Concentrically Braced Steel Structure*" Rep. No. UCB/EERC-86/10, University of California, Berkeley, California, 1986.

[2] Whittaker, A.S., Uang, C.-M., and Bertero, V.V., "*Earthquake Simulation Tests And Associated Studies of A 0.3-Scale Model of A Six Story Eccentrically Braced Steel Structure*" Rep. No. UCB/EERC-87/02, University of California, Berkeley, California, 1987.

[3] Uang, C.-M., "*Establishing R (or Rw) and Cd Factors for Building Seismic Provisions*" Journal of Structural Engineering, ASCE, Vol. 117, No. 1, 1991.

[4] Freeman, S.A., "*On the Correlation of Code Forces to Earthquake Demands*" Proc., 4th U.S.-Japan Workshop On Improvement of Build. Struct. Des. And Constr. Practices, Applied Technology Council, Redwood City, California, 1990.

[5] Osteraas, J.D. and Krawinkler, H., "*Strength and Ductility Considerations in Seismic Design*" Rep.No. 90, John A. Blume Earthquake Engineering. Center, Stanford University, California, 1990.

[6] Rahgozar, M.A. and Humar, J.L., "*Accounting for Overstrength In Seismic Design of Steel Structures*" Canadian Journal of Civil Engineering, 25, 1–5, 1998.

[7] Kappos, A.J., "*Evaluation of Behavior Factors on the Basis of Ductility and Overstrength Studies*" Engineering Structures, 21, 823–835, 1999.

[8] Balendra, T. and Huang, X. "*Overstrength and Ductility Factors for Steel Frames Designed According to BS 5950*" Journal of Structural Engineering, ASCE, Vol. 129, No. 8, 2003.

[9] Lee, D.G., Cho, S.H., and Ko H., "*Response Modification Factors for Seismic Design of Building Structures in Low Seismicity Regions*" Korea Earthquake Engineering Research Center, 2005.

[10] Kim, J., and Choi, H., "*Response Modification Factors of Chevron-Braced Frames*" Engineering Structures, 27, 2005.

[11] Miranda E., and Bertero V.V., "*Evaluation of Strength Reduction Factors for Earthquake-Resistant Design*" Earthquake Spectra, Vol. 10, No 2, 1994.

[12] Newmark, N.M. and Hall, W.J., "*Seismic Design Criteria for Nuclear Reactor Facilities*" Rep. No. 46, Building Practices for Disaster Mitigation, National Bureau of Standards, U.S. Department of Commerce, 1973.

[13] Lai, S.-P. and Biggs, J.M., "*Inelastic Response Spectra for Aseismic Building Design*" Journal of Structural Engineering, ASCE, Vol. 106, No. ST6, 1980.

[14] Riddell, R. and Newrnark, N.M., "*Statistical Analysis of the Response of Nonlinear Systems Subjected to Earthquakes*" Structural Research Series No. 468, University of Illinois, Urbana, 1979.

[15] Riddell, R., Hidalgo, P. and Cruz, E., "*Response Modification Factors for Earthquake Resistant Design of Short Period Structures*" Earthquake Spectra, Vol. 5, No. 3, 1989.

[16] Miranda, E., "*Site-Dependent Strength Reduction Factors*" Journal of Structural Engineering, ASCE, Vol. 119, No. 12, 1993.

[17] Nassar, A.A. and Krawinkler, H., "*Seismic Demands for SDOF and MDOF Systems*" Rep. No. 95, John A. Blume Earthquake Engineering Center, Stanford University, California, 1991.

[18] Borzi, B. and Elnashai, A.S., "*Refined Force Reduction Factors for Seismic Design*" Engineering Structures, 22, 2000.

[19] Wilson, E.L., "*Three-Dimensional Static and Dynamic Analysis of Structures: A Physical Approach with Emphasis on Earthquake Engineering*" Computers And Structures, Inc. Berkeley, California, 2002.

[20] Newmark N.M. and Hall W.J., "*EERI Monograph Series*" Earthquake Spectra and Design." Earthquake Engineering Research Institute, Oakland, California, 1982.

[21] Ashour S.A., "*Elastic Seismic Response of Buildings with Supplemental Damping*" Ph.D. Dissertation, University of Michigan, 1987.

[22] Wu J.P. and Hanson R.D., "*Inelastic Response Spectra With High Damping*" Journal of Structural Engineering, ASCE, Vol. 115, No. 6, 1989.

[23] Ramirez O.M., Constantinou M.C., Kircher C.A., Whittaker A.S., Johnson M.W., Gomez J.D., Chrysostomou C.Z., "*Development And Evaluation of Simplified Procedures for Analysis And Design of Buildings With Passive Energy Dissipation Systems*" Rep. No: MCEER-00-0010, Multidisciplinary Center for Earthquake Engineering Research (MCEER), New York, 2000.

[24] Ramirez O.M., Constantinou M.C., Whittaker A.S., Kircher C.A., Chrysostomou C.Z., "*Elastic And Inelastic Seismic Response of Buildings With Damping Systems*" Earthquake Spectra Vol. 18, No. 3, 2002.

[25] Lin Y.Y. and Chang K.C., "*A Study on Damping Reduction Factor for Buildings Under Earthquake Ground Motions*" Journal of Structural Engineering, ASCE, Vol. 129, No. 2, 2003.

[26] Furuta, H., Shinozuka, M. and Chen, Y.N., "*Probabilistic And Fuzzy Representation of Redundancy In Structural Systems*" Proc., 1st Int. Fuzzy Systems Associated Congr., Palma De Mallorca, Spain, 1985.

[27] Frangopol, D.M. and Curley, J.P., "*Damage States, Redundancy, and System Strength*" Proc., Effects of Damage and Redundancy on Struct. Performance, ASCE, 1987.

[28] Tang, J.P., and Yao, T.P. "*Evaluation of Structural Damage and Redundancy*" Proc., Effects of Damage And Redundancy On Struct. Performance, ASCE, 1987.

[29] Bonowitz, D., Youssef N. and Gross. J.L. "*A Survey of Steel Moment-Resisting Frames Buildings Affected by the 1994 Northridge Earthquake*" Rep. No. NISTIR 5625, National Institute of Standards and Technology, Gaithersburg, 1995.

[30] Wood, S.L., "*Performance of Reinforced Concrete Buildings During the 1985 Chile Earthquake*" EERI Spectra, November, 1991.

[31] Moses, F., "*Reliability of Structural Systems*" Journal of the Structural Division, ASCE, Vol. 100, No. 9, 1974.

[32] Gugerli, H. and Goel, S.C., "*Inelastic Cyclic Behavior of Steel Bracing Members*" Rep. No. UMEE 82R1, University of Michigan, Michigan, 1982.

[33] Aslani, F. and Goel, S.C., "*Experimental and Analytical Study of the Inelastic Behavior of Double Angle Bracing Members Under Severe Cyclic Loading*" Rep. No. UMCE 89-5, University of Michigan, Michigan. 1989.

[34] Kahn, L.F. and Hanson, R.D. "*Inelastic Cycles of Axially Loaded Steel Members*" Journal of the Structural Division, ASCE, Vol. 102, No. 5, 1976.

[35] Jain, A.K., Goel, S.C., and Hanson, R.D. "*Inelastic Response of Restrained Steel Tubes*" Journal of the Structural Division, ASCE, Vol 104, No 6, 1978.

[36] Jain, A.K., Goel, S.C., and Hanson, R.D. "*Hysteretic Cycles of Axially Loaded Steel Members*" Journal of the Structural Division, ASCE, Vol. 106, No. 8, 1980.

[37] Prathuansit, D., Goel, S.C., and Hanson, R.D. "*Axial Hysteresis Behavior with End Restraints.*" Journal of the Structural Division, ASCE, Vol. 104, No. 6, 1978.

[38] Popov, E. P. and Black, R.G. "*Steel Struts Under Severe Cyclic Loadings*" Journal of the Structural Division, ASCE, Vol. 107, No. 9, 1981.

[39] Lee, S. and Goel, S.C., "*Seismic Behavior of Hollow And Concrete-Filled Square Tubular Bracing Members*" Rep. No. UMCE 87-11, University of Michigan, 1987.

[40] Picard, A. and Beaulieu, D., "*Theoretical Study of the Buckling Strength of Compression Members Connected to Coplanar Tension Members*" Canadian Journal of Civil Engineering, Vol. 16, No. 3, 1989.

[41] Picard, A. and Beaulieu, D., "*Experimental Study of the Buckling Strength of Compression Members Connected To Coplanar Tension Members*" Canadian Journal of Civil Engineering, Vol. 16, No. 3, 1989.

[42] Krawinkler. H., "*Shear In Beam-Column Joints In Seismic Design of Steel Frames*" Engineering Journal, AISC, Vol. 15, No. 3, 1978.

[43] Bertero, V.V., Popov, E.P. and Krawinkler, H., "*Beam-Column Subassemblages Under Repeated Loading*" Journal of the Structural Division, ASCE, Vol. 98, No. 5, 1972.

[44] Bertero. V.V., Krawinkler, H. and Popov, E.P. "*Further Studies On Seismic Behavior of Steel Beam-To-Column Subassemblages*" Rep. No. EERC 73-27, University of California, Berkeley, California, 1973.

[45] Krawinkler, H., Bertero, V.V. and Popov, E.P. "*Inelastic Behavior of Steel Beam-To-Column Subassemblages*" Rep. No. EERC 71-7. University of California, Berkeley, California, 1971.

[46] Krawinkler, H., and Mohasseb, S. "*Effect of Panel Zone Deformations On Seismic Response*" Journal of Constructional Steel Research, Vol. 8, 1987.

[47] Schneider S. and Amidi .A, "*Seismic Behavior of Steel Frames With Deformable Panel Zones*" Journal of Structural Engineering, ASCE, Vol. 124, No. 1, 1998.

[48] Federal Emergency Management Agency (FEMA), "*NEHRP Recommended Provisions for Seismic Regulations for New Buildings 1994 Edition*" (FEMA222A), Washington, DC, July 1995.

[49] Federal Emergency Management Agency (FEMA), "*NEHRP Recommended Provisions for Seismic Regulations for New Buildings 1997 Edition*" (FEMA 302), Washington, DC, February 1997.

[50] Federal Emergency Management Agency (FEMA), "*NEHRP Recommended Provisions for Seismic Regulations for New Buildings 2000 Edition*" (FEMA 368), Washington, DC, March 2001.

[51] Federal Emergency Management Agency (FEMA), "*NEHRP Recommended Provisions for Seismic Regulations for New Buildings 2003 Edition*" (FEMA 450), Washington, DC, June 2004.

[52] Federal Emergency Management Agency (FEMA), "*NEHRP Guidelines for the Seismic Rehabilitation of Buildings*" (FEMA 273), Washington, DC, October 1997.

[53] Federal Emergency Management Agency (FEMA), "*NEHRP Commentary on the Guidelines for the Seismic Rehabilitation of Buildings*" (FEMA 274), Washington, DC, October 1997.

[54] Federal Emergency Management Agency (FEMA), "*Recommended Seismic design Criteria for New Steel Moment-Frame Buildings*" (FEMA 350), Washington, DC, June 2000.

[55] Federal Emergency Management Agency (FEMA), "*State of the Art Report on Systems Performance of Steel Moment Frames Subject to Earthquake Ground Shaking*" (FEMA 355C), Washington, DC, September 2000.

[56] Federal Emergency Management Agency (FEMA), "*State of the Art Report on Connection Performance*" (FEMA 355D), Washington, DC, September 2000.

[57] Federal Emergency Management Agency (FEMA), "*Prestandard and Commentary for the Seismic Rehabilitation of Buildings*" (FEMA 356), Washington, DC, November 2000.

[58] Federal Emergency Management Agency (FEMA), "*Improvement of Nonlinear Static Seismic Analysis Procedures - Draft Camera Ready*" (FEMA 440), Washington, DC, June 2005

[59] Federal Emergency Management Agency (FEMA), "*NEHRP Recommended Provisions for Seismic Regulations for New Buildings and Other Structures - Commentary*" (FEMA 303a), Washington, DC, February 1997

[60] Applied Technology Council (ATC), "*Structural Response Modification Factors*" (ATC-19), Redwood City, California, 1995

[61] Applied Technology Council (ATC), "*Seismic Evaluation and Retrofit of Concrete Buildings*" (ATC-40), Redwood City, California, 1996

[62] Applied Technology Council (ATC), "*Tentative Provisions for the Development of Seismic Regulations for Buildings*" (ATC-3-06), Redwood City, California, 1978

[63] Bayındırlık ve İskân Bakanlığı, "*Afet Bölgelerinde Yapılacak Yapılar Hakkında Yönetmelik (1998 değişiklikleri ile birlikte)*" Ankara, 1998.

[64] American Institute of Steel Construction Inc. (AISC), "*Load and Resistance Factor Design Specification for Structural Steel Buildings*" (LRFD 99) Chicago Illinois, December 1999.

[65] International Conference of Building Officials (ICBO), "*International Building Code*" *(IBC 2000)*, Whittier, California, 2000.

[66] International Conference of Building Officials (ICBO), "*Uniform Building Code*" (UBC 1997), Whittier, California, 1997.

[67] European Committee for Standardization (CEN), "*Design of Structures for Earthquake Resistance*" (Eurocode 8), Brussels, 1994.

[68] Computers and Structures Inc. (CSI), "*SAP2000 Integrated Software for Structural Analysis and Design* v9.03" Berkeley, California, 2004.

[69] Computers and Structures Inc. (CSI), "*SAP2000 Analysis Reference Manual*" Berkeley, California, 2004.

[70] American Institute of Steel Construction Inc. (AISC), "*Allowable Stress Design Specification for Structural Steel Buildings*" (ASD 89), Chicago Illinois, 1989.

[71] Türk Standardları Enstitüsü (TSE), "*Yapı Elemanlarının Boyutlandırılmasında Alınacak Yüklerin Hesap Değerleri*" (TS 498), Ankara, 1987.

[72] Veletsos, A.S. and Newmark N.M., "*Effect Of Inelastic Behavior On The Response Of Simple Systems To Earthquake Motions*" Proceedings of the 2nd World Conference on Earthquake Engineering, Tokyo, Japan 1960.

[73] Moghaddam, H. and Hajirasouliha I., "*An Investigation on the Accuracy of Pushover Analysis for Estimating the Seismic Deformation of Braced Steel Frames*" Journal of Constructional Steel Research" 2005.

[74] Krawinkler, H. and Seneviratna, G.D.P.K., "*Pros and Cons of a Pushover Analysis of Seismic Performance Evaluation*" *Engineering Structures*, Vol. 20, No. 4-6, 1998.

[75] Kim, S. and D'Amore, E., "*Pushover Analysis Procedure in Earthquake Engineering*" Earthquake Spectra, Vol. 15, No. 3, 1999

[76] Davies, J.M., "*Strain Hardening, Local Buckling and Lateral-Torsional Buckling In Plastic Hinges*" Journal of Constructional Steel Research 62, 27–34, 2006.

[77] Korkmaz A. And Sarı A., "*Evaluation of Lateral Load Pattern in Pushover Analysis*" Department of Civil Engineering, University of Texas at Austin, 2003.

[78] Chintanapakdee, C. and Chopra, A.K., "*Evaluation of Modal Pushover Analysis Using Generic Frames*" Earthquake Engng Struct. Dyn. 32:417–442, 2003.

[79] Chopra, A.K. and Goel, R.K., "*Evaluation of Nsp to Estimate Seismic Deformation: Sdof Systems*" Journal Of Structural Engineering, ASCE, Vol. 126, No. 4, 2000.

[80] Priestley, M.J.N., "*Performance Based Seismic Design*" *University of California, San Diego, 1999*

[81] Whalen, T.M., Archer, G.C. and Bhatia, K.M. "*Implications of Vertical Mass Modeling Errors on 2d Dynamic Structural Analysis*" *Struct. Design Tall Spec. Build.* 13, 305–314, 2004.

[82] Goto, Y. and Miyashita, S. "*Classification System for Rigid and Semirigid Connections*" Journal of Structural Engineering, ASCE, Vol. 124, No. 7, 1998.

[83] Abolmaali, A., Kukreti, A.R. and Razavi, H., "*Hysteresis Behavior of Semi-Rigid Double Web Angle Steel Connections*" Journal of Constructional Steel Research 59 1057–1082, 2003.

[84] Shen, J. ,and Astaneh, A.A., "*Hysteresis Model of Bolted-Angle Connections*" Journal of Constructional Steel Research 54, 317–343, 2000.

[85] Lee, S.S. and Moon, T.S., "*Moment-Rotation Model of Semi-Rigid Connections with Angles*" Engineering Structures 24, 227–237, 2002.

[86] Mofid, M. and Lotfollahi, M., "*On the Characteristics of New Ductile Knee Bracing Systems*" Journal of Constructional Steel Research 62 271–281, 2006.

[87] Tremblay, R., Archambault, M.H. and Filiatrault A., "*Seismic Response of Concentrically Braced Steel Frames Made With Rectangular Hollow Bracing Members*" Journal of Structural Engineering, ASCE, Vol. 129, No. 12, 2003.

[88] Schneider, S.P. and Amidi, A., "*Seismic Behavior of Steel Frames with Deformable Panel Zones*" Journal of Structural Engineering, ASCE, Vol. 124, No. 1, 1998.

[89] Richard, L. and Chen, W.F., "*Analysis and Design of Steel Frames Considering Panel Deformations*" Journal of Structural Engineering, ASCE, Vol. 121, No. 10, 1995.

APPENDIX A

A.1 PROPOSED RESPONSE MODIFICATION FACTORS

Table A.1.1: Response Modification Factors proposed in NEHRP 2003 [51]

Basic Seismic-Force-Resisting System	**Detailing Reference Section**	***R***	Ω_0
Bearing Wall Systems			
Special reinforced concrete shear walls	9.2.1.6	5	2½
Ordinary reinforced concrete shear walls	9.2.1.4	4	2½
Detailed plain concrete shear walls	9.2.1.2	2	2½
Ordinary plain concrete shear walls	9.2.1.1	1½	2½
Intermediate precast shear walls	9.2.1.5	4	2½
Ordinary precast shear walls	9.2.1.3	3	2½
Building Frame Systems			
Steel eccentrically braced frames with moment-resisting connections at columns away from links	AISC Seismic, Part I, Sec. 15	8	2
Steel eccentrically braced frames with non-moment-resisting connections at columns away from links	AISC Seismic, Part I, Sec. 15	7	2
Buckling-Restrained Braced Frames, moment-resisting Beam-column connections		8	2½
Special steel concentrically braced frames	AISC Seismic, Part I, Sec. 13	6	2
Ordinary steel concentrically braced frames	AISC Seismic, Part I, Sec. 14	5	2
Special reinforced concrete shear walls	9.2.1.6	6	2½
Ordinary reinforced concrete shear walls	9.2.1.4	5	2½
Detailed plain concrete shear walls	9.2.1.2	2½	2½
Ordinary plain concrete shear walls	9.2.1.1	1½	2½
Composite eccentrically braced frames	AISC Seismic, Part II, Sec. 14	8	2½
Composite concentrically braced frames	AISC Seismic, Part II, Sec. 12	5	2
Ordinary composite braced frames	AISC Seismic, Part II, Sec. 13	3	2
Composite steel plate shear walls	AISC Seismic, Part II, Sec. 17	6½	2½
Special steel plate shear walls		7	2
Moment Resisting Frame Systems			
Special steel moment frames	AISC Seismic, Part I, Sec. 9	8	3
Special steel truss moment frames	AISC Seismic, Part I, Sec. 12	7	3
Intermediate steel moment frames	AISC Seismic, Part I, Sec. 10	4½	3
Ordinary steel moment frames	AISC Seismic, Part I, Sec. 11	3½	3
Special reinforced concrete moment frames	9.2.2.2 & ACI 318, Chapter 21	8	3

Table A.1.1: Response Modification Factors proposed in NEHRP 2003 [51] (cont.)

Moment Resisting Frame Systems		***R***	Ω_0
Special steel moment frames	AISC Seismic, Part I, Sec. 9		
Special steel truss moment frames	AISC Seismic, Part I, Sec. 12	7	3
Intermediate steel moment frames	AISC Seismic, Part I, Sec. 10	4½	3
Ordinary steel moment frames	AISC Seismic, Part I, Sec. 11	3½	3
Special reinforced concrete moment frames	9.2.2.2 & ACI 318, Chapter 21	8	3
Intermediate reinforced concrete moment frames	9.2.2.3 & ACI 318, Chapter 21	5	3
Ordinary reinforced concrete moment frames	9.3.1 & ACI 318, Chapter 21	3	3
Special composite moment frames	AISC Seismic, Part II, Sec. 9	8	3
Intermediate composite moment frames	AISC Seismic, Part II, Sec. 10	5	3
Composite partially restrained moment frames	AISC Seismic, Part II, Sec. 8	6	3
Ordinary composite moment frames	AISC Seismic, Part II, Sec. 11	3	3
Special masonry moment frames	11.7	5½	3
Dual Systems with Special Moment Frames			
Steel eccentrically braced frames	AISC Seismic, Part I, Sec. 15	8	2½
Buckling-Restrained Braced Frame		8	2½
Special steel concentrically braced frames	AISC Seismic, Part I, Sec. 13	7	2½
Ordinary reinforced concrete shear walls	9.2.1.3	6	2½
Composite eccentrically braced frames	AISC Seismic, Part II, Sec. 14	8	2½
Composite concentrically braced frames	AISC Seismic, Part II, Sec. 12	6	2
Special steel plate shear walls		8	2½
Composite steel plate shear walls	AISC Seismic, Part II, Sec. 17	7½	2½
Special composite reinforced concrete shear walls with steel elements	AISC Seismic, Part II, Sec. 16	7	2½
Ordinary composite reinforced concrete shear walls with steel elements	AISC Seismic, Part II, Sec. 15	6	2½
Special reinforced masonry shear walls	11.5.6.3	5½	3
Intermediate reinforced masonry shear walls	11.5.6.2	4	3
Dual Systems with Intermediate Moment Frames			
Special steel concentrically braced frames *j*	AISC Seismic, Part I, Sec. 13	6	2½
Special reinforced concrete shear walls	9.2.1.4	6½	2½
Ordinary reinforced concrete shear walls	9.2.1.3	5½	2½
Ordinary reinforced masonry shear walls	11.5.6.1	3	3
Intermediate reinforced masonry shear walls	11.5.6.2	3½	3
Composite concentrically braced frames	AISC Seismic, Part II, Sec. 12	5½	2½
Ordinary composite braced frames	AISC Seismic, Part II, Sec. 13	3½	2½

Table A.1.2: Response Modification Factors proposed in ABYYHY [63]

BUILDING STRUCTURAL SYSTEM	Nominal Ductility Level Systems	High Ductility Level Systems
(1) CAST-IN-SITU REINFORCED CONCRETE BUILDINGS		
(1.1) Buildings in which seismic loads are fully resisted by frames	4	8
(1.2) Buildings in which seismic loads are fully resisted by coupled structural walls	4	7
(1.3) Buildings in which seismic loads are fully resisted by solid structural walls	4	6
(1.4) Buildings in which seismic loads are jointly resisted by frames and solid and/or coupled structural walls	4	7
(2) PREFABRICATED REINFORCED CONCRETE BUILDINGS		
(2.1) Buildings in which seismic loads are fully resisted by frames with connections capable of cyclic moment transfer	3	6
(2.2) Buildings in which seismic loads are fully resisted by single-storey hinged frames with fixed-in bases	-	5
(2.3) Buildings in which seismic loads are fully resisted by prefabricated solid structural walls	-	4
(2.4) Buildings in which seismic loads are jointly resisted by frames with connections capable of cyclic moment transfer and cast-in-situ solid and/or coupled structural walls	3	5
(3) STRUCTURAL STEEL BUILDINGS		
(3.1) Buildings in which seismic loads are fully resisted by frames	5	8
(3.2) Buildings in which seismic loads are fully resisted by single-storey hinged frames with fixed-in bases	4	6
(3.3) Buildings in which seismic loads are fully resisted by braced frames or cast-in-situ reinforced concrete structural walls		
(a) *Concentrically braced frames*	3	-
(b) *Eccentrically braced frames*	-	7
(c) *Reinforced concrete structural walls*	4	6
(3.4) Buildings in which seismic loads are jointly resisted by frames and braced frames or cast-in-situ reinforced concrete structural walls		
(a) Concentrically braced frames	4	-
(b) Eccentrically braced frames	-	8
(c) Reinforced concrete structural walls	4	7

A.2 FRAME MEMBER LABELS

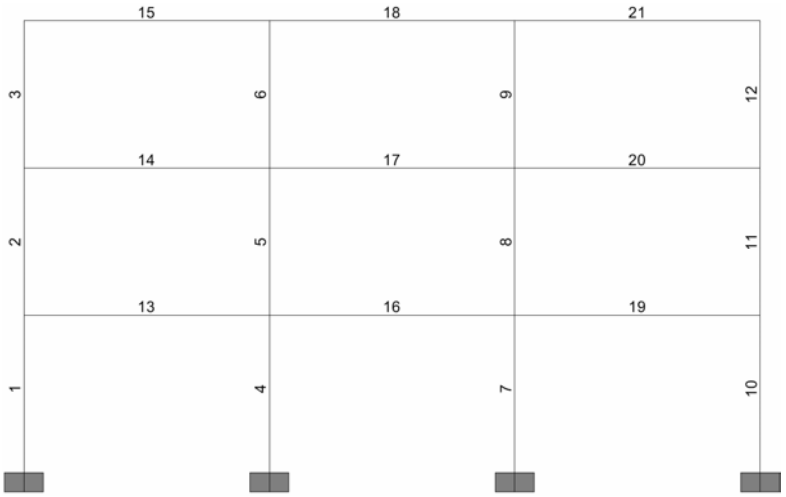

A-3-3

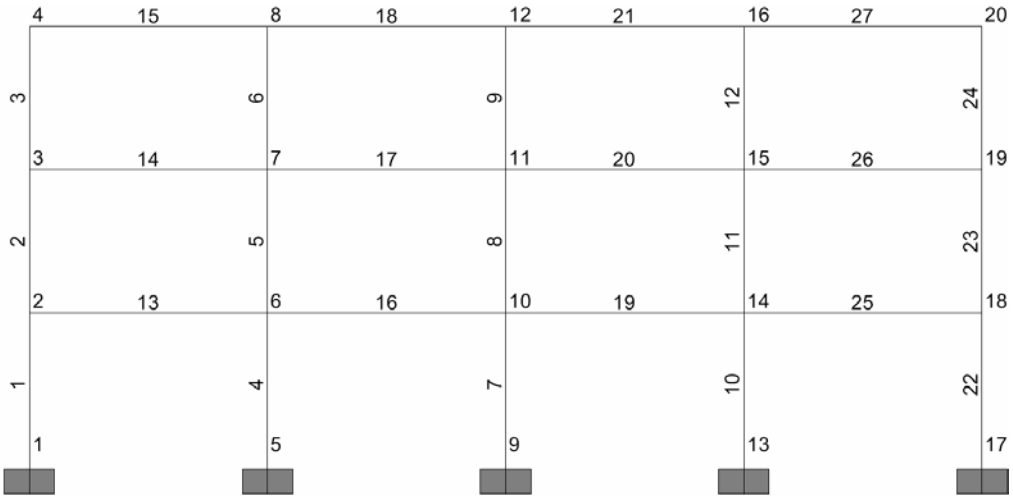

A-4-3

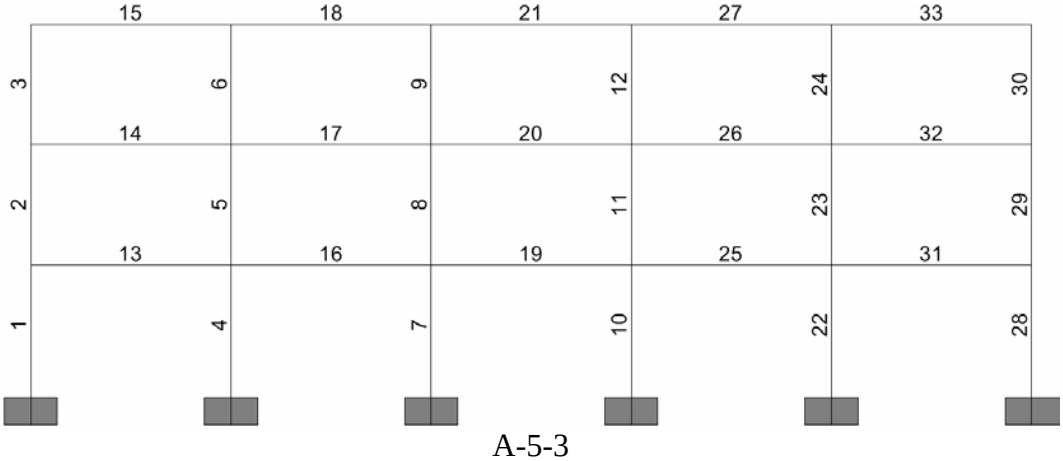

A-5-3

Figure A.2.1: Frames “A-3-3”, “A-4-3” & “A-5-3” member labels

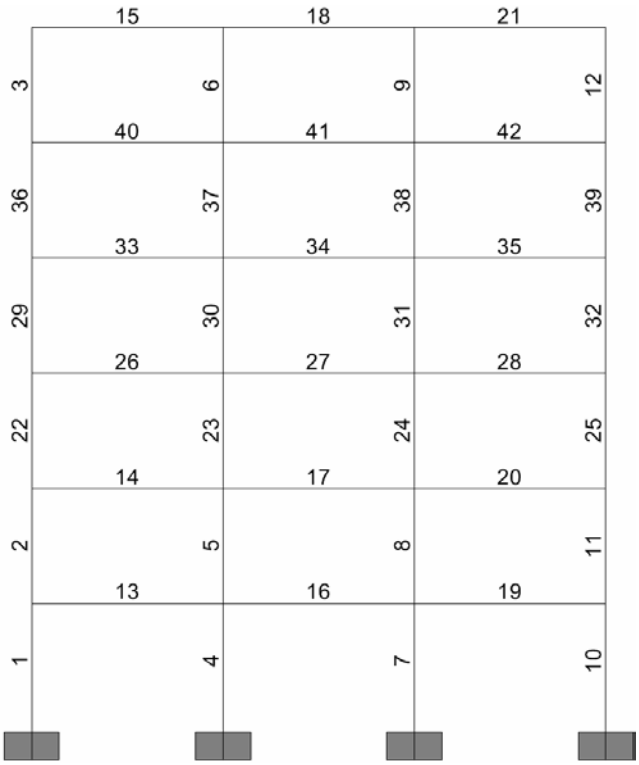

A-3-6

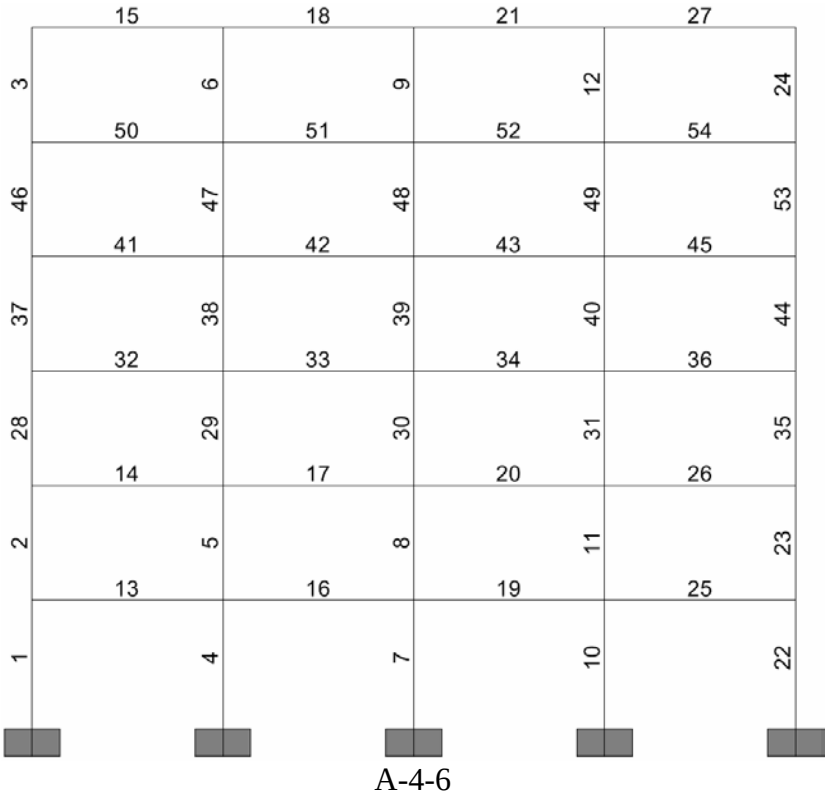

A-4-6

Figure A.2.2: Frames “A-3-6” & “A-4-6” member labels

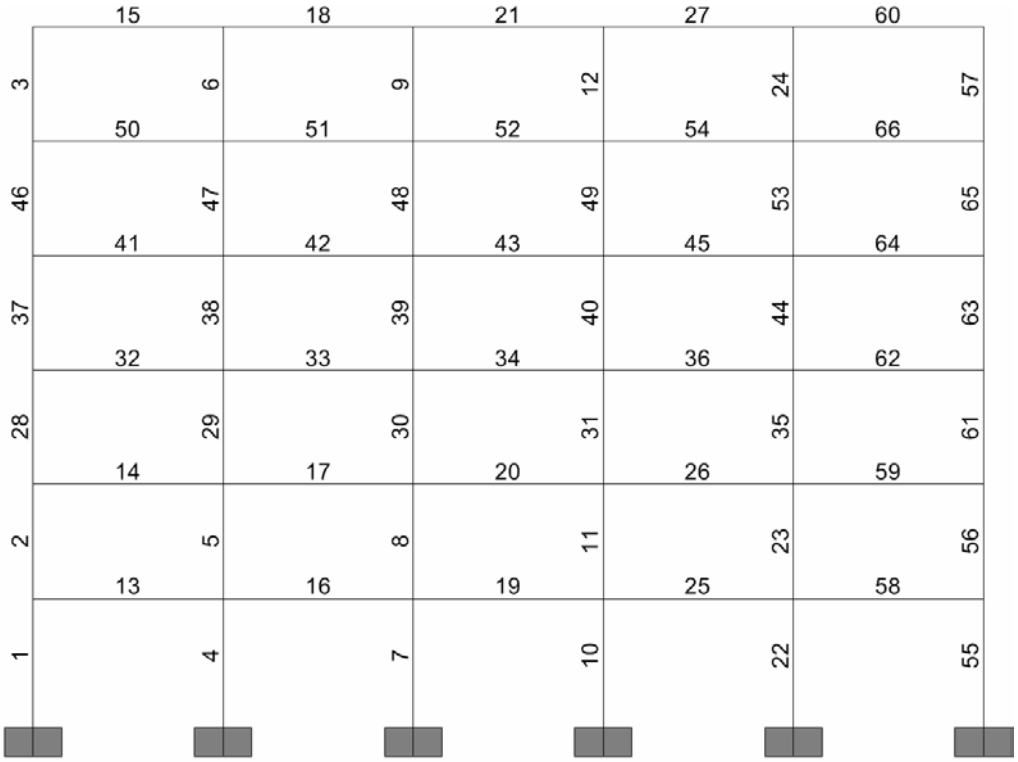

A-5-6

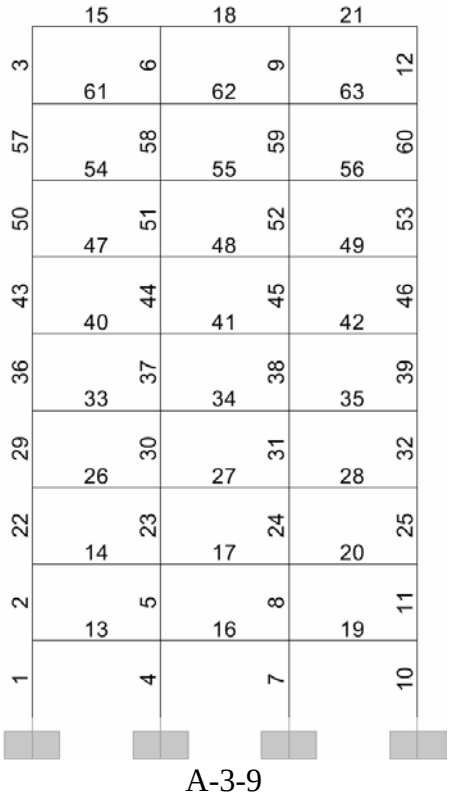

A-3-9

Figure A.2.3: Frames “A-5-6” & “A-3-9” member labels

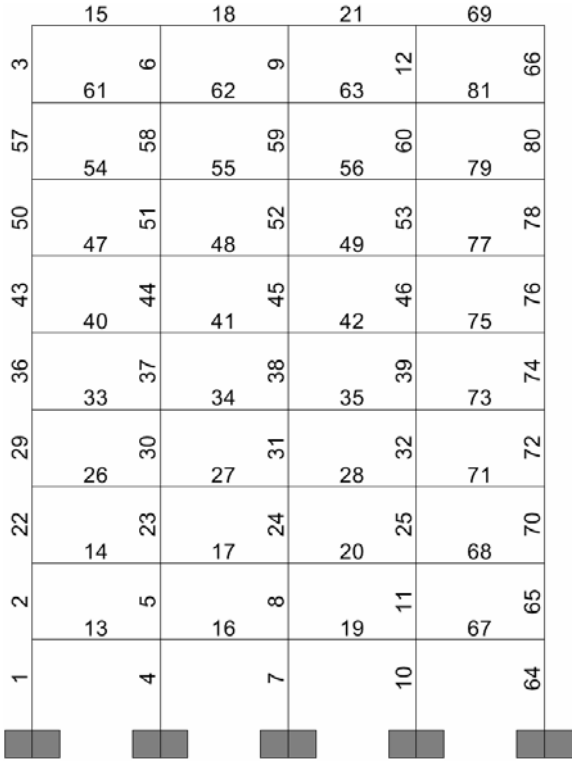

A-4-9

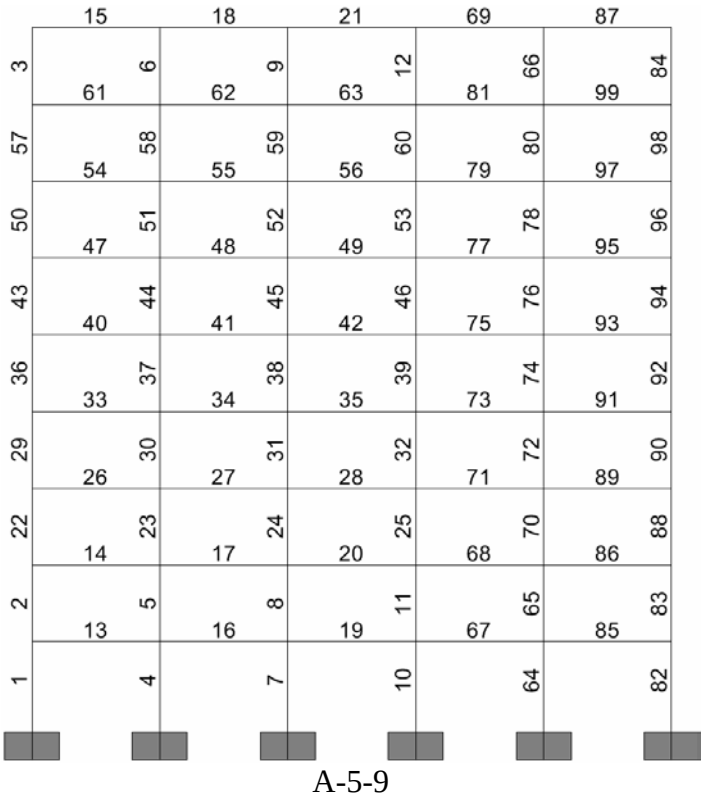

A-5-9

Figure A.2.4: Frames “A-4-9” & “A-5-9” member labels

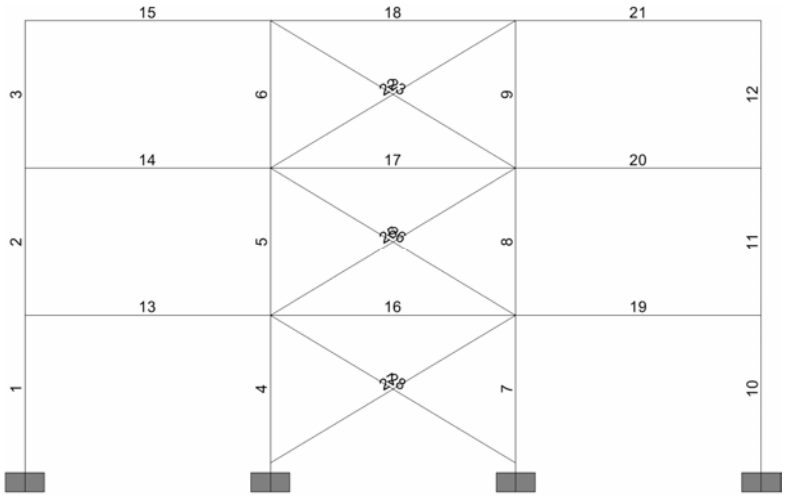

B-3-3

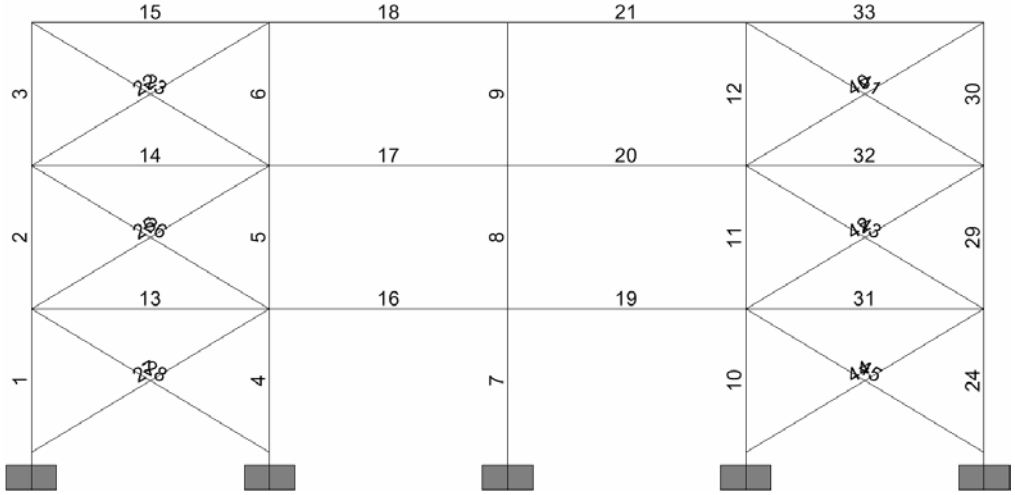

B-4-3

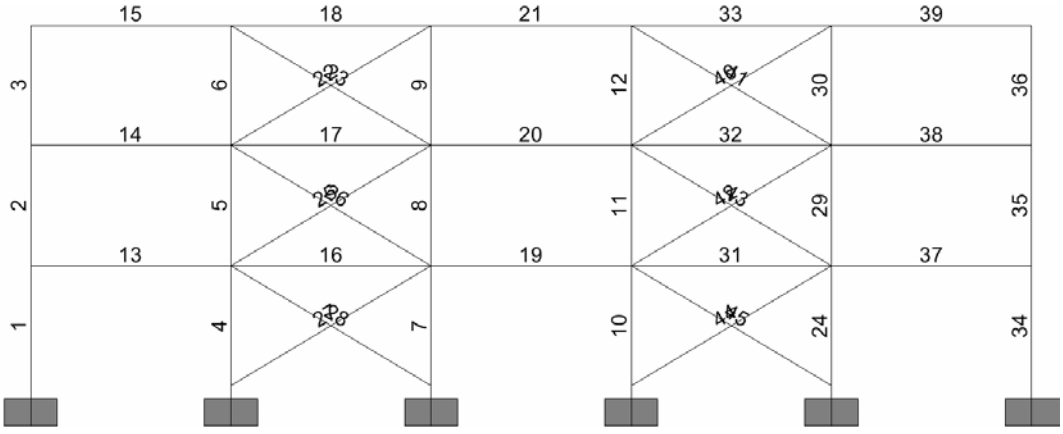

B-5-3

Figure A.2.5: Frames “B-3-3”, “B-4-3” & “B-5-3” member labels

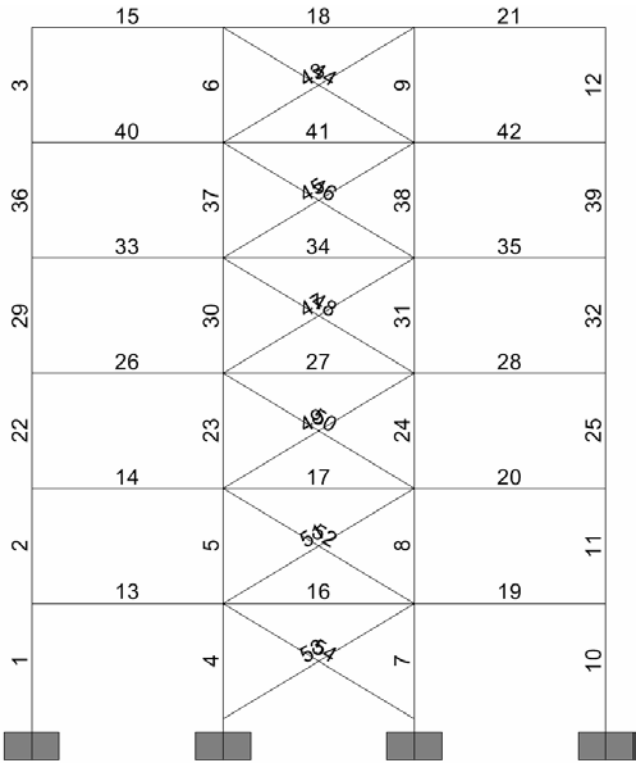

B-3-6

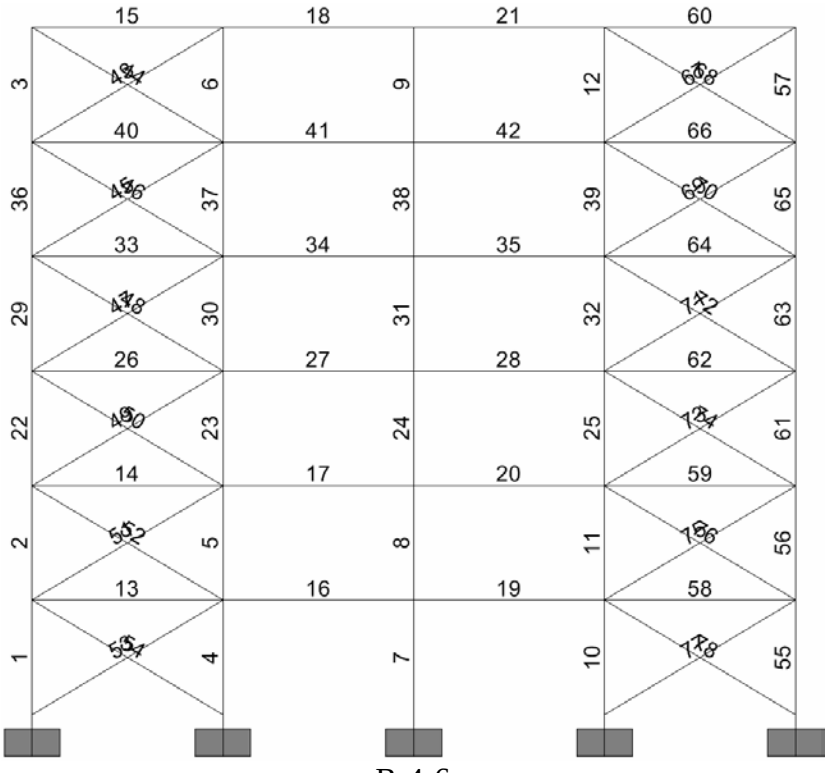

B-4-6

Figure A.2.6: Frames “B-3-6” & “B-4-6” member labels

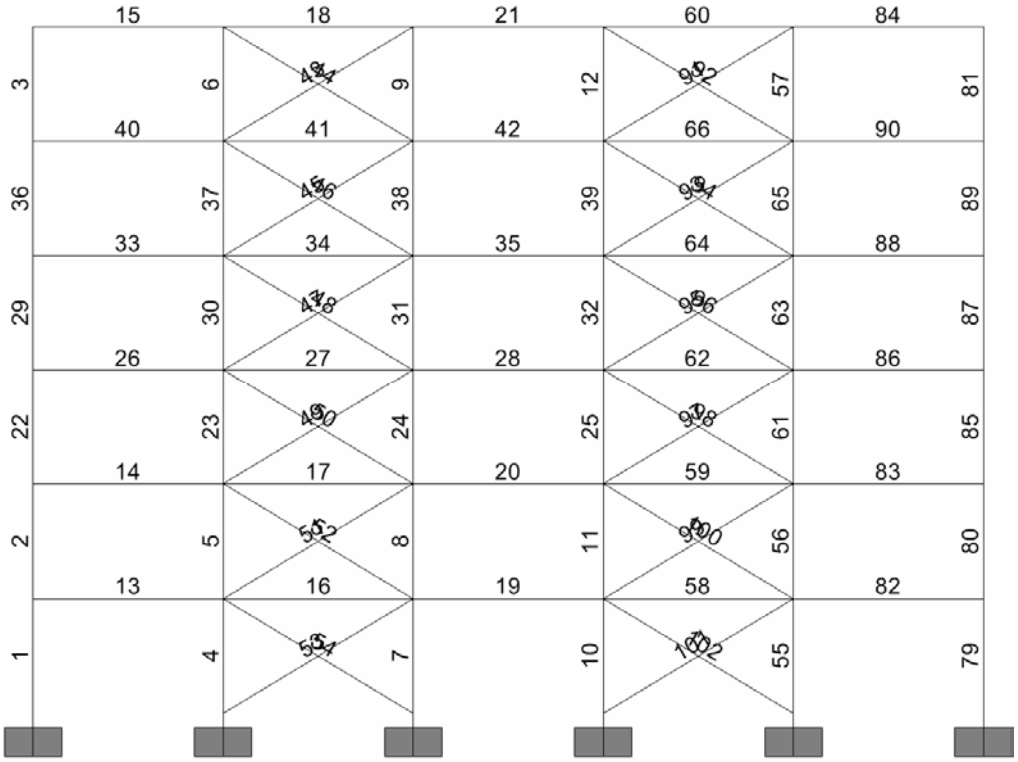

B-5-6

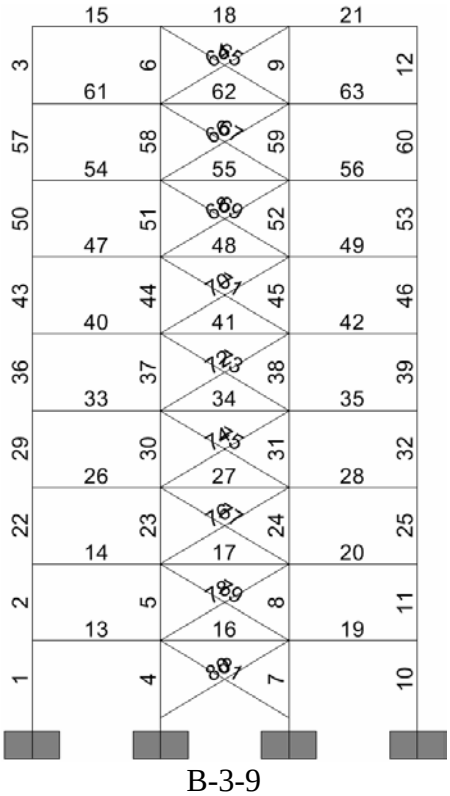

B-3-9

Figure A.2.7: Frames “B-5-6” & “B-3-9” member labels

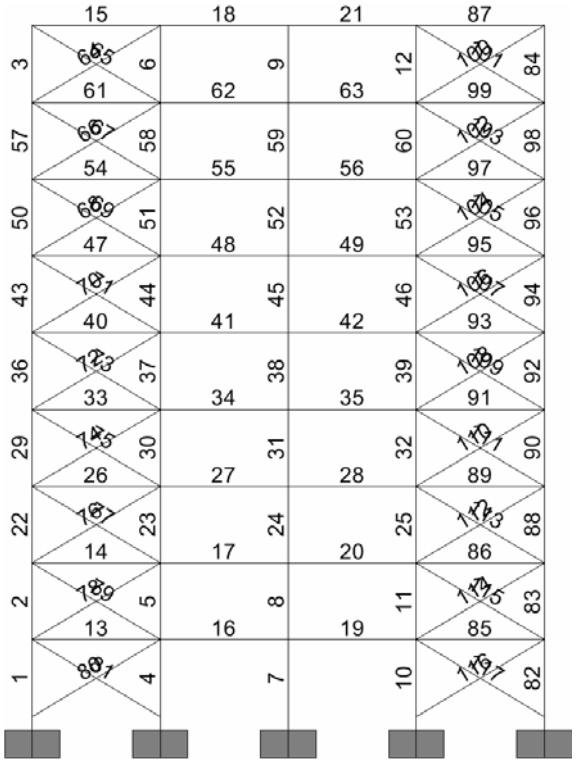

B-4-9

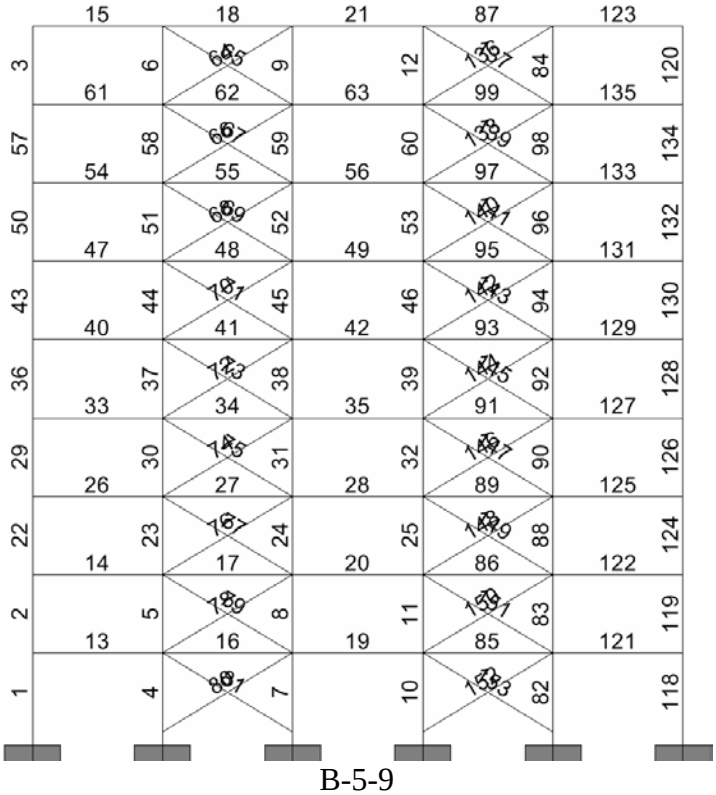

B-5-9

Figure A.2.8: Frames “B-4-9” & “B-5-9” member labels

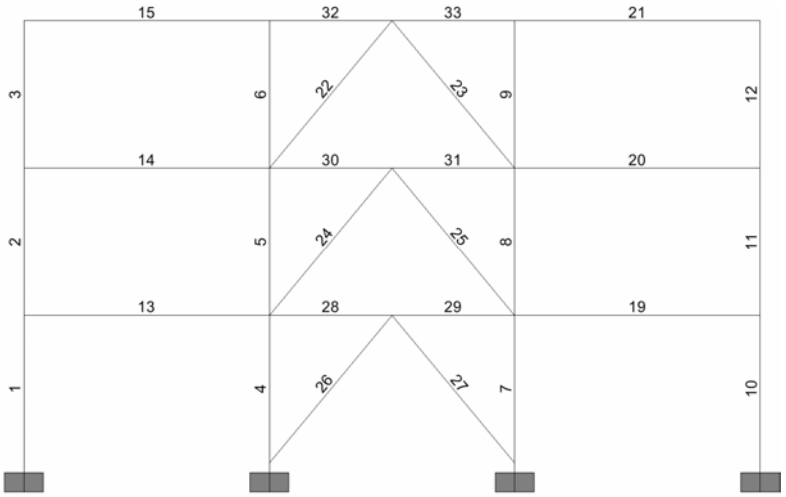

C-3-3

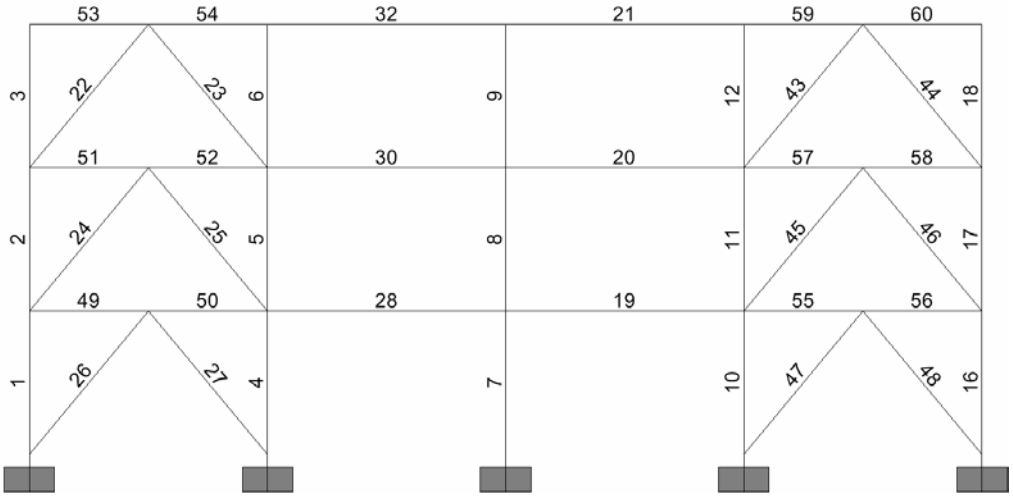

C-4-3

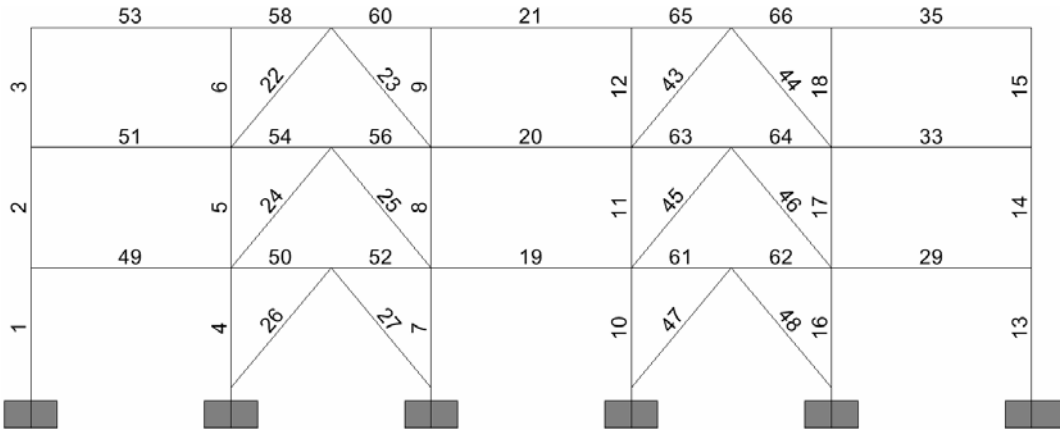

C-5-3

Figure A.2.9: Frames “C-3-3”, “C-4-3” & “C-5-3” member labels

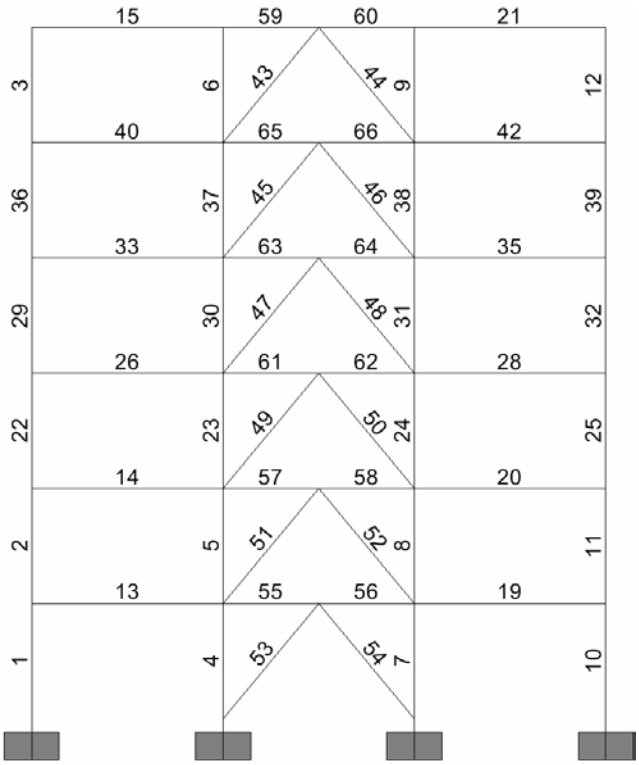

C-3-6

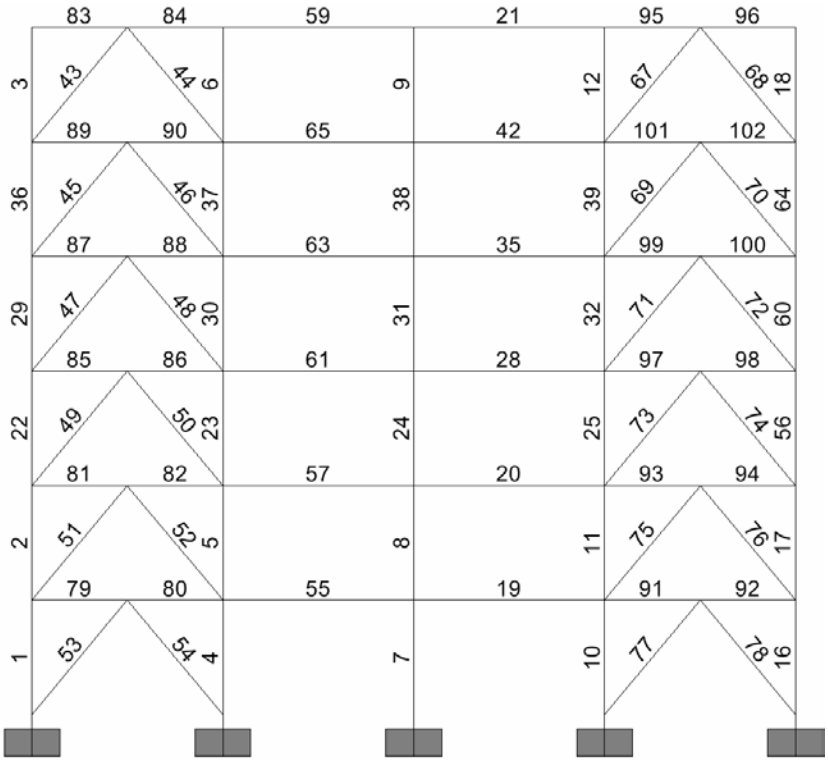

C-4-6

Figure A.2.10: Frames “C-3-6” & “C-4-6” member labels

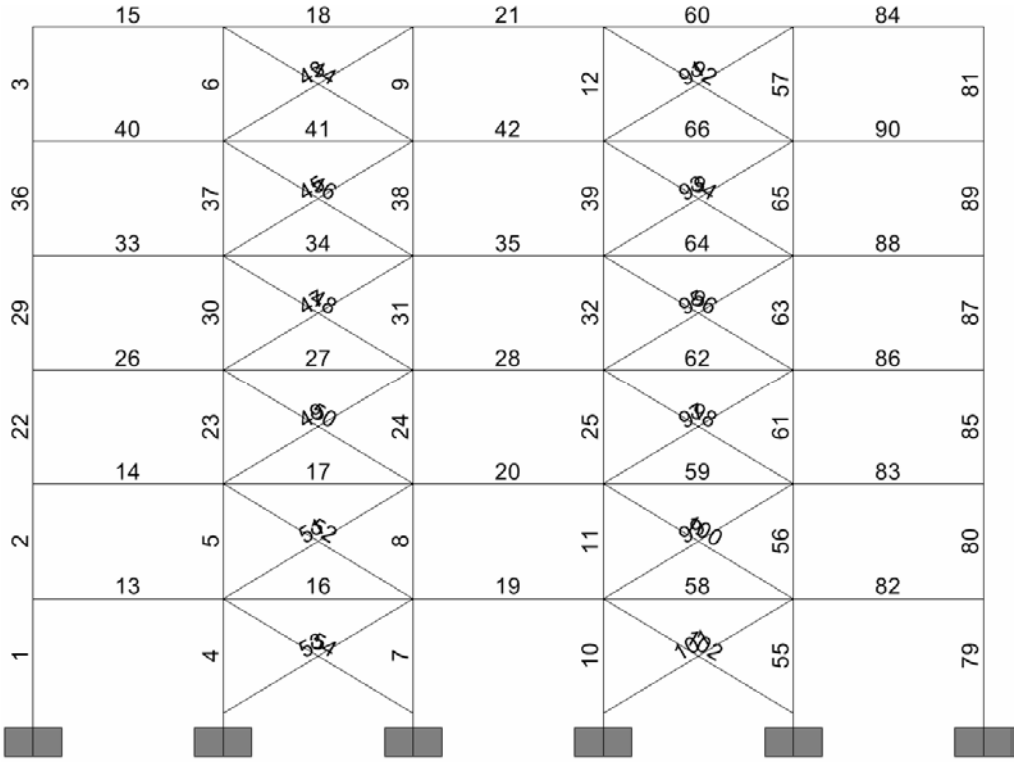

C-5-6

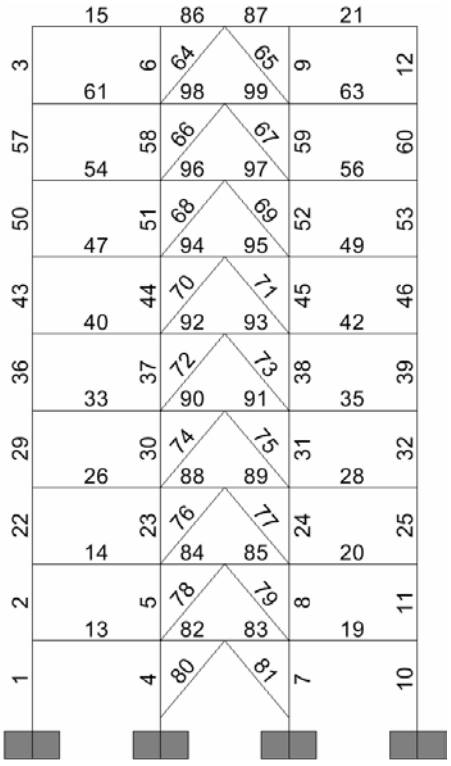

C-3-9

Figure A.2.11: Frames “C-5-6” & “C-3-9” member labels

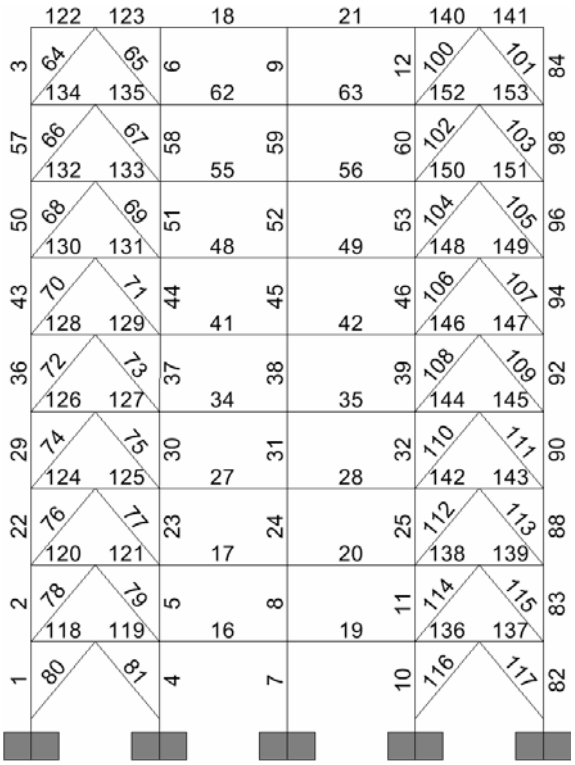

C-4-9

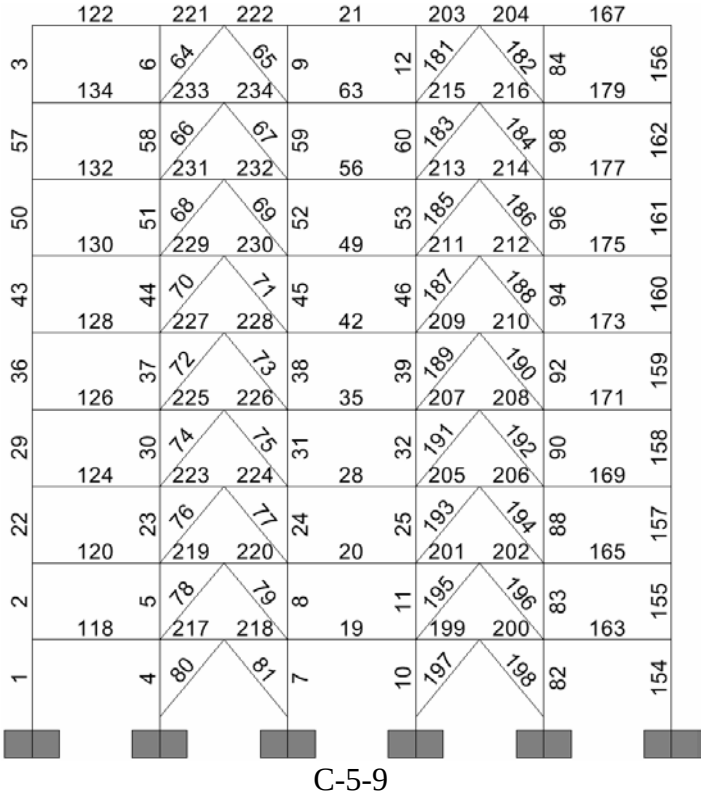

C-5-9

Figure A.2.12: Frames “C-4-9” & “C-5-9” member labels

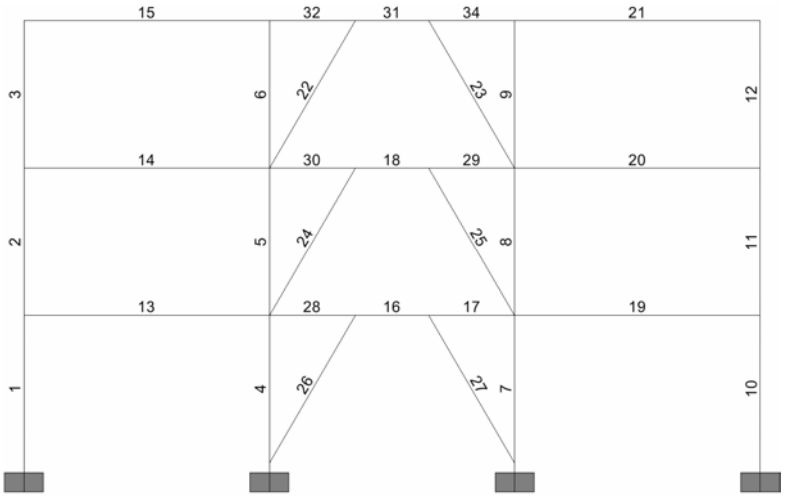

D-3-3

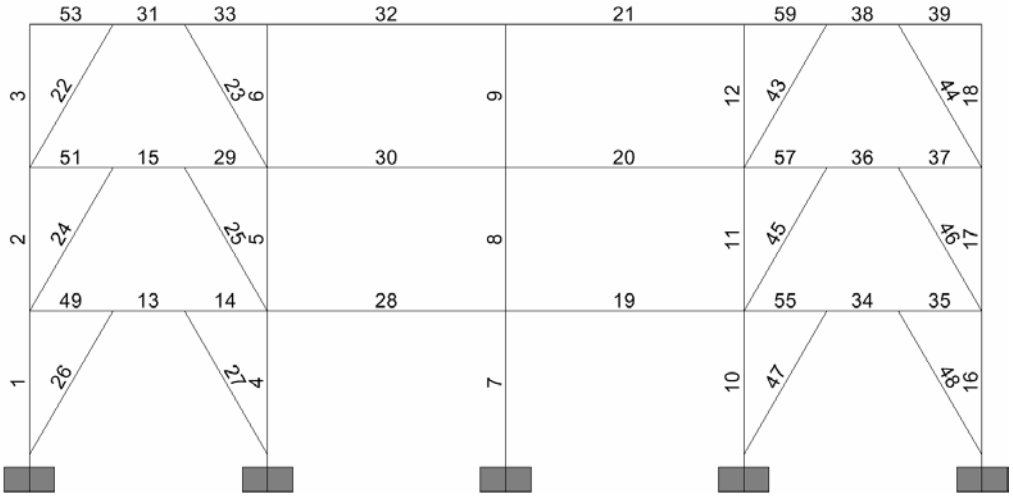

D-4-3

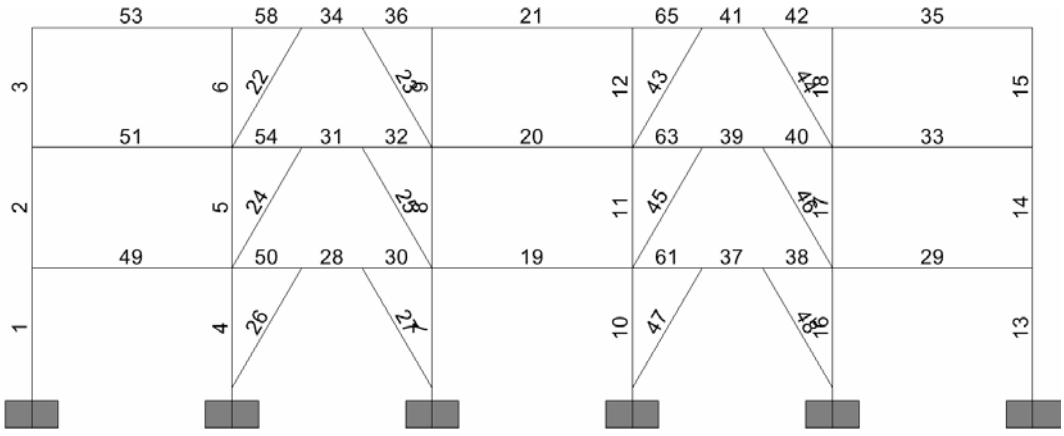

D-5-3

Figure A.2.13: Frames “D-3-3”, “D-4-3” & “D-5-3” member labels

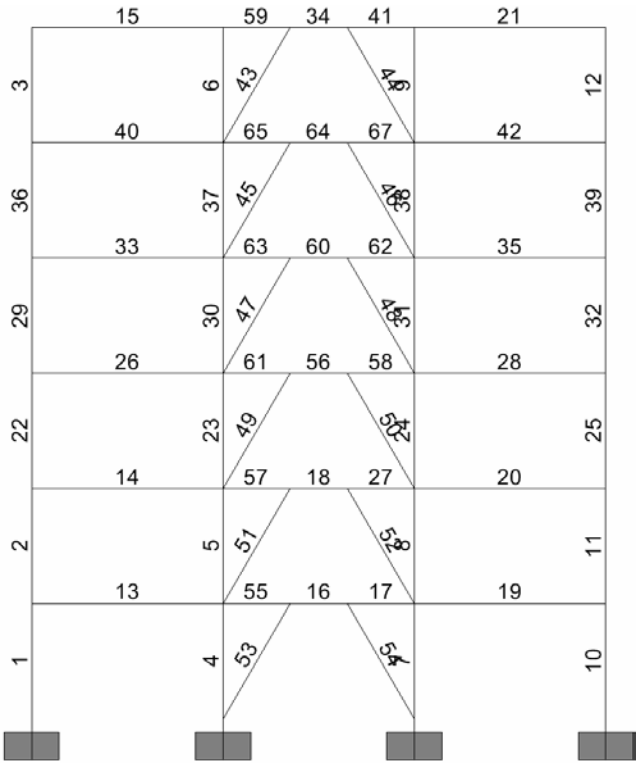

D-3-6

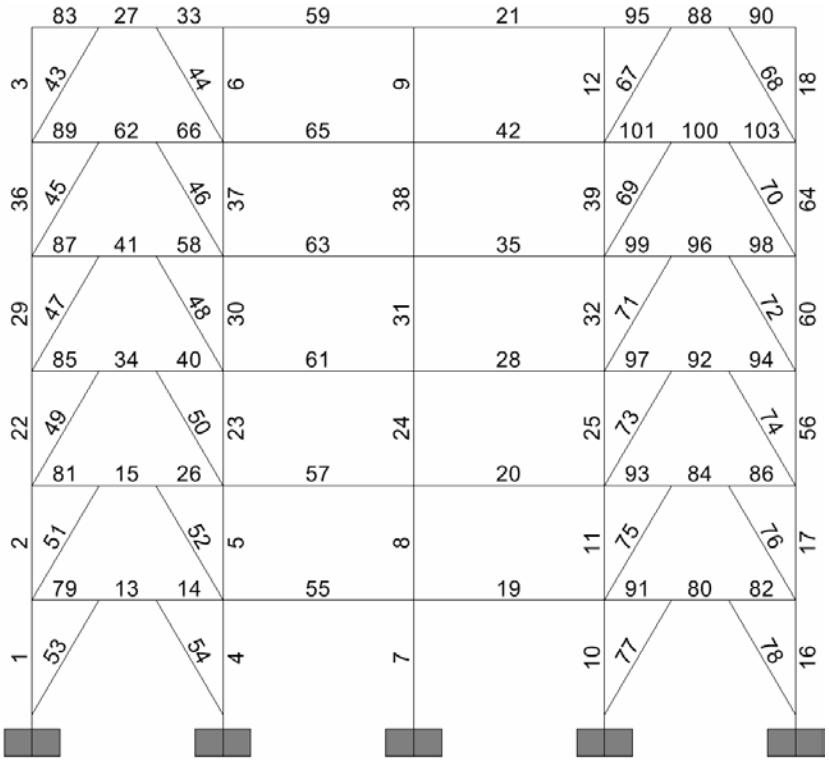

D-4-6

Figure A.2.14: Frames “D-3-6” & “D-4-6” member labels

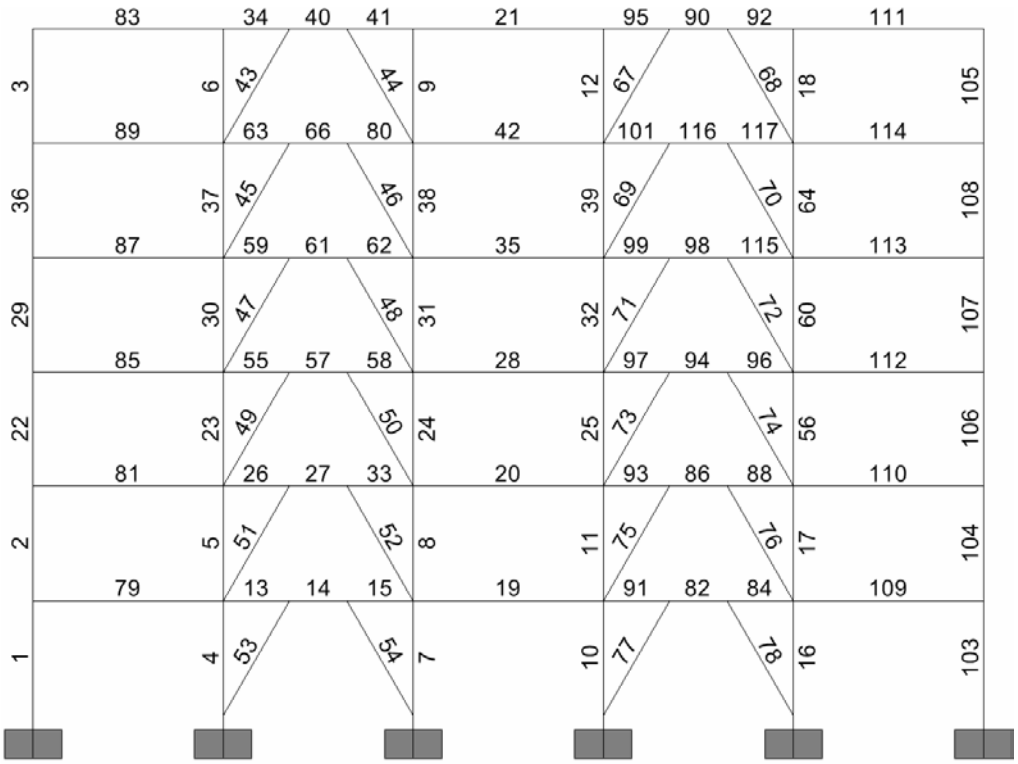

D-5-6

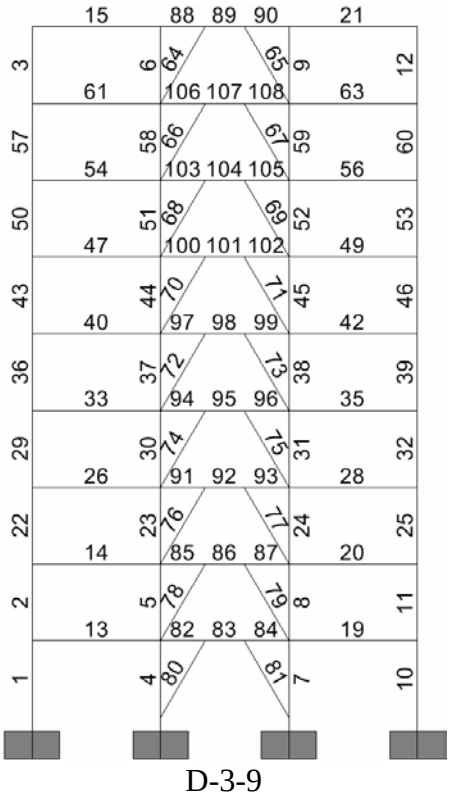

D-3-9

Figure A.2.15: Frames “D-5-6” & “D-3-9” member labels

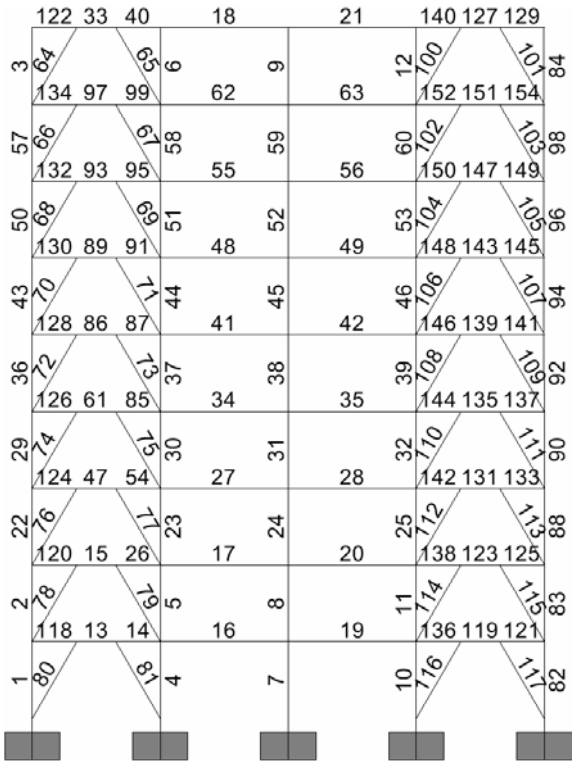

D-4-9

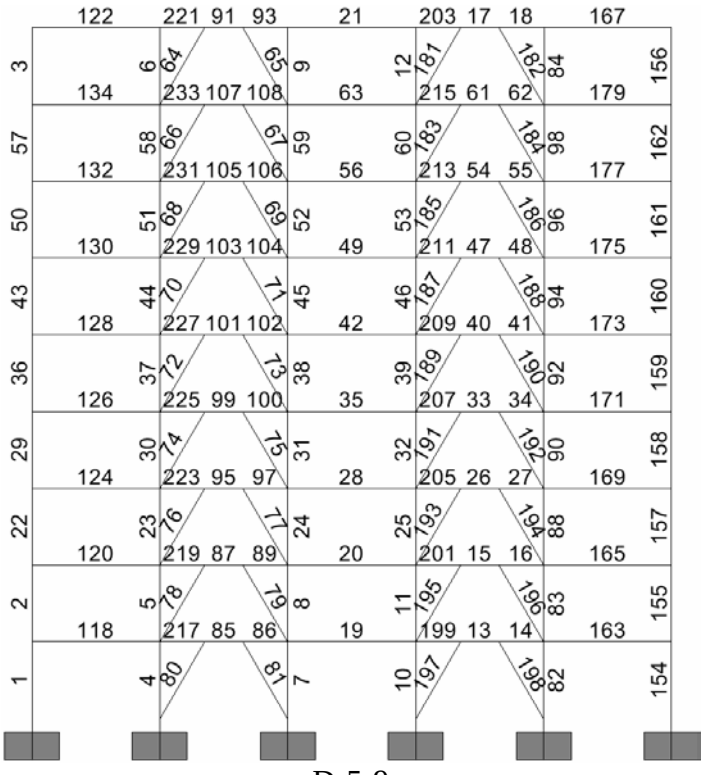

D-5-9

Figure A.2.16: Frames “D-4-9” & “D-5-9” member labels

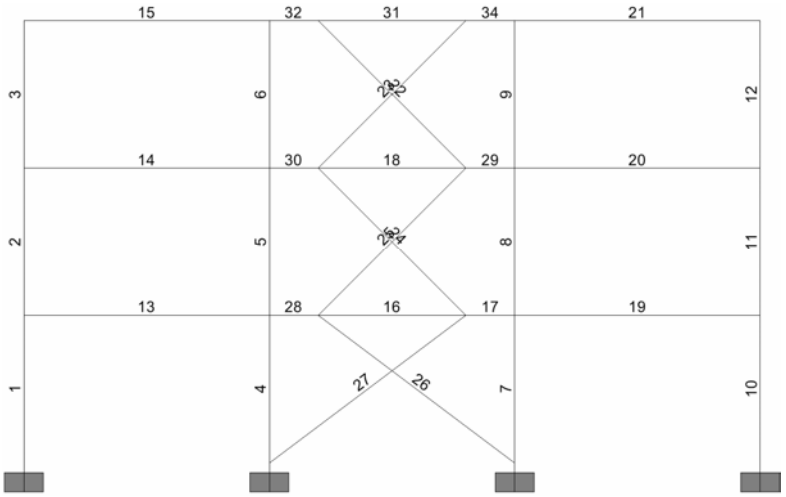

E-3-3

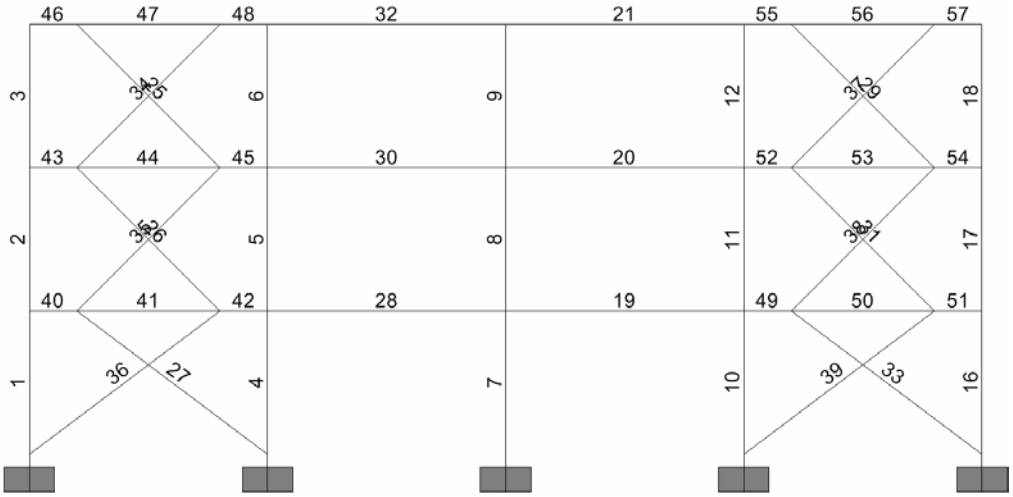

E-4-3

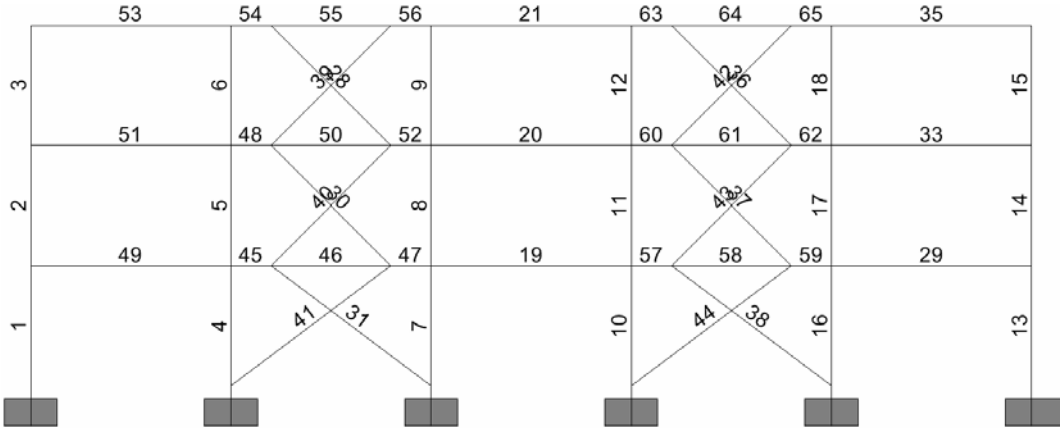

E-5-3

Figure A.2.17: Frames “E-3-3”, “E-4-3” & “E-5-3” member labels

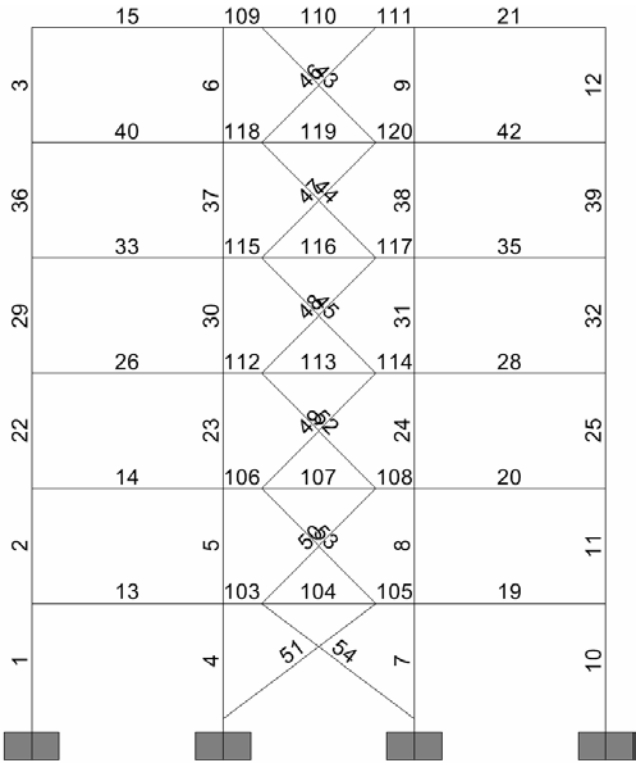

E-3-6

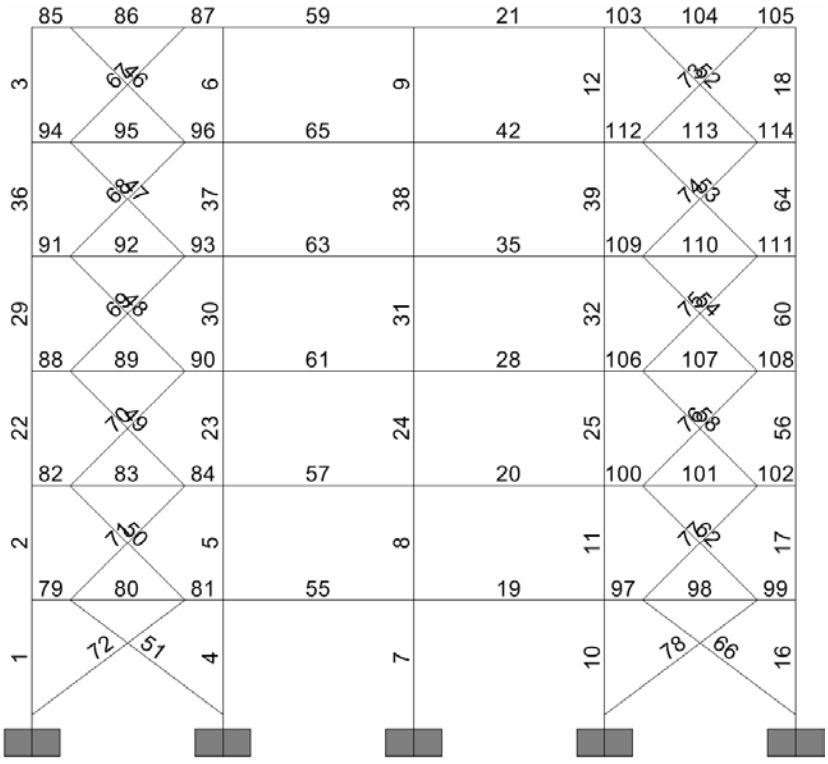

E-4-6

Figure A.2.18: Frames “E-3-6” & “E-4-6” member labels

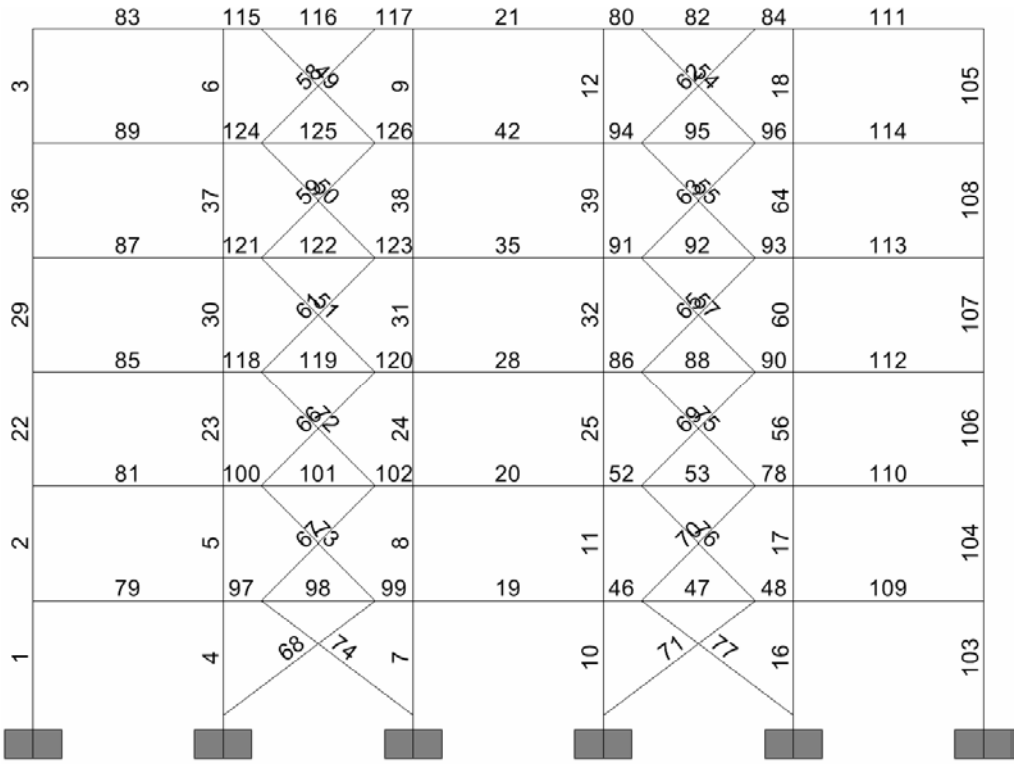

E-5-6

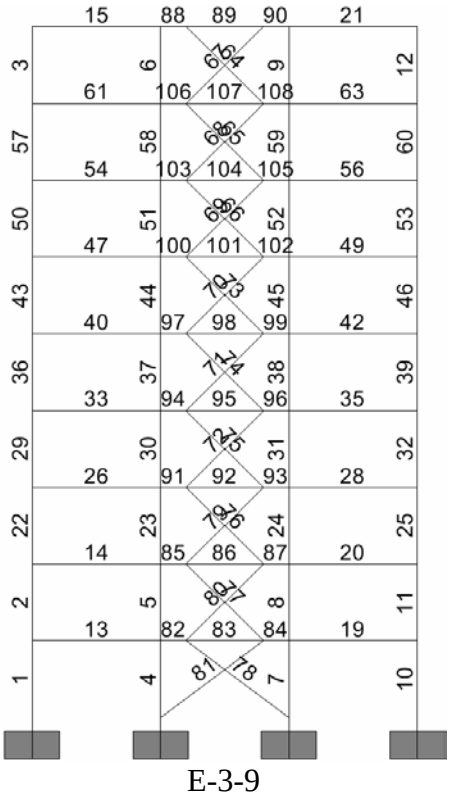

E-3-9

Figure A.2.19: Frames “E-5-6” & “E-3-9” member labels

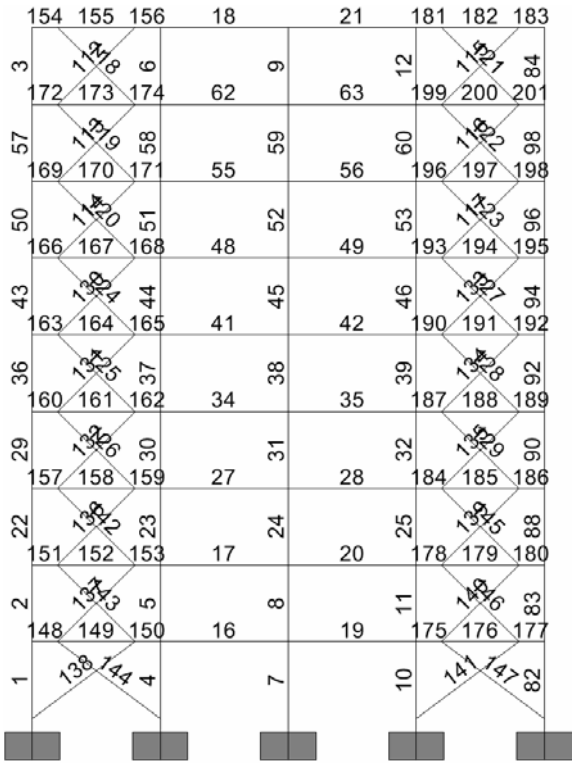

E-4-9

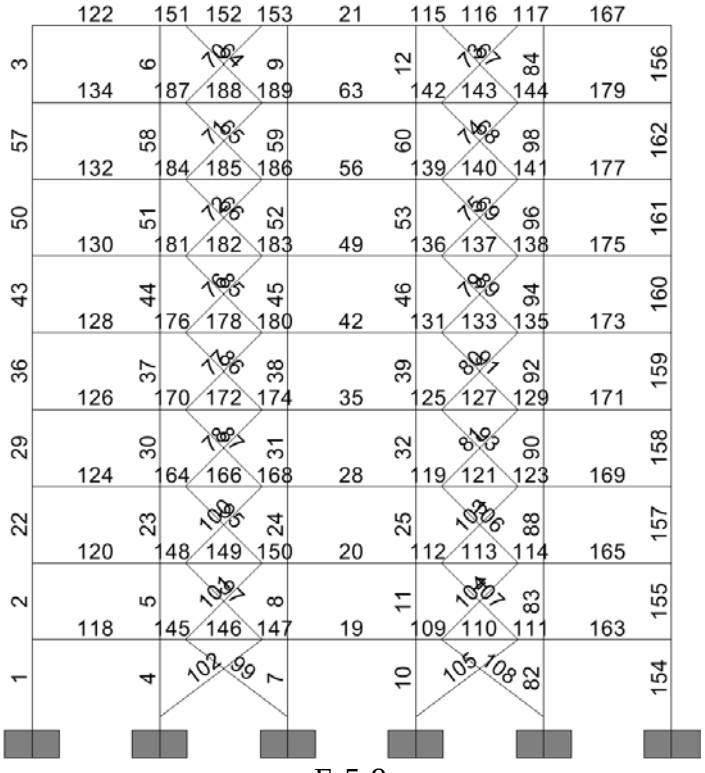

E-5-9

Figure A.2.20: Frames “E-4-9” & “E-5-9” member labels

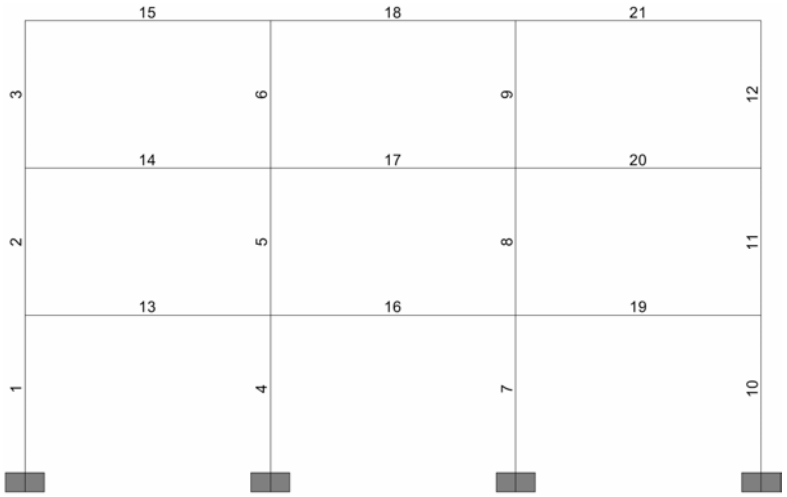

F-3-3

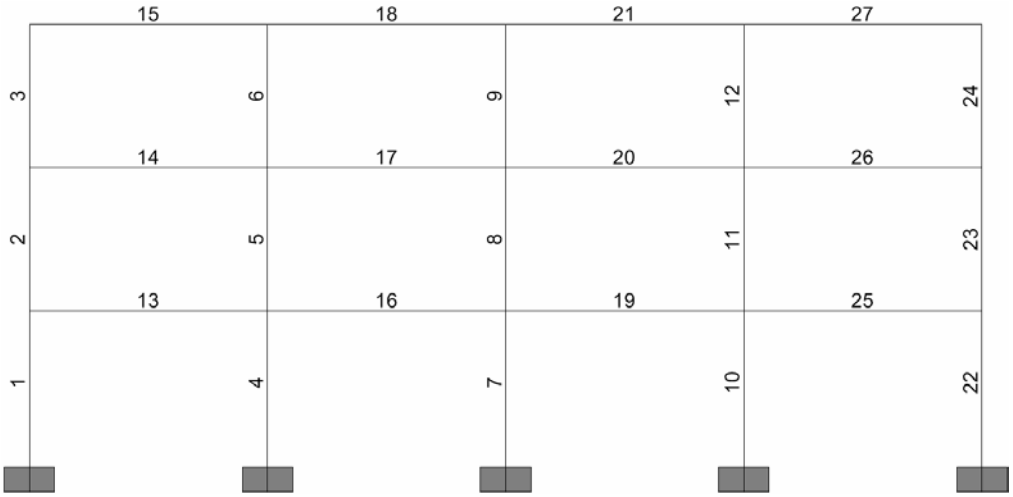

F-4-3

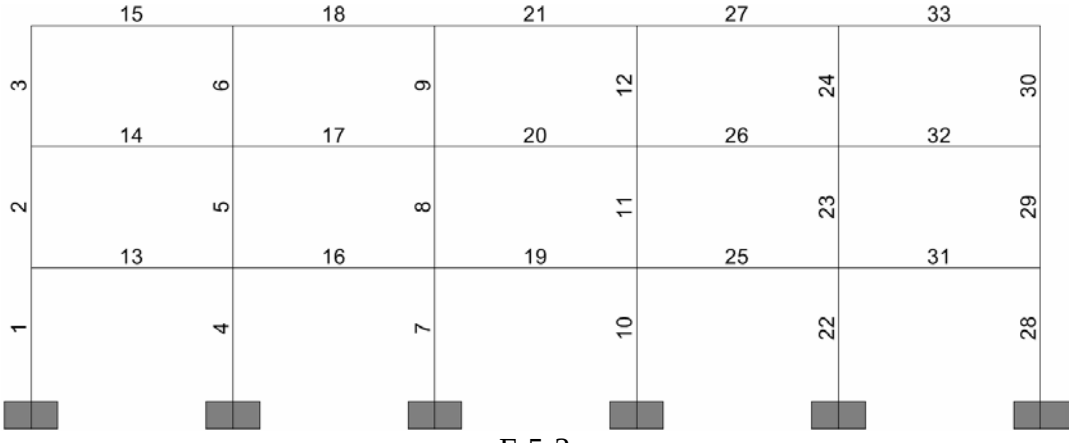

F-5-3

Figure A.2.21: Frames “F-3-3”, “F-4-3” & “F-5-3” member labels

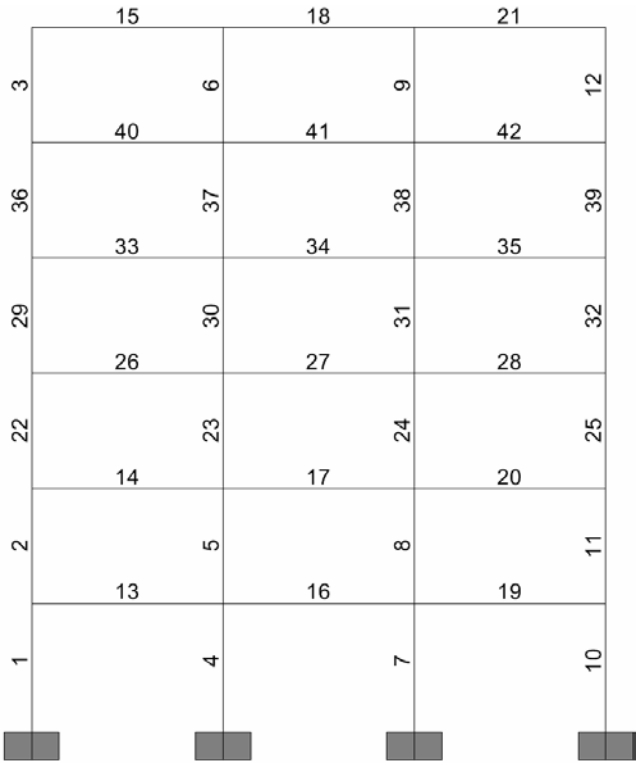

F-3-6

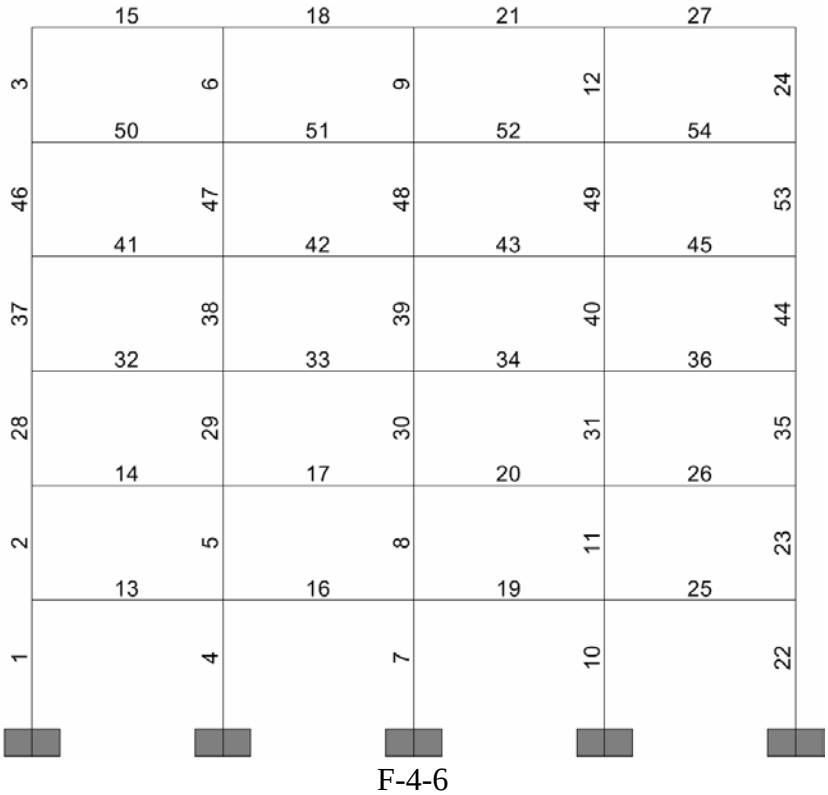

F-4-6

Figure A.2.22: Frames “F-3-6” & “F-4-6” member labels

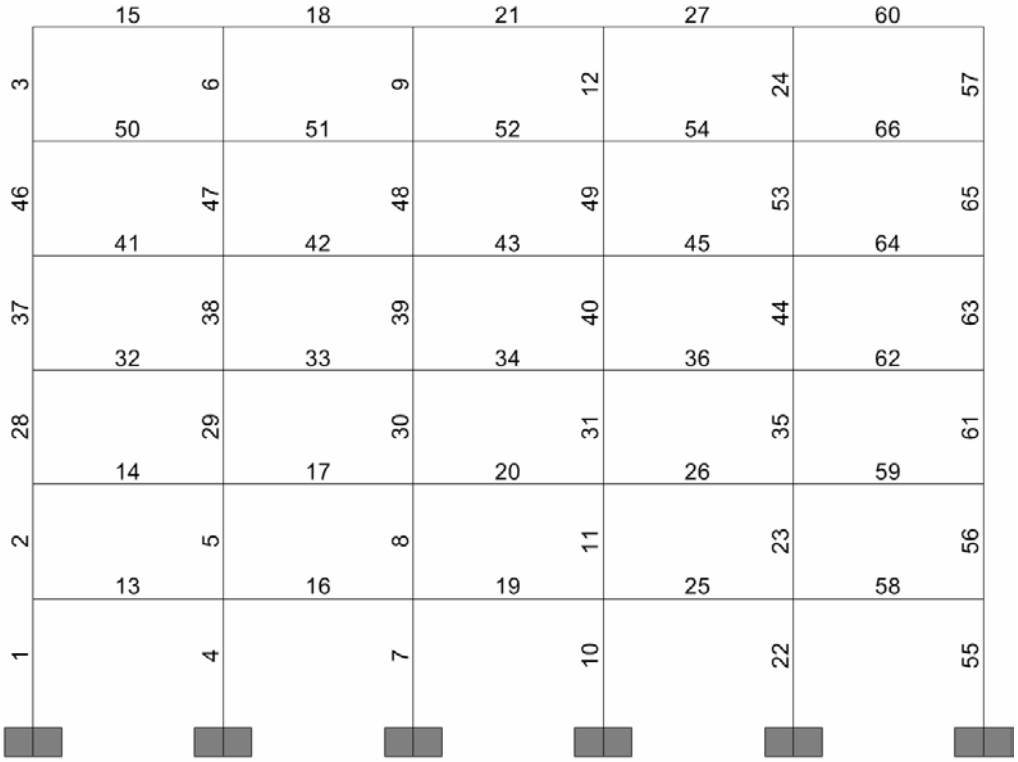

F-5-6

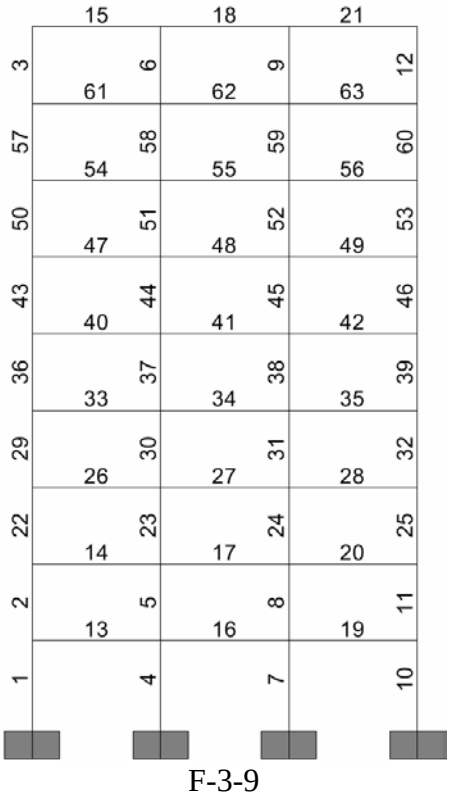

F-3-9

Figure A.2.23: Frames “F-5-6” & “F-3-9” member labels

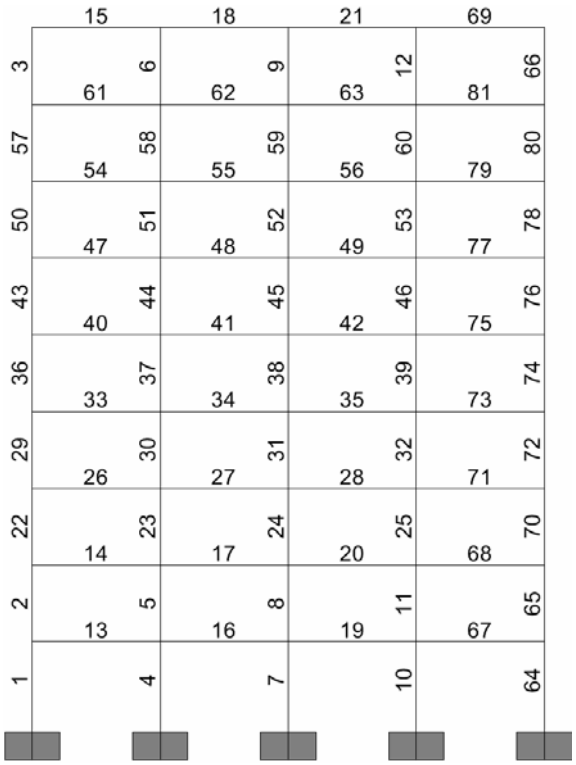

F-4-9

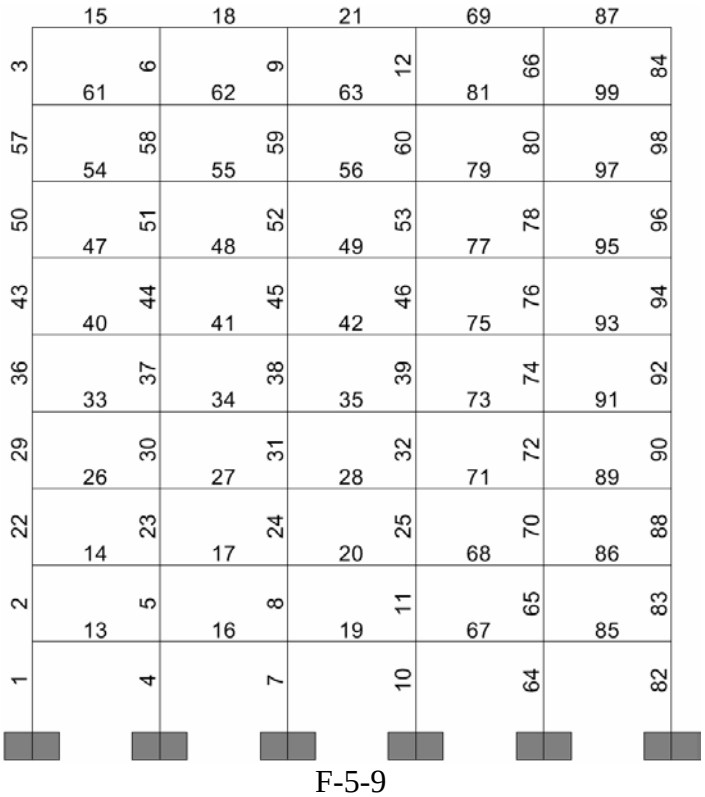

F-5-9

Figure A.2.24: Frames “F-4-9” & “F-5-9” member label

A.3 FRAME MEMBER SECTIONS

Table A.3.1: “A” Type frame member labels and corresponding cross-sections

	IPE 400	IPE 450	IPE 500	IPE 550	HE 360A	HE 400A	HE 450A
A-3-3	15,18,21	13,14,16,17,19,20	-	-	1~12	-	-
A-3-6	15,18,21	33,34,35,40,41,42	13,14,16,17,19,20,26,27,28	-	3,6,9,12,29,30,31,32,36~39	1,2,4,5,7,8,10,11,22,23,24,25	-
A-3-9	15,18,21	54~56,61~63	33~35,40~42,47~49	13,14,16,17,19,20,26~28	3,6,9,12,50~53,57~60	29~32,36~39,43,44,45,46	1,2,4,5,7,8,10,11,22~25
A-4-3	15,18,21,27	13,14,16,17,19,20,25,26	-	-	1~12,22~24	-	-
A-4-6	15,18,21,27	41~43,45,50~52,54	13,14,16,17,19,20,25,26,32~34,36	-	3,6,9,12,24,37~40,44,46~49,53	1,2,4,5,7,8,10,11,22,23,28~31,35	-
A-4-9	15,18,21,69	54~56,61~63,79,81	33~35,40~42,47~49,73,75,77	13,14,16,17,19,20,26~28,67,68,71	3,6,9,12,50~53,57~60,66,78,80	29~32,36~39,43~46,72,74,76	1,2,4,5,7,8,10,11,22~25,64,65,70
A-5-3	15,18,21,27,33	13,14,16,17,19,20,25,26,31,32	-	-	1~12,22~24,28~30	-	-
A-5-6	15,18,21,27,60	41~43,45,50~52,54,64,66	13,14,16,17,19,20,25,26,32~34,36,58,59,62	-	3,6,9,12,24,37~40,44,46~49,53,57,63,65	1,2,4,5,7,8,10,11,22,23,28~31,35,55,56,61	-
A-5-9	15,18,21,69,87	54~56,61~63,79,81,97,99	33~35,40~42,47~49,73,75,77,91,93,95	13,14,16,17,19,20,26~28,67,68,71,85,86,89	3,6,9,12,50~53,57~60,66,78,80,84,96,98	29~32,36~39,43~46,72,74,76,90,92,94	1,2,4,5,7,8,10,11,22~25,64,65,70,82,83,88

Table A.3.2: “B” Type frame member labels and corresponding cross-sections

	IPE 400	IPE 450	IPE 500	IPE 550	HE 200A	HE 220A	HE 340A	HE 360A	HE 500A	TUBE 120x120x10	TUBE 140x140x10	TUBE 160x160x10	TUBE 180x180x10
B-3-3	15,18,21	13,14,16,17,19,20	-	-	-	1~12	-	-	-	22,23,25~28	-	-	-
B-3-6	15,18,21	33~35,40~42	13,14,16,17,19,20,26~28	-	-	3,6,9,12,29,30~32,36~39	-	1,2,4,5,7,8,10,11,22~25	-	43~48	49~54	-	-
B-3-9	15,18,21	54~56,61~63	33~35,40~42,47~49	13,14,16,17,19,20,26~28	-	3,6,9,12,50~53,57~60	29~32,36~39,43~46	-	1,2,4,5,7,8,10,11,22~25	64~69	70~75	76~81	-
B-4-3	15,18,21,33	13,14,16,17,19,20,31,32	-	-	-	1~12,24,29,30	-	-	-	22,23,25~28,40~45	-	-	-
B-4-6	15,18,21,60	33~35,40~42,64,66	13,14,16,17,19,20,26~28,58,59,62	-	-	3,6,9,12,29~32,36~39,57,63,65	-	1,2,4,5,7,8,10,11,22~25,55,56,61	-	43~48,67~69,70~72	49~54,73~78	-	-
B-4-9	15,18,21,87	54~56,61~63,97,99	33~35,40~42,47~49,91,93,95	13,14,16,17,19,20,27,28,85,86,89	-	3,6,9,12,50~53,57~60,84,96,98	-	29~32,36~39,43~46,90,92,94	1,2,4,5,7,8,10,11,22~25,82,83,88	64~69,100~105	70~75,106~111	76~81,112~117	-
B-5-3	15,18,21,33,39	13,14,16,17,19,20,31,32,37,38	-	-	-	1~12,24,29,30,34~36	-	-	-	22,23,25~28,40~45	-	-	-
B-5-6	15,18,21,60,84	33~35,40~42,64,66,88,90	13,14,16,17,19,20,26~28,58,59,62,82,83,86	-	3,6,9,12,29~32,36~39,57,63,65,81,87,89	-	-	1,2,4,7,8,10,11,22~25,55,56,61,79,80,58	-	43~48,91~96	49~54,97~102	-	-
B-5-9	15,18,21,87,123	54~56,61~63,97,99,133,135	33~35,40~42,47~49,91,93,95,127,129,131	13,14,16,17,19,20,26~28,85,86,89,121,122,125	-	3,6,9,12,50~53,57~60,84,96,98,120,132,134	-	29~32,36~39,43~46,90,92,94,126,128,130	1,2,4,5,7,8,10,11,22~25,82,83,88,118,119,124	-	64~69,136~141	70~75,142~147	76~81,148~153

Table A.3.3: “C” Type frame member labels and corresponding cross-sections

	IPE 400	IPE 450	IPE 500	IPE 550	HE 360A	HE 400A	HE 450A	TUBE 120x120x10	TUBE 140x140x10	TUBE 160x160x10
C-3-3	15,21,32,33,13	14,19,20,28~31	-	-	1~12	-	-	22~27	-	-
C-3-6	15,21,59,60	33,35,40,42,63~66	13,14,19,20,26,28,55~58,61,62	-	3,6,9,12,29~32,36~39	1,2,4,7,8,10,11,22~25	-	43~48,49~54	-	-
C-3-9	15,21,86,87	54,56,61,63,96~99	-	-	3,6,9,12,50~53,57~60	29~32,36~39,43~46	1,2,4,5,7,8,10,11,22~25	64~69	70~75	76~81
C-4-3	21,32,53,54,59,60	19,20,28,30,49,50~52,55~58	33,35,40,42,47,49,90~95	13,14,19,20,26,28,82~85,88,89	1~12,16~18	-	-	22~27,43~48	-	-
C-4-6	21,59,83,84,95,96	35,42,63,65,87~90,99~101	19,20,28,55,57,61,79,80~82,85,86,91~94,97,98	-	3,6,9,12,18,29~32,36~39,60,64,102	1,2,4,5,7,8,10,11,16,17,22~25,56	-	43~48,67~72	49~54,73~78	-
C-4-9	18,21,122,123,140,141	55,56,62,63,132~135,150~153	34,35,41,42,48,49,126~131,144~149	16,17,19,20,27,28,118~125,136~139,142,143	3,6,9,12,50~53,57~60,84,96,98	29~32,36~39,43~46,90,92,94	1,2,4,7,8,10,11,22~25,82,83,88	64~69,100~105	70~75,106~111	76~81,112~117
C-5-3	21,35,53,58,60,65,66	19,20,29,33,49~54,56,61~64	-	-	1~18	-	-	22~27,43~48	-	-
C-5-6	21,59,83,95,96,111	35,42,63,65,87,89,99~102,113,114	19,20,28,55,57,61,79,81,85,91~94,97,98,109,110,112	-	3,6,9,12,18,29,30~32,36~39,60,64,105,107,108	1,2,4,5,7,8,10,11,16,17,22~25,56,103,104,106	-	43~48,67~72	49~54,73~78	-
C-5-9	21,122,167,203,204,221,222	56,63,132,134,177,179,213~216,231~234	35,42,49,126,128,130,171,173,175,207~212,225~230	19,20,28,118,120,124,163,165,169,199~206,217~220,223,224	3,6,9,12,50~53,57~60,84,96,98,156,161,162	29~32,36~39,43~46,90,92,94,158,159,160	1,2,4,5,7,8,10,11,22~25,82,83,88,154,155,157	64~69,181~186	70~75,187~192	76~81,193,198

Table A.3.4: “D” Type frame member labels and corresponding cross-sections

	IPE 400	IPE 450	IPE 500	IPE 550	HE 360A	HE 400A	HE 450A	TUBE 120x120x10	TUBE 140x140x10	TUBE 160x160x10
D-3-3	15,21,31,32,34	13,14,16~20,28~30	-	-	1~12	-	-	22~27	-	-
D-3-6	15,21,34,41,59	33,35,40,42,60,62~65,67	13,14,16~20,26~28,55~58,61	-	3,6,9,12,29,30~32,36~39	1,2,4,5,7,8,10,11,22~25	-	43~48	49~54	-
D-3-9	15,21,88,89,90	54,56,61,63,103~108	33,35,40,42,47,49,94~102	13,14,19,20,26,28,82~87,91~93	3,6,9,12,50~53,57~60	29~32,36~39,43~46	1,2,4,5,7,8,10,11,22~25	64~69	70~75	76~81
D-4-3	21,31~33,38,39,53,59	13~15,19,20,28~30,34~37,49,51,55,57	-	-	1~12,16~18	-	-	22~27,43~48	-	-
D-4-6	21,27,33,59,83,88,90,95	35,41,42,58,62,63,65,66,87,89,96,98,99,100,101,103	13~15,19,20,26,28,34,40,55,57,61,79,80~82,84~86,91~94,97	-	3,6,9,12,18,29~32,36~39,60,64	1,2,4,5,7,8,10,11,16,17,22~25,56	-	43~48,67~72	49~54,73~78	-
D-4-9	18,21,33,40,122,127,129,140	55,56,62,63,93,95,97,99,132,134,147,149,150,151,152,154	34,35,41,42,48,49,61,85~87,89,91,126,128,130,135,137,139,141,143~146,148	13~17,19,20,26~28,47,54,118~125,131,133,136,138,142	3,6,9,12,50~53,57~60,84,96,98	29~32,36~39,43~46,90,92,94	1,2,4,5,7,8,10,11,22~25,82,83,88	64~69,100~105	70~75,106~111	76~81,112~117
D-5-3	21,34,35,36,41,42,53,58,65	19,20,28~33,37~40,49~51,54,61,63	-	-	1~18	-	-	22~27,43~48	-	-
D-5-6	21,34,40,41,83,90,92,95,111	35,42,59,61~63,66,87,89,98,99,101,113~117	20,26~28,33,55,57,58,81,85,86,88,93,94,96,97,110,112	13~15,19,79,82,84,91,109	3,6,9,12,18,29~32,36~39,60,64,105,107,108	1,2,4,5,7,8,10,11,16,17,22~25,56,103,104,106	-	43~48,67~72	49~54,73~78	-
D-5-9	17,18,21,91,93,122,167,203,221	54~56,61~63,105~108,132,134,177,179,213,215,231,233	33~35,40~42,47~49,99~104,126,128,130,171,173,175,207,209,211,225,227,229	13~16,19,20,26,27,28,85~87,89,95,97,118,120,124,163,165,169,199,201,205,217,219,223	3,6,9,12,50~53,57~60,84,96,98,156,161,162	29~32,36~39,43~46,90,92,94,158~160	1,2,4,5,7,8,10,11,22~25,82,83,88,154,155,157	64~69,181~186	70~75,187~192	76~81,193~198

Table A.3.5: “E” Type frame member labels and corresponding cross-sections

	IPE 400	IPE 450	IPE 500	IPE 550	HE 360A	HE 400A	HE 450A	TUBE 120x120x10	TUBE 140x140x10	TUBE 160x160x10
E-3-3	15,21,31,32,34	13,14,16~20,28~30	-	-	1~12	-	-	22~27	-	-
E-3-6	15,21,109~111	33,35,40,42,115~120	13,14,19,20,26,28,103~108,112~114	-	3,6,9,12,29~32,36~39	1,2,4,5,7,8,10,11,22~25	-	43~48	49~54	-
E-3-9	15,21,88~90	54,56,61,63,103~108	33,35,40,42,47,49,94~102	13,14,19,20,26,28,82~87,91~93	3,6,9,12,50~53,57~60	29~32,36~39,43~46	1,2,4,5,7,8,10,11,22~25	64~69	70~75	76~81
E-4-3	21,32,46~48,55~57	19,20,28,30,40~45,49~54	-	-	1~12,16~18	-	-	25~27,29,31,33~39	-	-
E-4-6	21,59,85~87,103~105	35,42,63,65,91~96,109~114	19,20,28,55,57,61,79~84,88~90,97~102,106~108	-	3,6,9,12,18,29~32,36~39,60,64	1,2,4,5,7,8,10,11,16,22~25,56	-	46~48,52~54,67~69,73~75	49~51,58,62,66,70~72,76~78	-
E-4-9	18,21,154~156,181~183	55,56,62,63,169~174,196~201	34,35,41,42,48,49,160~168,187~195	16,17,19,20,27,28,148~153,157~159,175~180,184~186	3,6,9,12,50~53,57~60,84,96,98	29~32,36~39,43~46,90,92,94	1,2,4,5,7,8,10,11,22~25,82,83,88	112~123	124~135	136~147
E-5-3	21,35,53~56,63~65	19,20,29,33,45~52,57~62	-	-	1~18	-	-	28,30,31,36~44	-	-
E-5-6	3,6,9,12,18,29~32,36~39,60,64,105,107,108	1,2,4,5,7,8,10,11,16,17,22~25,56,103,104,106	-	-	21,80,82~84,111,115~117	35,42,87,89,91~96,113,114,121~126	19,20,28,46,47,48,52,53,78,79,81,85,86,88,90,97~102,109,110,112,118~120	49~51,54,55,57~59,61~63,65	66~77	-
E-5-9	21,115~117,122,151~153,167	56,63,132,134,139~144,177,179,184~189	35,42,49,125~133,135~138,170~176,178,180~183	19,20,28,109~114,118~121,123,124,145~150,163~166,168,169	3,6,9,12,50~53,57~60,84,96,98,156,161,161	29~32,36~39,43~46,90,92,94,158~160	1,2,4,5,7,8,10,11,22~25,82,83,88,154,155,157	64~75	76~81,85~87,89,91,93	95,97,99~108

Table A.3.6: “F” Type frame member labels and corresponding cross-sections

	IPE 400	IPE 450	IPE 500	IPE 550	HE 220A	HE 280A	HE 300A	HE 360A	HE 400A	HE 450A
F-3-3	15,18,21	13,14,16,17,19,20	-	-	1~12	-	-	-	-	-
F-3-6	15,18,21	33~35,40~42	13,14,16,17,19,20,26~28	-	3,6,9,12,29~32,36~39	1,2,4,5,7,8,10,11,22~25	-	-	-	-
F-3-9	15,18,21,54~56,61~63		33~35,40~42,47~49	13~17,19,20,26~28	3,6,9,12,50~53,57~60	-	-	29~32,36~39,43~46	1,2,4,5,7,8,10,11,22~25	-
F-4-3	15,18,21,27	13,14,16,17,19,20,25,26	-	-	1~12,22~24	-	-	-	-	-
F-4-6	15,18,21,27	41~45,50~54	13,14,16,17,19,20,25,26,32~34,36	-	-	-	3,6,9,12,24,37~40,44,46~49,53	1,2,4,5,7,8,10,11,22,23,28~31,35	-	-
F-4-9	15,18,21,69	54,55,56,61,62,63,79,81	33~35,40~42,47~49,73,75,77	13,14,16,17,19,20,26~28,67,68,71	-	3,6,9,12,50~53,57~60,66,78,80	-	-	29~32,36~39,43~46,72,74,76	1,2,4,5,7,8,10,11,22~25,64,65,70
F-5-3	15,18,21,27,33	13,14,16,17,19,20,25,26,31,32	-	-	-	1~12,22~24,28~30	-	-	-	-
F-5-6	15,18,21,27,60	41~45,50~52,54,64,66	13,14,16,17,19,20,25,26,32~34,36,58,59,62	-	-	-	3,6,9,12,24,37~40,44,46~49,53,57,63,65	1,2,4,5,7,8,10,11,22,23,28~31,35,55,56,61	-	-
F-5-9	15,18,21,69,87	54~56,61~63,79,81,97,99	33~35,40~42,47~49,73,75,77,91,93,95	13,14,16,17,19,20,26~28,67,68,71,85,86,89	-	3,6,9,12,50~53,57~60,66,78,80,84,96,98	-	-	29~32,36~39,43~46,72,74,76,90,92,94	1,2,4,5,7,8,10,11,22~25,64,65,70,82,83,88

A.4 NON-LINEAR FORCE DISPLACEMENT PARAMETERS for STRUCTURAL COMPONENTS

Table A.4.1: Non-linear Parameters for Beam & Column Type Components (FEMA-356 Table 5-6 [57])

Modeling Parameters and Acceptance Criteria for Nonlinear Procedures—Structural Steel Components

	Modeling Parameters			Acceptance Criteria				
	Plastic Rotation Angle, Radians		Residual Strength Ratio	Plastic Rotation Angle, Radians				
					Primary		Secondary	
Component/Action	a	b	c	IO	LS	CP	LS	CP
Beams—flexure								
a. $\frac{b_f}{2t_f} \le \frac{52}{\sqrt{F_{ye}}}$ and $\frac{h}{t_w} \le \frac{418}{\sqrt{F_{ye}}}$	$9\theta_y$	$11\theta_y$	0.6	$1\theta_y$	$6\theta_y$	$8\theta_y$	$9\theta_y$	$11\theta_y$
b. $\frac{b_f}{2t_f} \ge \frac{65}{\sqrt{F_{ye}}}$ or $\frac{h}{t_w} \ge \frac{640}{\sqrt{F_{ye}}}$	$4\theta_y$	$6\theta_y$	0.2	$0.25\theta_y$	$2\theta_y$	$3\theta_y$	$3\theta_y$	$4\theta_y$
c. Other	Linear interpolation between the values on lines a and b for both flange slenderness (first term) and web slenderness (second term) shall be performed, and the lowest resulting value shall be used							
Columns—flexure [2, 7]								
For $P/P_{CL} < 0.20$								
a. $\frac{b_f}{2t_f} \le \frac{52}{\sqrt{F_{ye}}}$ and $\frac{h}{t_w} \le \frac{300}{\sqrt{F_{ye}}}$	$9\theta_y$	$11\theta_y$	0.6	$1\theta_y$	$6\theta_y$	$8\theta_y$	$9\theta_y$	$11\theta_y$
b. $d\ \frac{b_f}{2t_f} \ge \frac{65}{\sqrt{F_{ye}}}$ or $\frac{h}{t_w} \ge \frac{460}{\sqrt{F_{ye}}}$	$4\theta_y$	$6\theta_y$	0.2	$0.25\theta_y$	$2\theta_y$	$3\theta_y$	$3\theta_y$	$4\theta_y$
c. Other	Linear interpolation between the values on lines a and b for both flange slenderness (first term) and web slenderness (second term) shall be performed, and the lowest resulting value shall be used							

Table A.4.1: Non-linear Parameters for Beam & Column Type Components (cont.) (FEMA-356 Table 5-6 [57])

Modeling Parameters and Acceptance Criteria for Nonlinear Procedures—Structural Steel Components (continued)

	Modeling Parameters			Acceptance Criteria				
	Plastic Rotation Angle, Radians		Residual Strength Ratio	Plastic Rotation Angle, Radians				
					Primary		Secondary	
Component/Action	a	b	c	IO	LS	CP	LS	CP
For $0.2 < P/P_{CL} < 0.50$								
a. $\frac{b_f}{2t_f} \le \frac{52}{\sqrt{F_{ye}}}$ and $\frac{h}{t_w} \le \frac{260}{\sqrt{F_{ye}}}$	—[3]	—[4]	0.2	$0.25\theta_y$	—[5]	—[3]	—[6]	—[4]
b. $\frac{b_f}{2t_f} \ge \frac{65}{\sqrt{F_{ye}}}$ or $\frac{h}{t_w} \ge \frac{400}{\sqrt{F_{ye}}}$	$1\theta_y$	$1.5\theta_y$	0.2	$0.25\theta_y$	$0.5\theta_y$	$0.8\theta_y$	$1.2\theta_y$	$1.2\theta_y$
c. Other	Linear interpolation between the values on lines a and b for both flange slenderness (first term) and web slenderness (second term) shall be performed, and the lowest resulting value shall be used							
Column Panel Zones	$12\theta_y$	$12\theta_y$	1.0	$1\theta_y$	$8\theta_y$	$11\theta_y$	$12\theta_y$	$12\theta_y$
Fully Restrained Moment Connections[13]								
WUF[12]	0.051-0.0013*d*	0.043-0.0006*d*	0.2	0.0126-0.0003*d*	0.0337-0.0009*d*	0.0284-0.0004*d*	0.0323-0.0005*d*	0.043-0.0006*d*
Bottom haunch in WUF with slab	0.026	0.036	0.2	0.0065	0.0172	0.0238	0.0270	0.036
Bottom haunch in WUF without slab	0.018	0.023	0.2	0.0045	0.0119	0.0152	0.0180	0.023
Welded cover plate in WUF[12]	0.056-0.0011*d*	0.056-0.0011*d*	0.2	0.0140-0.0003*d*	0.0318-0.0008*d*	0.0426-0.0008*d*	0.0420-0.0008*d*	0.056-0.0011*d*
Improved WUF-bolted web[12]	0.021-0.0003*d*	0.050-0.0006*d*	0.2	0.0053-0.0001*d*	0.0139-0.0002*d*	0.0210-0.0003*d*	0.0375-0.0005*d*	0.050-0.0006*d*
Improved WUF-welded web	0.041	0.054	0.2	0.0103	0.0312	0.0410	0.0410	0.054
Free flange[12]	0.067-0.0012*d*	0.094-0.0016*d*	0.2	0.0168-0.0003*d*	0.0508-0.0009*d*	0.0670-0.0012*d*	0.0705-0.0012*d*	0.094-0.0016*d*
Reduced beam section[12]	0.050-0.0003*d*	0.070-0.0003*d*	0.2	0.0125-0.0001*d*	0.0380-0.0002*d*	0.0500-0.0003*d*	0.0525-0.0002*d*	0.07-0.0003*d*
Welded flange plates								
a. Flange plate net section	0.03	0.06	0.2	0.0075	0.0228	0.0300	0.0450	0.06
b. Other limit states	force-controlled							
Welded bottom haunch	0.027	0.047	0.2	0.0068	0.0205	0.0270	0.0353	0.047
Welded top and bottom haunches	0.028	0.048	0.2	0.0070	0.0213	0.0280	0.0360	0.048
Welded cover-plated flanges	0.031	0.031	0.2	0.0078	0.0177	0.0236	0.0233	0.031

Table A.4.1: Non-linear Parameters for Beam & Column Type Components (cont.) (FEMA-356 Table 5-6 [57])

Modeling Parameters and Acceptance Criteria for Nonlinear Procedures—Structural Steel Components (continued)

	Modeling Parameters			Acceptance Criteria				
	Plastic Rotation Angle, Radians		Residual Strength Ratio	Plastic Rotation Angle, Radians				
					Primary		Secondary	
Component/Action	a	b	c	IO	LS	CP	LS	CP
Partially Restrained Moment Connections								
Top and bottom clip angle[g]								
a. Shear failure of rivet or bolt (Limit State 1)[g]	0.036	0.048	0.200	0.008	0.020	0.030	0.030	0.040
b. Tension failure of horizontal leg of angle (Limit State 2)	0.012	0.018	0.800	0.003	0.008	0.010	0.010	0.015
c. Tension failure of rivet or bolt (Limit State 3)[g]	0.016	0.025	1.000	0.005	0.008	0.013	0.020	0.020
d. Flexural failure of angle (Limit State 4)	0.042	0.064	0.200	0.010	0.025	0.035	0.035	0.070
Double split tee[g]								
a. Shear failure of rivet or bolt (Limit State 1)[g]	0.036	0.048	0.200	0.008	0.020	0.030	0.030	0.040
b. Tension failure of rivet or bolt (Limit State 2)[g]	0.016	0.024	0.800	0.005	0.008	0.013	0.020	0.020
c. Tension failure of split tee stem (Limit State 3)	0.012	0.018	0.800	0.003	0.008	0.010	0.010	0.015
d. Flexural failure of split tee (Limit State 4)	0.042	0.064	0.200	0.010	0.025	0.035	0.035	0.070
Bolted flange plate[g]								
a. Failure in net section of flange plate or shear failure of bolts or rivets[g]	0.030	0.030	0.800	0.008	0.020	0.025	0.020	0.025
b. Weld failure or tension failure on gross section of plate	0.012	0.018	0.800	0.003	0.008	0.010	0.010	0.015
Bolted end plate								
a. Yield of end plate	0.042	0.042	0.800	0.010	0.028	0.035	0.035	0.035
b. Yield of bolts	0.018	0.024	0.800	0.008	0.010	0.015	0.020	0.020
c. Failure of weld	0.012	0.018	0.800	0.003	0.008	0.010	0.015	0.015
Composite top clip angle bottom [g]								
a. Failure of deck reinforcement	0.018	0.035	0.800	0.005	0.010	0.015	0.020	0.030
b. Local flange yielding and web crippling of column	0.036	0.042	0.400	0.008	0.020	0.030	0.025	0.035

Table A.4.1: Non-linear Parameters for Beam & Column Type Components (cont.) (FEMA-356 Table 5-6 [57])

Modeling Parameters and Acceptance Criteria for Nonlinear Procedures—Structural Steel Components (continued)

	Modeling Parameters			Acceptance Criteria				
	Plastic Rotation Angle, Radians		Residual Strength Ratio	Plastic Rotation Angle, Radians				
					Primary		Secondary	
Component/Action	a	b	c	IO	LS	CP	LS	CP
c. Yield of bottom flange angle	0.036	0.042	0.200	0.008	0.020	0.030	0.025	0.035
d. Tensile yield of rivets or bolts at column flange	0.015	0.022	0.800	0.005	0.008	0.013	0.013	0.018
e. Shear yield of beam flange connection	0.022	0.027	0.200	0.005	0.013	0.018	0.018	0.023
Shear connection with slab[12]	$0.029-0.0002d_{bg}$	$0.15-0.0036d_{bg}$	0.400	$0.0073-0.0001d_{bg}$	--	--	$0.1125-0.0027d_{bg}$	$0.15-0.0036d_{bg}$
Shear connection without slab[12]	$0.15-0.0036d_{bg}$	$0.15-0.0036d_{bg}$	0.400	$0.0375-0.0009d_{bg}$	--	--	$0.1125-0.0027d_{bg}$	$0.15-0.0036d_{bg}$
EBF Link Beam[10, 11]								
a. $e \le \frac{1.6 M_{CE}}{V_{CE}}$	0.15	0.17	0.8	0.005	0.11	0.14	0.14	0.16
b. $e \ge \frac{2.6 M_{CE}}{V_{CE}}$	Same as for beams.							
c. $\frac{.6 M_{CE}}{V_{CE}} < e < \frac{2.6 M_{CE}}{V_{CE}}$	Linear interpolation shall be used.							
Steel Plate Shear Walls[1]	$14\theta_y$	$16\theta_y$	0.7	$0.5\theta_y$	$10\theta_y$	$13\theta_y$	$13\theta_y$	$15\theta_y$

1. Values are for shear walls with stiffeners to prevent shear buckling.
2. Columns in moment or braced frames shall be permitted to be designed for the maximum force delivered by connecting members. For rectangular or square columns, replace $b_f/2t_f$ with b/t; replace 52 with 110, and replace 65 with 190.
3. Plastic rotation = 11 $(1-1.7\ P/P_{CL})\ \theta_y$.
4. Plastic rotation = 17 $(1-1.7\ P/P_{CL})\ \theta_y$.
5. Plastic rotation = 8 $(1-1.7\ P/P_{CL})\ \theta_y$.
6. Plastic rotation = 14 $(1-1.7\ P/P_{CL})\ \theta_y$.
7. Columns with $P/P_{CL} > 0.5$ shall be considered force-controlled.
8. For high-strength bolts, divide values by 2.0.
9. Web plate or stiffened seat shall be considered to carry shear. Without shear connection, action shall not be classified as secondary. If beam depth, $d_b > 18$ inches, multiply m-factors by $18/d_b$.
10. Deformation is the rotation angle between link and beam outside link or column.
11. Values are for link beams with three or more web stiffeners. If no stiffeners, divide values by 2.0. Linear interpolation shall be used for one or two stiffeners.
12. d is the beam depth; d_{bg} is the depth of the bolt group.
13. Tabulated values shall be modified as indicated in Section 5.5.2.4.2, item 4.

Table A.4.1: Non-linear Parameters for Beam & Column Type Components (cont.) (FEMA-356 Table 5-6 [57])

Modeling Parameters and Acceptance Criteria for Nonlinear Procedures—Structural Steel Components

	Modeling Parameters			Acceptance Criteria				
				Plastic Deformation				
	Plastic Deformation		Residual Strength Ratio		Primary		Secondary	
Component/Action	a	b	c	IO	LS	CP	LS	CP
Braces in Compression (except EBF braces)[1]								
a. Double angles buckling in-plane	$0.5\Delta_c$	$9\Delta_c$	0.2	$0.25\Delta_c$	$5\Delta_c$	$7\Delta_c$	$7\Delta_c$	$8\Delta_c$
b. Double angles buckling out-of-plane	$0.5\Delta_c$	$8\Delta_c$	0.2	$0.25\Delta_c$	$4\Delta_c$	$6\Delta_c$	$6\Delta_c$	$7\Delta_c$
c. W or I shape	$0.5\Delta_c$	$8\Delta_c$	0.2	$0.25\Delta_c$	$5\Delta_c$	$7\Delta_c$	$7\Delta_c$	$8\Delta_c$
d. Double channels buckling in-plane	$0.5\Delta_c$	$9\Delta_c$	0.2	$0.25\Delta_c$	$5\Delta_c$	$7\Delta_c$	$7\Delta_c$	$8\Delta_c$
e. Double channels buckling out-of-plane	$0.5\Delta_c$	$8\Delta_c$	0.2	$0.25\Delta_c$	$4\Delta_c$	$6\Delta_c$	$6\Delta_c$	$7\Delta_c$
f. Concrete-filled tubes	$0.5\Delta_c$	$7\Delta_c$	0.2	$0.25\Delta_c$	$4\Delta_c$	$6\Delta_c$	$6\Delta_c$	$7\Delta_c$
g. Rectangular cold-formed tubes								
1. $\frac{d}{t} \le \frac{90}{\sqrt{F_y}}$	$0.5\Delta_c$	$7\Delta_c$	0.4	$0.25\Delta_c$	$4\Delta_c$	$6\Delta_c$	$6\Delta_c$	$7\Delta_c$
2. $\frac{d}{t} \ge \frac{190}{\sqrt{F_y}}$	$0.5\Delta_c$	$3\Delta_c$	0.2	$0.25\Delta_c$	$1\Delta_c$	$2\Delta_c$	$2\Delta_c$	$3\Delta_c$
3. $\frac{90}{\sqrt{F_y}} \le \frac{d}{t} \le \frac{190}{\sqrt{F_y}}$	Linear interpolation shall be used.							
h. Circular hollow tubes								
1. $\frac{d}{t} \le \frac{1500}{F_y}$	$0.5\Delta_c$	$9\Delta_c$	0.4	$0.25\Delta_c$	$4\Delta_c$	$6\Delta_c$	$5\Delta_c$	$8\Delta_c$
2. $\frac{d}{t} \ge \frac{6000}{F_y}$	$0.5\Delta_c$	$3\Delta_c$	0.2	$0.25\Delta_c$	$1\Delta_c$	$2\Delta_c$	$2\Delta_c$	$3\Delta_c$
3. $\frac{1500}{F_y} \le \frac{d}{t} \le \frac{6000}{F_y}$	Linear interpolation shall be used.							
Braces in Tension (except EBF braces)[2]	$11\Delta_T$	$14\Delta_T$	0.8	$0.25\Delta_T$	$7\Delta_T$	$9\Delta_T$	$11\Delta_T$	$13\Delta_T$
Beams, Columns in Tension (except EBF beams, columns)[2]	$5\Delta_T$	$7\Delta_T$	1.0	$0.25\Delta_T$	$3\Delta_T$	$5\Delta_T$	$6\Delta_T$	$7\Delta_T$

1. Δ_c is the axial deformation at expected buckling load.
2. Δ_T is the axial deformation at expected tensile yielding load.

Table A.4.2: Moment Frame Connection Types
(FEMA-356 Table 5-4 [57])

Steel Moment Frame Connection Types

Connection	Description[1, 2]	Type
Welded Unreinforced Flange (WUF)	Full-penetration welds between beam and columns, flanges, bolted or welded web, designed prior to code changes following the Northridge earthquake	FR
Bottom Haunch in WUF w/Slab	Welded bottom haunch added to existing WUF connection with composite slab[3]	FR
Bottom Haunch in WUF w/o Slab	Welded bottom haunch added to existing WUF connection without composite slab[3]	FR
Welded Cover Plate in WUF	Welded cover plates added to existing WUF connection[3]	FR
Improved WUF-Bolted Web	Full-penetration welds between beam and column flanges, bolted web[4]	FR
Improved WUF-Welded Web	Full-penetration welds between beam and column flanges, welded web[4]	FR
Free Flange	Web is coped at ends of beam to separate flanges, welded web tab resists shear and bending moment due to eccentricity due to coped web[4]	FR
Welded Flange Plates	Flange plate with full-penetration weld at column and fillet welded to beam flange[4]	FR
Reduced Beam Section	Connection in which net area of beam flange is reduced to force plastic hinging away from column face[4]	FR
Welded Bottom Haunch	Haunched connection at bottom flange only[4]	FR
Welded Top and Bottom Haunches	Haunched connection at top and bottom flanges[4]	FR
Welded Cover-Plated Flanges	Beam flange and cover-plate are welded to column flange[4]	FR
Top and Bottom Clip Angles	Clip angle bolted or riveted to beam flange and column flange	PR
Double Split Tee	Split tees bolted or riveted to beam flange and column flange	PR
Composite Top and Clip Angle Bottom	Clip angle bolted or riveted to column flange and beam bottom flange with composite slab	PR
Bolted Flange Plates	Flange plate with full-penetration weld at column and bolted to beam flange[4]	PR[5]
Bolted End Plate	Stiffened or unstiffened end plate welded to beam and bolted to column flange	PR[5]
Shear Connection w/ Slab	Simple connection with shear tab, composite slab	PR
Shear Connection w/o Slab	Simple connection with shear tab, no composite slab	PR

1. Where not indicated otherwise, definition applies to connections with bolted or welded web.
2. Where not indicated otherwise, definition applies to connections with or without composite slab.
3. Full-penetration welds between haunch or cover plate to column flange conform to the requirements of the AISC (1997) *Seismic Provisions*.
4. Full-penetration welds conform to the requirements of the AISC (1997) *Seismic Provisions*.
5. For purposes of modeling, the connection may be considered FR if it meets the strength and stiffness requirements of Section 5.5.2.1.